An investigation of interactions with extracellular matrix proteins mediated by the CCP modules of the metabotropic $GABA_B$ receptor

Elin Pless

Thesis submitted for the degree of Doctor of Philosophy in the Collage of Science and Engineering

2009

THE UNIVERSITY *of* EDINBURGH

Abstract

$GABA_B$ receptors are G-protein coupled receptors for the major inhibitory neurotransmitter in the mammalian central nervous system, γ-aminobutyric acid (GABA). The receptor is linked to a variety of disorders including epilepsy, pain, spasticity, drug addiction and cognitive impairment and is, therefore of major importance for drug discovery. The most abundant receptor isoforms $GABA_B$R1a and R1b differ by the presence in R1a of a pair of N-terminal extracellular complement control protein modules (CCP1 and CCP2) which - in other proteins - are generally involved in mediating specific protein-protein recognition. The CCP1 module contains disulphides but is natively disordered.

In the current work, the yeast two-hybrid system was used to confirm an interaction of CCP1 of $GABA_B$R1a with the extracellular protein fibulin-2. Further work with the yeast two-hybrid system extablished the novel interaction of the abundant extracellular matrix protein laminin, with $GABA_B$R1a CCP1, via its laminin globular (LG) domains. The laminin interaction was further characterised by surface plasmon resonance, demonstrating that several different domains are involved in the binding to the $GABA_B$ receptor CCPs. The primary binding site is located on laminin α5 LG4-5, but the E10 domains of the β1 chain and LG1-3 on α1 may also be involved.

The pharmacological properties of the $GABA_B$R1a and R1b isoforms were studied by transient expression in *Xenopus laevis* oocytes. It was demonstrated that the agonist baclofen, as well as the antagonist CGP55845, appear to be more potent at $GABA_B$R1b compared to $GABA_B$R1a. Intriguingly, when recorded in the precence of laminin, $GABA_B$R1b/R2 expressing oocytes exhibited an increased baclofen-evoked response while the response in $GABA_B$R1a/R2 was completely abolished.

In conclusion, the work demonstrates that laminin is a binding partner for $GABA_B$R1a CCPs. Such an interaction between the metabotropic GABA receptor and the extracellular matrix may lie behind the recently reported roles of GABA in neuronal migration and the laying down of neuronal circuitry during the development of parts of the central nervous system.

Acknowledgements

I would like to thank my supervisors Paul Barlow for allowing me to work on this challenging project and for supervision- especially towards the final stages of my PhD.

I would also like to thank my second supervisor David Wyllie for his support and guidance throughout the second half of my PhD and for inviting me into the field of neuroscience.

I want to thank our collaborators Julia White and Jeff McIlhinney for their knowledge and input.
I would further like to thank both the Sasaki group and the Bettler group for interesting and fruitful collaborations.
I am grateful to GlaxoSmithKline and BBSRC for their financial support of this project.

I would like to thank Tatako Sasaki for supplying me with laminin fragments and Niki Gray for supplying me with oocytes. I'm grateful to Randy Hall and Julia White for their kind gifts of plasmids for the electrophysiology study. I would like to thank Brian Collier for his in vitro transcription-translation contribution and Andy Cronhaw for his help with N-terminal sequencing. I would further like to thank Martin Weir for his Biacore expertise.
I would like to thank Stan Blein for showing me the ropes in the beginning and for interesting brain-storming sessions. I would like to thank all the members of the Barlow group, both past and present for all the help and encouragement over the years. I will miss the cheese and wine nights in the office! Also, thanks to everyone in the George Square neuroscience lab (Marc-Andre, Tim, Christos, Cathy, Phil) for making the hours spent at 'the rig' much more enjoyable!

A big thanks to my girls Yvonne, Lena, Renate and Silvia who are always ready with a smile, listening ear, helping hand or a glass of wine: thank you guys!! Also, a big thanks to my friends, close by and across the sea, for their love, friendship, and support.

Finally I would like to thank Duane for his love, everlasting positive outlook, and for always believing in me.
Special thanks to my parents for all their support, love and encouragement throughout my life, and being behind me all the way.

Declaration

I hereby declare that I composed this thesis entirely myself and that it describes my own research.

Elin Pless
Edinburgh
2009

Abbreviations

AD	activation domain
AMD	age-related macular degeneration
AMPA	α-amino-3-hydroxyl-5-methyl-4- isoxazolepropionic acid
ATF4	activation transcription factor 4
BMG	buffered minimal glycerol
BMM	buffered minimal methanol
BSA	bovine serum albumin
C4BP	complement 4b binding protein
CA1	*Cornu Ammonis* 1
CA3	*Cornu Ammonis* 3
cAMP	cyclic adenosine monophosphate
CC	coiled-coil
CCP	complement control protein
CCP1	complement control protein module 1
CCP2	complement control protein module 2
cDNA	complementary deoxyribonucleic acid
CNS	central nervous system
ConA	concanavalin A
CREB	cAMP response element binding protein
CRF	corticotrophin-releasing factor
cRNA	complimentary ribonucleic acid
DEAE	diethylaminoethyl
DEPC	diethylpyrocarbonate
DMSO	dimethyl sulfoxide
DNA	deoxyribonucleic acid
DNA-BD	deoxyribonucleic acid- binding domain
dNTPs	deoxynucleotide trisphosphates (N denotes A (adenine), C (cytosine), G (guanine), T (thymine) and U (uracil))
DTT	dithiothreitol
ECM	extracellular matrix
EDC	3-dimethyl-aminopropyl)carbodiimide

EDTA	ethylenediaminetetraacetatic acid
EGF	epidermal growth factor
EHS	Engelbreht-Holm Swarm
Endo-Hf	fusion of endoglycosidase H and maltose binding protein
EVH	enabled/VASP homology
FPLC	fast protein liquid chromatography
FTM2	fibulin type module 2
FTM3	fibulin type module 3
G protein	guanine nucleotide-binding protein
GABA	gamma aminobutyric acid
GDP	guanosine diphosphate
GIRK	G protein-coupled inwardly-rectifying potassium channel
GPCR	G-protein coupled receptor
GRK	GPCR regulatory kinase
GTP	guanosine triphosphate
HCL	hydrochloric acid
HNK-1	human natural killer-1
Ig	immunoglobulin
ITC	isothermal titration calorimetry
I-V	current-voltage
kDa	kilodaltons
KIR	inward rectifying potassium channel
LAMA	laminin alpha
LAMB	laminin beta
LAMC	laminin gamma
LB	Luria-Bertani medium
LE	laminin epidermal growth factor-like
LG	G-like domains
LTP	long term potentiation
MCS	multiple cloning site
MD	minimal dextrose
mGluR	metabotropic glutamate receptor
MOPS	3-{N-morpholino] propanesulfonic acid

M_w	molecular weight
NHERF	Na^+/H^+ exchange regulatory factor
NHERF	Na^+/H^+ exchange regulatory factor
NHS	*N-hydroxysuccinimide*
NMR	nuclear magnetic resonance
NTA	*nitrilotriacetic acid*
OD	optical density
PBP	periplasmic binding proteins
PCR	polymerase chain reaction
PDZ	acronym of the first letter of the three proteinsfirst discovered to share the domain: PSD95, DlgA and zo-1
PEG	polyethylene glycol
PMSF	phenylmethanesulfonyl fluoride
PNS	peripheral nervous system
R1	receptor 1
R2	receptor 2
RNA	ribonucleic acid
RU	resonance units
SD	synthetic dropout
SDS-PAGE	sodium dodecyl sulfate-polyacrylamide gel electrophoresis
SOC	super optimal broth with catabolite repression
SPR	surface plasmon resonance
TAE	tris-acetate-EDTA buffer
TBS	tris-buffered saline
TEVC	two-electrod voltage clamp
TM	transmembrane
tRNA	transfer ribonucleic acid
UTR	untranslated region
X-Gal	5-bromo-4-chloro-3-indolyl-beta-D-galactopyranoside
Y2H	yeast two-hybrid
YNB	yeast nitrogen base
YPD	yeast extract/peptone/dextrose
YPDA	yeast extract/peptone/dextrose/adenine

Table of contents

Table of figures, tables and equations

CHAPTER 1

Introduction

1 Chapter 1 Introduction

1.1 G-protein coupled receptors

The G-protein coupled receptors (GPCRs) are a large and diverse superfamily of membrane-bound receptor proteins, containing 1000-2000 members (Bockaert and Pin, 1999). The GPCR are involved in recognition and transduction of signals from a wide range of ligands such as neurotransmitters, nucleotides, odorants, hormones and lipids. They regulate the sensory recognition of pain, cognition, muscle contraction, odours, inflammation, immunity and many other phenomena. The receptors are classified based on sequence homology and pharmacology into six families that all possess a seven-transmembrane helix domain but differ in the length and function of their intra- and extracellular domains (Pin et al., 1999) as seen in Figure 1.

Family 1 (or A) includes β-adrenergic receptors and rhodopsin. Members of this family have ligand-binding sites located within the seven-transmembrane domains. Family 2 (or B) includes receptors for the hormones secretin and glucagon. These receptors have ligand-binding sites in their extracellular domains. Family 3 (or C) includes both calcium-sensing receptors and metabotropic $GABA_B$ and glutamate receptors, all of which contain a large extracellular ligand-binding domain. Family 4 (or D) includes pheromone receptors (VNs) and has a long N-terminal domain. Family 5 (or E) includes cyclic AMP receptors (Parent and Devreotes, 1996); these control development of *Dictyostelium discoideum,* but have yet to be detected in vertebrates.

Family 6 (or F) includes the frizzled and smoothened receptors involved in embryonic development, intracellular polarity and cell localisation. The N-terminal cysteine-rich domain contains the ligand binding site (Bockaert and Pin, 1999).

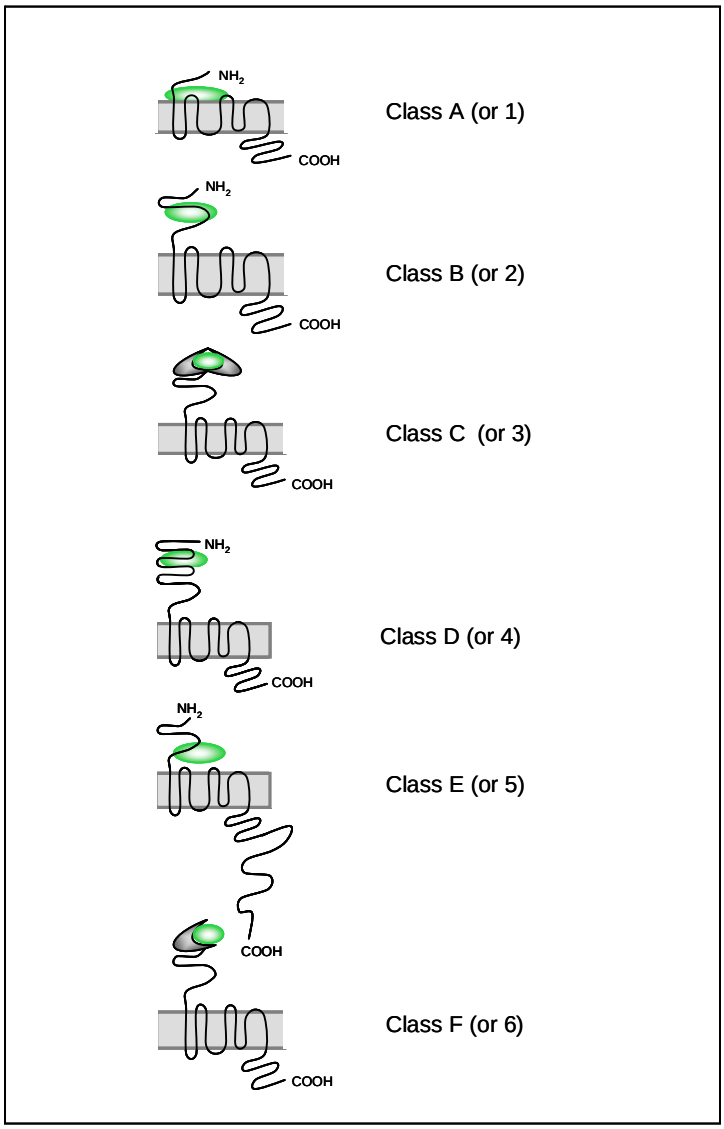

Figure 1 ***Families of G protein -coupled receptors***
GPCRs are subdivided into six super families, dependent on sequence homology and their native ligands. Family 1 has a ligand-binding site located within the seven-transmembrane domain. Family 2 has a ligand-binding site in the extracellular domain. Family 3 contains a large extracellular Venus flytrap ligand-binding domain. Family 4 has an extended N-terminal ligand-binding domain. Family 5 has an N terminal ligand binding site and an extended C terminal domain. Family 6 has an N-terminal cysteine-rich domain containing the ligand binding site. The ligand is shown in green. Figure based on (Bockaert and Pin, 1999).

GPCRs are so named because of their ability to couple to and regulate the activity of intracellular heterotrimeric G-proteins. The nature of the interaction between G-proteins and GPCRs is not fully understood to date but is likely to vary amongst different GPCR families. A large body of work on rhodopsin, for example, suggests that activation of the receptor leads to a change in the orientation of transmembrane (TM) region III and TM region VI, which involves the disruption of a putative salt-bridge, and the possible exposure of key residues involved in G-protein binding and activation (Bourne, 1997; Gether, 2000; Wess, 1997). Activation of the GPCR generates, in turn, a conformational change in the G-protein α-subunit (Gα) which leads to the exchange of GDP for GTP (Bourne, 1997; Bourne et al., 1991). The GTP-bound α-subunit then separates from the receptor and the β γ-subunits of the G-protein. Subsequently, both α-subunit and β γ-subunits regulate various signalling pathways including activation and inhibition of adenylate cyclase and regulation of calcium and potassium channels (Figure 2) (Hamm, 1998). Recently, Gα-GDP has been reported to bind to G protein-coupled inwardly-rectifying potassium channels (GIRKs), and specifically to GIRK1 (Rubinstein et al., 2009).

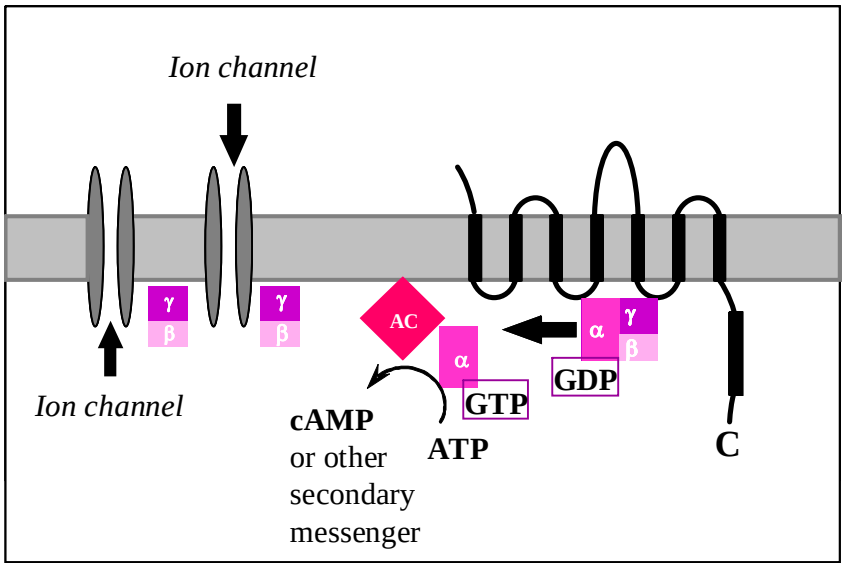

Figure 2 An example of *G-protein signalling*
Upon binding of ligand, the GPCR (shown in black) undergoes a conformational change and the Gα unit-bound GDP is exchanged for GTP. Gα binds to adenylyl cyclase and modulates cAMP (or alternative secondary messenger) signalling. Gβ/γ is released and binds to ion channels.

1.1.1 Desensitisation

Desensitisation reduces GPCR signalling even in the presence of agonist stimulation. This is an important physiological regulatory mechanism that protects against receptor overstimulation (Kristiansen, 2004; Tilakaratne and Sexton, 2005). In the absence of this mechanism, prolonged stimulation of a GPCR could promote, for example, excessive cell growth, which is a feature of many cancers. The regulation of signalling can operate directly at the receptor, or further downstream. Phosphorylation of the C-terminus, or the third intracellular loop, of receptors is mediated by GPCR regulatory kinases (GRKs) (Carman and Benovic, 1998) to phosphorylated sites of the receptor molecules. In general arrestins bind to the third intracellular loop or the C-terminus close to the membrane. The binding of arrestins hinders further interactions

with G-proteins that bind to the same area of the receptor, and they thereby desensitise G-protein-mediated signalling (Reiter and Lefkowitz, 2006). Binding of arrestins also targets the receptor for internalisation by attracting clathrin (Carman and Benovic, 1998; Lefkowitz, 1998). The receptor is later dephosphorylated and recycled to the cell surface (Ferguson et al., 1998). It has been suggested that arrestins are not only involved in the blocking of G-protein-mediated signalling but also the activation of other pathways involving recruitment of the tyrosine kinase Src, and subsequently activation of MAP kinases (Luttrell et al., 1996; Luttrell et al., 1999).

1.1.2 Protein-protein interactions

GPCRs were previously though to function as monomers and bind to trimeric G-protein with a stochiometry of 1:1. Lately, many GPCRs have been shown to dimerise, which may have an important role in receptor signalling (Bouvier, 2001; Marshall, 2001). GPCR dimerisation can occur between two identical receptor subunits forming a homodimer, as occurs for example in the case of β_2-adrenergic receptors (Hebert et al., 1996). Heterodimerisation between two different receptor protein subunits from the same subfamily can also occur - the $GABA_B$ receptors R1 and R2 (Jones et al., 1998; Kaupmann et al., 1998; White et al., 1998) provide an example.

1.1.2.1 Dimerisation and cross-talk

Many members of the GPCR family exist as either homo- or heterodimers (Franco et al., 2007; Marshall, 2001). Dimerisation may involve one or more of the receptor's extracellular, transmembrane and intracellular domains, and may occur via disulfide bridges and/or non-covalent interactions (Pin et al., 2003). The $GABA_B$ receptor (discussed further in section 1.2) was one of the earliest identified heterodimers, containing one $GABA_BR1$ subunit and one $GABA_BR2$ subunit (Jones et al., 1998; Kaupmann et al., 1998; White et al., 1998). It was initially thought that the receptor dimerises through interactions of the C-terminal tails of the subunits. However, it has been shown that isoform $GABA_BR1e$, which is naturally truncated and lacking the C-terminal domain, can nonetheless form heterodimers with $GABA_BR2$ (Schwarz et al., 2000) although the receptor remains inactive. Dimerisation of GPCRs is often essential for receptor trafficking and signalling, where one subunit might act as a chaperone for the other subunit, as is the case for the $GABA_B$ receptor (Margeta-Mitrovic et al., 2000) (discussed further in section 1.2.1).

There are an increasing number of studies suggesting cross-talk between different GPCR signalling pathways. The interaction between the dopamine D5 receptor and the $GABA_A$ γ2 subunit for example, inhibits signalling of both receptors (Liu et al., 2000). Interestingly, the $GABA_BR1$ subunit can heterodimerise with $GABA_A$ subunit γ2S to form cell surface-expressed receptors. The γ2S subunit does however also bind to the $GABA_BR1/R2$ heterodimer, resulting in an enhanced internalisation; this suggests

the two receptor classes are putatively involved in regulating each other (Balusuramanian et al 2004).

1.1.2.2 Intracellular interactions

A multitude of studies suggest that GPCRs interact with a range of binding partners besides G-proteins (Bockaert et al., 2004; Hall et al., 1998; Heuss and Gerber, 2000; Milligan and White, 2001). For example, GPCRs have been observed to interact with a family of proteins containing PDZ domains, which are amongs the most common protein-protein interaction domains. These domains generally bind stretches of three-four amino acid residues within the C-terminal sequences of partner proteins, although the target sequence varies greatly. One example is the β_2-adreneric receptor that interacts with the first PDZ-domain of the Na^+/H^+-exchange regulatory factor (NHERF) (Hall et al., 1998) in an agonist-dependent manner. It has been suggested that this binding is essential for β_2-adrenergic regulation of Na^+/H^+-exchange *in vivo* (Hall et al., 1998).

Binding of arrestins to GPCRs were long thought to be involved only in internalization of the receptor (discussed previously in section 1.1.1) (Pierce and Lefkowitz, 2001). β-arrestins were later shown to link receptors to various signalling cascades apart from G-protein-dependent signalling, such as Src family kinases (Luttrell and Lefkowitz, 2002) as illustrated in Figure 3. It has recently been shown that other parameters such as agonist concentration and receptor clustering can selectively activate G-protein-dependent receptor signalling or β-arrestin-regulated receptor signalling

(Violin and Lefkowitz, 2007), where agonists can selectively activate one signalling pathway without activating another (Gesty-Palmer et al., 2006; Wei et al., 2003).

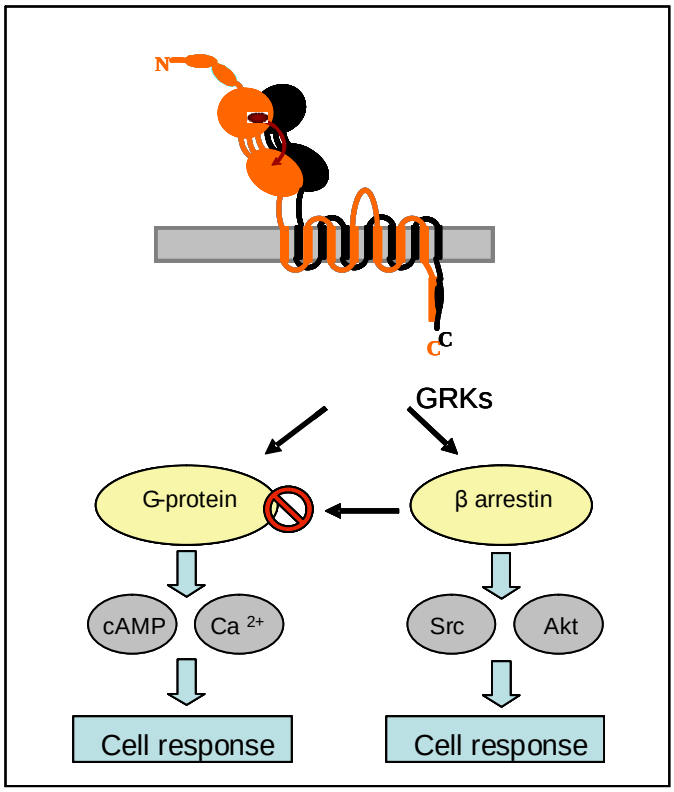

Figure 3 ***Receptor signalling via two distinctly different pathways***
The receptor (shown in orange and black) can be independently regulated by either G-protein-dependent receptor signalling, stimulating cyclic AMP and calcium, or β-arrestin-regulated receptor signalling, where β-arrestin binds to receptors phosphorylated by GRKs and thereby terminating G protein-coupled signalling (indicated by red symbol), and stimulating protein kinases Akt and Src.

Furthermore, binding of calmodulin to the serotonin receptor has been shown to be essential for β-arrestin binding and cell signalling (Labasque et al., 2008). Examples of other GPCR-interacting proteins include the Homer/Vesl proteins containing Enabled/VASP homology (EVH) domains that bind polyproline regions and the

metabotropic glutamate receptor (mGluR) group-1 proteins mGluR1a and mGluR5 contain a C-terminal sequence which interacts with EVH domains in all Homer isoforms (Ciruela et al., 2000). This interaction controls intracellular calcium release by regulation of the interaction of mGluR with the endoplasmic reticulum-based inositol triphosphate (IP_3) receptor (Tu et al., 1998).

The $GABA_BR1$ subunit has been shown to interact via its C-terminus with the activation transcription factor ATF4 (also known as cAMP response element binding protein, CREB2) (Nehring et al., 2000; Vernon et al., 2001; White et al., 2000) as well as members of the 14-3-3 family; this latter interaction appears to interfere with the dimerisation between $GABA_BR1$ and $GABA_BR2$. The $GABA_BR2$ subunit interacts with the transcription factor CHOP (Sauter et al., 2005) and the PDZ domain-containing protein $MUPP_1$ (Ige and Onadeko, 2001).

1.1.2.3 Extracellular interactions

The literature on extracellular binding partners for GPCR is much less extensive. Interactions on the extracellular surface are believed to play important roles in GPCR biology connected with pharmacology, localisation and signalling. The receptor's ligand-binding site is often located either in the large extracellular N-terminal domain or the extracellular loops of the seven-transmembrane regions (Bockaert and Pin, 1999).

The existence of protein-protein interaction motifs on the extracellular domains of GPCRs suggests roles such as receptor clustering, transmembrane signalling and localisation (Stacey et al., 2000). The extracellular matrix (ECM) protein neuronal

activity-regulated pentraxin (Narp) has been reported to aggregate α-amino-3-hydroxyl-5-methyl-4-isoxazolepropionic acid (AMPA) receptors in excitatory synapses by a direct or indirect interaction to AMPA-receptor subunits (O'Brien et al., 1999).

Germane to this thesis, the family-3 GPCR $GABA_BR1a$ subunit (but not the $GABA_BR1b$ subunit) contains a tandem-pair of protein-protein interaction domains known as complement control protein (CCP) modules (Blein et al., 2004; Martin et al., 2001; Tiao et al., 2008) thought to be involved in binding to other proteins, which will be discussed further in section 1.2.2.1. The ECM proteins tenascin-R and tenascin-C contains the HNK-1 carbohydrate and have been shown to interact and inhibit the activation of $GABA_B$ receptors (Saghatelyan et al., 2003). These modulator interactions have been further probed as alternative targets in drug discovery as discussed in section 1.2.5

1.2 The Gamma-aminobutyric Acid Type B ($GABA_B$) receptor

Gamma (γ) aminobutyric acid (GABA) is the major inhibitory neurotransmitter in the mammalian central nervous system (CNS) (Bettler and Tiao, 2006; Chebib and Johnston, 1999). It was discovered in the 1950s and is now known to inhibit mammalian neurons from firing action potentials. There are several other amino acid neurotransmitters besides GABA, namely glycine, glutamate and aspartate. GABA is synthesised from glutamate by the enzyme glutamic acid decarboxylase. There are three

receptors for GABA; these are the $GABA_A$, $GABA_B$ and $GABA_C$ receptors. $GABA_{A/C}$ receptors are responsible for fast (synaptic) inhibition and are generally classified as ionotropic voltage-gated receptors. $GABA_B$ receptors, on the other hand, are involved in slow, more prolonged (synaptic) inhibition and are classed as metabotropic GPCRs.

The $GABA_B$ receptor was identified in the 1980s (Bowery et al., 1979; Bowery et al., 1980; Bowery and Hudson, 1979; Hill and Bowery, 1981) Although the receptor was studied intensively with regards to its pharmacology, very little could be established about its molecular characteristics. In 1997 the $GABA_B$ receptor subunit R1 was identified (Kaupmann et al., 1997) and sequenced, and two splice variants - $GABA_B$R1a and $GABA_B$R1b - were isolated. The cloned receptor did not couple as efficiently to predicted signalling pathways as endogenous receptors, despite binding to agonists. Interestingly, agonist-binding affinities were found to be 100-fold lower than for native receptors (Kaupmann et al., 1997; Kaupmann et al., 1998) and the R1 subunit was detained in the endoplasmic reticulum instead of being expressed at the plasma membrane (Couve et al., 1998; White et al., 1998). The finding of a second subunit, $GABA_B$R2, was subsequently reported by several groups in 1998 (Jones et al., 1998; Kaupmann et al., 1998; Kuner et al., 1999; Martin et al., 1999; Ng et al., 1999; White et al., 1998).

1.2.1 Receptor topology

Like all the GPCRs, the $GABA_B$ receptor subunits has seven helical transmembrane stretches of 20-25 residues each, giving rise to three intracellular and

three extracellular loops. The ligand-binding properties of the $GABA_B$ receptor and other members of family 3 are quite different to other GPCR families due to its 'Venus-flytrap-like' ligand-binding site. The large N-terminal extracellular domains of the $GABA_B$ receptor subunits R1 and R2 (as well as other metabotropic receptors) share sequence similarities with periplasmic binding proteins (Pbp) of bacteria (O'Hara et al., 1993) each is comprised of two lobes linked by a hinge region (Figure 4). A number of studies indicate that upon binding of the ligand to the extracellular globular domains of the $GABA_BR1$ subunit, the two lobes close like a Venus flytrap (O'Hara et al., 1993; Quiocho, 1990) (Bockaert and Pin, 1999; Galvez et al., 1999). Despite the likely presence of a putative Venus flytrap domain in the $GABA_BR2$ subunit, residues involved in GABA binding are lacking (Kniazeff et al., 2002). Heterodimerisation (see section 1.1.2.1), probably though an interaction of the coiled-coil C-terminal domains of the R1 and R2 subunits, masks an arginine-rich endoplasmic reticulum-retention signal at the C-terminus of the R1 subunit, which otherwise restricts surface expression (Margeta-Mitrovic et al., 2000). It was later shown (Schwarz et al., 2000) that the two subunits can dimerise even in the absence of the C-terminal domains and that further sites for dimerisation must therefore be located elsewhere. The seven transmembrane helices of $GABA_BR2$ are thought to be involved in receptor activation, following ligand binding to $GABA_BR1$, through a conformational change that activates intracellular G-protein signalling (Galvez et al., 2001; Robbins et al., 2001) (shown in pink and purple in Figure 4). The Gα subunit binds to cyclic AMP and inhibits adenylate cyclase, while the Gβ/γ subunits bind to Ca^{2+} and K^+ channels at pre- and postsynaptic sites.

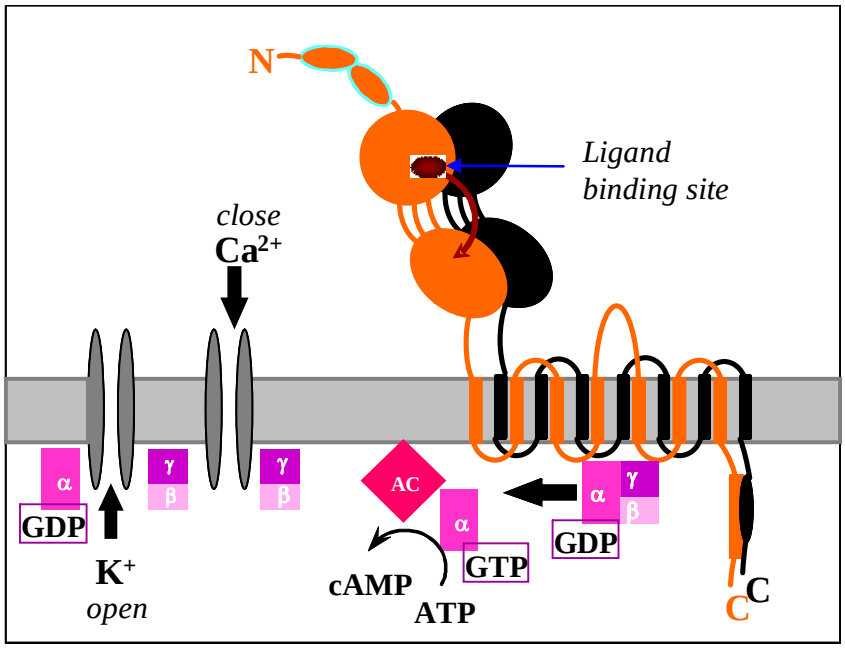

Figure 4 ***Schematic overview of the GABA$_B$ receptor subtypes and composition***
GABA$_B$ receptor subunit R1 is illustrated in orange and receptor subunit R2 in black. The ligand binding site lies within the two large lobes of the N-terminal extracellular domain of R1. Ligand binding to R1 results in a conformational change in the transmembrane domain of R2 which separates the α-subunit of the G-protein which binds to cyclic AMP and inhibits adenylate cyclase. The β- and γ-subunits of the G-protein regulate K^+ and Ca^{2+} channels.

1.2.2 Receptor isoforms

Native studies of GABA$_B$ receptors indicate pharmacologically and functionally distinct receptor subtypes (Dutar abd Nicoll 1988, Bonanno and Raiteri 1993). However, on a molecular level only two subtypes have been found and the pharmacological diversity observed in native studies has not been reproduced using recombinantly expressed receptors molecules (Bettler et al., 2004; Marshall et al., 1999). The limited molecular diversity originates primarily from the existence of two isoforms of the GABA$_B$R1 subunit (Figure 5), R1a and R1b (Kaupmann et al., 1997). The expression of the two isoforms is regulated by different promoters (Steiger et al., 2004).

The R1a and R1b isoforms are structurally identical with the exception of the 143 amino acid residues that form two CCP modules (or 'Sushi domains'), CCP1 and CCP2, present at the extracellular N terminus of R1a (Bettler et al., 1998; Hawrot et al., 1998). CREB has been shown to be involved in transcriptional regulation of isoform levels *in vivo* by binding to unique regions of the promoter (Steiger et al., 2004). In addition, there exists a human R1c splice variant that is the result of a 62-amino acid residue deletion of the second CCP module at the N terminus of $GABA_BR1$ (Martin et al., 2001). $GABA_BR1e$ is present in both humans and rat and is a truncated, soluble form of R1a lacking exon 11 encoding the transmembrane domain (Schwarz et al., 2000). The secreted isoform $GABA_BR1j$ has recently been reported, which is identical to $GABA_BR1a$ up to and including exon 4 (*i.e.* CCP1 and 2) but with a soluble C terminus lacking sequence homology to known proteins (Tiao et al., 2008). All $GABA_BR1$ isoforms are illustrated in Figure 5. Three splice variants of the $GABA_BR2$ subunit has been reported (Clark et al., 2000; Ng et al., 1999), however more recent analysis of the gene suggests these are cloning artefacts and in fact only one native form of R2 exists (Martin et al., 2001).

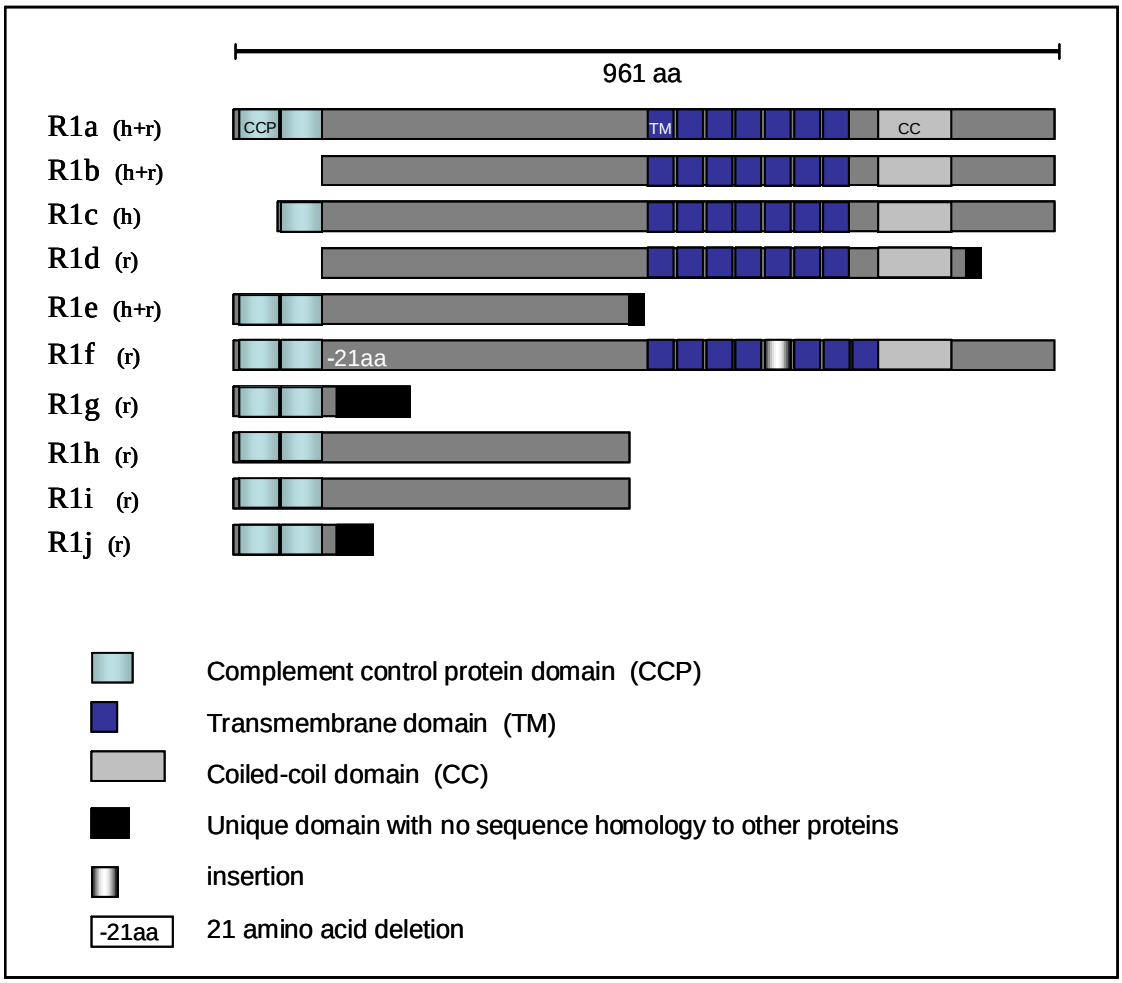

Figure 5 *$GABA_B$ R1 isoforms*
There are a large number of isoforms of the R1 subunit of the $GABA_B$ receptor, including four found in humans. R1a and R1b are the most abundant. CCP modules, transmembrane (TM) domains and coiled-coil (CC) domains are labelled. Scale is indicated at the top of the image. Isoform 1d, 1e, 1g and 1j have unique C- terminal tails (shown in black). R1f has a 21-amino acid deletion in the extracellular domain and an insertion in the transmembrane domain. Several of the truncated forms have insertions after exon 4, shifting the reading frame and thereby incorporating stop codons and truncations (Holter et al., 2005; Martin et al., 2001; Schwarz et al., 2000; Wei et al., 2001).

1.2.2.1 Complement control protein modules

Many proteins, particularly extracellular ones, are composed from arrays of domains or 'modules' characterised by the possession of distinct, consensus primary

sequences (Kirkitadze and Barlow 2001). The consensus sequence of each module-type normally defines a characteristic three-dimensional structure (Campbell and Downing, 1998). Databases of primary sequences reveal that some types of modules occur repeatedly in a range of different proteins, and in diverse combinations with other module-types. Thus, although the number of module-types is limited to hundreds, exon duplication and shuffling have created thousands of functionally different multiple-module proteins.

The CCP module is the predominant module-type in proteins involved in regulating complement activation, such as complement 4b-binding protein (C4BP) and factor H (DiScipio, 1992). CCP modules also occur widely in other types of proteins (see section 1.1.2.3), for example $GABA_BR1a$, the brain-specific seizure-related gene Sez-6 (Shimizu-Nishikawa et al., 1995) and Hikaru genki (hig), which has been suggested to have a neural-specific role in the development of CNS functions involved in locomotor activity (Hoshino et al., 1993). It has been shown that when CCP modules occur near the N terminus of cell-surface expressed proteins, they are often involved in ligand binding and interactions with other proteins (Hawrot et al., 1998; Hoshino et al., 1993).

A CCP module consists of approximately 60 amino acid residuess (Kristensen and Tack, 1986; Lehtinen et al., 2004). Many atomic-resolution structures of CCP modules have been solved (Grace et al., 2004; Uhrinova et al., 2003);(Blein et al., 2004). In all of these structures, five extended regions run parallel and antiparallel with the long axis of the prolate module causing N- and C-termini to lie at opposite ends. For some or all of their lengths these extended regions form β-strands that contribute to antiparallel

β-sheets, which wrap around a hydrophobic core. The four conserved cysteine residues form two disulfide bridges that stabilise the globular fold (Figure 6). These cysteines are disulfide-linked, Cys-I–Cys-III and Cys-II–Cys-IV (Barlow et al., 1991; Janatova et al., 1989; Blein et al., 2004).

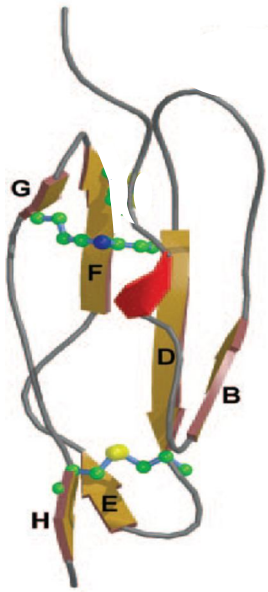

Figure 6 ***Structure of GABA$_B$R1a CCP2***
The CCP module structure has five extended regions that run parallel and antiparallel with the long axis module causing N- and C-termini to lie at opposite ends. β-strands contribute to antiparallel β-sheets, which wrap around a hydrophobic core. Four conserved cysteine residues form two disulfide bridges that stabilise the globular fold β-strands (β-strands indicated in brown and labeled B-H). The two disulphide bridges are shown in ball-and-stick representation. Structure from (Blein et al., 2004).

A recombinant version of the GABA$_B$R1a N-terminus (residues 17-159 in the GABA$_B$R1a rat sequence, numbering includes the protein signal sequence of GABA$_B$R1a (Hawrot et al., 1998)) was expressed in *Pichia pastoris*. Figure 7 shows the sequence of the two CCP modules, aligned by CLUSTALW (http://www.ebi.ac.uk/Tools/clustalw2/).

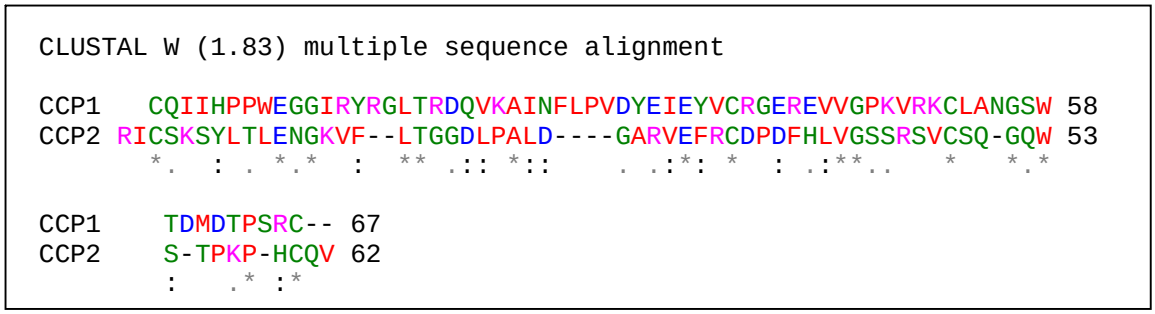

Figure 7 ***Sequence alignment of GABA$_B$R1a CCP1 and CCP2***
"*" illustrates an identical residue, "**:**" illustrates a conserved substitution and "**.**" illustrates a semi-conserved substitution.

The structures of CCP1 and CCP2 were extensively studied and shown to have strikingly different characteristics (Blein et al., 2004). Circular dichroism (CD) spectroscopy studies implied that the second CCP module (CCP2) remains stable at relative high temperatures and denaturing conditions. CCP1 on the other hand loses secondary structure under similarly harsh conditions. CCP2 is well structured with disulfide bridges and hydrophobic side chains protected at its core, while CCP1, despite possessing two disulphides, has a poorly structured hydrophobic core. An isotopically labelled version of GABA$_B$R1a CCP12 was used for determination of 3-D structure based on nuclear magnetic resonance (NMR) spectroscopy. The second of the two putative CCP modules present in this sequence was found to have a structure characteristic of other CCP modules. On the other hand, CCP1 appeared to be natively unfolded (Blein et al., 2004). Within the module-pair, CCP1 appears to be somewhat stabilised by the presence of CCP2 (Blein et al., 2004) compared to the isolated CCP1.

As mentioned above, in the instances where they occur toward the N-terminal end of a protein, CCP modules often participate in protein-protein interactions. It is therefore possible that the CCP domains of the GABA$_B$ receptor interact with auxiliary

proteins and this may affect the localisation of the R1a isoform, by influencing either its transport or retention or modulate its function. That the two CCP modules of the $GABA_B$ receptor have striking structural differences is therefore of potential interest. The open, disordered fold of CCP1 suggests the possibility that CCP1 participates in interactions with multiple protein-binding partners. This would explain some of the functional diversity observed in studies with native $GABA_B$ receptors.

1.2.3 Distribution and localisation

The $GABA_B$R1 and R2 subunits are widely expressed in the mammalian central nervous system. The expression pattern for the two subunits generally overlap, which is to be expected with the necessity for co-expression. Interestingly though, this is not always the case (Calver et al., 2000), which suggests the possibility of a different molecular nature of the receptor subunits in these tissues, as discussed in section 1.1.2.1. The highest expression levels of the receptor are found in the cerebellum and hippocampus but it is also present in the thalamus, cortex and brain stem (Clark et al., 2000; Mohler et al., 2001). Furthermore, $GABA_B$ receptors are found in a wide range of tissue including the peripheral nervous system and non-neural tissue such as smooth muscle, gut and pancreatic islets (Bowery, 1993; Ong and Kerr, 1990).

$GABA_B$ receptors are located both pre-and post-synaptically in the brain. Pre-synaptic receptors can be auto- or hetero-receptors that control the release of GABA, and other neurotransmitters, respectively, by inhibition of calcium ion channels. Post-synaptic receptors cause hyperpolarisation of the plasma membrane by gating inward

rectifying potassium (KIR) type channels (as discussed in the previous section). $GABA_BR1a$ is primarily located at pre-synaptic sites, while $GABA_BR1b$ is located at post-synaptic sites (Fritschy et al., 2004; Vigot et al., 2006).

There had been no solid experimental evidence supporting functional differences between isofoms until recently, when support for differential functions of the two isoforms, $GABA_BR1a$ and R1b, in the hippocampus was reported (Vigot et al., 2006). By knocking out one isoform at a time, the expression and function of each individual isoform could be studied *in vivo*. $GABA_BR1a$ appears to inhibit glutamate release at the connection between CA3 and CA1 regions of the hippocampus by forming heteroreceptors, while $GABA_BR1b$ mediates postsynaptic inhibition. $GABA_BR1a$ is selectively expressed in distal axons of CA3 neurons, indicating the putative involvement of CCP modules in retaining the heteroreceptor at this specific location (Vigot et al., 2006). In addition, separate physiological roles have been suggested for the $GABA_BR1a$ and R1b isoforms at layer 5 of pyramidal neurons in the neocortex. $GABA_BR1b$ appears to be involved in the blocking of Ca^{2+} currents in dendrites due to postsynaptic inhibition, whereas $GABA_BR1a$ is involved in presynaptic inhibition of GABA release (Perez-Garci et al., 2006). Interestingly, differences in expression levels of the $GABA_BR1$ isoforms during development and adult life in rat and human have been observed (Martin et al., 2001). $GABA_BR1a$ has been shown to be predominantly expressed during human and rat early development, with levels dropping rapidly after postnatal day five to moderate levels in adult brain. In contrast, $GABA_BR1b$ is undetectable at birth and expression levels increase after postnatal day five so that this is

the dominant isoform expressed in adult brain. $GABA_BR1c$ is expressed solely in foetal brain and at similar levels to $GABA_BR1a$ (Fritschy et al., 1999; Martin et al., 2001).

The fact that the isoforms that are more abundant during development, R1a and R1c, both contain CCP modules while the CCP-lacking isoform R1b is dominant in adult brain is intriguing. CCP modules have been found in other GPCRs (see section 1.2.2.1). The CCP module of neurocan was reported to interact with the L1 adhesion molecule of the immunoglobulin super family, which is linked to axonal outgrowth and neuronal cell migration, and ultimately to memory and learning (Oleszewski et al., 2000). This evidence suggesting a role of CCP modules in the developing brain forms the basis of an intriguing area of research. It has been reported that the CCP modules of $GABA_BR1a$ are involved in an interaction with the extracellular matrix protein fibulin (Ginham et al., 2002), which was further confirmed in our lab (Blein et al., 2004) but the functional relevance of this interaction, as well as others that have been mooted, is yet to be explored.

1.2.4 Pharmacological differences between $GABA_B$ receptor isoforms

A few studies have indicated distinct pharmacological properties for each of the two isoforms (Ng et al., 2001; Parker et al., 2004). Ng *et al* reported that gabapentin acts as an isoform-selective agonist of R1a; this would have provided the first tool capable of distinguishing the isoforms pharmaceutically. Subsequntly, it was suggested that gabapentin selectively activates postsynaptic R1a/R2 receptors but not presynaptic

receptors (Ng et al., 2001). Confusingly, another report claimed that gabapentin selectively activates presynaptic heteroreceptors (Parker et al., 2004). These contradictory findings have not been reproduced by others (Jensen et al., 2002; Lanneau et al., 2001; Shimizu et al., 2004), however. These claims and counter-claims meant further investigation.

Turning to the intracellular side, selective activation pathways mediated through a preference for G-protein isoforms has been reported for $GABA_BR1a$ and R1b. While R1a selectively signals via $G_{0\alpha A}$, R1b signals equally via $G_{0\alpha A}$ and $G_{i\alpha 2}$ (Leaney and Tinker, 2000). The same paper suggested that R1b (but not R1a) was able to activate KIRs directly, *i.e.* in absence of the R2 subunit that is normally needed for G protein signalling. This work therefore appears to show a distinct difference in signalling between the two isoforms.

1.2.5 Relevance to disease and possible therapies

The human gene for $GABA_BR1$ is located on chromosome 6p21.3, which is a genetic locus for a range of neurological disorders including schizophrenia, dyslexia and juvenile myoclonic epilepsy. On the other hand, the human gene for $GABA_BR2$ is located on chromosome 9q22.1, which is linked to hereditary sensory neurophathy type 1. The $GABA_B$ receptor has long been considered a promising drug target for disorders such as epilepsy, chronic pain, spasticity, drug addiction and cognitive impairment (Bowery, 2006; Marshall et al., 1999).

A number of selective, high- and low-affinity $GABA_B$ receptor antagonists have aided pharmacological and physiological studies of this receptor. The earliest known antagonists were the low-affinity binders saclofen, 2-hydroxy saclofen and phaclofen (Kerr et al., 1988; Kerr et al., 1987). Further development of high-affinity antagonists resulted in CGP35348 and the widely used CGP55845 followed by very high-affinity antagonists, including some radio-labelled ones, that were important in work leading to the initial expression cloning of the $GABA_B$ receptor (Davies et al., 1993; Kaupmann et al., 1997). Baclofen is the most commonly employed $GABA_B$ receptor agonist in humans. It is used for treatment of spasticity by decreasing spinal reflex transmission (Bowery, 1993) and has also been shown to decrease cravings for addictive substances like alcohol, cocaine and heroin. Despite the potential benefits of Baclofen, it is rapidly tolerated and can give numerous side-effects such as muscle relaxation, sedation and hyperthermia. The structures of agonist and antagonists are shown in Figure 8.

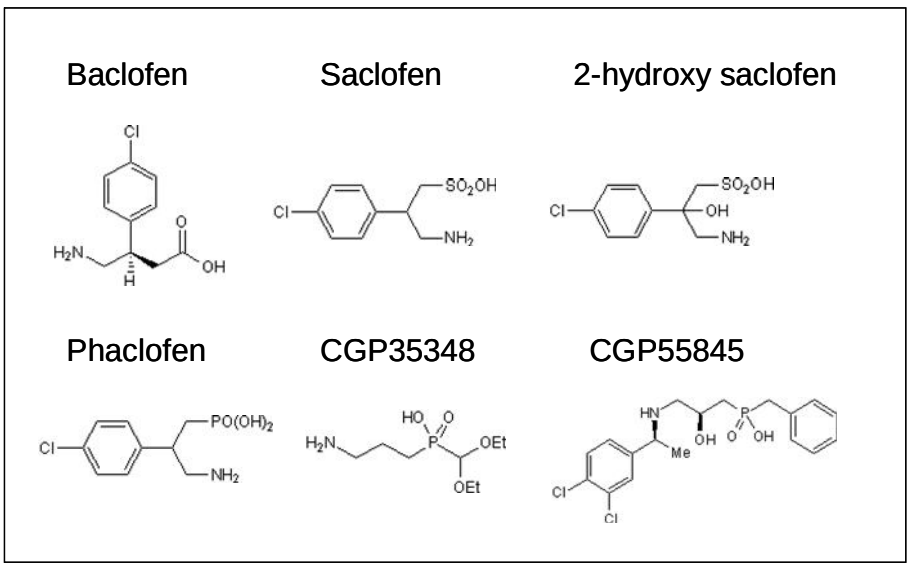

Figure 8 ***$GABA_B$ receptor agonist and antagonist structures***
Stuctures from Tocris Bioscience

An interesting alternative proposal for treatment is the use of allosteric modulators. These do not bind to the receptor at the ligand-binding site, but increase or decrease the inhibitory effect in the presence of an agonist (Bridges and Lindsley, 2008; Ross, 2007). One example of a target for drug design is the modulator Tenascin-R which upon binding to the $GABA_B$ receptor inhibits binding of GABA and thereby receptor-activated K^+ currents (Saghatelyan et al., 2003). Tenascin-R carries the HNK-1; a carbohydrate expressed by neuronal adhesion molecules and thought to be involved in induction of long term potentiation (LTP). When binding is disrupted by anti-HNK-1 antibody, receptor remains active (inhibitory function) and K^+ currents are restored (Saghatelyan et al., 2000; Saghatelyan et al., 2003). Furthermore, the positive modulator GS39783 has been reported to be efficient in treating anxiety without the undesired side effects of baclofen (Cryan et al., 2004).

1.3 The extracellular matrix

All cells in the human body are surrounded by a network of secreted macromolecules that make up the extracellular matrix (ECM). The ECM varies between different tissues, from a thick layer of matrix in epithelial tissue to thin sheets of extracellular protein in basement membrane, and plays an important role in complex communications between cells at various locations of the body. The basement membrane has a major impact on cell phenotypes as well as tissue compartmentalisation from development onwards. During development cells migrate by attaching to the basement membrane; it is furthermore involved in wound healing and nerve

regeneration. (Engvall, 1995; Timpl and Brown, 1996). The proteins of the ECM are continually produced to replace others that have been internalised during cell signalling or disturbed by cells migrating through the matrix. The major components of the basement membrane are laminin and collagen IV; both proteins form a large network by self-assembly. They also interact with each other and various other ECM proteins such as nidogen, fibulin and proteoglycans (Timpl and Brown, 1996). The apparent complexity of the basement membrane continues to expand (Erickson and Couchman, 2000), with the discovery of new protein members and isoforms such as endactin-2/nidogen-2 (Kimura et al., 1998; Kohfeldt et al., 1998) and argin (Nitkin et al., 1987). The structure of the ECM is tissue-specific consistent with its many functions, from barriers against tumour cells to substrates for cell attachment. The basement membrane is attached to cells by interactions with integrin receptors, primarily to laminin and collagen IV. The interactions between ECM components and cell surface receptors transmit signals across the cell membrane and thereby alter cell behaviour, as well as developmental fate. Intracellular signalling pathways connected with the ECM are highly conserved and a breakdown of the ECM can lead to uncontrolled cell growth and tissue death (Timpl and Brown, 1996).The ECM has been extensively studied in tissues other than the brain (Ekblom, 1995). The existence of ECM in the brain was earlier under debate but is now accepted and widely studied. A schematic overview of the extracellular matrix illustrates the complexity of the protein network (Figure 9). Many proteins are large, consisting of several chains and domains and are involved in specific interactions with neighbouring proteins as well as self-assembly.

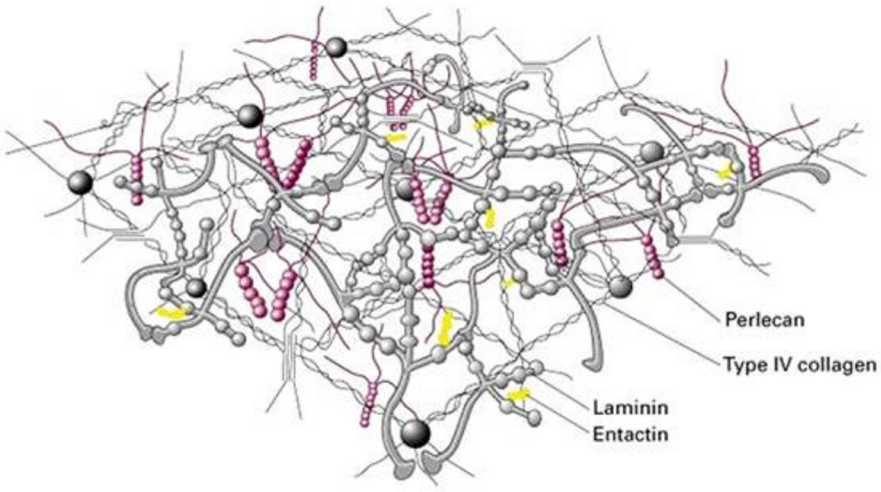

Figure 9 ***The complex network of the extracellular matrix***
The extracellular matrix is built up of a mixture of proteins. Laminin (grey crucifix) and collagen type IV (thin grey rods) are crosslinked together by entactin (yellow) and perlecan (pink). Picture adapted from (Lodish, 1995)

1.3.1 Laminins

1.3.1.1 Isoforms

The laminins are a major family of glycoproteins making up an important part of the ECM. Laminin-1, the first-described and most extensively studied member of this family, was isolated from mouse Engelbreht-Holm Swarm (EHS) tumour in 1979 (Timpl et al., 1979). The number of laminins identified in mammals has increased in recent years; to date, 15 isoforms have been recognised (Table 1), many with a unique expression pattern and distinct functions (Aumailley et al., 2005; Powell and Kleinman, 1997).

Table 1. *Overview of the 15 laminin isoforms*

Isoform	New nomenclature*	Chain composition
Laminin-1	111	α1β1γ1
Laminin-2	211	α2β1γ1
Laminin-3	121	α1β2γ1
Laminin-4	221	α2β2γ1
Laminin-5	332	α3β3γ2
Laminin-6	311	α3β1γ1
Laminin-7	321	α3β2γ1
Laminin-8	411	α4β1γ1
Laminin-9	421	α4β2γ1
Laminin-10	511	α5β1γ1
Laminin-11	521	α5β2γ1
Laminin-12	213	α2β1γ3
Laminin-13	522	α5β2γ2
Laminin-14	423	α4β2γ3
Laminin-15	523	α5β2γ3

*discussed further in section 1.3.1.2

Laminin consists of one α-chain, one β-chain and one γ-chain. There are five types of α-, three types of β- and three types of γ-chains, resulting in many possible combinations (Beck et al., 1990). Each chain is encoded by a different gene; α by the LAMA family, β by the LAMB family and γ by the LAMC family. Some laminin chains have been shown to be alternatively spliced; examples are the human α3 chain that is modified in the IIIa domain (see below) (Galliano et al., 1995; Ryan et al., 1994), γ2 that displays two variants with differences at the 3'-end (Airenne et al., 1996) and human β2 where alternative splicing occur at the 5'-untranslated region (UTR) of the mRNA transcript (Kallunki et al., 1992; Durkin et al., 1996). Other modifications include the proteolytic cleavage of polypeptide chains within already assembled laminins

(Colognato and Yurchenco, 2000); the cleaved fragment may remain bound to the main laminin protein.

1.3.1.2 Structure

The α-, β- and γ-chains of laminin form a large cruciform trimer with a molecular weight of approximately 800 kilodaltons (kDa). Coiled-coil regions, stabilised by inter-disulphide bonds, holds the three chains (as seen in Figure 10) (Engel, 1992; Maurer et al., 1995).

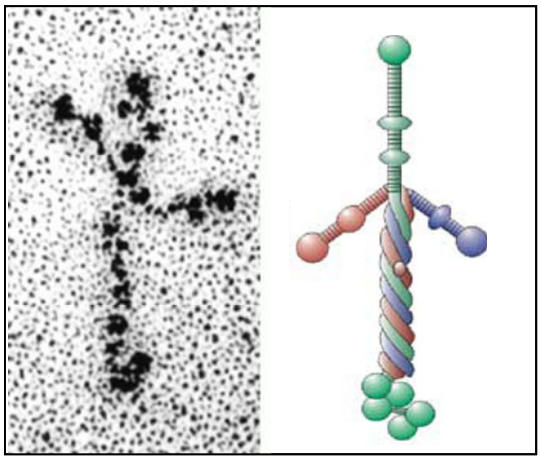

Figure 10 ***Electron microscopical visualisation and schematic structure of the Laminin heterotrimer***
The cruciform trimer of laminin consists of one α- (red), one β- (blue), and one γ (green) chain . Images (Aumailley et al., 2005; Engel, 1992). The C-terminus of the γ-chain contains five laminin globular (LG) domains, seen in green.

The laminin polypeptides consist of several types of structurally and sometimes functionally independent domains originally designated by the roman numerals I to IV (Figure 11) (Beck et al., 1990; Sasaki et al., 1988). These domains include epidermal

growth factor (EGF)-like repeats, coiled-coil domains (CC) and globular-like domains (LG) (Beck et al., 1990). A new nomenclature was proposed (Aumailley et al., 2005) to simplify the naming of laminin domains, where instead of βIV or γIV for example, the domains are named laminin N-terminal domain (LN), laminin epidermal growth factor domain (LE), laminin domain 4 α- and γ-chain (L4), laminin domain 4 β-chain (LF), laminin coiled coil domain (LCC) and laminin globular-like domain (LG) (Aumailley et al., 2005; Scheele et al., 2007). However, both nomenclatures are still being used at present (Figure 11).

A

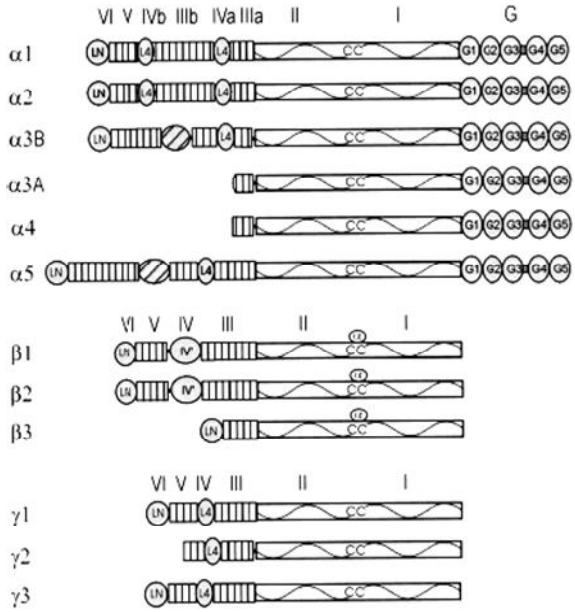

B

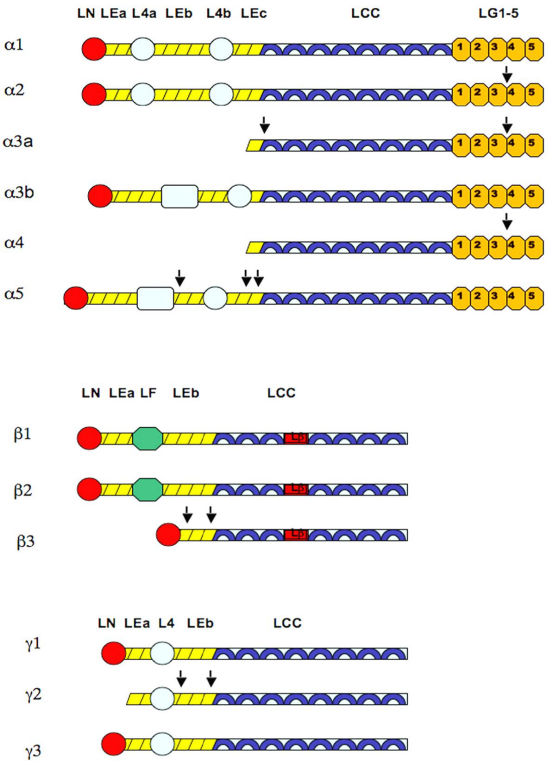

Figure 11 ***Schematic overview of domains making up laminin α-, β-, and γ-chains***
Figure A names laminin domains using the 'old' nomenclature (I,II,III,IV,V,VI), figure (Colognato and Yurchenco, 2000) while figure B names rodlike EGF-like tandems (LEa, LEb, LEc) and globular domains (LN, L4a, L4b, L4, LF) according to the new proposed nomenclature , figure (Tzu and Marinkovich, 2008).

The three-dimensional structure of the α2 LG4-5 domains (Hohenester et al., 1999; Tisi et al., 2000) has been determined. Furthermore, a protein corresponding to the α1 LG4-5 was recently crystallised (Harrison et al., 2007), as was LG4 of α3 (Kato-Takagaki et al., 2007); also known is the structure of the nidogen-binding γ1 EGFs (Stetefeld et al., 1996). Most recently determined is the crystal structure of α2 LG1-3 (Carafoli et al., 2009).

1.3.1.3 Expression and localisation

In non-neuronal tissue, laminins are primarily expressed in the basement membrane, where they assembly into a tightly structured network. In contrast, laminins expressed in the developing CNS form looser structures and are associated with neuronal cells, glia cells and axons (Colognato et al., 2005). In the peripheral nervous system (PNS), laminins are present in the basement membrane surrounding Schwann cells (Hagg et al., 1997; Miner, 2008). In higher vertebrates laminin is expressed in the CNS during development and to lesser extent in adult CNS (Colognato et al., 2005). It is continuously expressed in adult PNS (Engvall et al., 1990; Miner, 2008; Montell and Goodman, 1989). Laminin-10 (containing the chains α5, β1 and γ1) is a major isoform in mouse hippocampus (Indyk et al., 2003) and is crucial for brain development (Colognato and Yurchenco, 2000; Miner et al., 1998). Expression of laminin chains α1, α2, α4, α5, β1, β2, γ1 and γ3 is found in both developing and adult CNS in mammals. It is however not entirely clear which laminin isofoms are expressed where, as identical chains are shared between different laminin isofoms (Colognato et al., 2005).

Interestingly, the α1-containin laminin-1 is involved in the clustering of acetylcholine receptors in the brain (Siguyama 1997). However, the α5-containing laminin-10, which is the major laminin isoform in the hippocampus (Indyk et al., 2003), appears not to be involved.

1.3.1.4 Relevance of laminin to disease

Congenital muscular dysfunction, resulting from a mutation in LAMA2, associates with defects in the peripheral and central nervous system, such as epileptic seizures and reduced myelination, supporting the necessity for laminin in the mammalian nervous system (Mercuri et al., 1996; Sunada et al., 1995). Laminin, γ1 in particular, but also α1 and α5, have been implicated as important for kidney development (Scheele et al., 2007). They have been shown to be particularly important for the capillaries that filter waste from the blood to produce urine. Laminins are also linked to the growth of cancers; it is reported that the state of the basement membrane yields an indication of the severity of cancers, *e.g*. a disrupted basement membrane is an indication of more malignant tumours (Scheele et al., 2007). Mammary carcinomas, in contrast, have very low if any expression of laminin chains. The α1 chain is commonly absent in many basement membrane-containing carcinomas (Maatta et al., 2001).

1.3.2 The fibulin family

1.3.2.1 Structure

Fibulin proteins consist predominantly of a series of calcium-binding epidermal growth factor (EGF)-like modules, followed by a carboxy-terminal fibulin-type module, as illustrated in Figure 12 (Kobayashi et al., 2007; Timpl et al., 2003). The composition of each fibulin will be further discussed in the next section.

1.3.2.2 Isoforms

Fibulins are a family of seven extracellular matrix proteins, fibulin-1 to fibulin-7. Fibulin-1 and -2 are structurally similar and fall into the same subgroup. Fibulin-3, -4 and -5 are also subgrouped on the basis that they are much smaller in size. Alternative splicing of fibulin-1 results in four alternative proteins designed fibulin-1A-1D. Fibulin-2 forms a homodimer where two subunits, arranged in an anti-parallel manner, are linked by a disulphide bond (Timpl et al., 2003). Fibulin-3, -4 and -5 are structurally closely related, as seen in Figure 12. Fibulin-6, which is also referred to as hemicentin, contains 48 immunoglobulin domains (Argraves et al., 2003; Vogel and Hedgecock, 2001) .Fibulin-7 is the newest addition to the fibulin family and is reportedly the only of the fibulins that contains a CCP module (de Vega et al., 2007; de Vega et al., 2009).

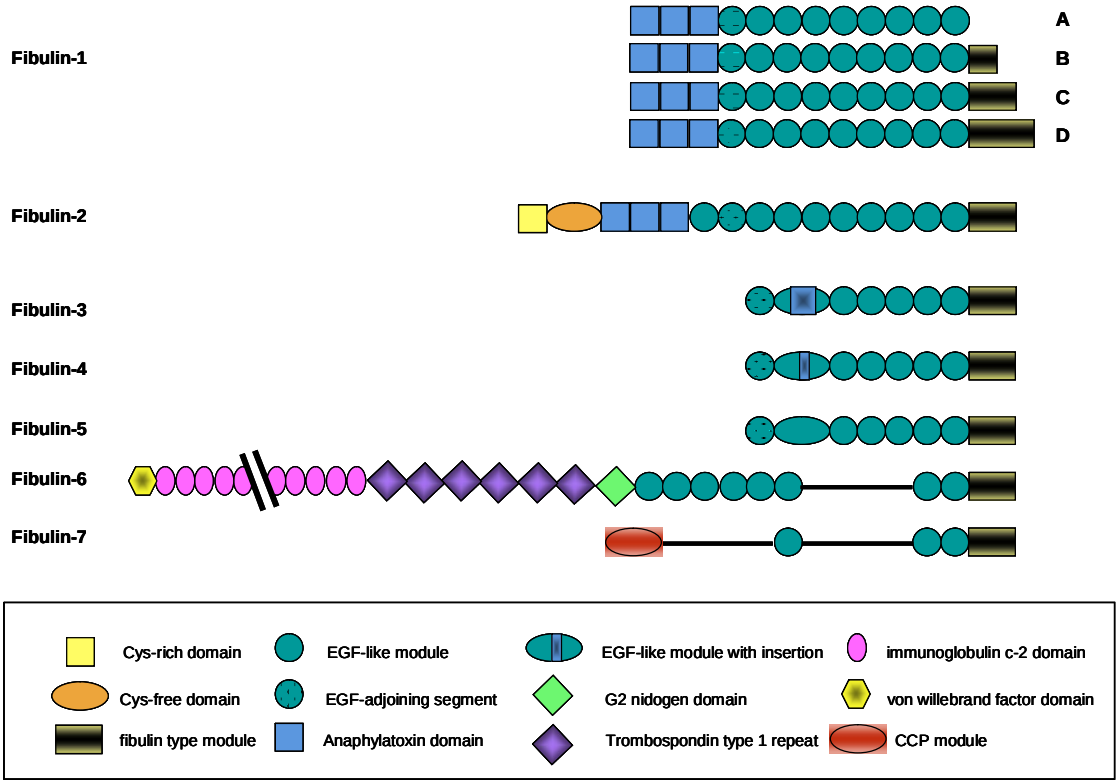

Figure 12 ***Illustration of the modular structure of the fibulin proteins***
The fibulin family consists of seven proteins. Each is built up predominantly from a string of EGF like domains that are linked to the C-terminal domain- further details in the figure; Fibulin-1 has four splice variants, 1A-1D, which varies at the C-terminus (Not all 48 immunoglobulin c-2 domains are illustrated due to space constaints). Figure based on (Argraves et al., 2003)

1.3.2.3 Distribution and localisation

Fibulins are expressed in the ECM. Fibulin-1, for example, is widely expressed within the matrix fibre and basement membranes of most organs. The other fibulin proteins have a more restricted distribution, with fibulin-2 expressed in fibroblasts and basement membranes and fibulin-3, -4 and -5 mainly expressed in larger blood vessels and some basement membranes (Timpl et al., 2003). Fibulin-6 is expressed in skin fibroblasts while fibulin-7 is expressed in teeth and hair follicles (de Vega et al., 2009).

Expression of fibulin-1 has an onset in early development and it is expressed at very high levels (10-50 µg/ml) in human serum. This is approximately 1000-fold higher concentration than other fibulins and ECM proteins. Fibulin-2 has a slightly later onset, but is still expressed at high levels during organ development. Interestingly, both fibulin-1 and -2 are expressed in the brain, suggesting a neuronal function for fibulins (Kobayashi et al., 2007; Timpl et al., 2003).

1.3.2.4 Relevance of fibulin to disease

Fibulins are known to regulate cell-growth, migration and morphology. Tumour suppressive and oncogenic roles have been reported for several members of the fibulin family. Fibulin-1D (Figure 12) is reported to be involved in breast cancers by suppressing the invasiveness of tumour cells (Argraves et al., 2003; Greene et al., 2003). Fibulin-1C is up-regulated in ovarian cancer. A number of ECM proteins like fibronectin and tenascin have also been found to be up-regulated in breast cancers (Loridon-Rosa et al., 1990; Mackie et al., 1987). Down-regulation of fibulin-2 has been reported in breast cancer tissue, which may aid cell migration and invasion in breast cancer (Yi et al 2007). Fibulin-4 is positive regulator and fibulin-5 is a dual positive and negative regulator of cell-growth (Gallagher et al., 2005). Fibulin-4 has further been reported to be up-regulated in colon cancer (Gallagher et al., 2001). Fibulin-3 and fibulin-6 are not known to have a role in cancer to date (Gallagher et al., 2005) Yi 2007).

Fibulins have furthermore been linked to inherited eye disorders. A mutation in the fibulin-3 gene has been linked to Malattia Leventinese (ML) macular dystrophy (Argraves

et al., 2003; Stone et al., 1999), whereas mutations in the fibulin-6 gene may predispose for age-related macular degeneration (AMD) in a small subset of the population, however it has little effect in the overall population (Fisher et al., 2007; Schultz et al., 2003).

1.4 Aims of study

The $GABA_B$ receptor isoform R1a has been shown to be expressed selectively within heteroreceptors at presynaptic sites as discussed previously. This would support the idea that the CCP modules present in R1a may be involved in localising these receptors to presynaptic sites. This may occur through interaction with extracellular proteins in an analogous fashion to the clustering of acetylcholine receptors via interactions with agrin and laminin (Sugiyama et al., 1997) (section 1.3.1.3). Interestingly, $GABA_B$R1a is the predominant isoform during CNS development. Similarly laminin and fibulin are also primarily expressed in the CNS during development. These observations are consistent with a functional role for these interactions in regulation of the developing brain. It has been shown that the CCP modules of R1a bind to the extracellular matrix protein fibulin-2 (Blein et al., 2004). It was speculated that the CCP modules are also involved in binding to other extracellular proteins. Thus the ECM interaction mediated by these modules requires further investigation.

These intriguing but tentative observations of interactions between the $GABA_B$ receptor and the ECM provided a starting point for the current project. In order to

establish a firmer basis for further study of this phenomenon it was necessary to validate or otherwise the preliminary work. Thus the first aim was to re-examine the interaction between the $GABA_BR1a$CCP modules and fibulin-2, with an emphasis on establishing which modules/domains are involved. It was also of interest to investigate a potential interaction with fibulin-3 that shares with fibulin-2 a unique C-terminal fibulin-like module. Given the predominance of laminins in the ECM and the large number of proteins reported to interact with the laminin family, the protein-protein interaction studies devised for fibulins could also be applied to laminins and laminin domains – this constitutes the next aim. All of these studies, which utilise yeast two-hybrid and surface plasmon resonance approaches, will be described in Chapters 2 and 3.

Having fleshed out the interaction data, the next aim was to investigate their functional implications. An important objective, given controversies in this area, was to investigate any pharmacological differences between $GABA_BR1a$ and $GABA_BR1b$. This was accomplished using oocyte-expressed isoforms and a two-electrode voltage clamp technique. The intention was then to employ a similar approach in order to facilitate an investigation of whether the pharmacological responses (*e.g.* to the agonist, baclofen) of the isoforms $GABA_BR1a$ and $GABA_BR1b$ is influenced by the presence of extracellular proteins (*e.g.* laminin). This work is described in Chapter 4.

CHAPTER 2

Yeast Two-hybrid binding study

2 Chapter 2 Yeast two-hybrid binding study

2.1 Aims

The first aim was to establish the yeast two-hybrid (Y2H) system as a means by which to further investigate protein-protein interactions mediated by the CCP modules of $GABA_BR1a$. The second aim was to validate or otherwise the previously proposed interaction between the $GABA_BR1a$CCP1 and the C-terminal module of the extracellular protein fibulin-2, and to investigate a potential interaction with the equivalent module of fibulin-3. The third aim was to characterise the putative interaction between the CCP modules of $GABA_BR1a$ and the extracellular matrix protein laminin, with an emphasis on establishing which laminin domains are involved.

2.2 Context

As outlined in the previous chapter, controversy persists as to whether pharmacological differences between the $GABA_B$ receptor isofoms are detectable when working *in vitro* or in *X. laevis* oocytes. But the situation must in any case be more sophisticated within the mammalian central nervous system wherein receptors operate in the presence of other, potentially interacting, proteins that are absent from experimentally more tractable model systems. To reiterate, the difference between isoforms $GABA_BR1a$ and R1b lies in the presence of two, tandemly arranged, CCP

modules on the N-terminal ectodomain of $GABA_BR1a$. There is a considerable amount of literature indicating that CCP modules (in general) participate in protein:protein interactions indicating that the CCP modules of $GABA_BR1a$ might also have such a role. To pursue this line of enquiry, it is necessary to identify and characterise the putative binding partners for these modules. In the current work, which builds on previous published and unpublished observations, the CCP modules of $GABA_BR1a$ were therefore studied to characterize their ability to bind ECM proteins. Fibulin domains were selected for study on the basis of previous report of interaction between $GABA_BR1a$ modules and fibulin 2 (Ginham 2002). The laminin globular (LG) domains were selected for study in this project because laminin is one of the most abundant ECM protein; moreover there is precedent for CCP module-LG domain interactions in the literature – specifically, the LG domains of protein S interact with CCP modules of C4b binding protein (C4BP) (Fernandez and Griffin, 1994; Hardig and Dahlback, 1996; Hardig et al., 1993; Hillarp and Dahlback, 1990)

2.3 Materials and Methods

2.3.1 Yeast two-hybrid background and theory

Identification of a protein's interaction partners affords valuable insight into its biological roles and mechanisms of action. With this in mind, Fields and Song (1989) invented the yeast two-hybrid (Y2H) system as a means of detecting protein-protein

interactions (Fields and Song, 1989). The system has since been modified to additionally detect protein-RNA and protein-ligand interactions (Coates and Hall, 2003). The Y2H system has been extensively used to study intracellular protein interactions including those involving the $GABA_B$ receptor (Durfee et al., 1993; White et al., 2002), but has also been applied successfully to the detection of extracellular protein-protein interactions (Overall et al., 2002; Oxford et al., 2004; Veroni et al., 2007). The Y2H system exploits a transcription factor - generally Gal4 or LexA. A schematic diagram summarizing the Gal4-based Y2H system is presented in Figure 13. The system relies on the utilization of two components: the Gal4 DNA-binding domain fused to protein 'bait' and the Gal4 transcription activation domain fused with protein 'prey'. When both fusion proteins are co-expressed, and provided the 'bait' and the 'prey' interact, a functional transcription factor is reconstituted from the resulting juxtaposition of the activation and DNA-binding domains. This activates transcription of reporter genes, typically *His3, Ade2, lacZ and Mel1*. The first two of these are yeast biosynthetic markers and their inclusion ensures selection can be carried out for organisms able to grow on media lacking histidine and adenine. The latter two reporter genes enable identification of 'positive' clones by a colourimetric assay of galactosidase activity.

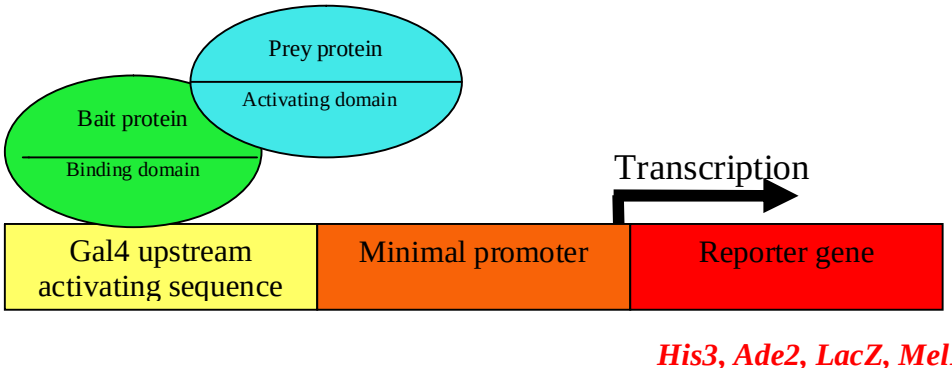

Figure 13 ***The principle of the Gal4 Y2H***
The bait protein is expressed as a fusion with the DNA-binding domain of the Gal4 transcription factor, the prey protein is expressed as a fusion with the Gal4 transcription-activating domain. Upon interaction of the bait and prey, mediated by their fusion partners, transcription is initiated leading to expression of reporter genes used to detect the interaction.

The Y2H system was originally designed to confirm binding between two known proteins that had already been suggested to interact on the basis of evidence from other methods. The system has additionally been employed to delineate the specific domains involved in such an interaction (Legrain and Selig, 2000; Stokes et al., 2007). Identifications of novel protein-binding partners using the Y2H system have been achieved by screening a cDNA library (Legrain and Selig, 2000). The 'Matchmaker Gal4 Two-Hybrid System 3' (Clonetech) was chosen for the current work on the grounds that this system enables detection of relatively weak or brief interactions between proteins – it has a detection limit in the region of K_D ~70 µM (Yang et al., 1995). The assay is carried out in a eukaryotic system *in vivo*, which increases the chance of correct conformation and folding of proteins, thus optimizing sensitivity and maximising the possibility of detecting an interaction. In the current study, this system was applied to investigate the interaction between $GABA_BR1a$CCP1 and C-terminal fragments of the ECM proteins fibulin-2, fibulin-3 and laminin α5.

2.3.2 Materials

2.3.2.1 Stock solutions and media

The following solutions were prepared in double-deionised water:

50% (w/v) polyethylene glycol (PEG) 3350

10 x tris/ethylenediaminetetraacetic acid (TE) buffer (0.1 M Tris-HCl, 10 mM EDTA, pH 7.5, autoclaved)

10 x LiAc (1 M lithium acetate, adjusted to pH 7.5 with dilute acetic acid, autoclaved)

Yeast extract/peptone/dextrose/adenine (YPDA) medium (to 1 L of *yeast* extract/peptone/dextrose (YPD) medium (Clontech), 15 ml of filter-sterilized 0.2 % (w/v) adenine hemisulfate was added, producing a final concentration of 0.003 % (w/v))

Polyethylene glycol (PEG)/LiAc solution (8 ml of 50% PEG (w/v), 1 ml of 10 x TE, 1 ml of 10 x LiAc)

10 x BU salts (70 g $Na_2HPO_4H_2$, and 30 g NaH_2PO_4 were dissolved in one litre of water, adjusted to pH 7, and autoclaved)

Z-buffer/x-gal solution (To 15 ml Z-buffer (60 mM Na_2HPO_4, 40 mM NaH_2PO_4, 10 mM KCl, 0.1 mM $MgSO_4$, pH 7.0) was added 60 µL of β-mercaptoethanol, 300 µl of a 20 mg/ml β X-gal stock solution (5-bromo-4-chloro-3-indolyl-β-D-galactopyranosode dissolved in N,N-dimethylformamide) which gives a final concentration of ~0.4 mg/ml).

2.3.2.2 Synthetic dropout (SD) base media plates

Agar plates were made up from the following constituents: yeast nitrogen base without amino acids (6.7 g); 20 g agar; 850 ml H_2O; and 100 ml 10x 'drop-out' solution (see below). Plates were autoclaved, allowed to cool to 55°C, then dextrose to 2% (w/v) and adenine to 0.2% (w/v) were added

Drop-out solutions: Three - 'low' 'medium' or 'high' - drop-out solutions contained a mixture of amino acids and nucleosides (adenine hemisulphate salt, L-arginine HCL, L-histidine HCL monohydrate, L-isoleucine, L-leucine, L-lysine HCL, L-methionine, L-phenylalanine, L-threonine, L-tryphtophan, L-tyrosine, L-uracil, L-valine, their concentrations are proprietary to Clontech). These were added to the Minimal SD Bases to make a defined medium lacking the specified nutrients as shown below:

"Low": minus leucine and tryptophan.

"Medium": minus leucine, tryptophan and histidine

"High": minus leucine, tryptophan, histidine and adenine

SD/Gal/ /Drop-out plates: Minimal SD base media plates were prepared as above, except the volume of water was reduced to 725 ml. Plates were autoclaved, and the following were added once the temperature had cooled to 55°C: 2% w/v dextrose; 0.2% w/v adenine, 1x BU salts see above), pH 7, 20 mg/l x-gal (see z-buffer/x-gal solution above)

2.3.2.3 Plasmid DNA preparation

Note: Buffers P1, P2, N3 and PE were all supplied as part of the Qiagen kit and their formulations are proprietary.

Re-suspension buffer: buffer P1, with addition of 140 µl of the Qiagen-provided RNase A solution

Lysis buffer: buffer P2

Neutralization buffer: buffer N3

Wash buffer: buffer PE, with addition of 100% ethanol (according to manufacturer's protocol)

2.3.2.4 Protein expression and purification

The following soulutions were pepared:

Buffered minimal glycerol medium (BMG): 100 mM potassium phosphate (pH 6); 1.34% (w/v) yeast nitrogen base (YNB; with $(NH_4)_2SO_4$ and without amino acids)**,** 1% (v/v) glycerol, 0.00004% (w/v) biotin)

Buffered minimal methanol medium (BMM): 100 mM potassium phosphate (pH 6); 1.34% (w/v) YNB (with $(NH_4)_2SO_4$ and without amino acids)**,** 0.5% (v/v) methanol, 0.00004% (w/v) biotin

For digest with Endo H_f: 5 ml of protein-containing supernatant (~0.25-0.3 mg/ml), 7.5 µl of Endo H_f (7500 U), 5 µl of protease-inhibitor cocktail (Sigma), 10 µl of 0.5M EDTA; Incubate for approximately 6 hours at 37 °C

ConA Buffers:

Binding buffer: 20 mM Tris-HCl pH 7.4 (16.8 ml 1 M Tris-HCl + 3.2 ml 1 M Tris Base) + 0.5 M NaCl

Elution buffer: 20 mM Tris-HCl pH 7.4 + 0.5 M NaCl + 0.5 M Methyl α-D-glucopyranoside

Cation-exchange chromatography buffers:

Binding buffer for CCP1 and CCP1-2: 12.5 mM NaAc pH 5.3

Binding buffer for CCP2: 50 mM NaAc pH 4.6

Elution buffer for CCP1 and CCP1-2: 12.5 mM NaAc pH 5.3 + 1 M NaCl

Elution buffer for CCP2: 50 mM NaAc pH 4.6 + 1 M NaCl

2.3.3 Methods

In the present study we set out to investigate the potential interactions of $GABA_BR1a$ with fragments of ECM proteins using the Y2H system. A previously published study (Blein et al., 2004) used a recombinantly expressed fibulin-2 C-terminal fragment to pull down $GABA_BR1a$ from solubilized rat synaptic plasma membranes, supporting an unpublished earlier observation (Dr. Julia White, GlaxoSmithKline,

personal communication). Thus the present study aimed to provide independent evidence for this putative interaction between $GABA_BR1$-CCP12 and fibulin using the Y2H system. Furthermore, it was hypothesized that the abundant ECM protein laminin might be an additional potential binding partner for $GABA_BR1a$ (as discussed in section 1.4) providing another target for the current Y2H-based investigation.

2.3.3.1 Generation of constructs for Y2H

For the bait, the cDNA for rat $GABA_BRCCP1$ (residues 17-98) was incorporated into the vector pGBKT7 DNA-BD (Clontech) by digesting a pET15b plasmid (Novagen) containing $GABA_BR1aCCP1$ (previously cloned by Dr Blein, Barlow group) and inserting the $GABA_BR1aCCP1$ fragment into a previously digested pGBKT7 DNA-BD vector. For the prey, the C-terminal fragment of fibulin-2 (FTM2) (residues 1068-1184) and the C-terminal fragment of fibulin-3 (FTM3) (residues 377-493), were inserted separately into the vector pGADT7 AD (Clontech) by digesting the pET41 plasmids (Novagen) containing FTM2 or FTM3 (previously cloned by Dr Blein), respectively, and inserting the fibulin fragments into separate, previously digested, pGADT7 vectors. The prey construct for laminin α5 laminin globular domains 1-5 (LAMA5 LG1-5) (residues 2733-3695) was created by amplifying the LAMA5 LG 1-5 from a cDNA library and blunt-end ligating the fragment into a pCR4blunt TOPO vector (Invitrogen). The TOPO vector was thereafter digested and the laminin fragment was inserted into a previously digested pGADT7 vector. Plasmid maps of the vectors pGBKT7 and pGADT7 used are presented in Figure 14.

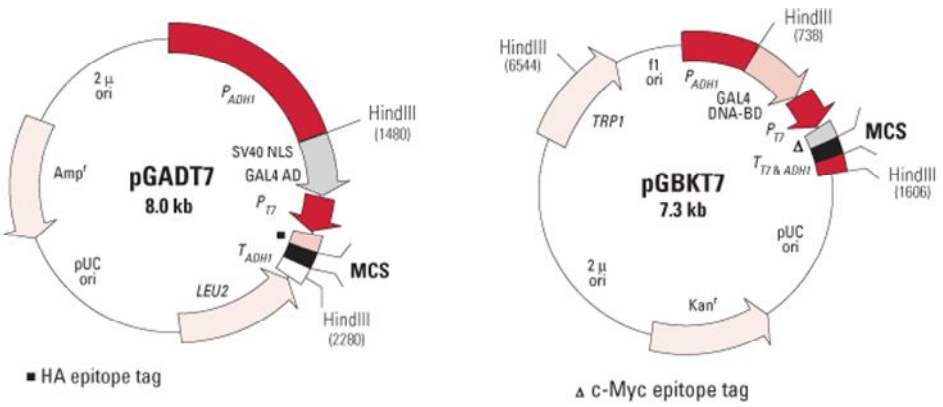

Figure 14 ***Plasmid maps of the two vectors pGBKT7 and pGADT7 used for Y2H studies***
A bait gene is expressed in pGBKT7 as a fusion to a Gal4 DNA-binding domain. The prey is expressed in pGADT7 as a fusion with the Gal4 transcriptional activating domain.

2.3.3.1.1 Primer design

The sequences of the genes under investigation were retrieved using www.ensemble.org. Primer sequences were designed, taking into account predicted secondary structure using Sigma-Genosys primer design (http://orders.sigma-genosys.eu.com). Finally the primer sequences were analysed using the Basic Local Alignment Search Tool (BLAST) to check for specificity to the genes of interest. Primers were synthesized commercially by Sigma-Genosys and re-suspended in ultrapure water for use at a concentration of 10 µM (for primer sequences see Appendix A.I).

2.3.3.1.2 Polymerase chain reaction

Conditions for the PCR were optimized by varying annealing temperatures from 50°C to 68°C. The following conditions, resulting in a single strong band of the correct size, were chosen for amplification of the genes;

An aliquot of 1 µl 10 mM dNTP (containing the four deoxyribonucleotides: dATP, dCTP, dGTP and dTTP) was mixed with 1 µl of 1:100 diluted plasmid DNA (approximately 200 ng), 1 µl forward-primer (10 µM), 1 µl reverse-primer (10 µM), 0.5 µl (2.5 U) Herculase hot-start polymerase, 5 µl Herculase 10x reaction buffer (Stratagene, Ca, USA) and 40.5 µl ultrapure water.

The PCR was carried out according to the following scheme:

95 ºC	2 min	
95 ºC	30 seconds	30 cycles
65 ºC*	30 seconds	
72 ºC	1 min	
72 ºC	10 min	
4 ºC	hold	

*or varied according to optimization

For the PCR, used to amplify the gene from the cDNA library, the following solutions were employed:

An aliquot of 1 µl 10 mM dNTP (containing the four deoxyribonucleotides: dATP, dCTP, dGTP and dTTP) was mixed with 1 µl (1 ng) Quick-clone cDNA universal human library (Clontech, UK), 1 µl forward-primer (10 µM), 1 µl reverse-primer (10 µM), 0.5 µl (2.5 U) Herculase hot-start polymerase, 5 µl Herculase 10x reaction buffer (Stratagene), 1.5 µl DMSO and 39 µl ultrapure water.

The PCR was carried out according to the following scheme:

95 ºC	2 min		
95 ºC	30 seconds	10 cycles	*decrease 0.5 ºC per cycle until 55 ºC
60 ºC*	30 seconds		
72 ºC	3 min		
95 ºC	30 seconds	25 cycles	
55 ºC	30 seconds		
72 ºC	3 min		
72 ºC	10 min		
4 ºC	hold		

2.3.3.1.3 Restriction digests

The pGBKT7 and pGADT7 cloning vectors were digested with the restriction enzymes *Nde*I/*BamH1* and *Nde*I/*Xho*I respectively. The pET15b plasmid already containing $GABA_BR1a$-CCP1 was digested with the restriction enzymes *Nde*I/*BamH1*, and the pET41 plasmids already containing FTM2 or FTM3 were digested with the restriction enzymes *Nde*I/*Xho*I. The pCR4blunt TOPO vector containing the amplified LAMA5 LG1-5 was digested with *EcoR1*, The pGADT7 vector was similarly digested with *EcoR1*.

For the digest reactions the following procedure was adopted:

Sample of 1 µg of DNA (plasmid DNA) were added to 1.5-ml Eppendorf tubes containing restriction-digest mix, which was made up of the following: 1 µl (20 U) *Nde1* and 1 µl (20 U) *BamH1*, 2 µl *BamH1*-buffer, 2 µl 10 x bovine serum albumin (BSA) and

11 µl ultrapure water (CCP1 construct) or 1 µl (20 U) *Nde1* and 1 µl (20 U) *Xho1*, 2 µl 10 x BSA, 2 µl buffer 4, and 11 µl ultrapure water (FTM2 and FTM3 constructs)/ 1 µl (20 U) *EcoR1*, 2 µl *EcoR1*-buffer, and 14 µl ultrapure water (LAMA5 LG1-5 construct) (all New England Biolabs). The DNA-digest mixtures were incubated at 37°C for 60 minutes. The digested DNA products were analysed by SDS-PAGE and gel-purified using a kit from Qiagen.

2.3.3.1.4 Ligation

For ligation reactions the following procedure was used:

An aliquot containing approximately 10 ng of PCR-product DNA was added to a ligation reaction volume including 1 µl (2000 U) 'Quick T4 DNA ligase', 10 µl 2x Quick ligation reaction buffer (132 mM Tris-HCl, 20 mM $MgCl_2$, 2 mM dithiothreitol, 2 mM ATP, 15% polyethylene glycol (PEG 6000), pH 7.6) (all from New England Biolabs), 50 ng restriction-digested and gel-purified vector. The reaction was incubated at room temperature for 10 minutes together with a negative control reaction (containing water instead of DNA insert).

2.3.3.1.5 Transformation

For transformations *E. coli* Top10 competent cells (Invitrogen CA, USA) were used. The following procedure was applied:

Top10 competent cells were transformed with products of ligation by heat shock. An aliquot of 50 µl of Top10 cells were removed from a -80 ℃ freezer and thawed on ice before a 5 µl aliquot of ligation mix was added and gently mixed. The mixture was left on ice for 30 minutes before the heat-shock step. The cell-ligation mix was incubated in a water bath at 42°C for 45 seconds and then placed on ice for two minutes. The cell mixture was resuspended in 1.0 ml of super optimal broth with catabolite repression (SOC) medium (Invitrogen) and incubated at 37°C with shaking at 200 rpm for 60 minutes. Subsequently, 50-200 µl of the mix was plated on Luria-Bertani (LB) agar plates containing 50 µg/ml ampicillin and incubated at 37°C overnight.

2.3.3.2 Yeast two-hybrid assay

2.3.3.2.1 Preparation of plasmid DNA

Colonies were picked from the selective plates and inoculated into 5.0 ml of LB medium containing 50 µg/ml ampicillin and incubated at 37°C with shaking overnight. Cells were pelleted by centrifugation at 13000 rpm for 60 seconds in a bench-top centrifuge (Eppendorf, Hamburg, Germany). Recombinant plasmids were purified from cell pellets by alkaline lysis using the Qiaprep miniprep kit (Qiagen, UK). Following re-suspension of the cell pellet in buffer P1, cells were lysed by addition of buffer P2 for up to five minutes and then neutralized by buffer N3 and gentle mixing. The suspension was centrifuged for 10 minutes in the bench-top centrifuge to pellet the precipitate and the supernatant was transferred to a Qiaprep silica-gel membrane column. The column

was centrifuged at 13000 rpm for 60 seconds in the bench-top centrifuge and the flow-through was discarded. The DNA-containing membrane was washed with buffer PE, the flow-through discarded and the centrifugation step was repeated. Finally, the membrane column was transferred to a clean Eppendorf microfuge tube and the purified plasmid DNA was eluted with 50 µl double-distilled water by centrifugation at 13000 rpm for 60 seconds. Plasmid DNA was analysed by analytical restriction-enzyme digests and PCR to confirm correct insertion of the gene, followed by DNA sequencing to confirm a correct reading frame.

2.3.3.2.2 Yeast transformation

Preparation of competent cells was undertaken using the following procedure:

A 1-ml aliquot of YPDA media was inoculated with a fresh colony of *Saccharomyses cerevisiae* strain Y190 (one-three weeks old) and thoroughly resuspended by vortexing. The inoculated media were transferred to a 1-liter flask containing 50 ml of YPDA media. The culture was incubated at 30 ºC overnight until $OD_{600} > 1.5$, whereupon 30-40 ml of the culture was transferred to a 2-liter flask containing 300 ml YPDA media and diluted in order to achieve an OD_{600} of 0.2-0.3. The culture was further incubated at 30 ºC for 2-3 hours until OD_{600} reached 0.4-0.6 and cells where then pelleted at 1000 x g for five minutes at room temperature. The supernatant was discarded and the cell pellet was re-suspended in a total volume of 25-50 ml sterile H_2O by vortexing, then centrifuged

again. The cell pellet was finally re-suspended in a volume of 1.5 ml freshly prepared 1 x TE/LiAc buffer.

The following protocol was used for transforming yeast cells:

1. Prepare 10 ml of PEG/LiAc buffer
2. Mix solutions containing 0.1 µg of pGBKT7-BD/Bait, 0.1 µg of pGADT7-AD/prey and 0.1 mg of herring-testes carrier DNA in 1.5-ml Eppendorf tubes
3. Add 0.1 ml of yeast competent cells to each tube. Mix by vortexing
4. Add 0.6 ml of sterile PEG/LiAc solution to each tube, vortex at high speed
5. Incubate at 30 º C for 30 minutes with shaking
6. Heat shock for 15 minutes in a 42º C water bath
7. Chill on ice for 1-2 minutes
8. Spin for one minutes at 7000 rpm in table-top centrifuge (Eppendorf)
9. Remove supernatant
10. Re-suspend in 0.5 ml of H_2O
11. Plate 100 µl (50-150 µl) of cells on selective media

2.3.3.2.3 Colony-lift filter assay

Colonies were screened using a colony-lift filter assay. Colonies were lifted from plates onto Hybond-C nitrocellulose membranes (Amersham Biosciences, Uppsala, Sweden). Colonies containing the interacting proteins should produce galactosidase (*Mel1* or *LacZ* selection) which produces a blue colour in the presence of X-gal. The galactosidase assay was carried out according to the Clontech Matchmakers protocol with some alterations (0.4 mg/ml β X-gal instead of 0.32 mg/ml was used, and the filter was submerged in liquid nitrogen *twice* and allowed to thaw in between). The membranes

were incubated for up to eight-ten hours. Positive and negative controls were performed in parallel.

The following protocol was used for colony-lift filter assay:

1. Pre-soak Whatman filters in a petri dish containing 2.5-3 ml of z-buffer/X-gal solution
2. Using forceps, place a Hybond-C nitrocellulose membrane over the surface of a plate of colonies to be assayed. Gently rub the filter with the forceps to help colonies cling to the filter
3. Mark filter and plate with holes to identify orientation of filter with respect to agar
4. Carefully lift filter off agar plate with forceps and transfer to pool of liquid nitrogen for 10 seconds
5. Remove filter and let thaw. Repeat procedure
6. Place filter, colony side up, on pre-soaked Whatman filter
7. Incubate at 30 ºC until blue (positive) colonies appear

2.3.3.2.4 Average intensity assay

A representative selection of colonies was picked from a plate (five-ten colonies) and the mixed pool of colonies was streaked onto a Whatman filter and incubated for two days at 30 °C. The same procedure was carried out for the negative and positive controls. A galactosidase assay was performed using the pool of colonies (an identical procedure as for colony-lift assay, except that the Whatman filter bearing the pool of colonies was transferred to liquid nitrogen and then placed on Whatman filter pre-soaked in z-buffer/X-gal solution), to get an average intensity of colour arising from the

putative interaction in the overall population. This made it easier to compare the intensities of colour arising from the interactions between $GABA_BR1a$-CCP1 and FTM2, $GABA_BR1a$-CCP1 and FTM3, and $GABA_BR1a$-CCP1 and LAMA5 LG1-5 with the positive and negative controls.

For average intensity assay the following protocol was observed:

1) Pick a representative selection of colonies (five-ten colonies) from the same plate and streak the mix onto a Whatman filter in a circular shape. Place the Whatman filter on a selective media agar plate and incubate for two days at 30 °C
2) Pre-soak unused Whatman filters in a petri dish containing 2.5-3 ml of z-buffer/x-gal solution
3) Transfer the colony bearing Whatman filter with forceps to pool of liquid nitrogen for 10 seconds
4) Remove filter and let thaw. Repeat procedure if necessary
5) Place filter, colony side up, on pre-soaked Whatman filter
6) Incubate at 30 ºC until any blue colonies appear

2.3.3.3 Immuno-dotblot assaying

2.3.3.3.1 Generation of protein for immuno-dotblot assay

Rat $GABA_BR1a$CCP1, (residues 17-98) -CCP2 (residues 96-159) and -CCP12 (residues 17-159) were originally cloned by Dr Blein. The $GABA_BR1a$CCP12 expressing *P. pastoris* KM71 strain was plated on minimal dextrose (MD) agar plates using sterile technique and grown for two days at 30 ºC. A single colony was used to

inoculate 10 ml of buffered minimal glycerol (BMG) medium. The starter culture was incubated at 30 ºC for two days with shaking at 250 rpm and then used to inoculate a further 1 litre of BMG medium which was divided equally into four 1-litre baffled conical flasks. The cultures were incubated for an additional two days at 30 ºC with shaking at 250 rpm (or until the $OD_{600\ nm}$ reached approximately 14 units) in preparation for induction of $GABA_BR1aCCP12$ expression. The yeast cells were pelleted by centrifugation at 1800 g for five minutes at room temperature, the supernatant was discarded and the cell pellets were resuspended in 200 ml of buffered minimal methanol (BMM) medium. The cultures were then incubated at 25 ºC with shaking at 250 rpm to achieve induction of protein expression. The cells were pelleted by centrifugation and resuspended in fresh induction media daily, followed by continued incubation. The supernatant was filtered through a 0.2-µm syringe filter and stored at -20 ºC in the presence of 5 mM EDTA and 1 mM phenylmethanesulfonyl fluoride (PMSF) (final concentrations) while awaiting purification. The EDTA and the PMSF inhibit metalloproteases and serine proteases respectively. The *P. Pastoris* supernatants were filtered through a 0.2-µm filter and concentrated at 4 °C from 1 litre down to 20 ml using a N_2-pressurized stirred cell (Millipore) containing a membrane with a molecular weight cut-off of various sizes depending on the protein. For CCP1-2 a 5000 M_w cut-off membrane was used, for CCP1 a 3000 M_w cut-off membrane and for CCP2 a 1000 M_w cut-off membrane was used for concentration of the supernatant.

In preparation for purification the concentrated supernatants containing either CCP1 or CCP12 were buffer-exchanged into 12.5 mM sodium acetate (pH 5.3) while supernatant containing CCP2 was buffered in 50 mM sodium acetate (pH 4.6), using a

PD10 column (GE healthcare). A crude purification was carried out by cation-exchange chromatography using a MonoS column (Mono S HR 5/5, Amersham Biosciences, Little Chalfont, UK) operated at 1 ml/min on an AKTA FPLC system. A representative trace and corresponding SDS-PAGE gel of the initial purification step is shown in Figure 15. The protein was eluted with a 0–1 M NaCl gradient over 25 column volumes. The $GABA_BR1aCCP1$, -2 and CCP12 recombinantly expressed proteins elutes at 0.4-0.5 M NaCl.

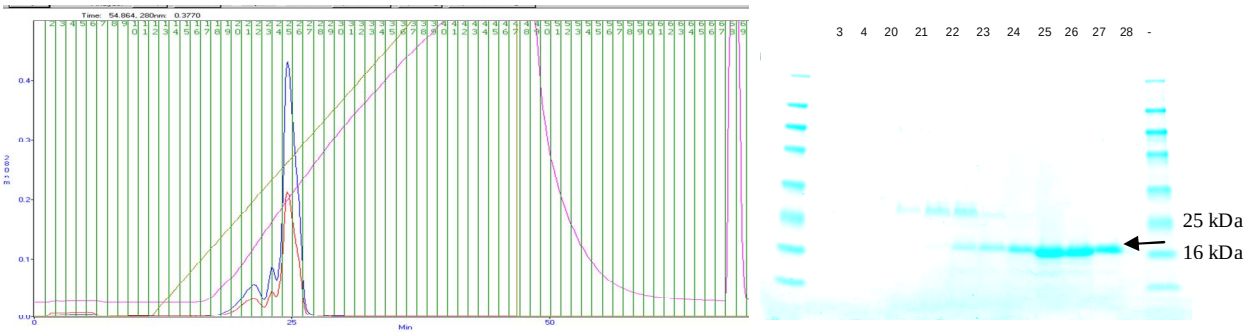

Figure 15 ***Initial purification of recombinantly expressed $GABA_BR1aCCP12$ by cation exchange chromatography***
Chromatogram to the left and SDS-PAGE to the right show separation of $GABA_BR1aCCP12$ from host cell proteins when purified by MonoS cation-exchange chromatography. The A_{280} absorbance trace, salt gradient and conductivity are shown in blue, pink and brown respectively. $GABA_BR1aCCP12$ with a molecular weight of 16.2 kDa is indicated by arrow.

N-glycosylation sites present at Asn23 and Asn83 required deglycosylation with Endoglycosidase H_f (NEB, 6000 units/mg of recombinant protein) for 7 h at 37 °C for constructs CCP1 and CCP12. Traces of glycosylated material were removed by concanavalin A (conA)-sepharose chromatography (Amersham Biosciences). ConA binds molecules that contain α-D-mannose, and the cleaved protein was collected in flow-through mode. Endoglycosidase H_f was removed by cation-exchange

chromatography using a MonoS column (a representative SDS-PAGE gel is shown in Figure 16).

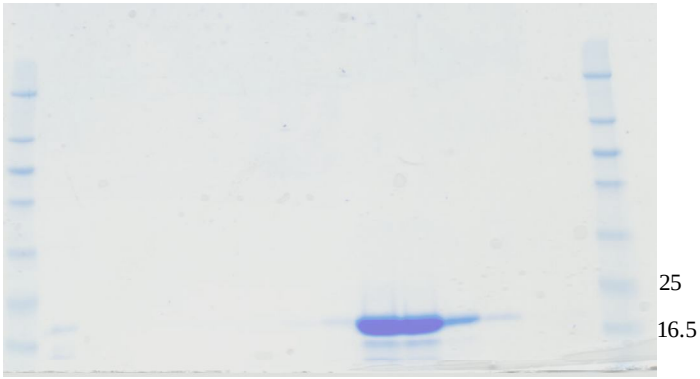

Figure 16 ***$GABA_BR1aCCP12$ final purification by MonoS cation exchange chromatography***
$GABA_B$R1aCCP12, sized 16.2kDa, was purified in three chromatography steps. Faint smaller molecular weight bands present in some preparations, as seen on this gel indicate small amounts of degradation products. The protein sample was run on 10-20% acrylamide Tris-HCl SDS-PAGE under reducing conditions and stained with EZ Blue (Sigma).

Yields of protein were in the order of 4-5 mg/l of growth medium. Protein concentrations were calculated from optical density measurements at 280 nm and a theoretical extinction coefficient based on the protein sequence (ProtParam Tool, available at www.expasy.org). The N-terminal sequence of each protein construct was confirmed by amino acid sequencing (Dr. A. Cronshaw, University of Edinburgh, UK). Mass spectrometry was carried out by S Blein at the Joseph Black facilities, University of Edinburgh.

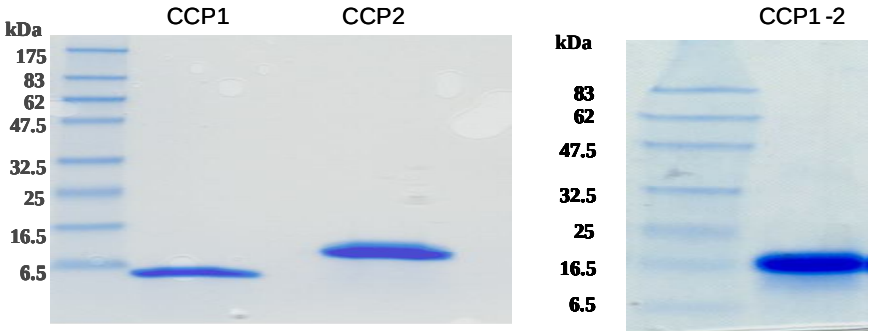

Figure 17 ***SDS-PAGE showing the recombinantly expressed and purified $GABA_BR1a$ modules CCP1, CCP2 and CCP12***
Samples were run on 10-20 % acrylamide Tris-glycine SDS-PAGE under reducing conditions and protein sizes are shown by the protein markers on the left side of the gels.

2.3.3.3.2 Immunodetection of protein

Western immunoblotting and co-immunoprecipitation techniques were not able to detect binding of laminin to $GABA_BR1aCCP12$. Indeed, no interaction could be detected in any method that involved running the protein on SDS-PAGE. A dot-immunoblot was used as an alternative method for detection of these putative protein interactions.

Dot-blot assays were carried out as follows:

A sample containing 4 pmol of the potential partner protein (various sources of laminin, SDS-PAGE can be seen in Figure 30) were dotted on a nitrocellulose membrane and air-dried for five minutes. Non-specific binding of antibodies was blocked by incubation of the membrane, in a 2% (w/v) solution of non-fat dried milk powder in tris-buffered saline (TBS)**,** for one hour at ambient temperature. The membrane was then incubated in the presence of 2 µM $GABA_BR1aCCP12$ protein overnight. Following incubation, the membrane was washed three times in TBS-tween (0.05% v/v) and probed for proteins

with antibodies. The membrane was incubated with a primary sheep antibody s908 (raised against $GABA_BR1aCCP1$) diluted 1:100 in TBS-tween containing 2% (w/v) non-fat dried milk powder at room temperature for two hours. The membrane was then washed three times for 10 minutes with TBS-tween containing 2% (w/v) non-fat dried milk powder, followed by incubation with a secondary monoclonal anti-sheep/goat antibody, A8062 (Sigma, Gillingham UK), for one hour at room temperature. The secondary antibody was diluted 1:25000 in TBS-tween with 2% (w/v) non-fat dried milk powder. The membrane was finally washed three times for ten minutes with TBS-tween. All incubations were carried out on a rocking platform. For detection of alkaline phosphatase, BCIP®/Nitro-blue tetrazolium chloride was employed and the alkaline phosphatase substrate kit (Sigma, UK) was used as a substrate for detection of alkaline phosphatase on immunoblots. The substrate tablet was dissolved in 10 ml of water and incubated with the membrane for up to ten minutes or until protein bands were visible.

2.4 Results

2.4.1 Establishment of the Y2H system for investigating of interactions mediated by the $GABA_BR1a$CCPs

The C-terminal LG domains of laminin were selected as candidates for an interaction with the CCPs of $GABA_BR1a$ as there is precedent for CCP module-LG domain interactions in the literature. A cartoon illustrating the composition of laminin can be seen in Figure 20. It was initially attempted to amplify the entire α5 chain from a human cDNA library. However, this fragment is very large (~400 kDa) and the attempt proved unsuccessful.

In the present study, the cDNA encoding the gene for LAMA5 LG1-5 (residues 2733-3695) was successfully amplified from a human cDNA library and inserted into the pCR®4Blunt-TOPO® cloning vector (Invitrogen, Paisley UK). The *Nde*1/*Xho1* restriction sites were incorporated by PCR and the DNA fragment was inserted into the *Nde*1/*Xho*1 sites of the cloning vector pGADT7 AD (Clontech) (Figure 18). Orientations and correct reading frames of all constructs were confirmed by restriction digests and automated sequencing.

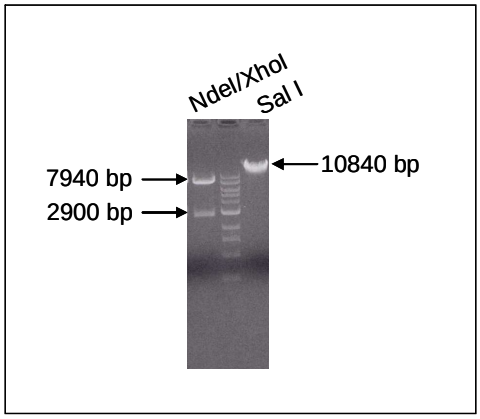

Figure 18 ***Y2H construct for LAMA5 LG1-5***
Double digest (restriction enzymes *NdeI/XhoI*) demonstrating that the construct containing the incorporated gene LAMA5 LG1-5 (2900 bp) was incorporated into the plasmid pGADT7. The full size of the construct (10840 bp) is demonstrated by its linearisation with restriction enzyme *SalI.*

Furthermore, the cDNA encoding the gene for rat $GABA_BR1a$CCP1 (residues 17-98) was successfully amplified by PCR and inserted into the *Nde*1/*Nco*1 sites of the cloning vector pGBKT7 DNA-BD (Clontech). Additionally, cDNA encoding the genes of the C-terminal tail of FTM2 (residues 1068-1184) and FTM3 (residues 377-493) were successfully inserted, separately, into the *Nde*1/*Xho*1 sites of the cloning vector pGADT7 AD (Clontech) (Figure 19).

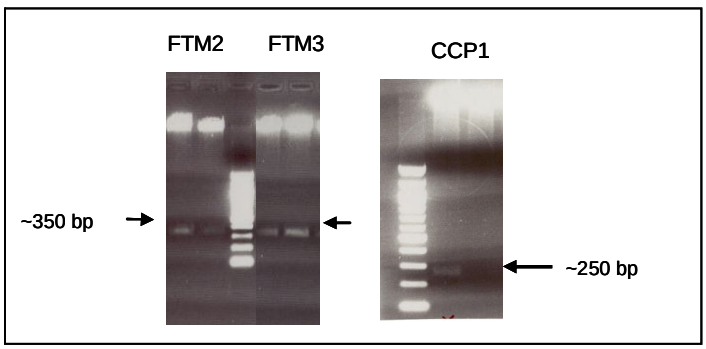

Figure 19 ***Y2H constructs for CCP1, FTM2 and FTM3***
Double digests (restriction enzymes *NdeI/XhoI* and *NdeI/NcoI* respectively) demonstrating that constructs contained the incorporated genes. FTM2 and FTM3 (both 348 pb) were incorporated into the plasmid pGADT7. CCP1 (243 bp) was incorporated into the plasmid pGBKT7.

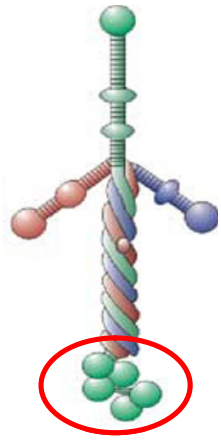

Figure 20 ***Cartoon illustrating the composition of laminin***
The protein consists of the three chains; α in green, β in red, and γ in blue. The α-chain contains five C-terminal LG domains, circled in red. Cartoon (Aumailley et al., 2005)

2.4.1.1 Control experiments

Prior to performing the Y2H assay, it was important to verify that the constructs were able to express protein. In order to establish this, *in-vitro* transcription-translation experiments were carried out to demonstrate protein expression. Yeast two-hybrid assays with single-construct transformations were employed to confirm that no construct gave a positive result when expressed alone. *In vitro* transcription-translation was used to ensure expression of protein by the genes encoding the $GABA_BR1a$CCPs, fibulin C-terminal modules FTM2 and FTM3 and the LAMA5 LG1-5. [^{35}S]-Cys-labeled protein fragments were prepared by *in vitro* transcription-translation of the plasmids used in the Y2H study employing the TNT® T7/SP6 coupled reticulocyte lysate system as described by the manufacturer (Promega). The *in vitro* transcription-translation assay was kindly performed by Dr Brian Collier, MRC Edinburgh. The reactions carried out using rabbit reticulocyte lysate demonstrated that the constructs were indeed able to produce the

desired proteins *in vitro*. As seen in the photographic film illustrating the transcription-translation in Figure 21, the plasmid carrying the gene for $GABA_BR1aCCP1$ produced protein of the expected size (9.4 kDa), as did the plasmids for FTM2 (13.3 kDa) and FTM3 12.9 kDa) and the plasmid for LAMA5 LG1-5 (104 kDa).

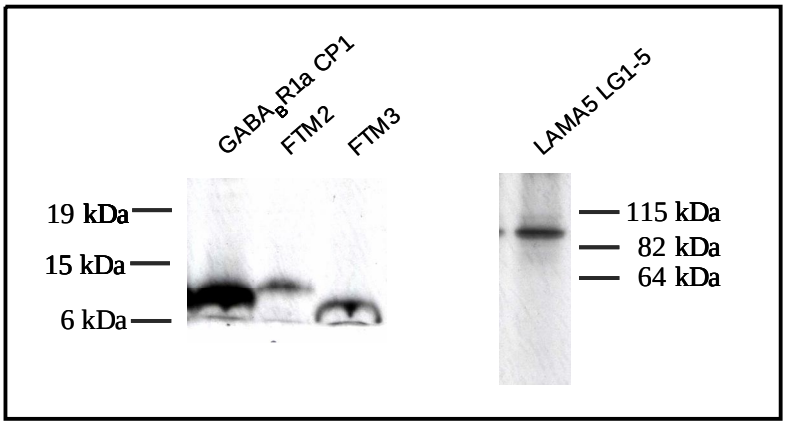

Figure 21 ***Photographic film demonstrating the in vitro transcription-translation of constructs used in Y2H studies***
$GABA_BR1aCCP1$ (9.4 kDa), FTM2 (13.3 kDa) FTM3 (12.9 kDa) and LAMA LG1-5 (104 kDa) are successfully produced and of the correct size *in vitro*.

Single-construct transformations were carried out for all constructs used in the present study as a negative control to confirm that no single protein gave a positive signal in the Y2H system. All constructs were individually transformed into *S. cerevisiae* and the recombinant organisms were tested for growth on media lacking specific nutritients and for enzymatic activity. No constructs were able to promote growth on media that lacked other nutrients than the specific one produced by that particular construct. Similarly, no construct alone promoted enzymatic activity when screened in a galactosidase assay as demonstrated in Figure 22. Thus all constructs were

shown to behave as desired and could subsequently be used in co-expression experiments to screen for interactions.

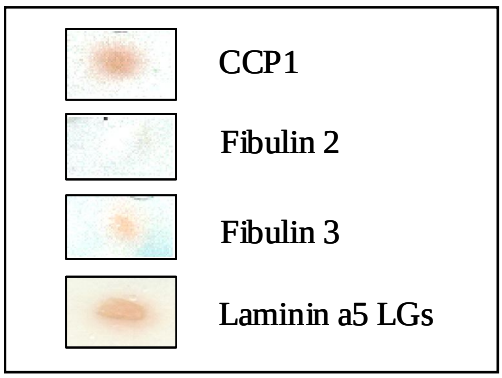

Figure 22 ***Single construct transformations***
All constructs were tested for suitability in the Y2H assay, to confirm that no construct alone could achieve enzymatic activity. All constructs tested negative by producing white/pink colonies. If a protein can produce enzymatic activity without an interacting partner, it would give a false-positive result (blue colour).

2.4.1.2 Co-expression of potentially interacting proteins

The two plasmids pGBKT7 and pGADT7, containing bait and prey respectively, were co-transformed into the *S. cerevisiae* strain, AH109, employing a standard lithium acetate transformation protocol with some alterations (see below). Screening of transformants was carried out using nutritional markers by selecting for colony growth on low *(-Leu/-Trp),* medium *(-Leu/-Trp/-His3)* or high *(-Leu/-Trp/-His3/-Ade2)* stringency media plates. In accordance with standard procedures, low-stringency screening is used if the interaction is known to be weak or if the bait binds transiently with other proteins. In this case, a weak interaction and possibly multiple binding partners are suspected so screening was carried out using low *(-Leu/-Trp),* and medium

(-Leu/-Trp/-His3) stringency plates. Positive and negative controls were used in parallel with the test proteins, as summarised in Table 2. Positive clones were analysed for colony growth and β-galactosidase activity using an X-gal based colorimetric assay.

In the current work colony growth and enzymatic activity as reflected in the development of a blue colour, were judged by eye. A test was considered to be weakly positives if it resulted in activation of just the *LacZ* reporter, while a strongly positive test is one where activation of both the *LacZ* and *His3* reporter occurs. Thus potential interactions between pairs of proteins were categorized as follows. A 'strong positive' interaction was recorded if an intense blue/green colour developed, most or all of the colony area was colored in the average-intensity assay and rapid colony growth occurred. A'weak positive' interaction was characterized by the formation of colonies with a pale blue/green colour, only the outer edges of the colony area becoming colored in the average intensity assay and poor colony growth. A negative result *i.e*. 'no interaction' was characterized by a lack of colony growth or by very slow growth of (or beige) colonies.

Table 2 *Controls for Yeast two-hybrid screening assays*

POSITIVE CONTROLS:

pCL1
Encodes the full-length Gal4 protein.

pGBKT7-T + pGADT7-53
SV40 large T-antigen and murine p53 protein are known to interact and therefore these colonies would be expected to be positive by Y2H.

NEGATIVE CONTROLS:

pGBKT7-T
Encodes only a fusion of the SV40 large T-antigen and the Gal4 activating domain (*i.e.* no transactivating domain).

pGBKT7-T + pGADT7-Lam
SV40 large T-antigen and human lamin C are known not to interact with each other and therefore these colonies would be expected to be negative in the Y2H.

Initially, transformation efficiencies were poor. A number of routes were subsequently explored with the aim of optimising the transformation protocol. For example, in an attempt to overcome the problem of a low number of transformants, the addition of DMSO prior to heat-shocking of the cells was excluded, which increased efficiency (since in this study, excluding this component from the transformation reaction generally increased the transformation efficiency by generating more colonies). Furthermore, the post-transformation incubation time was increased for some slow-growing constructs and this was accompanied by close monitoring of enzymatic assay activity.

2.4.2 Validation of the interactions between $GABA_BR1aCCP1$ and FTM2 and FTM3

2.4.2.1 Colony-lift filter assay

Co-transformations of the constructs for $GABA_BR1aCCP1$ and FTM2, as well as for the constructs for $GABA_BR1aCCP1$ and FTM3 were performed as described above. Positive clones were selected for on minimal media, transferred by lifting the colonies to nitrocellulose membranes and subjected to a colorimetric β-galactosidase assay. Each experiment was carried out in triplicate with consistent results. A strong positive interaction between $GABA_BR1aCCP1$ and FTM2 was observed, as can be seen in Figure 23. On the other hand $GABA_BR1aCCP1$ and FTM3 show only a weakly positive result in the colony-lift assay (Figure 23).

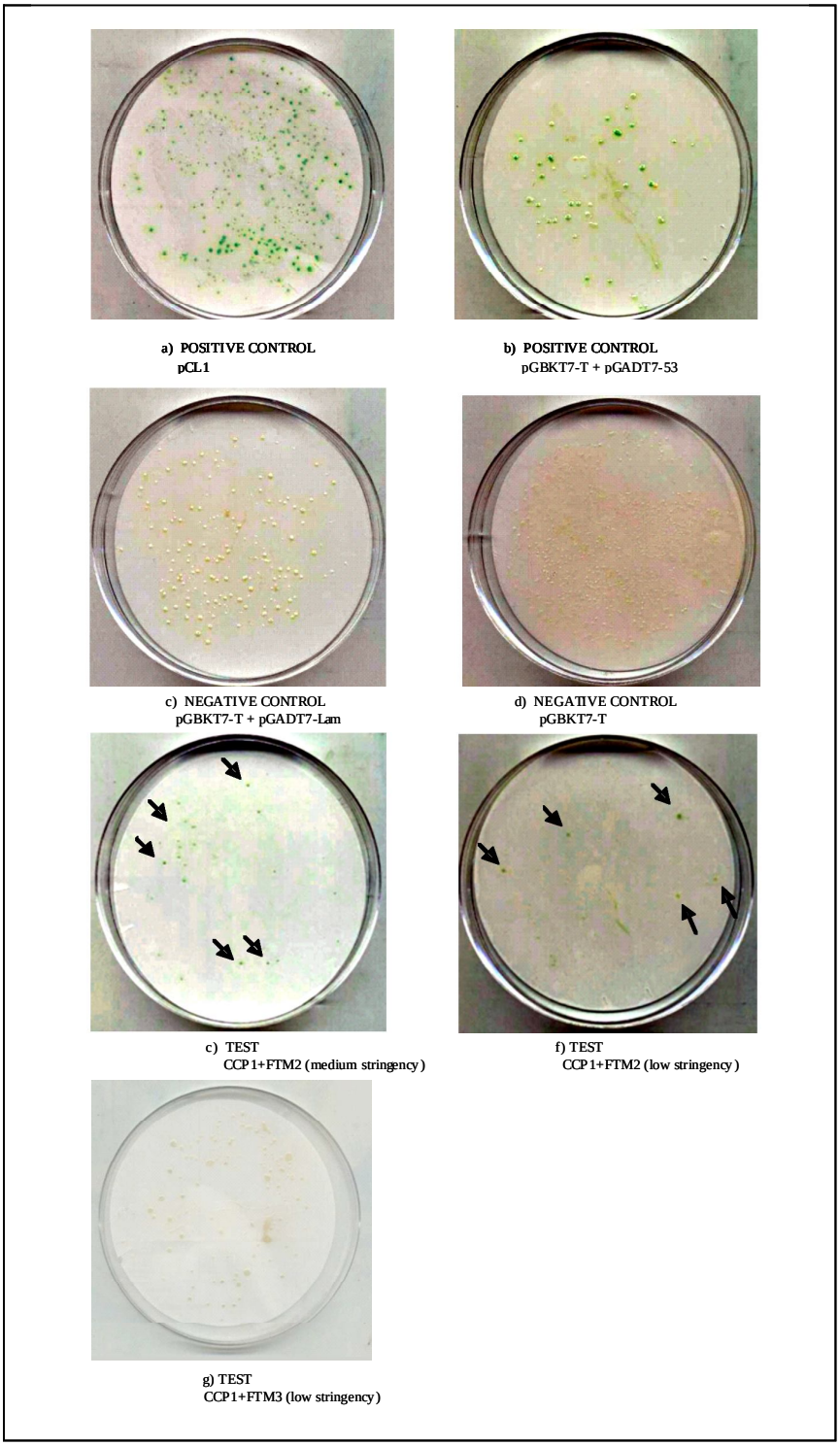

Figure 23 ***Colony-lift filter assay***
The assay shows a strong positive result (blue colour) for the interaction between $GABA_BR1a$CCP1 and FTM2 (e and f) and a weakly positive result (blue colour) for the interaction between $GABA_BR1a$CCP1 and FTM3 (g). Arrows indicate positive clones. Positive controls (a and b) (blue), negative controls (c and d) (white).

2.4.2.2 Average intensity assay

In order to investigate the approximate strength of a putative interaction between these two proteins using the Y2H assay, a representative sample of the population consisting of ten colonies, was examined. To achieve this, the colonies were pooled and re-streaked on Whatman filter paper, and then analysed for growth and enzymatic activity. The intensity of enzymatic response was judged by eye and then classified (strong, weak or negative) according to the criteria listed above.

The results from an average-intensity assay for the interaction of $GABA_BR1aCCP1$ with FTM2 and FTM3 are shown in Figure 24. The assay was repeated in triplicate and gave reproducible outcomes. These results confirm a strong positive result for the interaction between $GABA_BR1aCCP1$ and FTM2, and a weakly positive result for the $GABA_BR1aCCP1$ with FTM3 interaction. It may be concluded that $GABA_BR1aCCP1$ interacts more strongly with FTM2 than with FTM3, in the Y2H system.

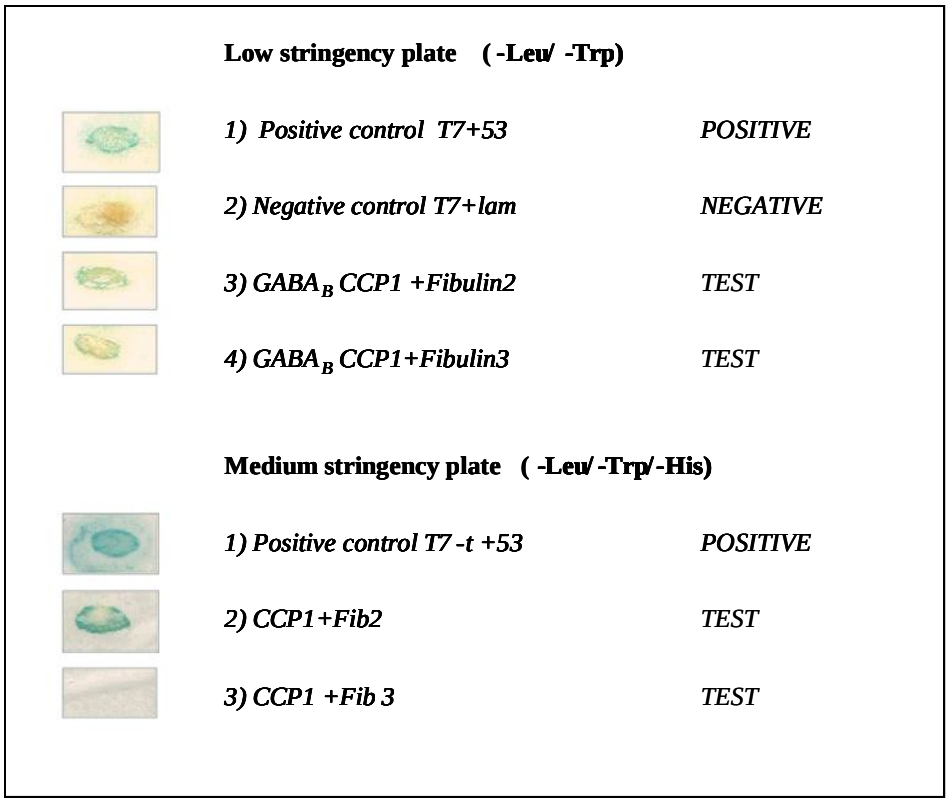

Figure 24 ***Average-intensity assay for the putative interactions of GABA$_B$R1aCCP1 with FTM2 and FTM3***

Galactosidase assays were performed on a pool of ten colonies in each case. Low stringency assays: 1) Positive control T7+53 (blue) 2) Negative control T7+lamin (white/pink) 3) CCP+FTM2 gives a strong positive signal, 4) CCP+Fib3 gives a weakly positive signal. Medium-stringency assay: 1) Positive control T7+p53 (blue), 2) CCP+Fib2 gives strong positive signal consistent with a physiologically meaningful interaction between these proteins, 3) CCP+Fib3 gives negative/inconclusive results.

2.4.3 Characterisation of the potential interaction between $GABA_BR1aCCP1$ and laminin α5 LG 1-5

2.4.3.1 Colony lift assay

Co-transformations of the constructs for $GABA_BR1aCCP1$ and LAMA5 LG1-5 were performed as described earlier. Positive clones were selected for on minimal media, transferred by colony-lift to nitrocellulose membranes and subjected to β-galactosidase assay. Each experiment was carried out in triplicate and delivered consistent results.

A weakly positive result was obtained for the interaction between $GABA_BR1aCCP1$ and LAMA5 LG1-5 as shown in Figure 25. No colony growth was observed on medium- or high-stringency plates, (*i.e*. with three or four sources of nutrition lacking from the growth media).

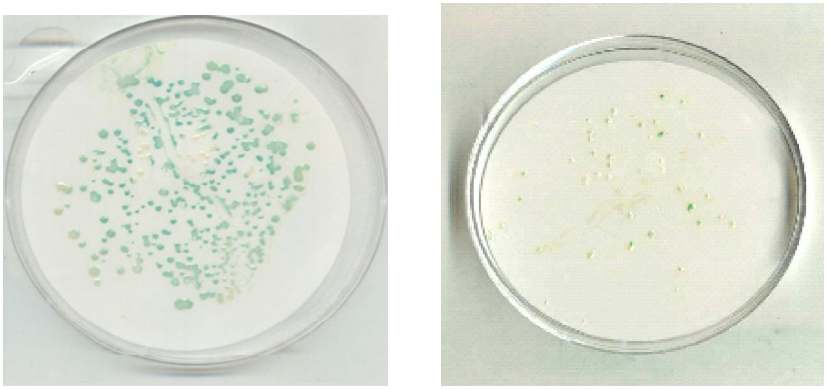

a) POSITIVE CONTROL
pCL1

b) POSITIVE CONTROL
pGBKT7-T + pGADT7-53

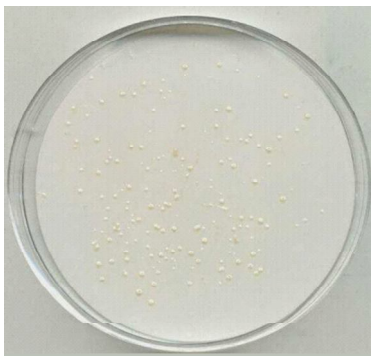

c) NEGATIVE CONTROL
pGBKT7-T + pGABT7-Lam

d) NEGATIVE CONTROL
pGBKT7-T

e) TEST
CCP1+LAMA5 LG (low)

Figure 25 ***Colony-lift filter assay showing a weakly positive result for the potential interaction of GABA$_B$R1aCCP1 with LAMA5 LG1-5***
Positive controls (blue colour) are shown in a) and b) and negative controls (white/pink colour) are shown in c) and d) (as summarized inTable 2). e) shows a weakly positive outcome for the interaction between GABA$_B$R1aCCP1 and LAMA5 LG1-5 on low-stringency plates (blue colour).

2.4.3.2 Average-intensity assay

The results from an average-intensity assay for the interaction between $GABA_BR1aCCP1$ and LAMA5 LG1-5 are shown in Figure 26. The assay was performed in triplicate with reproducible results. The weakly positive signal obtained is consistent with a weak or transient interaction between LAMA5 LG1-5 and $GABA_BR1aCCP1$.

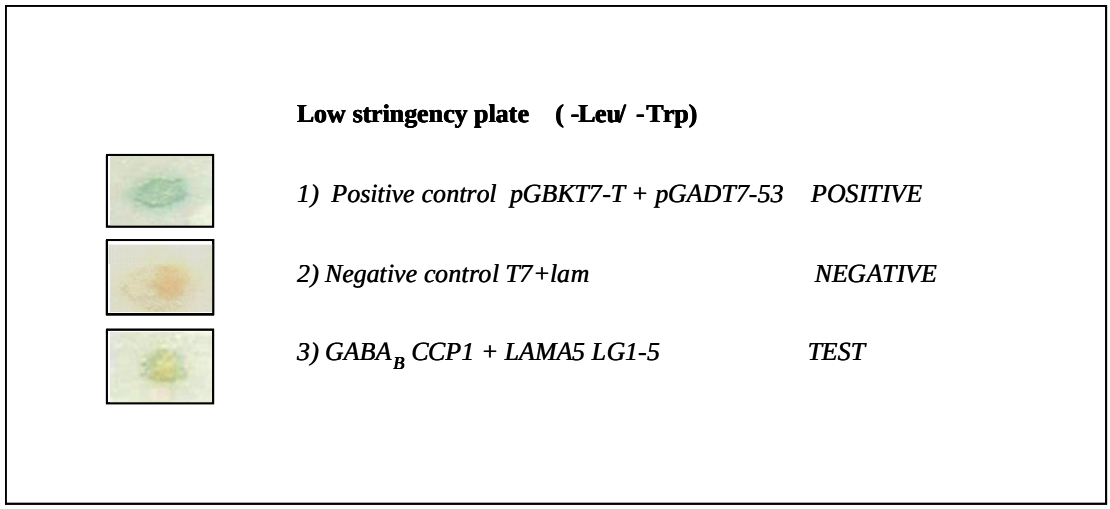

Figure 26 ***Average-intensity assay***
β-galactosidase assays were performed on a pool of ten colonies in each case. 1) Positive control- T7+p53 (blue), 2) Negative control- T7+lamin (white/pink) 3) $GABA_BR1aCCP1$ + LAMA5LG1-5 exhibits a weak or transient interaction as indicated by the weakly positive result (blue) of Y2H under low-stringency conditions.

2.4.3.3 Immuno-dotblots

Immuno-dotblots were used as a means of providing an alternative approach to the investigation of interactions between the CCP modules of $GABA_BR1a$ and laminin. A nitrocellulose membrane was dotted with a variety of laminin-derived fragments and

then incubated with recombinantly expressed $GABA_BR1aCCP12$ prior to washing (as described previously). The membrane was then probed with $GABA_BR1aCCP1$-specific antibody, followed by an alkaline phosphatase conjugated secondary antibody (as described in 0) which was detected with BCIP®/Nitro-blue tetrazolium chloride alkaline phosphatase substrate. The experiment was performed in triplicate and gave reproducible results.

There is literature precedence for an interaction between CCPs of C4BP and LG modules of protein S (Fernandez and Griffin, 1994; Hardig and Dahlback, 1996; Hardig et al., 1993; Hillarp and Dahlback, 1990). In a collaborative experiment (J. White, personal communication) an interaction of $GABA_BR1aCCP12$ was detected with one or more components in a commercial preparation of laminin, using a pull-down assay. This source of laminin contains the chains α5, β1 or β2 and γ1. Hence, recombinantly expressed LAMA5 LG1-3 and LAMA5 LG4-5 (kindly provided by Dr. Sasaki, Max-Planck Institute) were tested for interaction with $GABA_BR1aCCPs$. As illustrated by the immuno-dotblot in Figure 27, a positive signal was observed for LAMA5 LG4-5, while only a very weak interaction was inferred for LG1-3. However, laminin-1 (α1, β1, γ1) seemed to interact relatively strongly with the CCPs, which suggests the presence of more than one interaction-site on the full length-laminin protein.

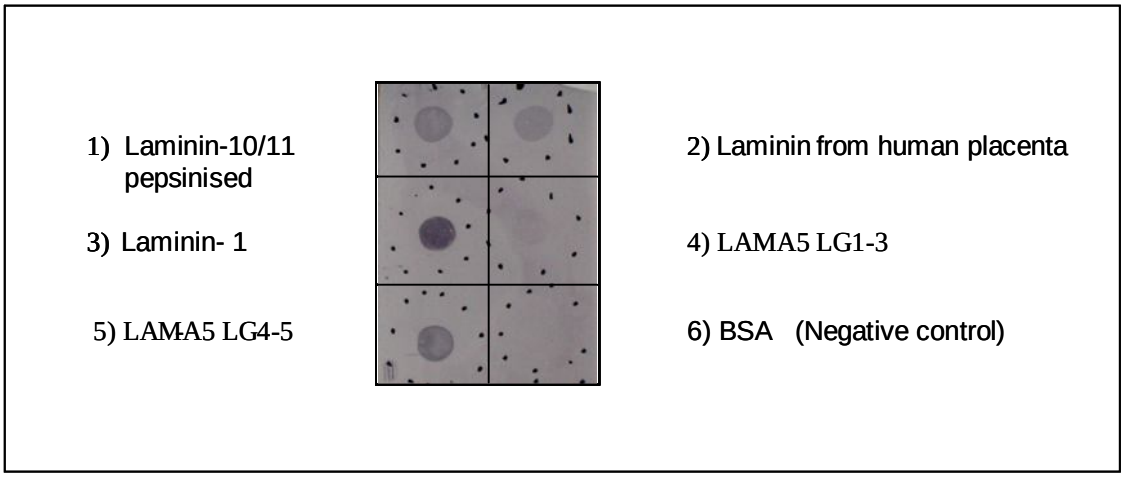

Figure 27 ***Immuno-dotblot demonstrating the interaction of GABA$_B$R1aCCP12 with several laminin preparations***
Nitrocellulose membrane was probed with alkaline phosphatase-conjugated GABA$_B$R1aCCP1 specific antibody and detected with BCIP®/Nitro-blue tetrazolium chloride alkaline phosphatase substrate.

2.5 Discussion

2.5.1 The Y2H was established as a system to investigate protein-interaction partners of the $GABA_BR1a$ CCP modules

A striking feature of the $GABA_B$ receptor is the presence in the extracellular domain of the $GABA_BR1a$ subunit of two CCP modules. These modules are of a type that, in other proteins, has been shown to engage in specific protein-protein interactions. The identification of physiologically relevant protein interaction partners for the CCP modules of $GABA_BR1a$ could open up a new line of investigation since it might point to novel functions of the receptor. The proteins of the ECM are obvious candidates. The current work involved establishing whether previous, mainly unpublished, reports of interactions with laminin and fibulin could be confirmed and elaborated upon.

The first task was to establish in the lab appropriate techniques for investigating protein-protein interactions. Initially, it was necessary to address the question: Is the yeast two-hybrid (Y2H) system a suitable method to use in the study of weak interactions such as are suspected to occur between the $GABA_BR1a$CCPs and fibulin, and $GABA_BR1a$CCPs and laminin? Although the Y2H is primarily used for high-throughput screening of interacting proteins, there is literature precedent for its use in investigating known or suspected interaction between two proteins (Miernyk and Thelen, 2008; Mukherjee, 2001). The concern once the system has been established is to

analyse the data vigorously and judge whether the outcome is reliable. A major potential pitfall is the occurrence of false-positive results. To minimize the possibility of false-positive readings in the present study, clones were re-tested, and only classified as true positives in cases where an interaction was observed in both colony-lift and average-intensity assays. The YTH results were then cross-checked by performing an alternative, independent assay based on immuno-dotblot (Rual et al., 2005; Stelzl et al., 2005). Another drawback of Y2H is that the test proteins are generally overexpressed, thus artificially enhancing the concentration of the potential binding partners. To minimize this problem, the Y2H system employed in the current study uses low-copy number plasmids. With this approach there remains a risk of false-negatives due to low expression (Lalonde et al., 2008).

Although the Y2H system has the benefit of being a eukaryotic, *in vivo*, method it could be argued that expression of mammalian proteins in non-native cells, *i.e.* yeast cells in this case, may not allow for correct protein folding and post-translational modification. Pertinent to the current study, the extracellular protein domains under investigation, expressed as fusion proteins with Gal4 domains may not appear as folded entities in the yeast nucleus (*i.e.* where they need to be if they are to contribute to transcription factors). In particular, proteins imported into the nucleus are unlikely to contain disulphide bonds (such as are present within CCP modules, for example) due to the reducing environment within both the cytoplasm and nucleoplasm. Nonetheless, there are several examples in the literature of the use of Y2H to detect protein interactions between extracellular proteins (Lee et al., 2005; Overall et al., 2002; Oxford et al., 2004). The nucleus may be regarded as a ‘less stressful’ environment compared to

the cell surface, and therefore it is possible that some protein domains will fold correctly despite the absence of stabilizing disulphide bridges, as has been further argued in the literature (Overall et al., 2002). In this respect it is interesting to note that CCP1 of $GABA_BR1a$ is a natively unfolded domain that presumably folds upon binding to an interaction partner (Blein et al., 2004).

2.5.2 Screening for $GABA_BR1a$CCP1 interaction with fibulin-2 (FTM2) and potentially with fibulin-3 (FTM3)

It was successfully demonstrated in the present study that the proposed interaction of $GABA_BR1a$CCP1 with the C-terminal fragment of fibulin-2, FTM2, is detectable using the Y2H. This result confirms and strengthens unpublished data collected by Dr Julia White (personal communication). An interaction of the $GABA_BR1a$CCP1 with the equivalent domain of fibulin-3, FTM3, could not be conclusively identified by Y2H in the current study. A $GABA_BR1a$CCP1/FTM2 interaction was later confirmed by pull-down experiments (Blein et al., 2004).

The possibility that both modules (*i.e.* CCP12) are required for the interaction with FTM3 was investigated using immuno-dotblots where the double module was used as an interacting partner (data not shown). Still no interaction could be detected for FTM3. The observation by Y2H that $GABA_BR1a$CCP binds to FTM2 over FTM3 is intriguing. The fibulin fragments used in the present study are the C-terminal fragments, and there is 20% sequence identity between them as shown in Figure 28, approximately 28% of residues are conserved substitutions.

Figure 28 ***Sequence alignment of C-terminal fragments of fibulin-2 and fibulin-3 used in the current Y2H study***
24 of 116 residues are identical ~ 20%. 33 of 116 residues are conserved substitutions ~ 28%

2.5.3 The putative interaction between the CCP modules of GABA$_B$R1a and laminin has been further characterised

It the current study, a weak or transient interaction of the GABA$_B$R1aCCP1 with the LAMA5 LGs was demonstrated by Y2H, although it is very close to the detection limit. Indeed less colony growth was observed (in colony-lift assays) for the GABA$_B$R1aCCP1:LAMA5 LG1-5 interaction compared to the weak or transient GABA$_B$R1aCCP1:FTM3 interaction described in the previous section. By using the immuno-dotblot technique, a more definite result for interaction with laminin was obtained. It was also successfully demonstrated by immuno-dotblot that several commercially available sources of laminin interact with GABA$_B$R1aCCP12. It was further determined by immunoblotting that α5 LG4-5 out of the five LG modules of the C-terminal fragment of LAMA5 is sufficient for this interaction. It was hypothesized that by testing laminin-1 (α1, β1, γ1), a negative result would help to rule out the β1 and γ1 chains as participating interaction partners. However, a positive result was obtained. Nonetheless, this potentially physiologically relevant interaction of a CCP module from

the $GABA_B$ receptor with LAMA5 LG1-5 adds a second example of CCP modules that interact with LG domains, discussed previously in the case of C4BP (Fernandez and Griffin, 1994; Hardig and Dahlback, 1996; Hardig et al., 1993; Hillarp and Dahlback, 1990).

In the immuno-dotblot assay, the recombinantly expressed $GABA_BR1aCCP12$ double module, rather than the single CCP1 module, was used when screening for the laminin interaction. Although the first CCP module (CCP1) appears to be sufficient for interaction according to surface plasmon resonance (Chapter 3), the second CCP module (CCP2) may help to stabilize the interaction. The use of CCP12 in the immuno-dotblot, might explain why this assay gave a stronger positive result (compared to Y2H) for the interaction with the LAMA5 LGs.

It therefore remains to be tested if CCP1 is sufficient for the interaction with laminin as tentatively inferred from Y2H. Alternative techniques for verifying protein-protein interactions detected by Y2H include surface plasmon resonance-based methods and isothermal titration calorimetry (ITC) techniques. Detection of a transient or weak interactions may require special techniques such as chemical cross-linking (Miernyk and Thelen, 2008; Trakselis et al., 2005). Further work using surface plasmon resonance is described in Chapter 3.

In conclusion, this chapter has shown for the first time that laminin is an interacting partner for $GABA_BR1aCCP1$, and that the α5 LG domains appear to be involved in this interaction. Furthermore, the binding of the C-terminal fragment of fibulin-2 (FTM2) with $GABA_BR1aCCP1$ is consistent with reports from other studies.

CHAPTER 3

Surface plasmon resonance study

3 Chapter 3 Surface plasmon resonance studies

3.1 Aims

The first aim was to establish in our laboratory surface plasmon resonance (SPR), performed on a Biacore instrument, as an independent biochemical technique by which to verify the interaction of the $GABA_BR1a$CCP modules with the extracellular proteins laminin-1 and laminin-10/11. The second aim was to use SPR to assess the extent to which one or both of the CCP modules are required for these interactions. The third aim was to employ SPR to investigate which domains or fragments of laminin are involved in binding to $GABA_BR1a$CCP12.

3.2 Context

There exists substantial literature precedent for direct participation of CCP modules in protein:protein interaction sites. These small disulfide-stabilised protein modules have a conserved three-dimensional structure that serves as a framework for the support of variable loops and turns endowing considerable potential diversity in molecular recognition capabilities. Typically, two or three contiguous CCP modules contribute to a specific protein-binding site. It is therefore noteworthy that it is the presence or absence of the tandem pair of N-terminal CCP modules in $GABA_BR1$ that distinguishes the two most abundant receptor isofoms. The possibility that these modules mediate interactions with other proteins is intriguing; such interactions might

introduce a previously unobserved pharmacological distinction between the receptor isoforms, or they might be important in establishing differences in spatial or temporal distributions of receptor sub-types. Identification and characterisation of the putative binding partners is therefore highly desirable. Results obtained from the Y2H study (see Chapter 2) encouraged further investigation of the involvement of the CCP modules in the proposed interaction with laminin.

3.3 Materials and methods

3.3.1 Surface Plasmon Resonance Theory

Surface plasmon resonance (SPR) is a phenomenon that occurs when plane-polarised light strikes the interface between two media of different refractive indices. In the Biacore system the interface occurs between a glass sensor chip and aqueous buffer. The glass, which has a higher refractive index than the buffer, is coated with a gold film. Total internal reflection is a condition that pertains when a light beam hits this interface at a specific angle called the plasmon resonance angle, θ_{SPR}, and is reflected back into the medium from which it came. Under these circumstances the incoming light causes free electrons (plasmons) on the gold surface to resonate.

Binding of molecules to the matrix on the back of the gold surface (furthest away from the glass) causes a change in refractive index. This can be detected as a change in the plasmon resonance angle. There are various types of sensor chips. The most common one, the CM5 chip, has a carboxymethylated dextran matrix attached to the back of the

gold surface. One of the interacting proteins, called the ligand, is covalently attached to the matrix (*e.g.* by amine coupling) while the putative binding partner, called the analyte, is passed over the surface of the sensor chip at a set flow rate. A binding event results in a change in the refractive index, which is detected in a real-time sensogram. The sensogram shows binding as resonance units (RU) versus time, where the resonance units represent the change in θ_{SPR}. One resonance unit corresponds approximately to the binding of one picogram per mm^2 of analyte. Surface plasmon resonance can be used to measure both kinetics and affinity; *i.e.* how fast and how strong the binding is.

3.3.2 Materials

3.3.2.1 Buffers and reagents

Table 3 *List of buffers and reagents used during the current study*

Buffer*	**Reagent**
Sensor chip activation solution	1:1 N-hydroxysuccinimide (NHS) : N-ethyl-N-(3-dimethyl-aminopropyl)carbodiimide (EDC)
Coupling buffer	10 mM sodium acetate, pH 4.0/4.5/ 5.0/ 5.5
Regeneration buffer	30 mM or 50 mM NaOH
HBS-P^+ running buffer	0.01 M HEPES, 0.15 M NaCl and 0.05% v/v Surfactant P20, pH 7.4

*All buffers were supplied by Biacore.

3.3.2.2 Sensor chips

Table 4 *List of sensor chips used during the current study*

Sensor chip*	Description
Series S sensor chip CM5 (certified)	carboxymethylated dextran
Series S sensor chip SA (certified)	**c**arboxymethylated dextran pre-immobilized with streptavidin for immobilization of biotinylated interaction partners
Series S sensor chip NTA (certified)	carboxymethylated dextran pre-immobilized with nitrilotriacetic acid (NTA*). His-tagged molecules are immobilized via Ni^{2+}/NTA chelation

*All sensor chips were supplied by Biacore.

3.3.2.3 Proteins

The protein laminin-1 was purchased from Sigma (product number: L2020, from basement membrane of Engelbreth-Holm-Swarm mouse sarcoma) while laminin-10/11 was purchased from Chemicon (catalogue number AG56P, from human placenta). Recombinantly expressed laminin fragments α1 LG1-3, α1 LG4-5, α5 LG1-3 and α5 LG4-5 were generously provided by Dr Takako Sasaki, Max-Planck Institute for Biochemistry. The analyte proteins $GABA_BR1a$CCP1, -CCP2 and -CCP12 were cloned, recombinantly expressed and purified as described in Chapter 2. The CCP module-containing proteins were exchanged into sodium acetate buffer, freeze-dried and, prior to running SPR experiments, resuspended in HBS-P^+ running buffer (see Table 3). Protein concentrations were determined by measuring absorbance (280 nm) on an Ependorf BioPhotometer. All proteins were analysed by 10-20% acrylamide tris-glycine SDS-PAGE to determine purity (Figure 29 and Figure 30).

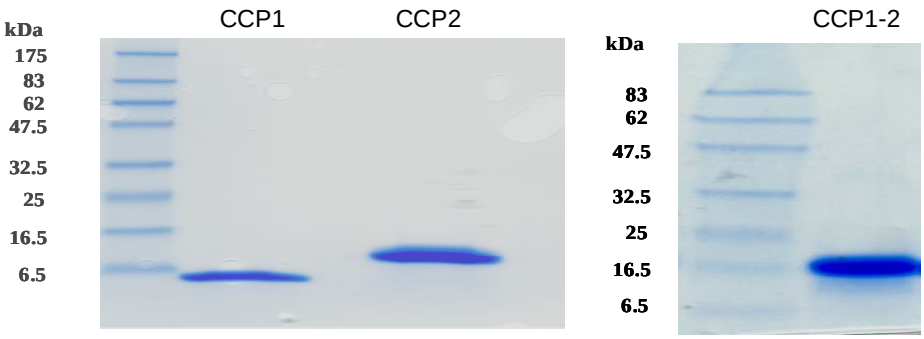

Figure 29 ***10-20 % tris-glycine SDS-PAGE showing the protein used in the SPR study***

As previously shown in figure 17. Samples were run under reducing conditions and protein sizes are shown by the protein markers on the left side of the gels. The gel was run as described in the standard methods. $GABA_BR1aCCP1$, -CCP2 and -CCP12 are all of a high standard of purity as judged by SDS-PAGE at this loading.

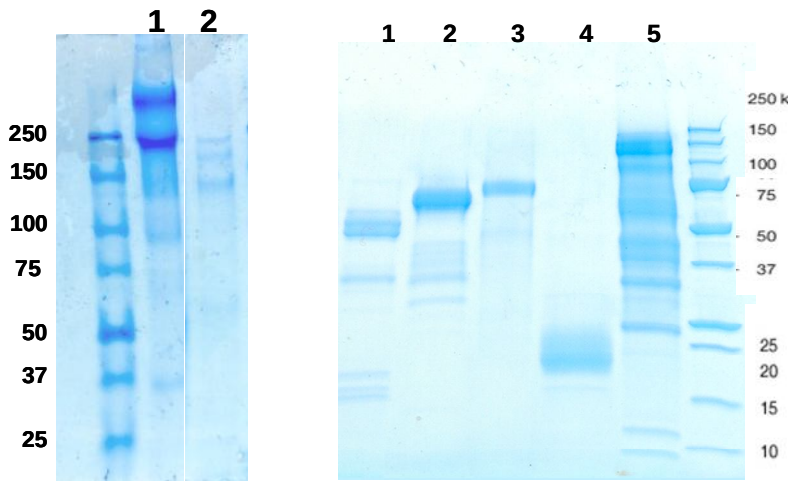

Figure 30 ***SDS-PAGE showing laminin proteins used in the SPR study***
Left-hand side: (5% TBE gel) **Full-length laminins.** Lane 1) Laminin-1 (mouse sarcoma-L2020). The individual chains appear as the dominant 400-kDa and 200-kDa bands under reducing conditions, although several additional bands in the region of 35 to 130 kDa are also visible. Lane 2) Laminin-10/11 (human placenta- AG56P); in this pepsinised preparation the dominant bands appear as approximately 130 kDa, 160 kDa and 200 kDa, although several smaller bands in the region of 60 kDa and 100 kDa are just visible. **Right-hand side:** ***(10-20 % tris-glycine gel)*** **laminin fragments.** Lane 1) α5 LG4-5. The dominant band is 40 kDa, but degraded protein or contaminants are visible by SDS-PAGE. Lane 2) Recombinant β1 VI/V. The dominant band is 60 kDa, but some minor contaminants are present. Lane 3) LN73. The dominant band is 75 kDa and this preparation appears fairly clean by SDS-PAGE. Lane 4) LN65. The dominant band is 25 kDa, however this band appears degraded and smeary by SDS-PAGE. Lane 5) LN78. This fragment of 450 kDa consists of three chains that have been pepsinised and would be expected to run separately under reduced conditions. In fact, a range of bands are present.

3.3.3 Methods

3.3.3.1 The Biacore T100 instrument

The SPR data was collected on a Biacore T100 system in the School of Biological Sciences at the King's Buildings, University of Edinburgh. The T100 system features four detector flow-cells, which can be used in single, paired or serial runs. Running buffer or buffered sample solution is passed through the flow-cells continuously. In the following experiments, the flow-cells were used pair-wise and treated identically, except that the ligand was immobilised on only one flow-cell. Thus the other flow-cell can be used as a reference to measure background or non-specific binding.

3.3.3.2 Pre-concentration

Pre-concentration of ligands on the CM5 sensor surface was performed by means of electrostatic attraction. This procedure was performed to optimise conditions for the subsequent immobilisation. The ligand in coupling buffers of different pH values was passed over an inactivated sensor surface. Effective pre-concentration should take place at a pH that lies between the pK_a of the dextran surface (pH 3.5) and the isoelectric point of the ligand (Figure 31). The pre-concentration of the ligand at various pH values is shown in a series of sensograms in Appendix B.I, a representative example is illustrated in Figure 32.

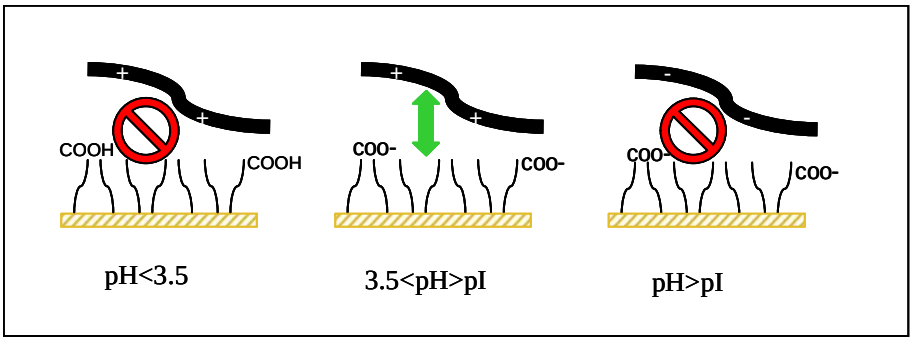

Figure 31 ***Illustration of pre-concentration of the ligand on the chip sensor surface by electrostatic attraction at a suitable pH.***
Pre-concentration should take place at a pH that lies between the pK_a of the dextran surface (pH 3.5) and the isoelectric point of the ligand. Under these conditions the overall charge of the protein will be positive and the charge of the dextran surface will be negative, creating an electrostatic interaction between the two.

The example shown is for $GABA_BR1aCCP12$ passed over an untreated sensor surface at four different pH values, followed by glycine buffer at pH 2 to regenerate the surface.

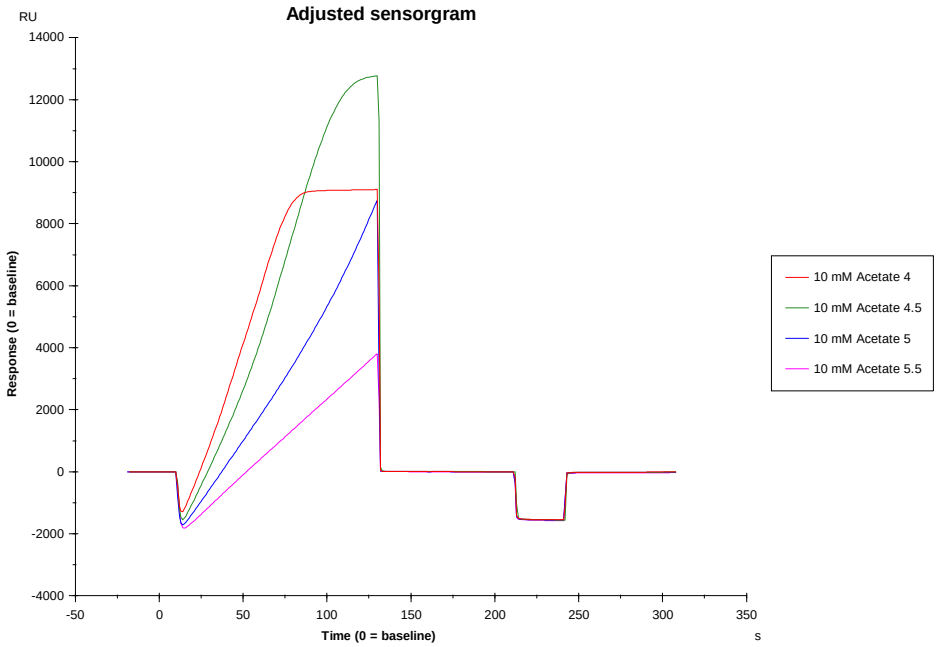

Figure 32 ***Sensogram of pre-concentration of $GABA_BR1aCCP12$***
The ligand was diluted in four differenly pH-ed buffers (see key), injected over the chip surface and analysed for electrostatic attraction to the chip surface. On this basis, pH 5.5 was selected for amine coupling.

3.3.3.3 Immobilisation of ligand

The ligands in this study were immobilised on CM5 chips unless otherwise stated. Alternative sensor chips used in the current study were SA- and NTA chips. Ligands were covalently linked to the dextran matrix of the CM5 chip using amine coupling, which is the most common method. The amine-coupling chemistry is illustrated in Figure 33. Immobilisation was carried out by activating the sensor surface with a mixture of N-hydroxysuccinimide (NHS) and 1-ethyl-3-(3-dimethylaminopropyl) carbodiimide hydrochloride (EDC) and thereafter attaching the ligand via its amine groups at a flow rate of 5 µl/min. Any unbound active ester groups on the sensor surface were then deactivated using ethanolamine, pH 8.5. A reference surface was created by inactivating the N-hydroxysuccinimide esters with ethanolamine without prior addition of ligand.

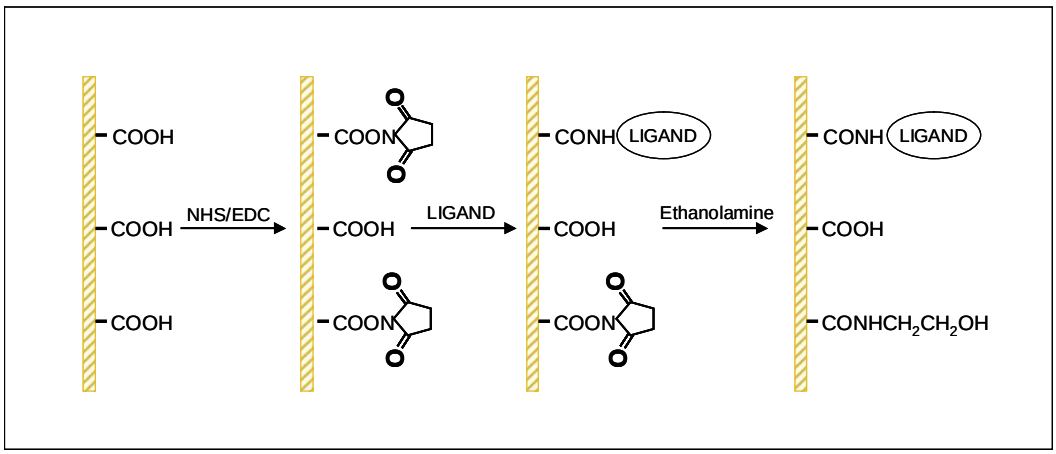

Figure 33 ***Amine-coupling chemistry on the surface of a CM5 chip***
The dextran matrix is represented by the long, patterned vertical line. The ligand attaches to the sensor surface via its primary amine groups. Any remaining active ester groups are inactivated by ethanolamine.

A representative sensogram recorded during immobilisation of a ligand is shown in Figure 34**,** which is for amine-coupling of laminin-1 to a CM5 chip. All sensograms recorded for ligand immobilisations can be found in Appendix B.II. A stock of the ligand at 20-30 µg/ml was made up in coupling buffer at pH values between 4.5 and 5.5 (depending on pre-concentration data, Table 5) and passed over the activated surface of flow-cell 2. A reference surface was created on flow-cell 1, as described earlier. The optimal amount of ligand that should be immobilised on the sensor surface was determined by Equation 1, where R_{max} was set to 100. The amount of laminin-1 immobilised on the chip corresponded to 5070 response units (RU).

Equation 1 *Immobilisation level is determined by the below equation*

$$R_{\max} = \frac{analyte\ M_W}{ligand\ M_W} * R_L * S_m$$

R_{max} describes the binding capacity of the sensor surface and is normally set to 100-300 RU to minimise mass transfer

R_{max} was set to 100 RU

R_L *:* immobilisation level

S_m *:* stocichiometric ratio (=1)

analyte (CCP1-2) *:* 16 200 Da

ligand (laminin-1) *:* 800 000 Da

R_L was calculated to be 4938 RU

Table 5 *Immobilization conditions. CM5 sensor chips were used unless otherwise stated*

Ligand name	Stock concentration of ligand	pH for immob	R_L (immobilization level)	Actual immob.	M_w ligand (Dalton
Laminin-1	30 µg/ml	5.0	4938 Ru	5070 Ru	800 000
Laminin-10/11	40 µg/ml	4.0	455 Ru	390 Ru	(pepsinised)
CCP12	10 µg/ml	5.5	81 Ru	235	16 200
CCP12 (SA*)	50 nM	-	235 Ru	230 Ru	16 200
α1 LG1-3	20 µg/ml	5.5	506 Ru	612 Ru	82 000
α1 LG4-5	20 µg/ml	5.5	272 Ru	465 Ru	44 000
α5 LG4-5 (NTA*)	200 nM	-	493 Ru	429 Ru	40 000

**alternative sensor chip used, as described in* Table 4

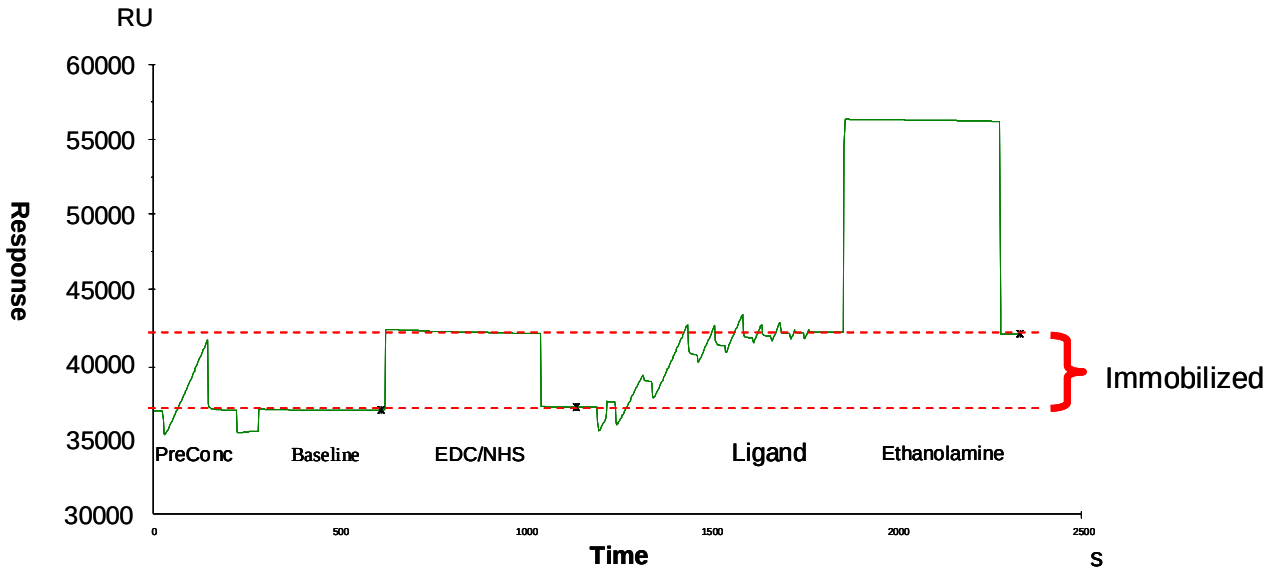

Figure 34 ***Immobilisation of the ligand laminin-1 on a CM5 sensor chip***
The dashed red line highlights the baseline before immobilisation, and the brace shows the increase in baseline after immobilisation. The amount of ligand immobilised produced a response of 5070 RU.

Streptavidin coupling was performed by first conditioning both the SA sensor-chip test surface and reference surface with three injections of 1 M NaCl in 50 mM NaOH followed by an injection of a 50 nM solution of biotinylated CCP12 on the test surface. When the desired immobilisation was reached, the remaining active groups were blocked by an injection of 1 mM biotin on both surfaces.

His-tag coupling was performed by conditioning both the NTA sensor-chip test surface and the reference surface with two injections of 50 mM NaOH, followed by an injection of 500 µM $NiSO_4$ in HBS-P+ buffer over the test surface. Both surfaces were stripped with 350 mM EDTA in PBS-P+. Finally the test surface was primed with 500 µM $NiSO_4$ in HBS-P+ followed by injection of His-tag labelled protein to desired immobilisation level.

3.3.3.4 Analyte binding

All analyses were performed on a Biacore T100 at a flow-rate of 30 µl/min. Prior to injection of analyte, both flow-cell surfaces were equilibrated with HBS-P^+ buffer. Individual analytes at various concentrations were injected over both the flow-cell that contained immobilised ligand, and over the reference flow-cell (containing no ligand), for 60 or 180 seconds and association data were collected. The surfaces were then washed with HBS-P^+ buffer for a further 300 seconds and dissociation data were collected. After each injection the chip surface was washed with regeneration buffer; 20 mM NaOH was chosen as the regeneration buffer because 50 mM $MgCl_2$, 1 M NaCl (data not shown), and 10 mM glycine pH 3 all proved to be unsuccessful (Figure 35).

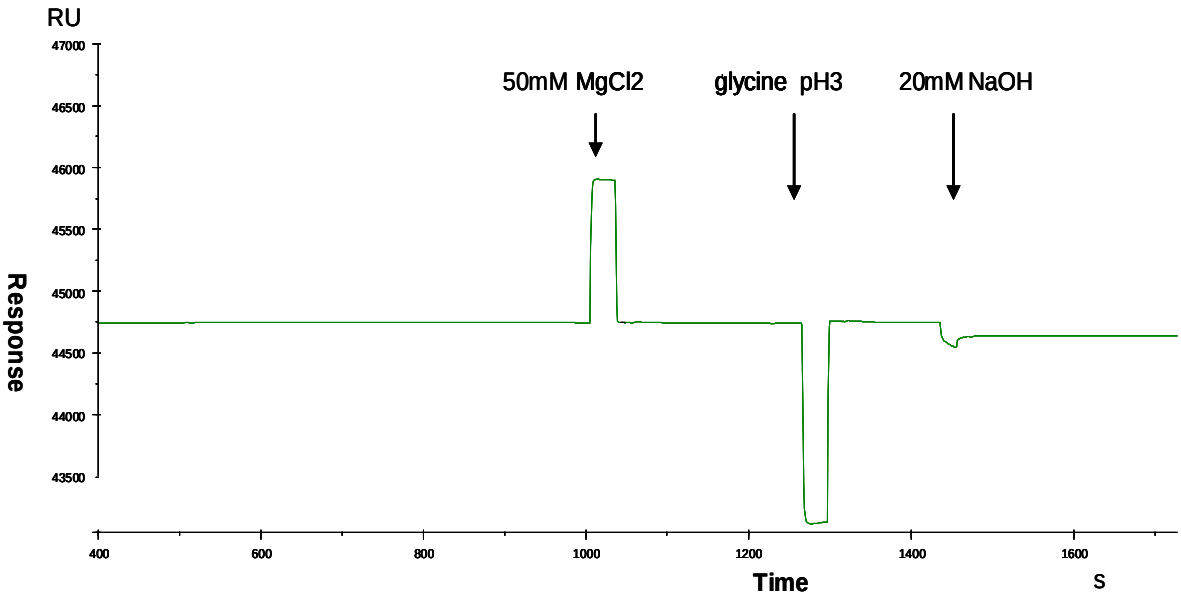

Figure 35 ***Regeneration scouting***
Various methods of regeneration were investigated in order to break up the interaction complexes under study, prior to a new injection of analyte. The sensogram shows a trace from the active surface (not reference-subtracted). $MgCl_2$, glycine and NaCl all proved unsuccessful at regenerating the surface. Sodium hydroxide successfully regenerated the surface; unfortunately it could destroy the active protein surface over time so only a very low concentration of 20 mM was used.

3.3.3.5 Data analysis

Data were analysed, and the association and dissociation constants (k_a and k_d), were calculated, using the Biacore T100 evaluation software version 1.1. In some cases the kinetic rates of binding and dissociation were too fast to fit accurately to sensogram curves, and therefore k_a and k_d could not be measured. Determination of the affinity constant (K_D), which is calculated as the concentration of ligand required to occupy 50% of available binding sites, was also attempted; however this was not possible in cases where an insufficient amount of ligand was available to achieve responses which reached equilibration.

3.4 Results

3.4.1 Determination of the interaction of $GABA_BR1aCCP$ modules with laminin-1 and laminin-10/11

The results of the SPR experiments are shown in figures 36-41, where the laminin-10/11 interaction with the various $GABA_BR1a$ modules are illustrated in figures 36-38 and the laminin-1 interaction with the modules are illustrated in figures 39-41. The results show that the double module $GABA_BR1aCCP12$ binds to laminin-10/11 immobilised on a CM5 chip (Figure 36). This interaction had previously been demonstrated in immuno-dotblot assays (as illustrated in 2.4.3.3). The sensograms show that the predominant mode of binding involves fast-on, fast-off kinetics consistent with a low (*e.g.* $K_d = 10^{-4} – 10^{-3}$ M) affinity. Furthermore, as shown in Figure 39, $GABA_BR1aCCP12$ also binds to immobilised laminin-1. In this case, there are at least two components to the sensorgrams; a fast-on, fast-off (low affinity) process is superimposed on a much slower association/dissociation (higher affinity). It proved unfeasible to extract any reliable affinity constants from this data, as the response does not reach equilibrium. Interestingly, the number of response units recorded for the interaction with laminin-1 is greater than obtained with laminin-10/11 despite the same level of each laminin having been coupled to the chip (100 RU) – this implies laminin-1 has, overall, a higher affinity for $GABA_BR1aCCP12$ compared to lamininin-10/11.

The binding of single-module, $GABA_BR1aCCP1$, to the immobilised laminin-10/11 (Figure 37), is dominated by a slow association rate ($k_a = 150\ ms^{-1}$) and a complex

dissociation curve that has a very slow component. Due to strong binding of CCP1 to both laminin surfaces, the regeneration protocol is insufficient at successive higher concentrations of analyte, which explains the poor reproducibility obtained for the highest CCP1 concentrations in the binding level plot (Figure 42). Attempts to fit the sensorgrams to various models – 1:1 binding, bivalent analyte, two-state reaction – were unsuccessful and therefore it was not possible to extract a K_d value for this interaction. Nonetheless, the overall slow-on/slow-off behaviour is consistent with a high-affinity aspect to the binding. The sensorgrams for $GABA_BR1aCCP1$ binding to laminin-1 (Figure 40) are particularly difficult to interpret and could be explained in several ways including the possibility of non-specific aggregation/precipitation at the chip surface – therefore these data were not considered further.

In the case of $GABA_BR1aCCP2$, binding to both laminin-10/11 (Figure 38) and laminin-1 (Figure 41) produces very low responses, although there is some evidence of slow on and off-rates. Furthermore, the interaction appeared to have reached saturation prior to the end of the injection, which was not the case for the CCP1 module interaction. In summary, module CCP2 shows a much weaker binding compared to both the CCP1 module (for laminin-10/11) and the CCP12 double module.

In general, the analyses of the interactions studied were reproducible, as indicated by the superimposable response curves of the duplicate injections; the exception is the CCP1 module injected at higher concentrations.

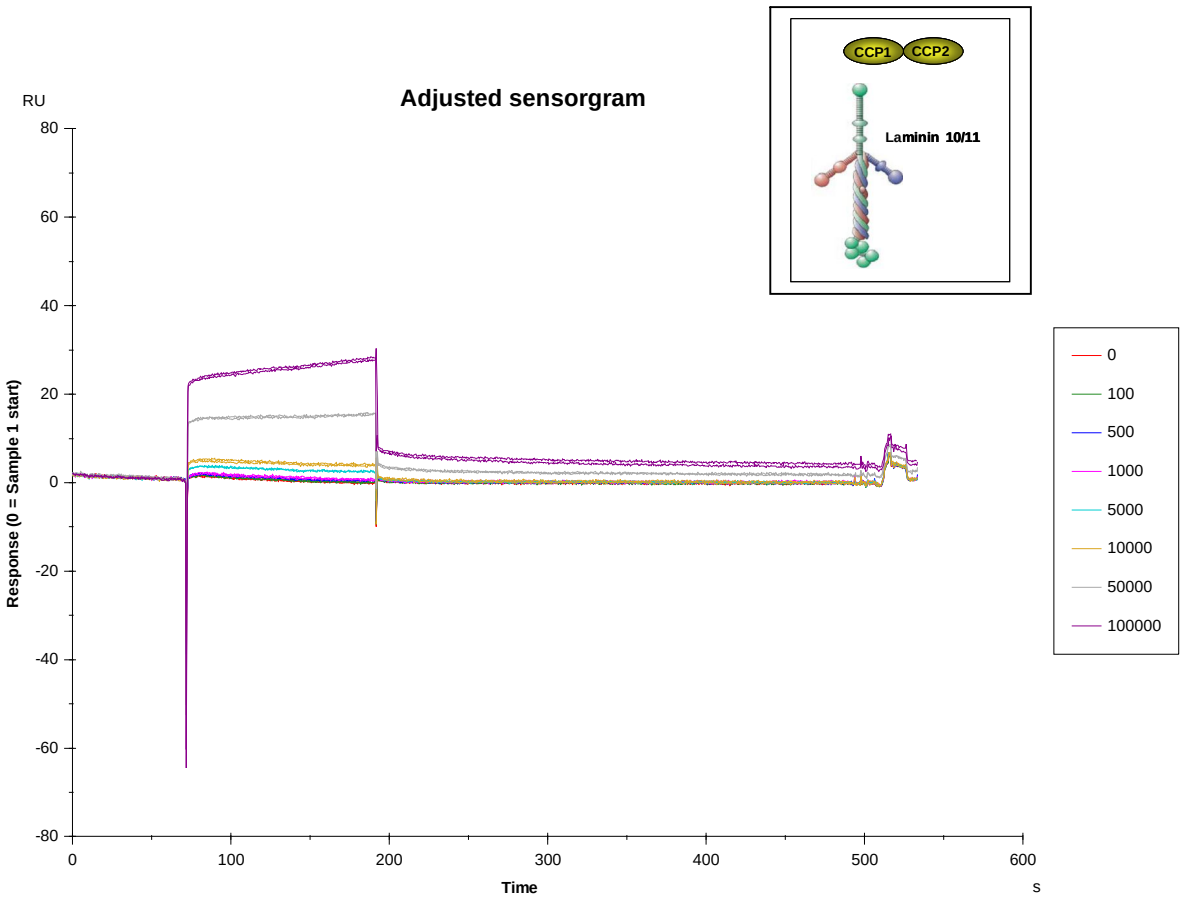

Figure 36 *Sensogram illustrating the binding of the GABA$_B$R1aCCP12 to laminin-10/11*
The CCP12 module-pair was injected over the sensor surfaces at concentrations ranging from 100 nM - 100 µM (see key, concentrations in nM). The inset shows the proteins tested for interaction in the experiment. Adjustment of sensogram consists of the reference readings beeing subtracted from the data.

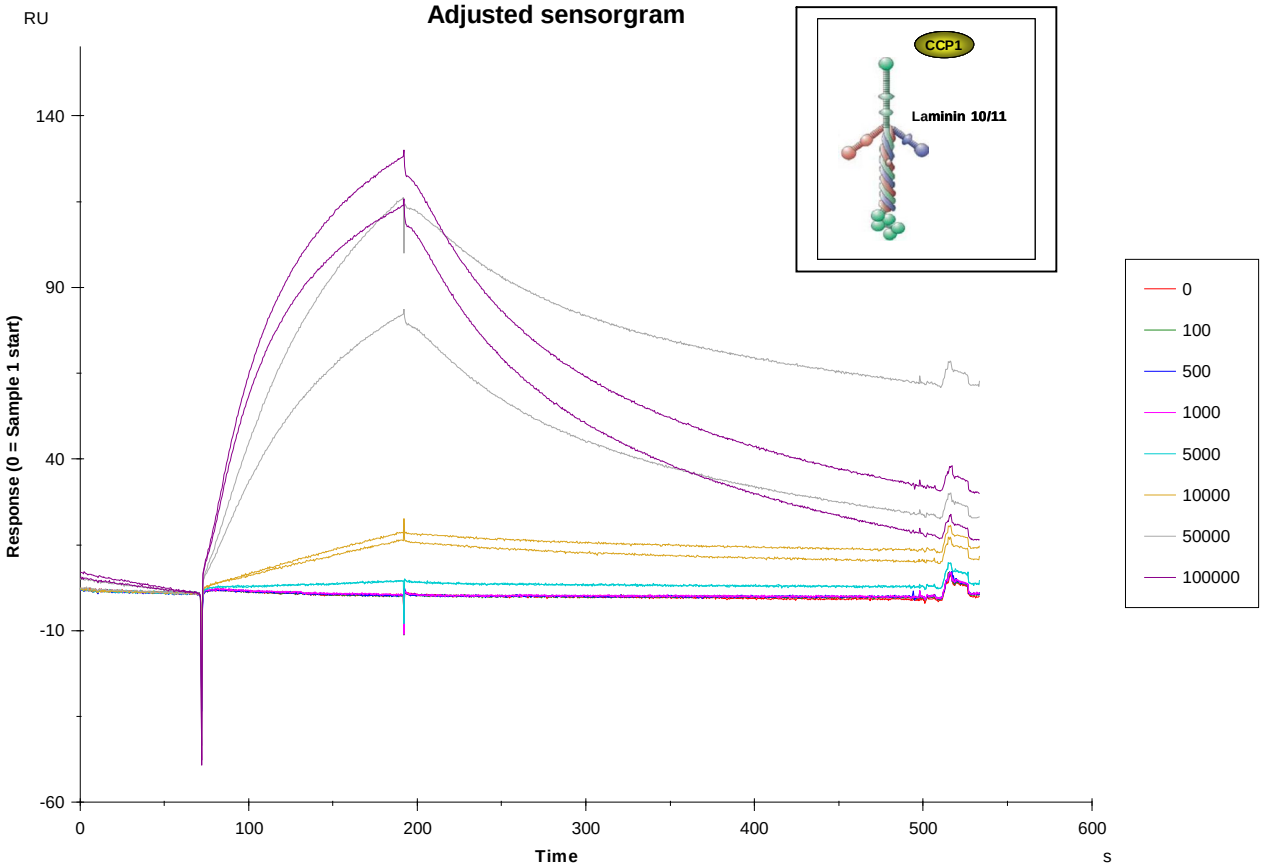

Figure 37 ***Sensogram illustrating the binding of the GABA$_B$R1aCCP1 to laminin-10/11***
The CCP1 module was injected over the sensor surfaces at concentrations ranging from 100 nM - 100 µM (see key, concentrations in nM). Other figure legend as in Figure 36.

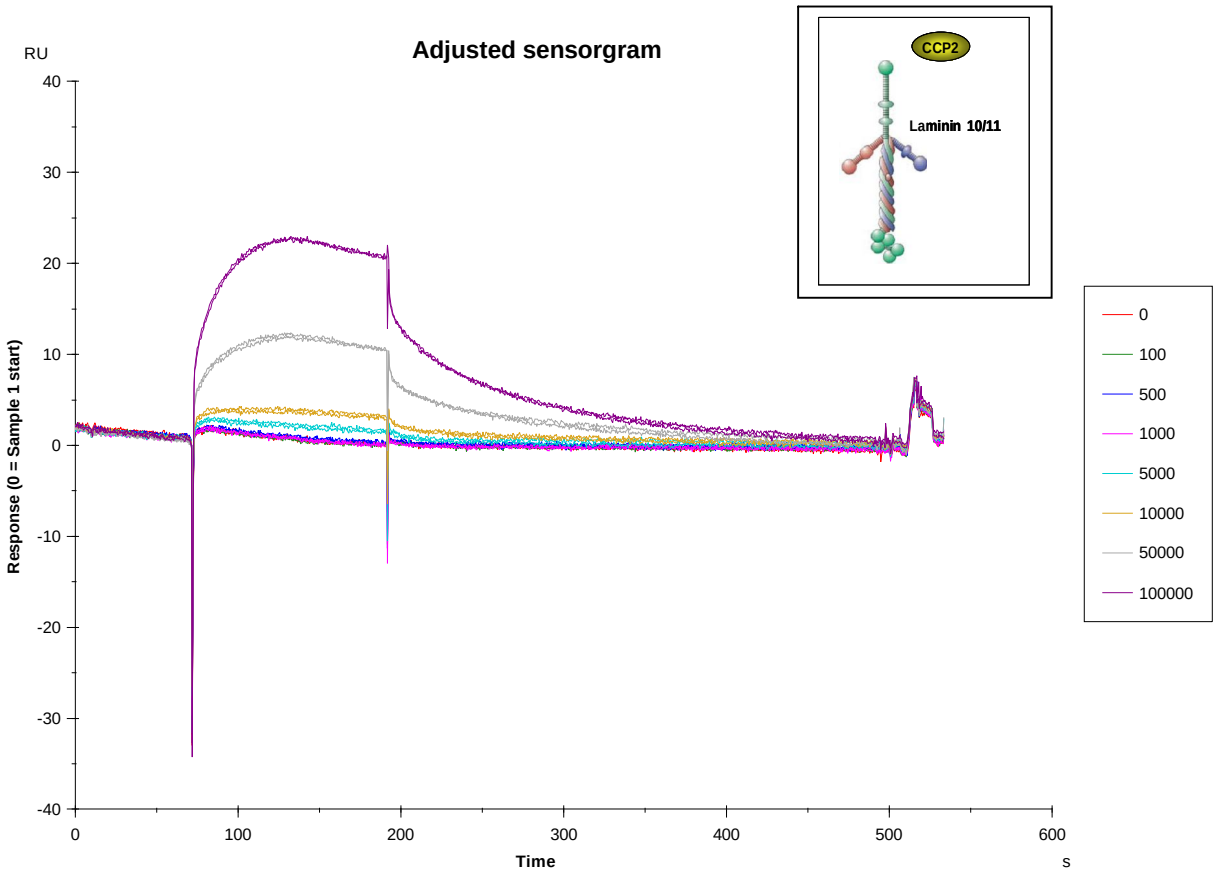

Figure 38 ***Sensogram illustrating the binding of GABA$_B$R1aCCP2 to laminin-10/11***
The CCP2 module was injected over the sensor surfaces at concentrations ranging from 100 nM - 100 µM (see key, concentrations in nM). Other figure legend as in Figure 36.

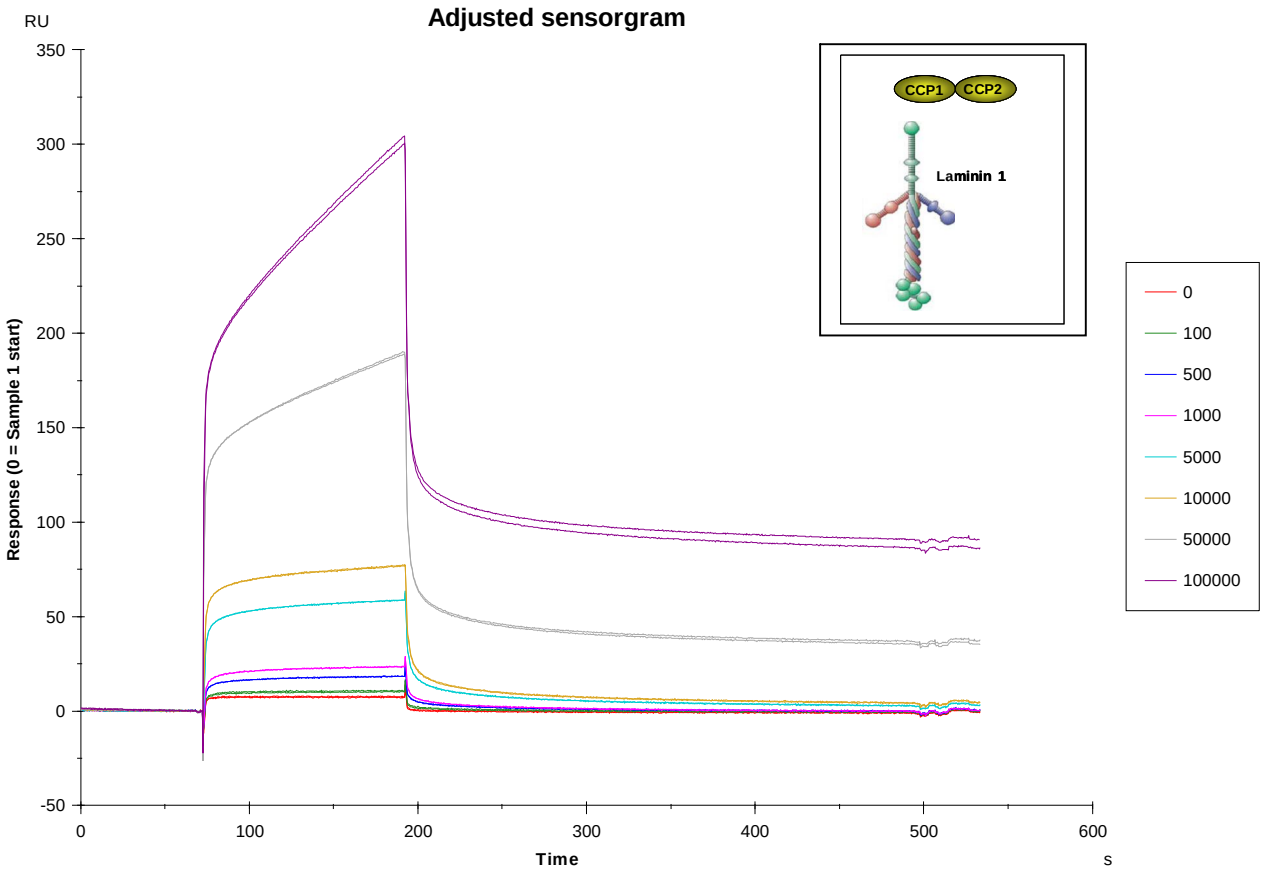

Figure 39 ***Sensogram illustrating the binding of $GABA_BR1aCCP12$ to laminin-1***
The CCP12 module-pair was injected over the sensor surfaces at concentrations ranging from 100 nM - 100 µM (see key, concentrations in nM). Other figure legend as in Figure 36.

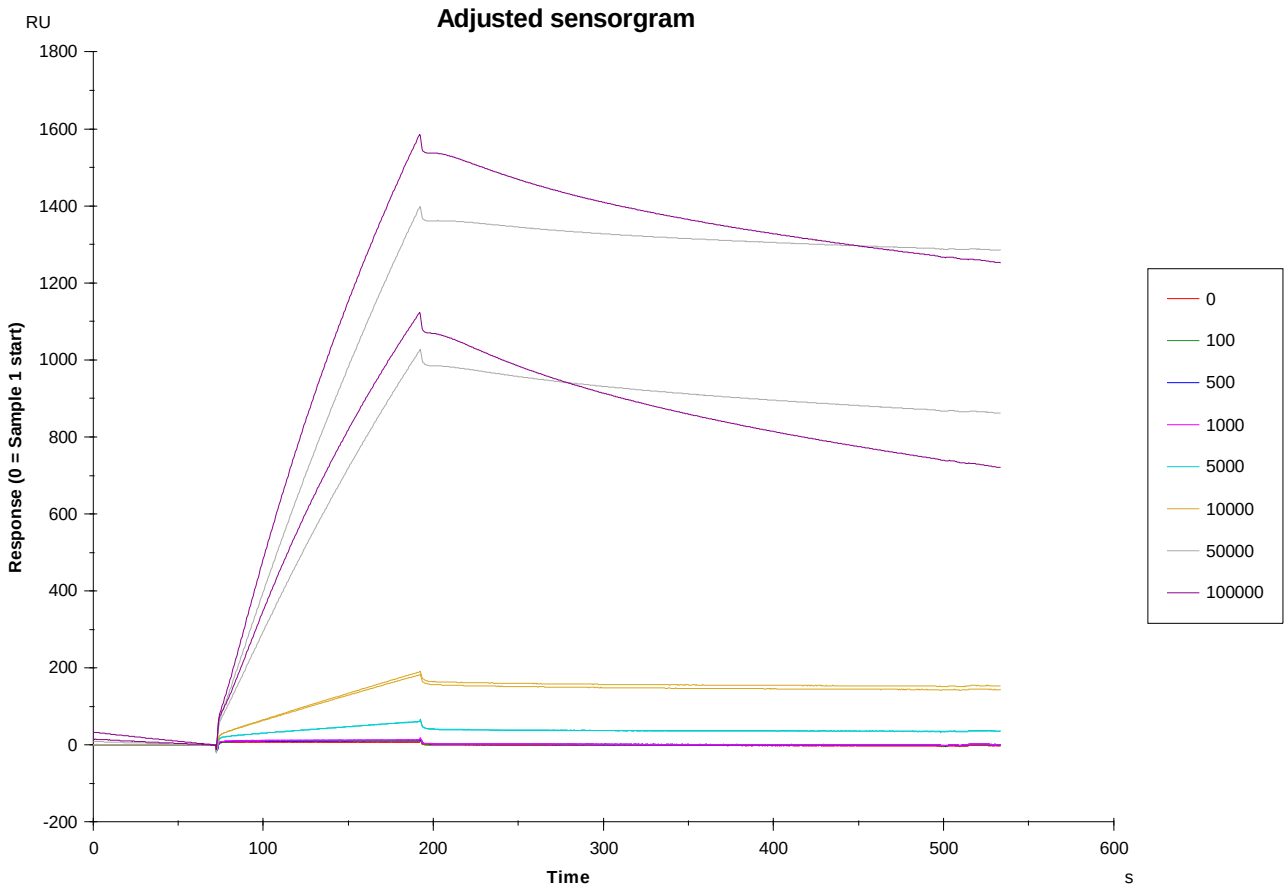

Figure 40 ***Sensogram illustrating the binding of GABA$_B$R1aCCP1 to laminin-1***
The CCP1 module was injected over the sensor surfaces at concentrations ranging from 100 nM - 100 µM (see key, concentrations in nM). Other figure legend as in Figure 36.

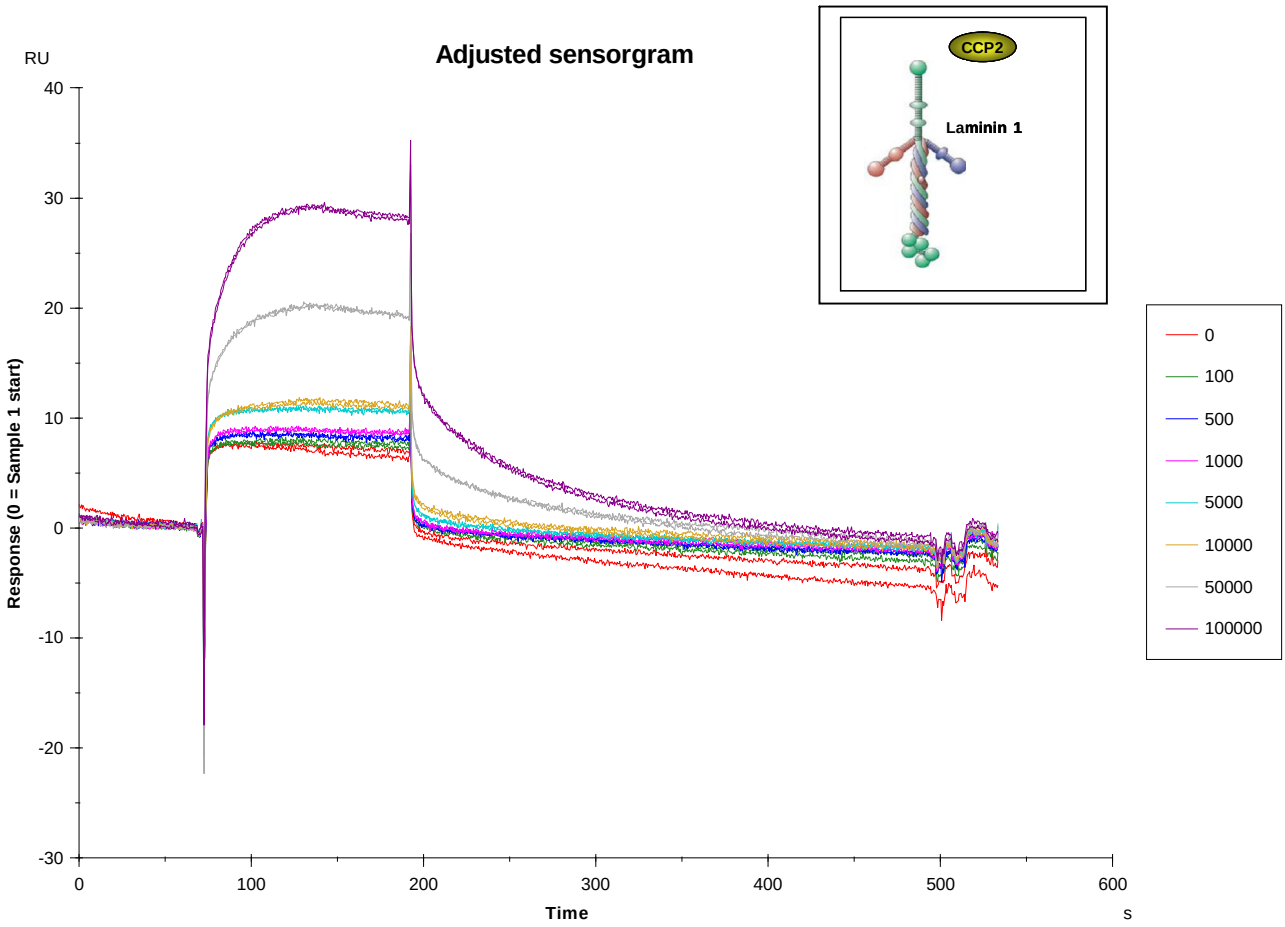

Figure 41 ***Sensogram illustrating the binding of GABA$_B$R1aCCP2 to laminin-1***
The CCP2 module was injected over the sensor surfaces at concentrations ranging from 100 nM - 100 µM (see key, concentrations in nM). Other figure legend as in Figure 36.

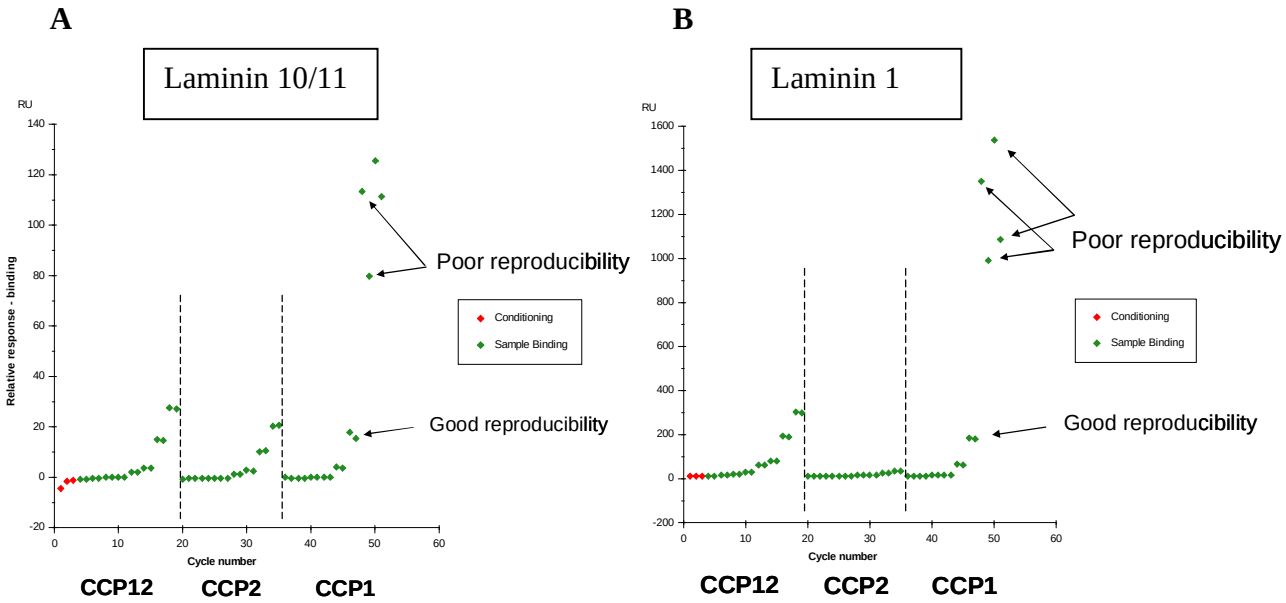

Figure 42 ***Binding level plots providing an overview of the binding levels of the $GABA_BR1aCCP$ modules to laminin-10/11 and laminin-1 respectively***
Plot A represents binding to immobilised laminin-10/11. Plot B represents binding to immobilised laminin-1. Each green point represents a binding response, injected ligands (in increasing concentrations) are labelled below the plots. Due to the difficulties in regenerating the chip surface after CCP1 injections, the last data points exhibited poorer reproducibility *i.e.* duplicate injections did not produce similar responses.

To further verify the binding, $GABA_BR1aCCP12$ was immobilised on a CM5 chip in order for the interaction to be studied in reverse, *i.e.* using laminin as the analyte. However, this proved unsuccessful initially, as the amine-coupled CCP modules appeared not to bind laminin-1 or laminin-10/11 (data not shown). An alternative immobilisation strategy for immobilisation was therefore used, whereby $GABA_BR1aCCP12$ that had been labelled with biotin (previously, by Dr Stan Blein) was coupled to a streptavidin-coated (SA) sensor-chip surface. In this new format, $GABA_BR1aCCP12$ was successfully shown to bind to laminin-1 (Figure 43); a weak but detectable interaction was also observed in the case of laminin-10/11 (Figure 44). This

strategy for immobilising $GABA_BR1aCCP12$ was adopted for further studies involving the screening of laminin fragments, as described in 3.4.2.

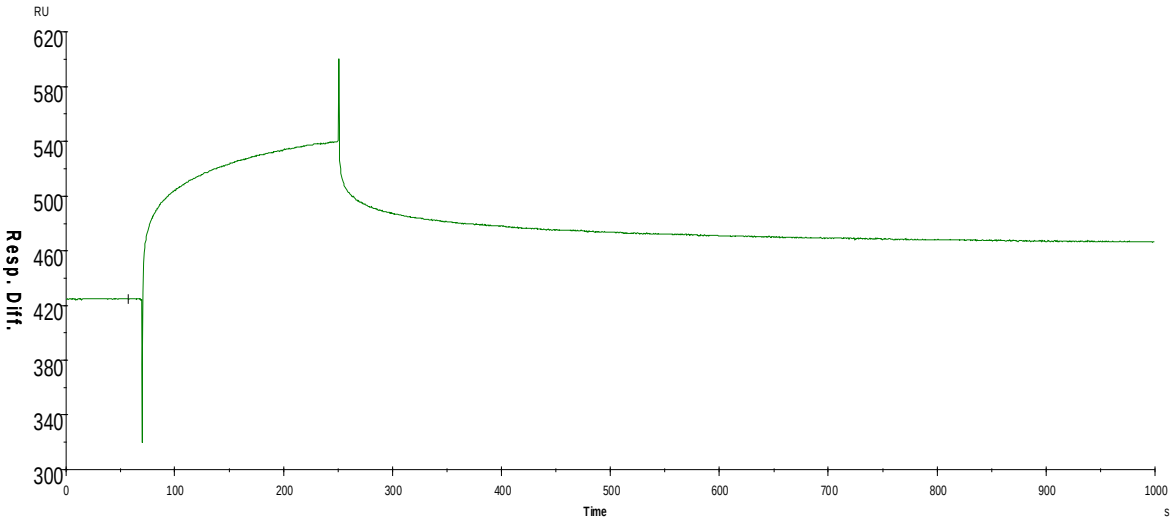

Figure 43 Laminin-1 binds to immobilised $GABA_BR1aCCP12$
The biotinylated CCP12 was immobilised on an SA-sensor chip surface. A sensogram resulting from injection of 1 µM laminin-1 demonstrates binding to $GABA_BR1a$-CCP12. The reference reading has been subtracted from the data.

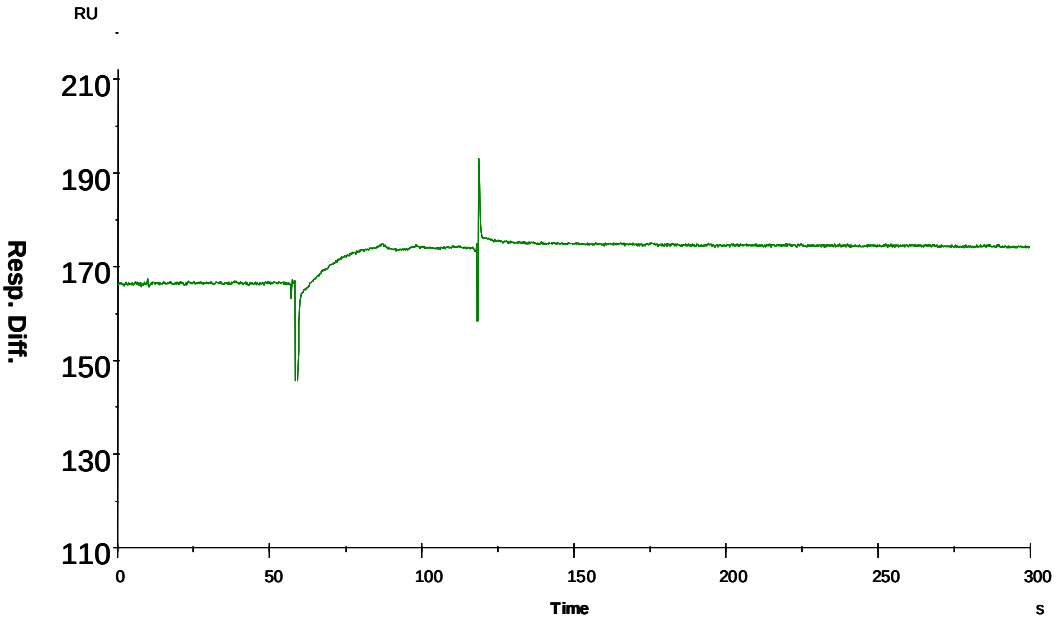

Figure 44 *Laminin-10/11 binds very weakly to immobilised $GABA_BR1aCCP12$*
Biotinylated *CCP1-2 was immobilised on an SA sensor chip.* The sensogram illustrates an injection of 0.5 µM laminin-10/11 and shows that the protein is binding weakly but detectably to $GABA_BR1a$-CCP12 immobilised in this orientation. The reference reading has been subtracted from the data.

3.4.2 Screening of laminin fragments as interaction partners for $GABA_B$ receptor modules CCP12

A range of laminin fragments was employed to map the potential protein interaction domains within laminin. These had been recombinantly expressed, or obtained by digestion of full-length laminin, and subsequently purified by Dr Takako Sasaki.

Table 6 Fragments of laminin screened for interaction with $GABA_B$R1aCCP12. The fragments are shown in Figure 45.

Fragment	**M_W (kDa)**
LN 86 (fullength laminin-1)	800
L2020 (laminin-1) [Sigma]	800
LN 78 (E1X-Nd)	450
LN 65 (E10)	25
LN65a (P1X)	350
LN73 (E4)	75
Recombinant α1 VI/V	60
Recombinant α1 VIb/IIIa	150
Recombinant β1 VI/V	60
Reconbinant γ1 VI/V	60
Recombinant α1 LG1-3	82
Recombinant α1 LG4-5	44
Recombinant α5 LG1-3	57
Recombinant α5 LG4-5	39.5

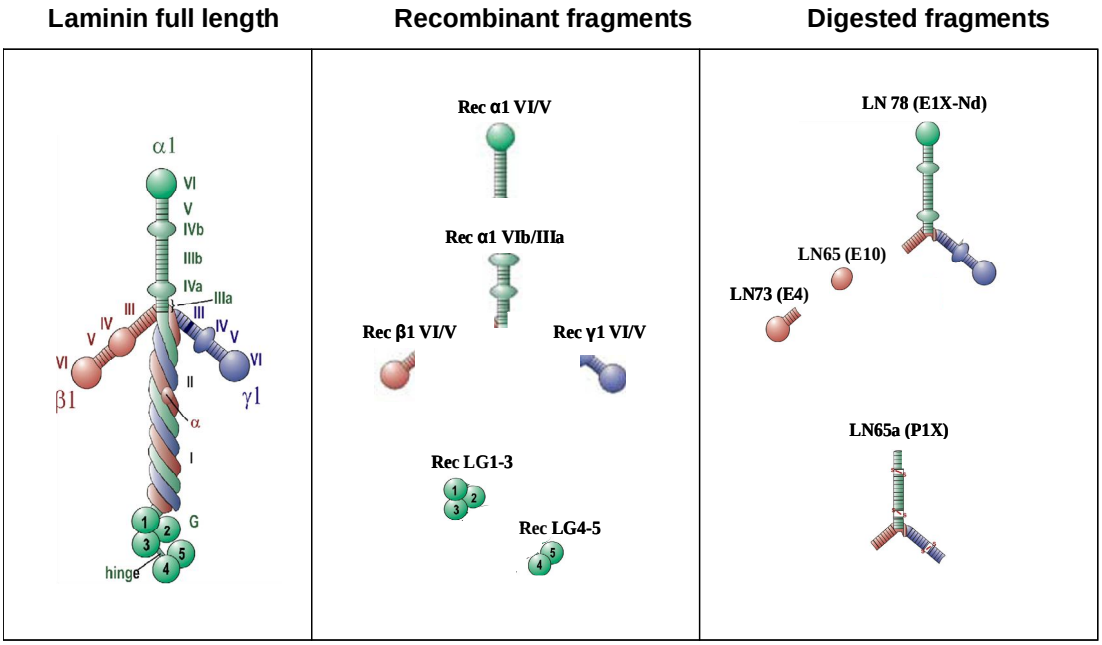

Figure 45 ***Overview of laminin fragments used in screen, as described in Table 6***
The laminin fagments were either recombinantly expressed or digested from intact laminin and purified (provided by Sasaki). The chains are coloured as previously described in Figure 10.

Sensograms for the different laminin fragment binding (or otherwise) to CCP12 are shown in Figure 46.

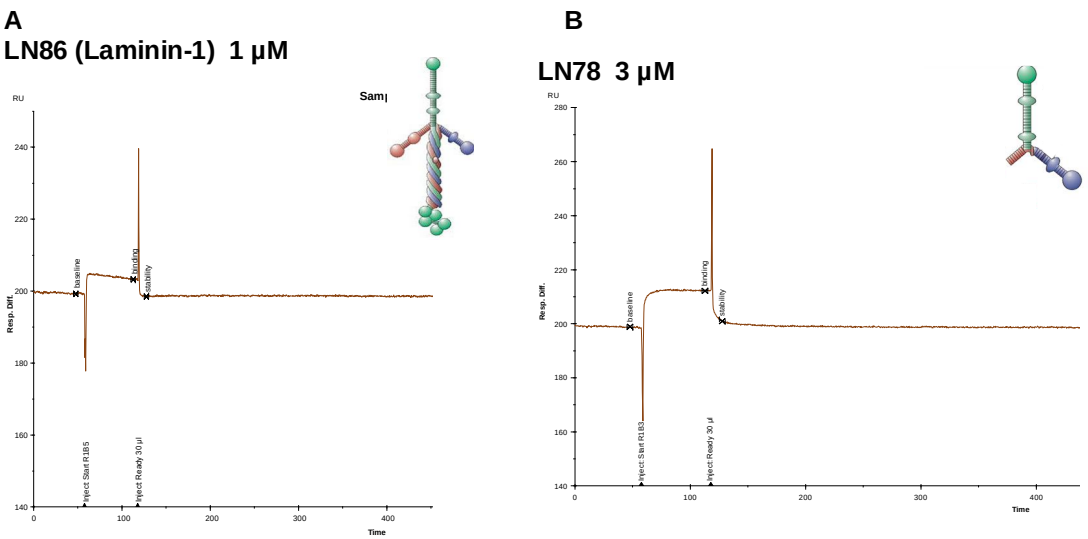

Figure 46 ***Sensograms showing the range of laminin fragments described in Table 6 injected over immobilised GABA$_B$R1a-CCP12***
The reference readings have been subtracted from the data. Inserted image illustrate the laminin fragment used as analyte for each sensogram. The responses can also be found in Table 7.

C
LN 65a 3 µM

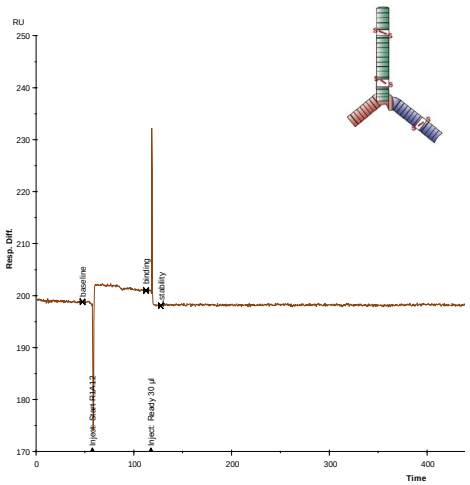

D
LN65 3 µM

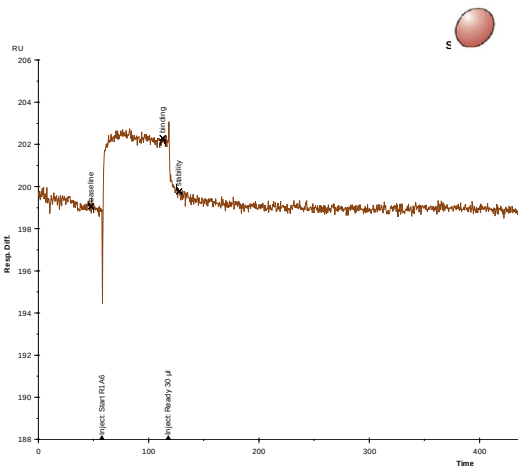

E
LN73 2 µM

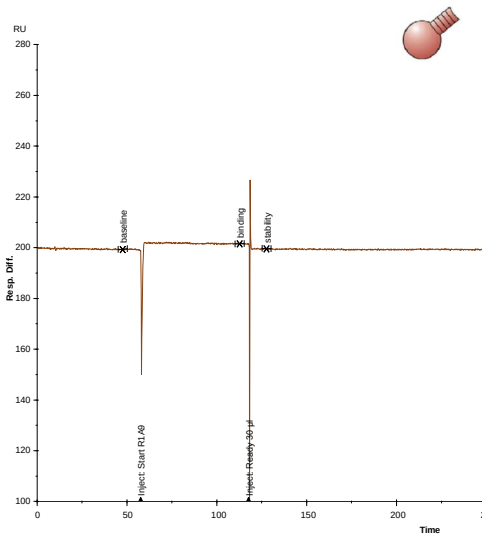

F
rec α1 VI/V 3 µM

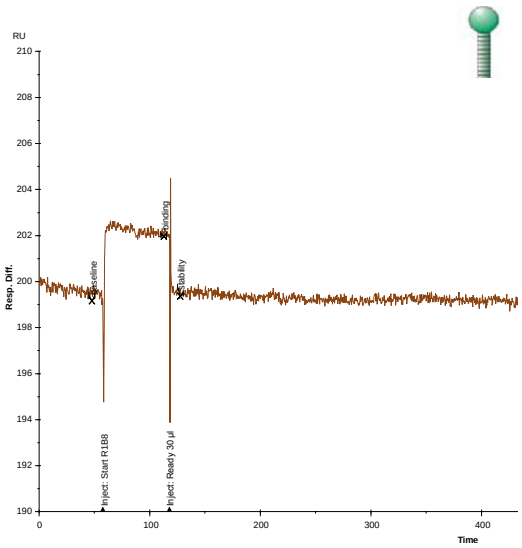

Figure 46 continued.
Spikes seen at the beginning/end of injections are due to running- and sample buffers not being perfectly matched. The reference readings have been subtracted from the data. The responses can also be found in Table 7.

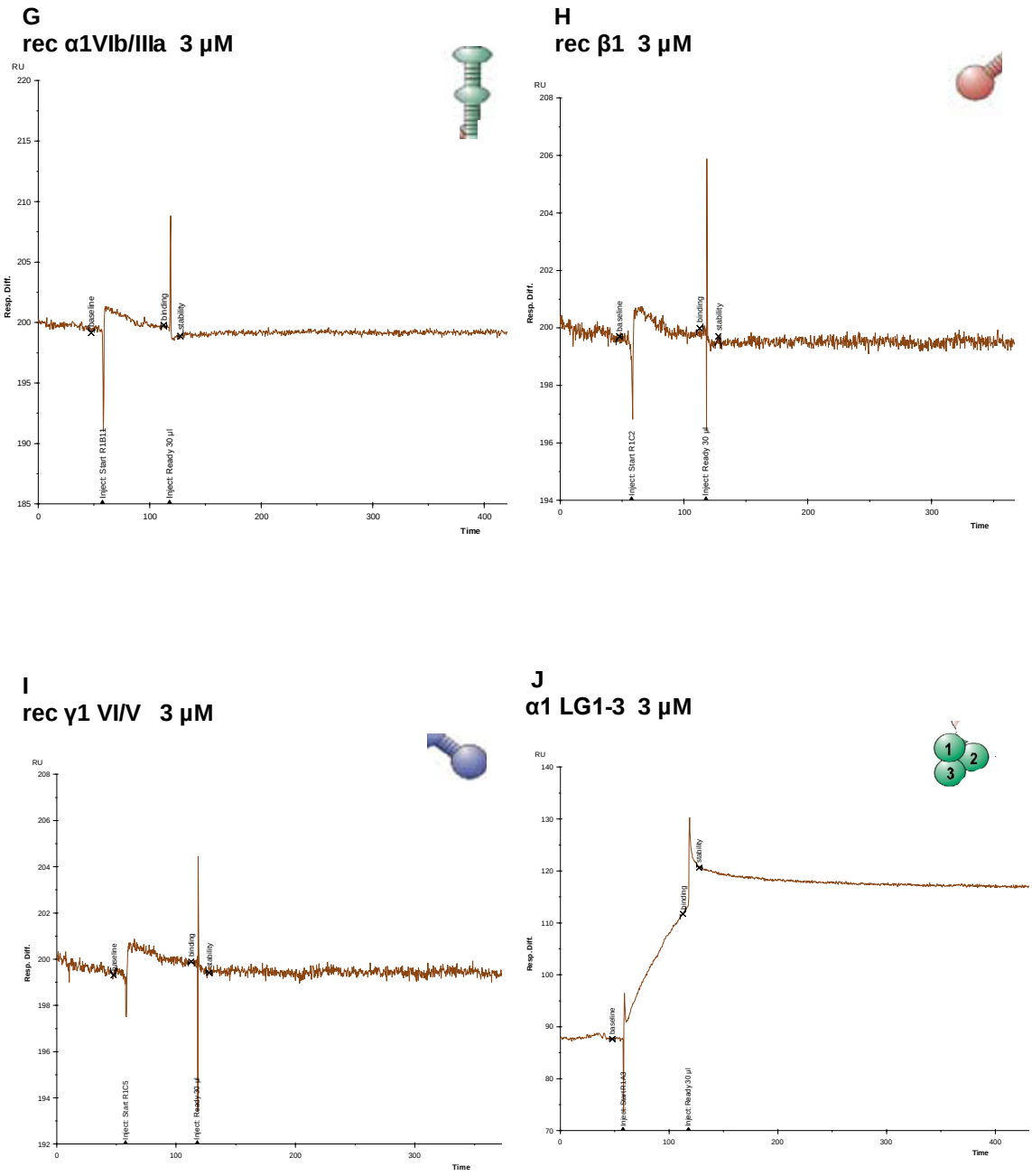

Figure 46 continued. ***Sensograms showing the range of laminin fragments described in Table 6 injected over immobilised GABA$_B$R1a-CCP12***
The reference readings have been subtracted from the data. The responses can also be found in Table 7.

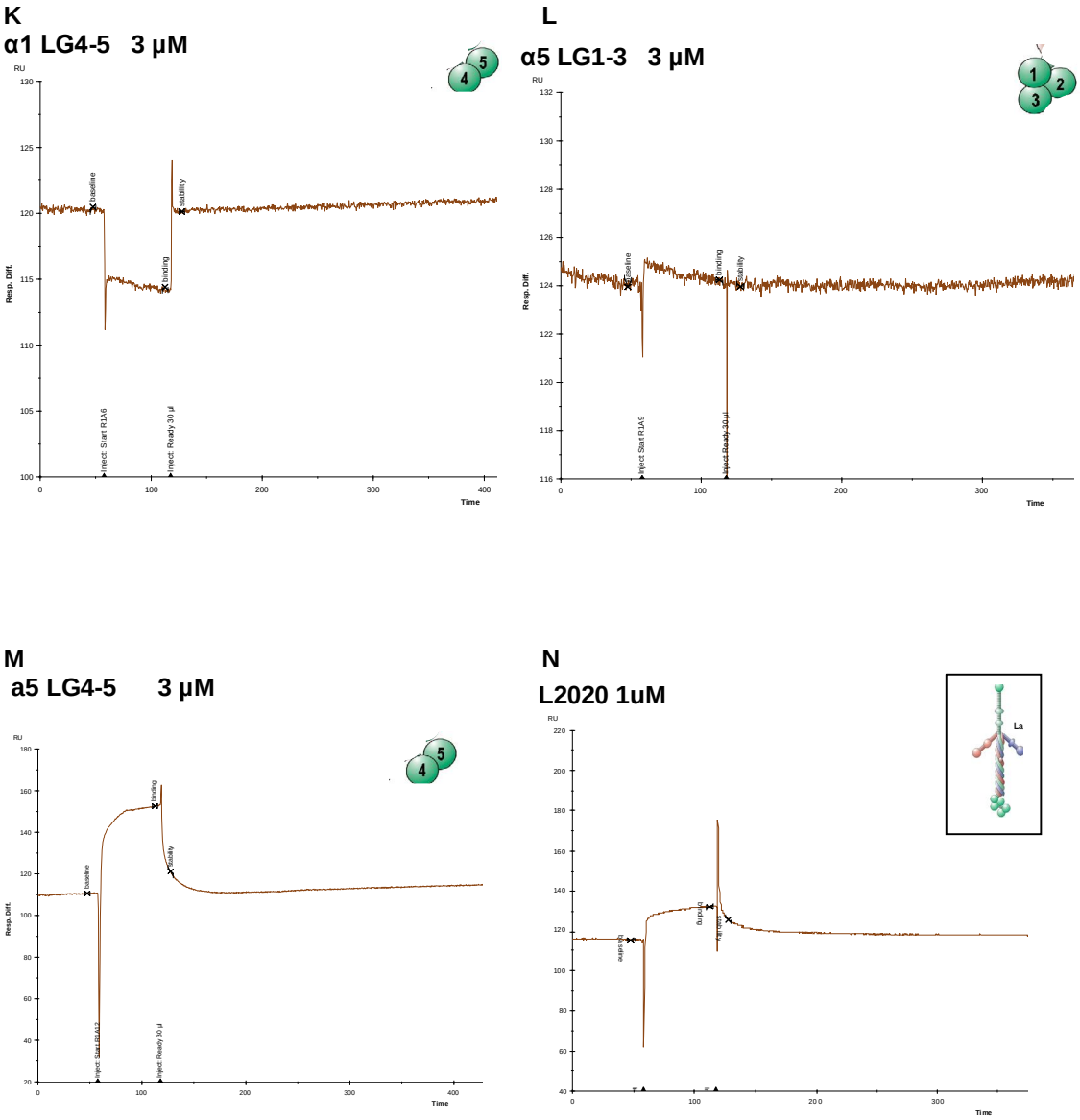

Figure 46 *continued.*
Spikes seen at the beginning/end of injections are due to running- and sample buffers not being perfectly matched. The α1 LG4-5 fragment gives a negative response, indicating that the fragment binds non-specifically and more to the reference surface. The reference readings have been subtracted from the data. The responses can also be found in Table 7.

The sensograms obtained from SPR experiments in which these fragments were injected over biotin-immobilsed $GABA_BR1aCCP12$ are shown in Figure 46. Interestingly, the shapes of the sensograms for the interaction between α1 LG1-3 and $GABA_BR1aCCP12$ are similar to those of the difficult-to-interpret sensograms obtained for the laminin-1/ $GABA_BR1aCCP1$ interaction; this might suggest similar events - aggregation or precipitation, for example - occurring in both cases. The interaction between α5 LG4-5 and $GABA_BR1aCCP12$, on the other hand, is the most convincing, and appears to be of higher affinity compared to the other fragments screened. This result is in agreement with the immuno-dotblots (Section 2.4.3.3). The α1 LG4-5 fragment gives a negative response, which is most likely caused by nonspecific binding to the reference surface. The LG4-5 of the α1- and α5 chains are 25% identical (and have 32% conserved substitutions) as seen by the sequence alignment in Figure 47.

```
CLUSTAL 2.0.10 multiple sequence alignment


Lama1_LG4-5      KKLSVELSIRTFASSGLIYYMAHQN--QADYAVLQLHGGRLHFMFDLGKGRTKVSHPALL 58
Lama5_LG4-5      NWPSLSMHVLPRSSRGLLLFTARLRPGSPSLALFLSNGHFVAQMEGLG-TRLRAQSRQRS 59
                 :  *:.: : . :* **: : *: .  ... *::  :*  :  * .**  * :..

Lama1_LG4-5      SDGKWHTVKTDYVKRKGFITVDGR---ESPMVTVVGDGTMLDVEGLFYLGGLPSQYQARK 115
Lama5_LG4-5      RPGRWHKVSVRWEKNRILLVTDGARAWSQEGPHRQHQGAEHPQPHTLFVGGLPASSHSSK 119
                   *:**.*.. : *.: ::..**    ..       :*:       :::****:. :: *

Lama1_LG4-5      IGNITHSIPACIGDVTVNSKQLDKDSPVSAFTVNRCYAVAQEGTYFDGSGYAALVKEGYK 175
Lama5_LG4-5      LP-VTVGFSGCVKRLRLHGRPLGAPTRMAGVTP-CILGPLEAGLFFPGSGGVITLDLPGA 177
                 :  :* .:..*:  : ::.: *.  : ::..*     .  : * :* *** .  :.

Lama1_LG4-5      VQSDVNITLEFRTSSQNGVLLGISTAKVD-AIGLELVDGKVLFHVNNGAGRITAAYEPKT 234
Lama5_LG4-5      TLPDVGLELEVRPLAVTGLIFHLGQARTPPYLQLQVTEKQVLLRADDGAGEFSTSVT--R 235
                 . .**.: **.*. : .*::: :. *:.   : *::.: :**::.::***.::::

Lama1_LG4-5      ATVLCDGKWHTLQANKSKHRITLIVDGNAVGAESPHTQSTSVDTNNPIYVGGYPAGVKQK 294
Lama5_LG4-5      PSVLCDGQWHRLAVMKSGNVLRLEVDAQSNHTVGP-LLAAAAGAPAPLYLGGLPEPMAVQ 294
                 .:*****:** * . ** : : * **.::  : .*   :::..:  *:*:** *  :  :

Lama1_LG4-5      CLRSQTSFRGCLRKLALIKS 314
Lama5_LG4-5      PWP--PAYCGCMRRLAVNRS 312
                      .:: **:*:**: :*
```

Figure 47 ***Sequence alignment of laminin α1 lG4-5 and α5 lG4-5***

In order to compare the responses for each fragment used in this interaction study, the response was reported as 'RUs per kilodalton' (kDa) (Table 7). This was necessary as the response signal measured depends on the molecular weight of the analyte - *i.e.* a large analyte gives a larger RU value than a small analyte for the same number of molecules bound to the sensor surface.

Table 7 *Responses, normalised for molecular weight, obtained on the Biacore T100 when various laminin fragments were injected over $GABA_BR1aCCP12$ immobilised on a CM5-sensor chip.*

Fragment	**CCP12 response (RU) for 3 µM ligand, unless otherwise stated**	**Analyte M_W(kDa)**	**Normalised response (RU/kDa)**
LN 86 (laminin-1)	5 (1 µM)	800	0.0063 (0.19*)
LN 78 (EX1Nd)	13.6	450	0.030
LN 65 (E10)	3.2	25	0.13
LN65a (P1X)	2.2	350	0.006
LN73 (E4)	2.2 (2 µM)	75	0.029 (0.044*)
Recombinant α1 VI/V	2.6	60	0.043
Recombinant α1 VIb/IIIa	0.2	150	0.0013
Recombinant β1 VI/V	0.2	60	0.0033
Reconbinant γ1 VI/V	0.4	60	0.0067
Reconbinant α1 LG1-3	24.7	82	0.20
Reconbinant α1 LG4-5	-5.9	44	-
Reconbinant α5 LG1-3	0.1	57	0.0018
Reconbinant α5 LG4-5	41.9	39.5	1.1
L2020 (laminin-1)	85.0 (1 µM)	800	0.11 (0.31*)

* If further normalised to a 3 µM analyte concentration, and based on an assumption that this concentration is << Kd

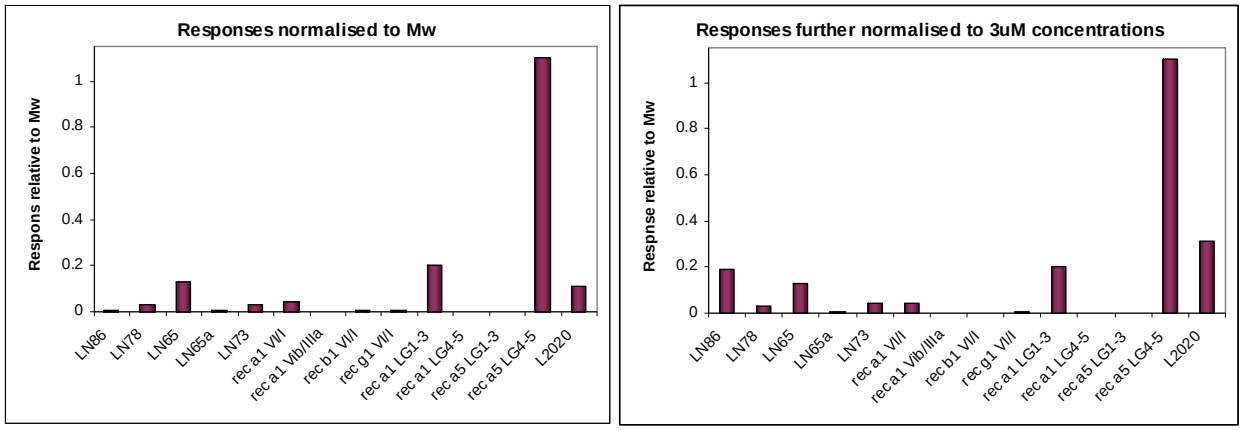

Figure 48 ***Bar graphs illustrating a comparison of the responses for each laminin fragment***
The two bar graphs show the two alternative analyte normalisations discussed in Table 7. The fragments α5 LG4-5, α1 LG1-3, LN 65 (E10) and full length laminin-1 (L2020) (figure 46, panel M, panel J, pandel D and panel N respectively) appear to bind the best to $GABA_BR1aCCP12$. However, from inspection of the sensograms inFigure 46, the interaction of α1 LG1-3 is questionable and might be an artefact of precipitation.

Since laminin-1 and laminin-10/11 had been shown to interact with $GABA_BR1aCCP12$, both in immuno-dotblot assays (see Section 2.4.3.3) and by SPR it was decided to investigate these interactions in more detail. The recombinantly expressed α1 LG1-3 and α1 LG4-5 (*i.e.* fragments from the α-chain of laminin-1) and α5 LG4-5 (*i.e.* a fragment of laminin-10/11) were immobilised (by amine-coupling) on a CM5 chip surface. The active surfaces were used to test for binding of some or all of $GABA_BR1aCCP12$, -CCP1 and -CCP2. No detectable binding could be demonstrated (data not shown). In an alternative strategy, a hexa-His-tagged version of α5 LG4-5 (provided by Dr Takako Sasaki) was immobilised on a NTA sensor chip; injection of $GABA_BR1aCCP12$ over this sensor chip yielded sensorgrams (Figure 49) that are similar, overall, to the results obtained when the double CCP module contruct was flowed over immobilised full-length laminin (Figure 39). Evidence for binding to α5

LG4-5 immobilised on the NTA-chip was also obtained for both $GABA_BR1aCCP1$ (Figure 50) and $GABA_BR1aCCP2$ (Figure 51), however, as with full-length laminin-1, the CCP1 fragment appears to dissociate very slowly from the test surface, possible due to aggregation/precipitation.

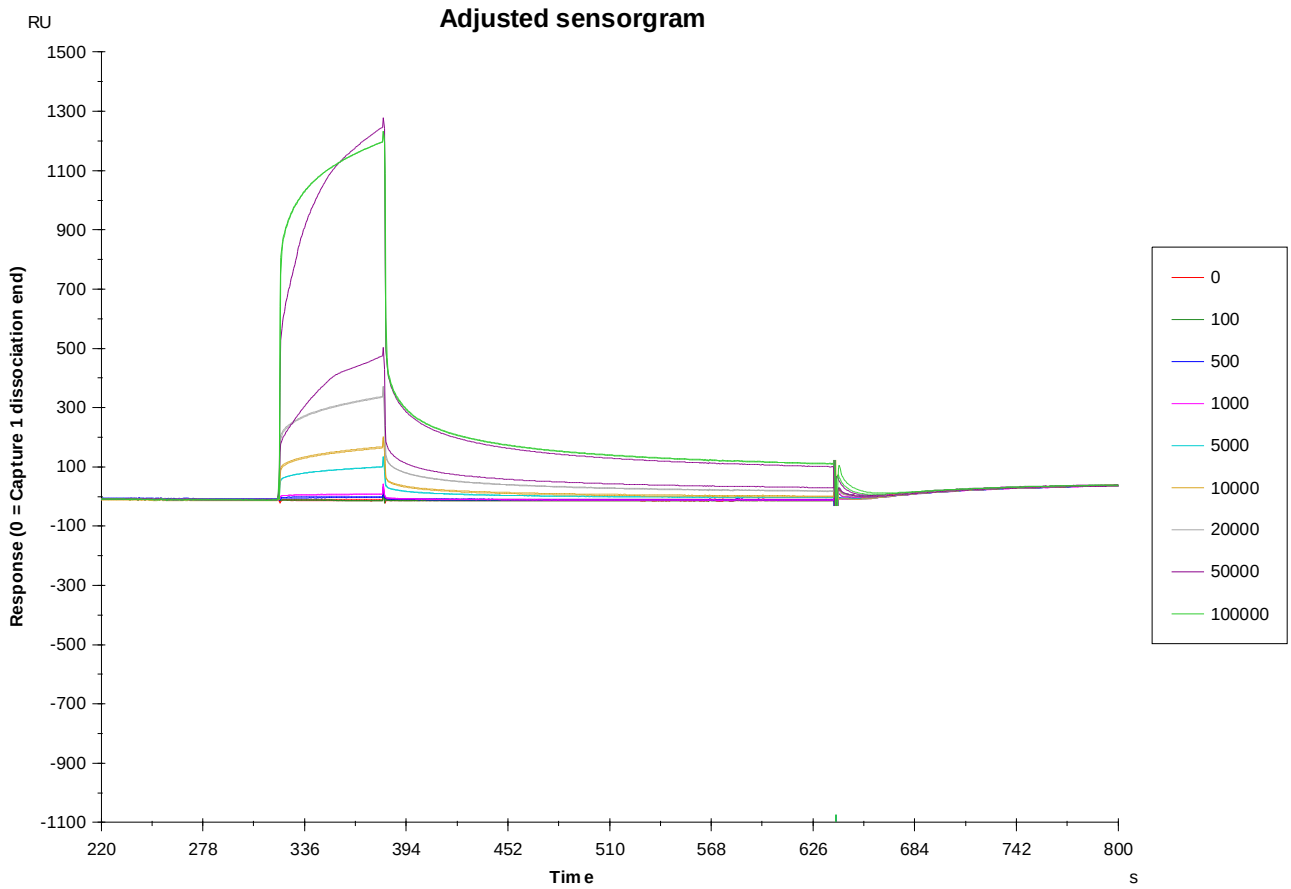

Figure 49 ***Sensogram illustrating the binding of $GABA_BR1aCCP12$ to α5 LG4-5***
The CCP12 double module was injected over the NTA sensor chip surfaces at concentrations ranging from 100 nM - 100 µM (see key, concentrations in nM). Adjustment of sensogram was performed by subracting reference readings from the data.

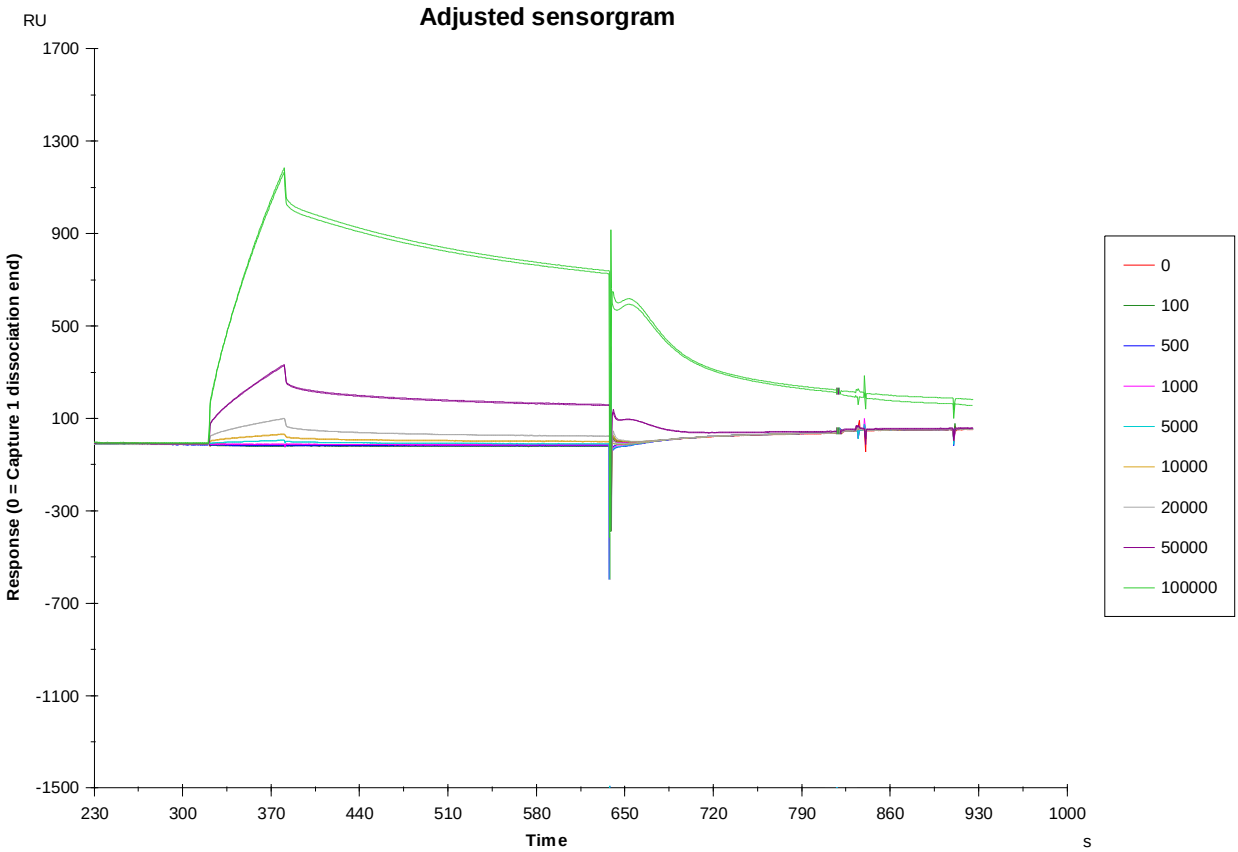

Figure 50 ***Sensogram illustrating the binding of $GABA_BR1aCCP1$ to α5 LG4-5***
The CCP1 single module was injected over the NTA sensor chip surfaces at concentrations ranging from 100 nM - 100 µM (see key, concentrations in nM). Adjustment as in Figure 49.

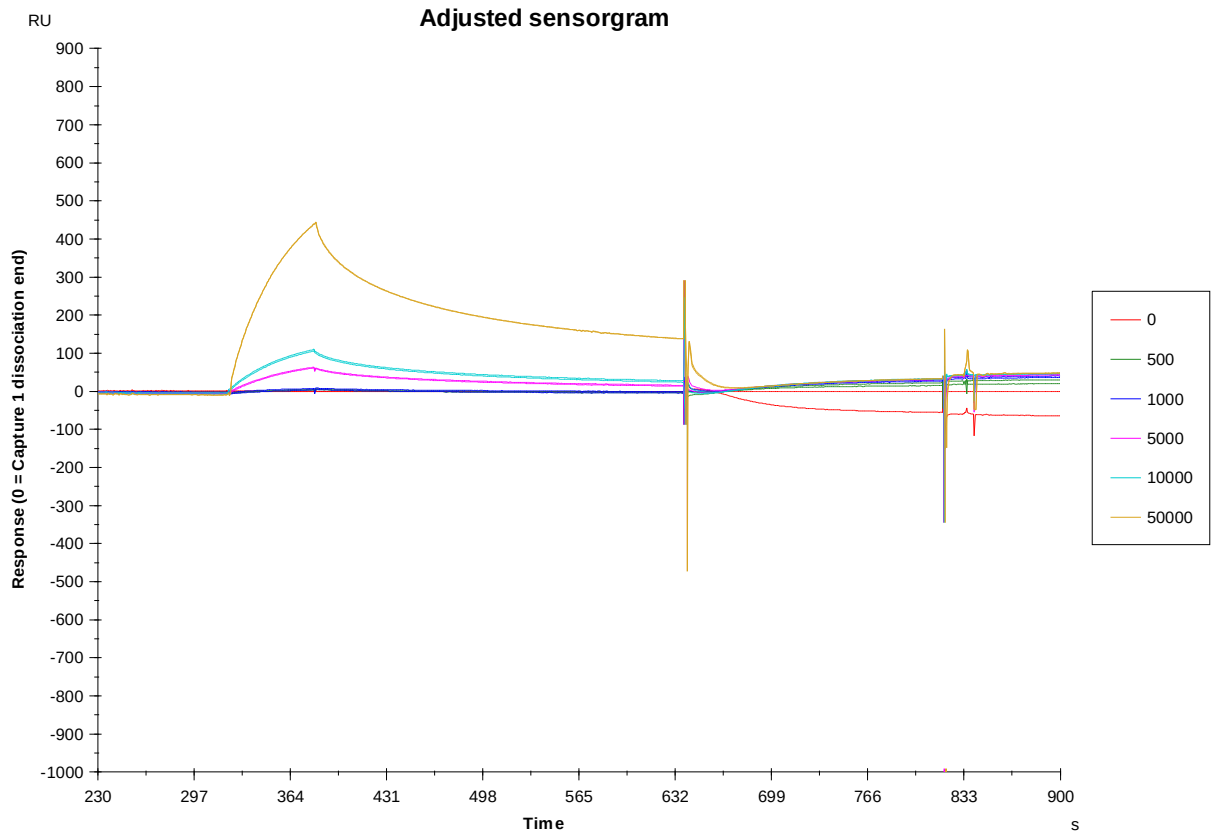

Figure 51 ***Sensogram illustrating the binding of $GABA_BR1aCCP2$ to α5 LG4-5***
The CCP2 single module was injected over the NTA sensor chip surfaces at concentrations ranging from 100 nM - 100 µM (see key, concentrations in nM). Adjustment as in Figure 49.

3.5 Discussion

As was mentioned previously, there is a substantial precedent for the involvement of CCP modules at sites of interaction between two proteins. Most examples in the literature are drawn from the mammalian complement system (Kirkitadze and Barlow, 2001). The β-strand rich three-dimensional structures of CCP modules feature loops and turns of diverse length and sequence that are conducive to specific molecular recognition processes. Furthermore, the cooperation of tandem CCP modules, connected by a short linker of non-conserved residues, in formation of a common binding site adds a further dimension of potential diversity. Frequently, the CCP modules concerned lie at the N-terminal end of the protein; for example, N-terminal CCP modules of factor H, C4b-binding protein alpha-chain, membrane cofactor protein, and complement receptor types 1 and 2, all participate in protein-protein interactions. In the case of the $GABA_B$ receptor it is the presence of the pair of an N-terminal pair of CCP modules in $GABA_B$R1a that distinguished it from $GABA_B$R1b, these being the two most abundant receptor subtypes (Hawrot et al., 1998).

As was described in the Introduction, the N-terminal CCP module of the $GABA_B$ receptor module-pair has properties characteristic of a natively unstructured domain (despite the presence of two intact disulphides) (Blein et al., 2004) – such domains may adopt a more compactly folded form upon binding to a partner in interactions that are often “low-affinity but high-specificity” in nature, and are typical of multivalent cell-cell or cell-extracellular matrix contacts (Dyson and Wright, 2005; Blein et al., 2004) Indeed, the previous chapter presented evidence - based on yeast-two-hybrid (Y2H)

studies (reinforced by immuno-dotblots) – suggesting the extracellular matrix proteins laminin and fibulin serve as protein binding partners for the $GABA_BR1a$ N-terminal region. The second of the $GABA_BR1a$ CCP modules is compactly folded and has the appearance of a typical CCP-module structure – in theory it could serve as a mere spacer, or it could provide the initial binding contacts with a partner protein in an interaction that involves subsequent folding of the N-terminal module.

Thus – based on the literature, biochemical intuition and the results of the previous chapter - various theories presented themselves in respect of the functional role of the $GABA_BR1a$ CCP module pair. Our first hypothesis was that there is a directly detectable interaction (corresponding to the one that can only be inferred from the Y2H results) between one, or both, of the $GABA_BR1a$ CCP modules and one or more domains of the abundant extracellular matrix protein laminin (or fibulin). This notion progressed to a model for binding in which the two modules act in a synergistic manner when it comes to recognition of ECM proteins with the N-terminal module providing most of the specificity and a slow off-rate for the complex, while the second module contributes binding energy to the initial encounter. In turn, the formation of a specific complex with laminin (for example) could modulate pharmacological activity, or localise receptors to specific regions of the cell surface, or have developmental consequences – for example in modulation of synapse formation or neurite outgrowth. This is studied further in chapter 4.

3.5.1 Surface plasmon resonance (SPR) verified interaction of $GABA_BR1a$ CCP modules with laminin-1 and laminin-10/11

Some of these ideas were tested by the work described in this chapter (and some will be tested in the work of the next chapter). In particular, the interaction with laminin warranted further investigation due to the predominance of this protein as a major constituent of basal lamina. Biochemical support (in addition to the previously reported immuno-dotblots) and quantification were required to back up the Y2H study and hence to add credibility to a claim for this putative protein-protein interaction being physiologically relevant. This was particularly important for the current study since the physiological interactions under investigation are extracellular in nature while Y2H is a technique that detects interactions as they occur between two proteins on the regulatory region of a gene within the nucleus. Having established the existence of a biochemically detectable interaction (discussed below), it was desirable to identify which domains or modules of the respective proteins are involved. With respect to the two $GABA_BR1a$CCP modules it was hoped to establish their relative contributions and whether they cooperate in binding. On the laminin side, it was important to discover which domains are involved in the interaction since this might shed light on which members of the laminin family (see Introduction) are likely to be involved; moreover knowledge of whereabouts on the large laminin molecule the CCP module(s) dock could have implications for the functional consequences of the interaction.

The method of choice in this study was surface plasmon resonance on the basis that it uses relatively small amounts of material and can detect and quantify weak

interactions. From the $GABA_B$ receptor side, constructs containing one or both of the two CCP modules were convenient to work with although they do not provide any insight on the potential role of the remainder of the large extracellular domain(s) in the interaction. The commercially available laminin-1 is a preparation from mouse Engelbreth-Holm-Swarm tumors, which produces large amounts of basement membrane. The main components of the basement membrane of mouse sarcoma are laminin and type-IV collagen. Traces of collagen are removed by subsequent high-salt (1.7 M NaCl) extractions, followed by DEAE-cellulose separation; nonetheless a small amount of contamination by this protein may be present as evident by several further bands in the range 35–130 kDa that are apparent on SDS-PAGE below the predominant laminin bands of 440 kDa and 220 kDa (Figure 30). The laminin-1 preparation thus contains naturally synthesised protein that is likely to be correctly folded and processed. The commercially available laminin-10/11 preparation (mainly laminin-10) was prepared from human placenta, by high-salt extraction and mild pepsin digest followed by affinity purification using a monoclonal anti-laminin antibody. Small protein contaminants were present in addition to the expected pepsinised 130 and 160 kDa components, according to analysis by SDS-PAGE. Furthermore, the mild pepsin treatment may have damaged binding sites present on the protein, which may explain why this preparation appears less potent than laminin-1 at binding $GABA_B$R1aCCP12. Overall, the laminin-1 preparation appeared to be cleaner and less heterogeneous than the laminin-10/11 preparation.

The SPR results presented in this chapter confirm that a direct interaction occurs between laminin-1 and the double module $GABA_B$R1aCCP12. The sensorgrams

obtained (Figure 39) show clearly that the interaction is dominated by a "slow-on; slow-off process". Such an observation normally reflects high-affinity binding (*i.e.* in the sub-μM range). While it did not prove possible in the current work to extract an accurate K_d from the experimental data, this inference of tight binding supports the physiological relevance of the originally Y2H-based finding. Although an interaction does not need to be tight in order to be important (for example it may be part of a multi-valent cell-cell interaction), a higher-affinity interaction is less likely to be non-specific. The difficulty in fitting the SPR data to any of the standard models for intermolecular interactions arises from what appears to be a convolution of a tight and a weak interaction; and this has a number of possible explanations. It might be that only a portion of the laminin-1 preparation is fully active; according to such a theory, this fully functional population of molecules is responsible for the high-affinity component of the sensorgram, while superimposed on this could be weaker binding (to for example clipped or unfolded laminin-1 molecules). Another theory is that the procedure of amine-coupling used for immobilisation of laminin-1 on the carboxymethylated dextran matrix of the sensor chip would have generated a heterogeneous mixture of orientations of the bound molecule and therefore the complete or partial occlusion of a range of potentially important binding surfaces. There is also the potential for two physiological binding sites – with very different affinities - for CCP modules on the same laminin-1 protein molecule. Finally, from the perspective of the $GABA_B$ receptor, it is feasible that the natively unfolded state of CCP1 could result in a more complex mode of binding than that represented in any of the models utilised by the fitting software. For example, the requirement for folding on the surface of laminin might not affect the measured on-rate

(dominated by the initial encounter) but could disfavour dissociation (as monitored by the off-rate). Such a complex curve will not fit a standard 1:1 fit, while using a complex model or exponentials will not necessarily give a more meaningful model (Rich and Myszka, 2008).

It was subsequently shown that, in respect of binding to full-length laminin-1, neither of the single CCP modules yielded SPR data (Figure 40 and Figure 41) that was as convincing as the equivalent data obtained with the double module (Figure 39). In the case of the N-terminal module, CCP1, it was not possible to detect much dissociation of module from the laminin-bearing chip surface. This could reflect either a very slow off-rate due to formation of a tight complex; but it could also reflect irreversible precipitation of the unfolded module on the matrix (albeit in a laminin-dependent manner, since data from the control flow-cell has been subtracted from the curves shown). The CCP1-laminin-10/11 interaction (Figure 37) furthermore appears to be partially limited to mass transport at higher concentrations of analyte, increasing the risk of re-binding of analyte before it can diffuse away. On the other hand, CCP2 produced only a very small number of response units in the SPR experiments with laminin-1. Overall these data (for CCP1, CCP2 and CCP12 binding) are consistent with the idea that CCP1 is the dominant interaction site and binding involves a kinetically complex reaction in which CCP1 adopts a more compact fold upon binding to its target. They are also not inconsistent with the idea that the two modules participate cooperatively in the binding process - CCP2 provides an initial weak docking surface, while CCP1 provides the specificity.

The results in this chapter also confirm that the $GABA_BR1aCCP$ modules bind lamininin-10/11 although this is a "fast-on: fast- off process" (Figure 36). This is at first sight a curious result given the slow-on: slow-off binding observed with laminin-1. It is important to recall (see above) that the laminin-10/11 preparation contains pepsinized molecules (while laminin-1 does not) – and that overall the laminin-10/11 preparation has more degradation problems than the laminin-1. Given this inferior quality it is somewhat surprising that CCP1 alone appears to binds laminin-10/11 with slow off- and on-rates– it is worth scrutinising the data and observing that this latter interaction gives rise to a higher number of response units compared to CCP12. It might be that what is being observed here is binding to a subpopulation of the molecules on the chip that are functionally intact.

3.5.2 Screening of laminin fragments for binding to $GABA_BR1aCCP12$

In a subsequent more detailed study of the interaction between laminin and $GABA_BR1a$, a range of truncated proteins covering large parts of the vast laminin molecule (although excluding the coiled-coil region) were investigated as potential binding partners. A goal here was to explore which of the laminin domains contributes most prominently to the interaction. The truncated products screened in this study included both pepsinised native laminin fragments and recombinantly expressed regions of laminin. Some of the preparations appeared to contain contaminations and/or

degradation as judged from SDS-PAGE (Figure 30), however it was not attempted to purify these fragments further due to very limited amount of available material.

Protein:protein interactions involving laminins are generally complex in nature as a consequence of their very large size and the presence of numerous domains and multiple chains. While laminin was reported to interact with its 67-KDa receptor via an EGF-like domain on its short beta arm (Panayotou et al., 1989), most cellular receptors of laminins (including integrins, dystroglycan and syndecan) interact with the globular (LG) domains or the VI domain of the long alpha-chain (Suzuki, Yokoyama, Nomizu, *2005*). In the light of these results, it is intriguing (Figure 51) that a His-tagged laminin LG4-5 construct, immobilized on the SPR sensor chip, exhibited "slow-on, slow-off" binding kinetics with $GABA_BR1aCCP2$ (and a response of over 400 RU). This interaction between CCP modules and LG4-5 was also detected by SPR performed in the inverse sense (Figure 46, panel 15) with the $GABA_BR1a$ CCP12 immobilized on the chip and LG4-5 as analyte, although the response is smaller (41.9 RU for a 39.5-kDa fragment) and the on- and off-rates are somewhat higher. It is difficult to ensure that immobilization of the CCP12 modules mimics their orientation *in vivo*, allowing full access to binding sites. Biotinylated protein was shown to be more active than protein immobilised with standard amine-coupling. However, the CCP12 modules appear to be more active as an analyte. Indeed all of the studies performed with immobilized $GABA_BR1aCCP12$ produced small responses that require cautious interpretation.

For example, it appears that fragment LN78 (Figure 46, panel B) bound significantly more strongly to immobilised CCP12 than did LN65a (13.6 RU compared to 2.2 RU - these fragments are similar in molecular weight, *i.e.* 450 and 350 kDa,

respectively). This is interesting as the very weakly (or non-) binding LN65a fragment is identical to LN78 with the exception of the N-terminal V/VI domains of all three chains (see Figure 52). The LN73 and LN65 fragments, which correspond to the N-terminal two domains of the β1 chain present in laminin-1 and laminin-10/11, respectively, showed only weak binding (giving rise to 2.2 RU and 3.2 RU for these small fragments of 75 and 25 kDa, respectively). The recombinantly expressed fragment β1 V1/V also bound weakly (3.6 RU for a 60-kDa fragment) to CCP12. The recombinantly expressed α1 LG1-3 fragment gave a significant response of 24.7 RU (82-kDa fragment). However, the sensogram looks similar to that obtained for CCP1:laminin-1 (Figure 40), with little or no dissociation, which may suggest precipitation on the sensor chip surface. Overall, according to this survey of fragments (summarized in Figure 52), the LG domain region appears to dominate the interaction with CCPs, while other regions may contribute to binding.

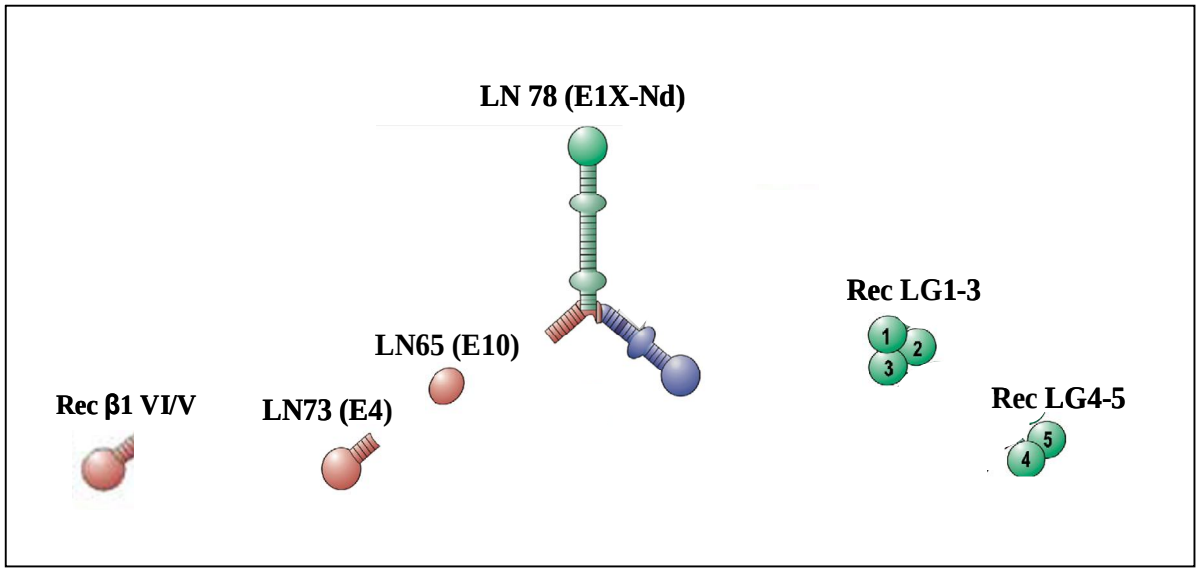

Figure 52 ***Cartoon illustrating an overview of the binding laminin fragments in the current study***
Laminin fragments LN78, LN73, LN65 and β1 V1/V contribute to binding of $GABA_BR1a$ CCPs, while the recombinant α5 LG4-5 fragment appears to dominate the interaction. The response seen for the recombinant α1 LG1-3 fragment may be caused by precipitation on the sensor chip surface.

A similar situation may prevail for the interaction with acetylcholinesterase; it was recently reported that acetylcholinesterase also interacts with these LG domains, specifically with the alpha chain LG4 domain (Johnson et al., 2008), while a previous report (Paraoanu and Layer, 2004) had implicated the beta chain IV domain of laminin in acetylcholinesterase binding. This suggests the intriguing possibility of $GABA_BR1a/2$ competing for the same binding sites on laminin as acetylcholinesterase. Finally it is worth reiterating that CCP modules of C4BP bind LG domains of Protein S (Hardig and Dahlback, 1996; Hardig et al., 1993; Hillarp and Dahlback, 1990; Fernandez and Griffin, 1994) and therefore a CCP-LG interaction is not unprecedented.

CHAPTER 4

Two-electrode voltage clamp study

4 Chapter 4 Two-electrode voltage clamp study

4.1 Aims

The first aim of the work described in this chapter was to establish, in our laboratory, *Xenopus laevis* oocytes as a model system with which to characterize some functional aspects of the $GABA_B$ receptor. The second aim was to use a two-electrode voltage clamp technique to investigate pharmacological differences between the oocyte-expressed isoforms $GABA_BR1a$ and $GABA_BR1b$. The third aim was to use this technique to investigate pharmacological responses to the agonist, baclofen, of the isoforms $GABA_BR1a$ and $GABA_BR1b$ in the presence of the extracellular protein, laminin.

4.2 Context

The function and pharmacology of the $GABA_B$ receptor have previously been studied extensively in *Xenopus* oocytes and membrane preparations (Billinton et al., 1999; Pfaff et al., 1999; White et al., 1998) Nonetheless, the functional role of the two N-terminal CCP modules of $GABA_BR1a$ remained unclear. In the previous two chapters, it was established that these CCP modules are able to mediate interactions between the receptor and the extacellular matrix. Not only were such interactions detected in a Y2H approach, they could also be measured in an *in vitro* setting using surface plasmon resonance. For example in the case with laminin-1, the interaction displays slow-

on/slow-off characteristics that are consistent with specificity and high-affinity (as opposed to a random non-specific interaction). This interaction was dominated by contacts between the CCPs and laminin α5 LG domains 4 and 5. Such an observation immediately raises the question: what is the functional role of this interaction? One possibility is that laminin modulates the response of the receptor to GABA. In this respect it is worth noting that GABA, as well as being the dominant inhibitory neurotramitter in adult CNS, contributes to many developmental processes (Bolteus, 2006). Acting through both the ionotropic and metabotropic GABA receptors, GABA can influence cell proliferation and neuronal migration (Manent and Represa 2007). These cellular processes are intimately associated with the extracellular matrix that provides both physical support for cells and the medium through which they move and communicate. Thus some complex interplay between GABA, the $GABA_B$ receptor and the extracellular matrix could exist, with the CCP modules playing a central role. If laminin binding modulates the affinity of the receptor for GABA, this should be detectable using standard pharmacological approaches. In the current study the pharmacology of the two isoforms and the potential functional impact of the presence of laminin were examined.

4.3 Materials and Methods

4.3.1 *Xenopus laevis* oocyte expression system

The oocyte from the South African clawed toad, *Xenopus laevis,* is a well-characterised and extensively used model system within the field of molecular pharmacology. Notably the surface of the oocyte bears few endogenous ion channels and receptors, which makes it a suitable model for studying expression and function of recombinantly expressed ion channels and receptor proteins *in vivo*. Ovaries in adult female frogs mainly contain stage V and VI oocytes, which are fully grown (~1.2 mm in diameter) and best suited for experimental studies. The cells have a characteristic division into two halves: the pale white-yellow vegetal pole, and the dark-brown animal pole that contains the nucleus (as seen in Figure 53).

Figure 53 *Xenopus laevis* toad and oocyte
To the left: an image of a South African clawed toad, *Xenopus laevis*. **To the right**: an image of oocytes undergoing micro-injection. The animal and vegetal poles are clearly visible in dark brown and pale yellow respectively.

4.3.2 Materials

4.3.2.1 TEVC reagents

Table 8 *Buffers and reagents used during all two-electrode voltage clamp (TEVC) experiments for characterisation of the $GABA_BR1a$ and $GABA_BR1b$ isoforms*

Buffers	**Reagent**
Barth's solution, pH 7.35	88 mM NaCl 1 mM KCl 2.4 mM $NaHCO_3$ 0.82 mM $MgCl_2$ 0.77 mM $CaCl_2$ 15 mM Tris-Hcl 50 IU/ml penicillin 50 µg/ml streptomycin
TEVC external buffer "low [K]" adjusted to pH 7.35 with 1 M NaOH	115 mM NaCl 2.5 mM KCl 1.8 mM $CaCl_2$ 10 mM Hepes 10 µM EDTA
TEVC external buffer "medium [K]" adjusted to pH 7.35 with 1 M NaOH	90 mM NaCl 25 mM KCl 1.8 mM $CaCl_2$ 10 mM Hepes 10 µM EDTA
TEVC external buffer "high [K]" adjusted to pH 7.35 with 1 M NaOH	75 mM NaCl 40 mM KCl 1.8 mM $CaCl_2$ 10 mM Hepes 10 µM EDTA

Table 9 *Drugs and concentrations used for TEVC experiments.*
All drugs were diluted to the desired concentration in 'TEVC external buffer med [K^+]' (Table 8). All reagents were supplied by Tocris (Bristol UK)

Drugs	Concentrations
Baclofen ($GABA_B$ receptor agonist)	1 µM, 3 µM, 10 µM, 100 µM
CGP55845 ($GABA_B$ receptor antagonist)	0.1 µM, 0.3 µM, 1 µM, 3 µM, 5 µM, 10 µM

4.3.2.2 Primer design

The sequences of the genes under investigation were confirmed using www.ensemble.org. Primers were designed using Sigma-Genosys software, synthesized commercially by Sigma-Genosys and re-suspended in ultra-pure water for use at a concentration of 10 µM. (For the sequences of primers used in this study, see Appendix C.I).

4.3.2.3 Constructs encoding $GABA_B$ receptor subunits and GIRK subunits

Constructs encoding the genes for human $GABA_BR1a$, $GABA_BR1b$, $GABA_BR2$ and rat inward-rectifying potassium (KIR) channel subunits GIRK3.1 and GIRK3.4 were obtained from Dr Julia White (GlaxoSmithKline, Stevenage UK) ($GABA_BR1a$) and Dr Randy Hall (Emory University, Atlanta, USA) (all others). $GABA_BR1a$ had been cloned into the expression vector pcDNA3.1 (Invitrogen) and RNA transcription *in vitro* is driven by the T7 promoter. $GABA_BR1b$, $GABA_BR2$ and KIR channel subunits GIRK3.1 and GIRK3.4 had been cloned into the expression vector pSGEM (as

illustrated in Figure 54), which is a modified version of pGEMHE, optimised for *Xenopus* oocyte expression since it contains 3' and 5'-untranslated regions (UTR) from *Xenopus* β-Globin and a polyA tail (Villmann et al., 1997). These help stabilise the RNA transcript and aid translation in the oocyte. RNA transcription *in vitro* is driven by the SP6 promoter (Plasmid map can be found in Appendix C.II).

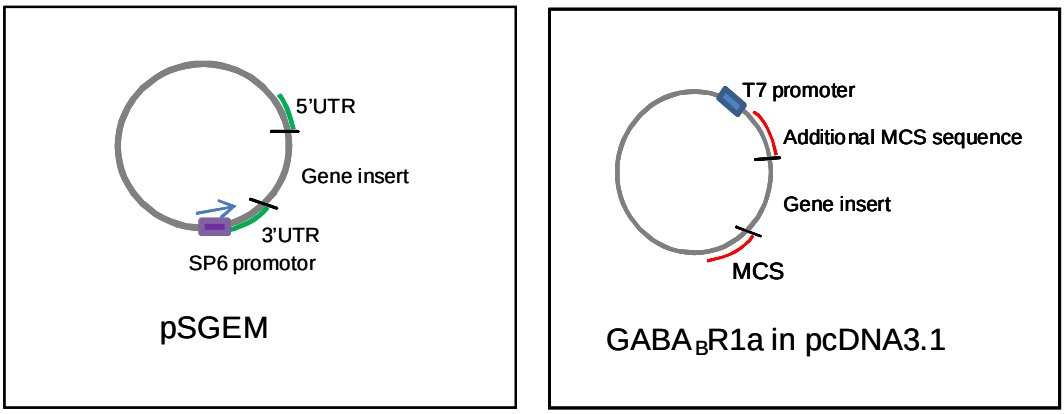

Figure 54 ***Plasmid maps***
Left hand side*:** Plasmid diagram of pSGEM, a plasmid derived from pGEMHE (Liman et al., 1992). ***Right hand side: Gene-Plasmid maps illustrating the additional MCS in the plasmid pcDNA3.1 leading to disruption of transcription.

4.3.3 Methods

4.3.3.1 Generation of a new GABA$_B$R1a construct

The GABA$_B$R1a construct in vector pCDNA3.1, as supplied at the outset of this work, failed to transcribe cRNA *in vitro*. Restriction-enzyme digestion and automated sequencing of the construct revealed an additional multiple-cloning site in the plasmid containing unwanted restriction sites. The presence of these undesirable restriction sites

resulted in a separation of the T7 promoter from the gene encoding $GABA_BR1a$ following the digestion step used to linearise the plasmid. Several alternative strategies were therefore explored in an attempt to overcome this problem and achieve higher expression levels of the $GABA_BR1a$ isoform. A direct cloning approach to moving the $GABA_BR1a$ cDNA from the pcDNA3.1 vector to the alternative, *Xenopus*-optimised, pSGEM vector was hindered because there were no mutually compatible restriction sites shared between the multiple cloning sites of the respective vectors. A subsequent attempt at introducing appropriate restriction sites by PCR amplification of the entire R1a gene proved difficult.

4.3.3.1.1 Incorporation of restriction sites utilising an oligo nucleotide adapter

An adaptor was designed to incorporate new restriction sites into the pSGEM vector (Villmann et al., 1997). The adaptor consisting of two oligonucleotide sequences that were designed so that when allowed to anneal, external overhangs would result in matching restriction sites for *Not*I and *Xho*I; an internal restriction site for *Xba*I was also included within the sequences (Figure 55). Subsequently, the vector pSGEM was digested with the restriction enzymes *Not1* and *Xho1*, and an attempt was made to incorporate the adaptor into the pSGEM vector. The final steps would have entailed digestion of pSGEM and pcDNA3.1 with *Xba1/Xho1,* and then incorporation of the digested $GABA_BR1a$ insert into pSGEM. Due to difficulties encountered in annealing the two short oligoneucleotide sequences to each other, under a range of annealing conditions, no product could be detected. Note that due to the small size of the adaptor -

approximately 20 base pairs - it was difficult to follow the attempted creation of the adapter visually on an agarose gel.

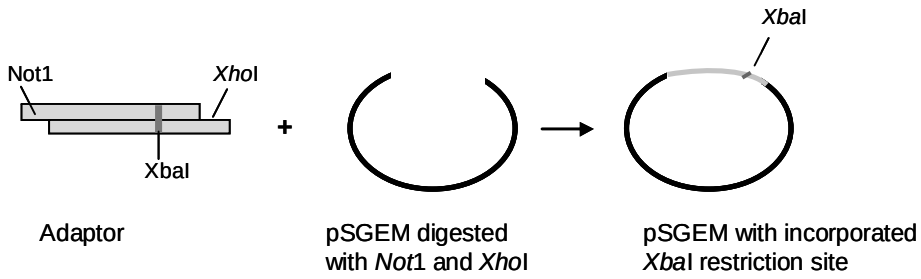

Figure 55 ***Illustration of adaptor designed to incorporate desired restriction sites into the pSGEM vector.***

4.3.3.1.2 Cloning the gene for $GABA_BR1a$ into pRSSP

In response to these difficulties, a new construct for $GABA_BR1a$ expression was generated in the pRSSP vector (derived from the pSP64T vector) (Veyhl et al., 2006), which contains many of the elements present in the pSGEM vector used for the other constructs, and is particularly well-suited for facilitated expression in *Xenopus* oocytes (Kuner and Schoepfer, 1996). The pRSSP construct was generated using a multistep cloning approach (Figure 65).

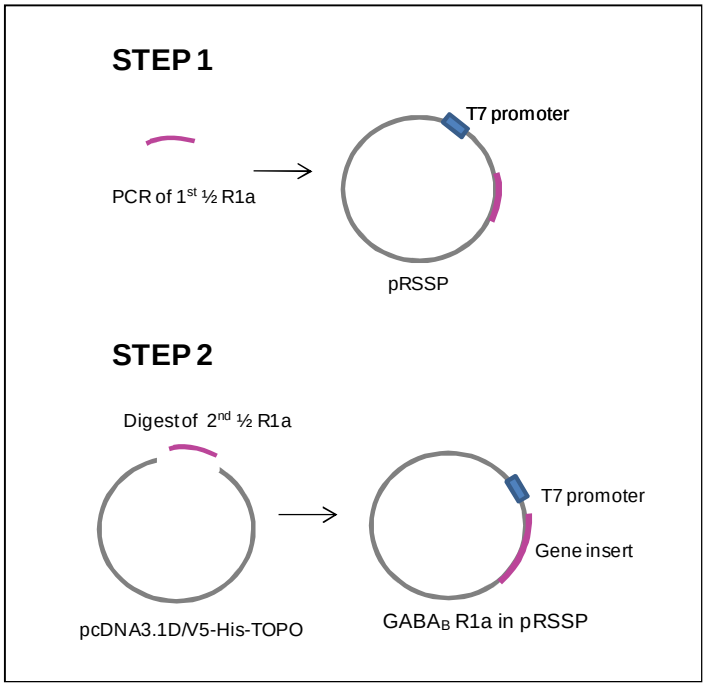

Figure 56 ***Two-step cloning approach***
A two-step cloning approach was used to insert the $GABA_BR1a$ gene into the pRSSP plasmid, in which part of the $GABA_BR1a$ gene was amplified by PCR and inserted into pRSSP followed by insertion of the remaining part of gene by restriction digests.

To minimise the risk of mismatched base pairs when amplifying such a relatively large gene, a fragment was generated by PCR-amplifying only the first part of the $GABA_BR1a$ gene (Figure 58) from the previously prepared pcDNA3.1D/V5-His-TOPO construct, incorporating new *AflIII* and *BglII* sites. The pRSSP vector was digested with restriction enzymes *NcoI* and *BglII* (Figure 58), and the PCR-generated fragment of the $GABA_BR1a$ gene was incorporated into pRSSP (the *AlfIII* and *NcoI* recognition sites are compatible in their digestion pattern, because of degenerate sites at *AlfIII*, Figure 57).

Recognition Site *Alf*III:
5′...ACRYGT...3′ 3′...TGYRCA...5′
Recognition Site *Nco*I:
5′...CCATGG...3′ 3′...GGTACC...5′

Figure 57 ***The restriction enzymes AlfIII and NcoI have compatable recognition sites***
*Alf*III has a degenerate site, which means that the enzyme will recognise both A and G in the 'R' position and both C and T in the 'Y' position

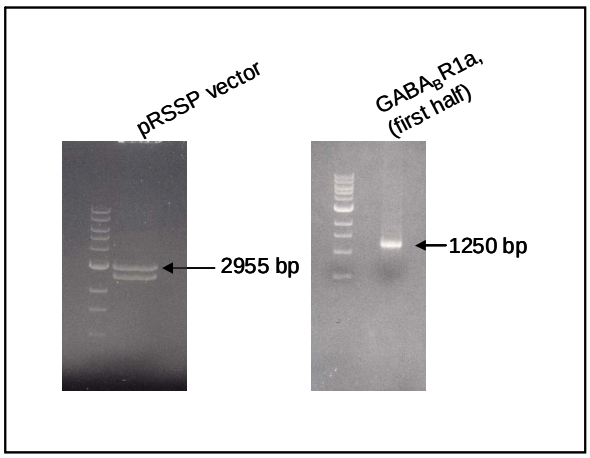

Figure 58 ***Agarose gel for first cloning step***
Left-hand side: digest of pRRSP vector with restriction enzymes *NcoI* and *BglII* to separate vector from previously (unrelated) incorporated gene. The upper band of 2955 bp was gel purified. **Right-hand side:** PCR amplification of the first half of the GABA$_B$R1a gene to incorporate new *AflIII* and *BglII* sites.

In step 2 of the procedure, the second half of the GABA$_B$R1a gene was digested from pcDNA3.1D/V5-His-TOPO using *BglII*/*XhoI* and the resulting fragment was inserted into the *BglII*/*XhoI* sites of the pRSSP vector (Figure 59), which already contained the first fragment of the GABA$_B$R1a gene from the previous step.

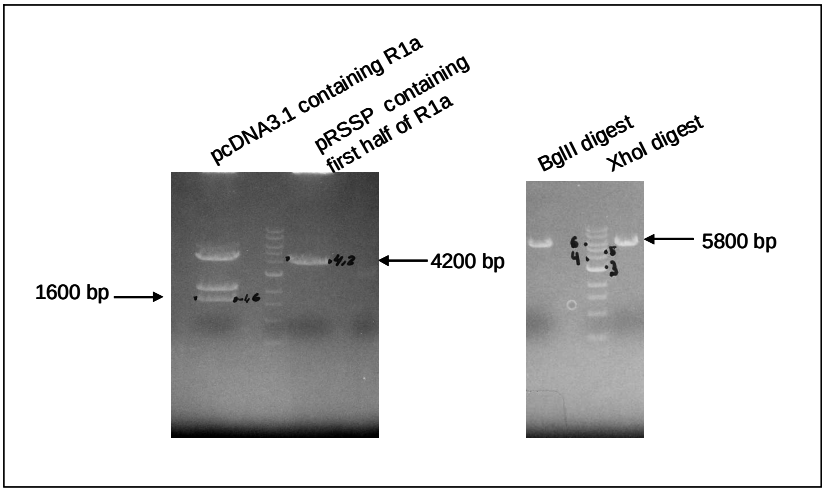

Figure 59 ***Agarose gel for second cloning step***
Left-hand side: Restriction digest of pcDNA3.1 construct with *BglII* and *XhoI* to isolate the second half of the $GABA_BR1a$ gene. The gene fragment of 1600 bp was gel purified. The pRRSP contruct containing the first half of $GABA_BR1a$ was digested with *BglII* and *XhoI*, removing 16 bp and the remaining plasmid of 4200 bp was gel purified. **Right-hand side:** The final construct was digested with *BglII* and *XhoI* separately to verify the incorporation of the whole $GABA_BR1a$ gene, giving a fragment of 5800 bp.

4.3.3.1.3 Polymerase chain reaction (PCR)

Conditions for the PCR were optimized by varying annealing temperatures from 50 °C to 68 °C. The following conditions, resulting in a single strong band of the correct size, were chosen for amplification of the genes.

An aliquot of 1 µl 10 mM dNTP (containing the four deoxyribonucleotides: dATP, dCTP, dGTP and dTTP) was mixed with 1 µl of 1:100-diluted plasmid DNA (approximately 200 ng), 1 µl forward-primer (10 µM), 1 µl reverse-primer (10 µM), 0.5 µl (2.5 U) Herculase hot-start polymerase, 5 µl Herculase 10x reaction buffer (Stratagene, Ca, USA) and 40.5 µl ultrapure water.

The PCRs were carried out according to the following scheme:

95 ºC	2 minutes	
95 ºC	30 seconds	30 cycles
65 ºC*	30 seconds	
72 ºC	1 minute	
72 ºC	10 minutes	
4 ºC	hold	

*or varied according to optimization

4.3.3.1.4 General restriction digest procedure

In the restriction enzyme digestion procedure, 2 µg DNA (plasmid DNA or PCR product) was added to microcentrifuge (Eppendorf) tubes containing restriction enzyme digest mix, which was made up of 1 µl (10 U) of each restriction enzyme, 2 µl NEBuffer (compatible with the restriction enzymes used), 2 µl 10x BSA (for some digests only) and 11 µl ddH_2O (all from New England Biolabs). The DNA digest mixtures were incubated at 37 °C for one hour. The digested DNA products were analysed by agarose gel and purified using a gel-purification kit from Qiagen.

4.3.3.2 Ligation and transformation procedures for all constructs

A 2-µl aliquot of the PCR-generated DNA for $GABA_BR1a$ was added to a ligation reaction mixture including Quick T4 DNA ligase, Quick ligation reaction buffer 2x (New England Biolabs), 0.5 µl (50 ng) of restriction-digested and gel-purified vector.

The reaction was incubated, at room temperature, for ten minutes and performed in parallel with a negative control reaction (containing water instead of the DNA insert).

4.3.3.3 Transformation

E. coli "One Shot Top10" competent cells (Invitrogen, UK) were subjected to transformation by heat shock, as follows. An aliquot of 50 µl of Top10 cells was removed from a -80 °C freezer and thawed on ice before 2 µl of the ligated product (see above) was added and gently agitated. The mixture was left on ice for 30 minutes before the heat-shock step. The cell-ligation mixture was then incubated in a water bath at 42 °C for 45 seconds and then placed on ice for two minutes. The mixture was then re-suspended in 1.0 ml of SOC medium (Invitrogen) and incubated at 37 °C, with shaking at 200 rpm for 60 minutes. Aliquots of 50-200 µl of the mixture were plated on LB agar plates containing 50 µg/ml ampicillin and incubated at 37 °C overnight.

4.3.3.4 Preparation of plasmid DNA

Colonies were picked from the selective plates and inoculated into 5.0 ml of LB medium containing 50 µg/ml ampicillin, then incubated at 37 °C, with shaking, overnight. Cells were then pelleted by centrifugation at 13000 rpm for 60 seconds. Recombinant plasmids were purified from cell pellets by alkaline lysis using the Qiaprep miniprep kit (Qiagen). Following re-suspension of the cell pellet in buffer P1, cells were lysed by addition of buffer P2 for up to five minutes and then neutralized by addition of buffer N3 and gentle mixing. The suspension was centrifuged in a table-top centrifuge

(Eppendorf) for ten minutes to accumulate the precipitate, and then the supernatant was transferred to a Qiaprep silica-gel membrane column. The column was spun at 13000 rpm for 60 seconds in an Eppendorf bench-top centrifuge and the flow-through was (ultimately) discarded. The membrane-bound DNA was washed with buffer PE, the flow-through discarded and the centrifugation step repeated. Finally, the membrane column was transferred to a fresh (and carefully cleaned) Eppendorf microcentrifuge tube, and the purified plasmid DNA was eluted with 50 µl ddH_2O by centrifugation at 13000 rpm for 60 seconds. The plasmid DNA was analysed by analytical restriction enzyme digest and PCR in order to confirm the correct insertion of the gene, followed by DNA sequencing to confirm a correct reading frame.

4.3.3.5 In vitro cRNA synthesis from $GABA_BR1a/R1b/R2$ and GIRK cDNA constructs

RNA was synthesised from mini-prep/midi-prep-derived DNA using a modified protocol for the RiboMax™ (Promega, Madison) large-scale RNA production system with T7 polymerase (for $GABA_BR1a$ in pcDNA3.1), or SP6 RNA polymerase (for $GABA_BR1a$ in pRSSP, $GABA_BR1b$/-R2 and GIRK3.1/-3.4, all in pSGEM). All solutions and materials were handled with gloves to avoid RNase contamination. Solutions were made up from diethylpyrocarbonate (DEPC)-treated water. DEPC-treated water was made by adding one gram of DEPC to one litre of double-distilled water (ddH_2O) and incubated overnight at room temperature, followed by autoclaving to inactivate the DEPC.

4.3.3.6 Template linearization

DNA constructs were linearised using the unique restriction sites displayed in Table 10 prior to RNA synthesis.

Table 10 *Restriction enzymes for linearising DNA constructs prior to RNA synthesis*

DNA construct	**Restriction site used**
R1a in pcDNA3.1	*Bsp*HI
R1b in pSGEM	*Nhe*I
R2 in pSGEM	*Nhe*I
GIRK 3.1 in pSGEM	*Mlu*I
GIRK 3.4 in pSGEM	*Mlu*I
R1a in pRSSP	*Mlu*I

Approximately 10 µg of plasmid DNA was added to 40 µl of digestion mixture that contained 4 µl restriction enzyme buffer (New England Biolabs), 30 U of restriction enzyme, (and for *Nhe*I digestions, 4 µl of BSA) and the remaining volume was made up to 100 µl with DEPC-treated ddH_2O. The DNA mixture was incubated at 37 ºC for one hour and then analysed by loading 1 µl onto a 1% (w/v) agarose gel made up with Tris-acetate-EDTA (TAE) -buffer that was also used as running buffer. The gel was run at 10 V/cm. The digested DNA was subsequently cleaned by phenol/chloroform extraction followed by chloroform extraction. Finally, the DNA was precipitated with 3 M NaAc (pH 5.2) and 100% ethanol.

4.3.3.7 cRNA synthesis and purification

On the assumption that 50% (5 µg) of the digested DNA had been recovered following linearization and purification, the RNA synthesis reaction mixture was made up as follows: 8.5 µl of digested DNA template re-suspended in DEPC-treated ddH_2O, 4 µl of mixture containing 25 mM each of ATP, UTP and CTP and 8 mM GTP , 1.5 µl of 10 mM $m^7G(5')ppp(5')G$ sodium capping, 4 µl of SP6 or T7 polymerase buffer and 2 µl SP6 or T7 polymerase. The reaction mixture was incubated at 37 ºC for one hour and then analysed by loading 1 µl onto a 1 % agarose gel made up with TAE-buffer that was also used as running buffer. The gel was run at 10 V/cm.

For purification, the RNA reaction mixture was made up to 100 µl with DEPC-treated ddH_2O. Contaminating DNA was removed by addition of 20 µl 2 M NaAc, pH 4, followed by 50 µl water-saturated phenol and 10 µl chloroform. The mixture was vortexed, centrifuged and the aqueous phase transferred to a clean Eppendorf microcentrifuge tube. An equal volume of isopropanol was added and the resulting mixture was incubated at –20 °C overnight. The mixture was then centrifuged at 13000 rpm for 30 minutes at 4 °C in an Eppendorf bench-top centrifuge and the supernatant discarded. The pellet was washed in 70% ethanol and re-suspended in 20 µl nuclease-free water. The RNA products were analysed by loading 1 µl on a 0.8% agarose gel containing formaldehyde in 5x MOPS buffer. A sample buffer mixture containing 1.5 µl of 5 x MOPS buffer, 2.6 µl formaldehyde and 7.5 µl formamide, and a loading buffer mixture containing 2 µl loading buffer and 0.5 µl (1 mg/ml) ethidium bromide, were incubated at 65 °C for three minutes. An aliquot of 11 µl of the sample buffer mixture

and 2.5 µl of the loading buffer mixture were then added to each one-µl RNA sample, and sample mixtures were incubated at 65 °C for a further three minutes. Then 1x MOPS buffer was used as running buffer, and the gel was run at 10 V/cm. RNA concentrations were determined from optical density measurements at 260 nm.

4.3.3.8 RNA sample preparation for oocyte micro-injection

The cRNAs for $GABA_BR1a$ or $GABA_BR1b$, $GABA_BR2$, GIRK 3.1 and GIRK 3.4 were mixed in a nominal ratio (by weight) of 8:8:1:1. The ratio was determined based on baclofen-evoked currents being large enough to be able to detect whithout the oocyte being compromised by the holding potential becoming too large, and avoiding excessively high expression levels of injected protein. Mixtures were diluted ten-fold with nuclease-free water in order to yield appropriate expression levels, resulting in measurable baclofen-evoked currents (approximately 0.3 µA for R1a and 3 µA for R1b). The optimal amount of cRNA injected per oocyte is displayed in Table 11.

Table 11 *Optimised ratios of cRNA mixtures used to micro-inject oocytes.*

	R1	**R2**	**GIRK 3.1**	**GIRK 3.4**
R1a mix	15 ng	15 ng	1.8 ng	1.8 ng
R1b mix	15 ng	15 ng	1.8 ng	1.8 ng

4.3.3.9 Preparation of stage V-VI oocytes

Xenopus laevis were anesthetised and the ovarian lobes were removed surgically (surgery performed by members of Dr Niki Gray's group, human genetics unit, MRC Edinburgh). Oocytes were separated manually into bundles of 10-20 oocytes and treated with collagenase type-1A (50 U/ml) for 30 minutes at room temperature with shaking. Following collagenase treatment the oocytes were washed three times with Barth's solution and then left to recover at 19 °C overnight. The following day the oocytes were defolliculated manually and RNA was injected using a Nanoject injector (Drummond Scientific, USA). Each oocyte was injected with 46 nl RNA (33.6 ng total amount RNA) and placed in an individual well of a 24-well plate containing 1.8 ml of Barth's solution. The oocytes were incubated at 19 °C for 2-5 days to allow expression of receptors and ion channels to occur, prior to use for TEVC recordings.

4.3.3.10 Two-electrode voltage clamp (TEVC) recordings

The TEVC recordings were made with a Geneclamp 500 amplifier (Axon Instruments, UK) and responses to 10 μM baclofen were measured at a holding potential of –100 mV. Voltage and current electrodes for recordings were made of thin-walled borosilicate glass (GC150TF-7.5, Harvard Apparatus, Kent) pulled using a PP-830 electrode puller (Narashige Instruments, Japan) and filled with 3 M KCl. The electrode resistances ranged between 0.2 and 0.5 MΩ. Oocyte were placed in a recording chamber containing TEVC external buffer "low [K]" (*i.e.* 2.5 mM potassium, Table 8) and impaled with the voltage and current electrodes. At this stage the oocyte was

continuously perfused with buffer. The resting potential of each oocyte was noted and it was thereafter voltage-clamped at -100 mV. The holding current for each oocyte was noted whereupon the perfusion buffer was changed to TEVC external buffer "medium [K]" (*i.e.* 25 mM potassium cloride). Experiments were carried out that involved recording the responses of a $GABA_BR1a/R2$ or $GABA_BR1b/R2$-expressing oocyte to the agonist baclofen and the antagonist CGP55845. All drugs were made up in TEVC external buffer "medium [K]" and perfused at a rate of ~8 ml/min.

4.3.3.11 Current-Voltage response curves

The current-voltage (I-V) relationship of GIRK3.1/3.4-activated currents expressed in oocytes was also studied using TEVC. The I-V relationship was determined from the response of oocytes co-expressing $GABA_BR1a/GABA_BR2$ and GIRK3.1/3.4, or oocytes co-expressing $GABA_BR1b/GABA_BR2$ and GIRK3.1/3.4, in the presence of 10 µM baclofen by step depolarisations from -100 to -20 mV in 20 mV increments. Data from four or five oocytes for each isoform are averaged. The theoretical membrane equilibrium is -31 mV, according to the Nernst equation, when external potassium (K^{+ext}) is 40 mM.

$$E_K = \frac{RT}{zF} \ln \frac{[K^+]_{out}}{[K^+]_{in}}$$

Where E_K is the electric potential across the membrane due to the potassium concentration gradient, R is the universal gas constant (8.3 J K^{-1}), T is the absolute

temperature in Kelvin, $[K^+]_{out}$ and $[K^+]_{in}$ are the potassium concentrations outside and inside membrane, zF is the number of electric charges carried by a mole of K^+ ; z is the valency of ion species (1 for K^+) and F is the Faraday constant 9.65×10^{4} C mol^{-1}.

4.3.3.12 Protein expression

Due to lack of suitable antibodies for western blotting, protein expression levels proved difficult to test experimentally. Instead *in vitro* transcription-translation was explored. [^{35}S]-Cys-labeled protein fragments were prepared by *in vitro* transcription-translation of the plasmids used in the TEVC study using the TNT® T7/SP6-coupled reticulocyte lysate system as described by the manufacturer (Promega). The *in vitro* transcription-translation assay was kindly performed by Dr B. Collier, human genetics unit, MRC Edinburgh. The reactions carried out using rabbit reticulocyte lysate demonstrated that the constructs were able to produce the desired proteins *in vitro*. As seen in the autoradiograph (Figure 60) of the *in vitro* transcription-translation, the plasmids carrying the genes for $GABA_BR1b$ (94 kDa), $GABA_BR2$ (105 kDa), $GABA_BR1a$ (108 kDa), GIRK 3.1 (56 kDa) and GIRK 3.4 (47 kDa) all produced protein of the expected sizes.

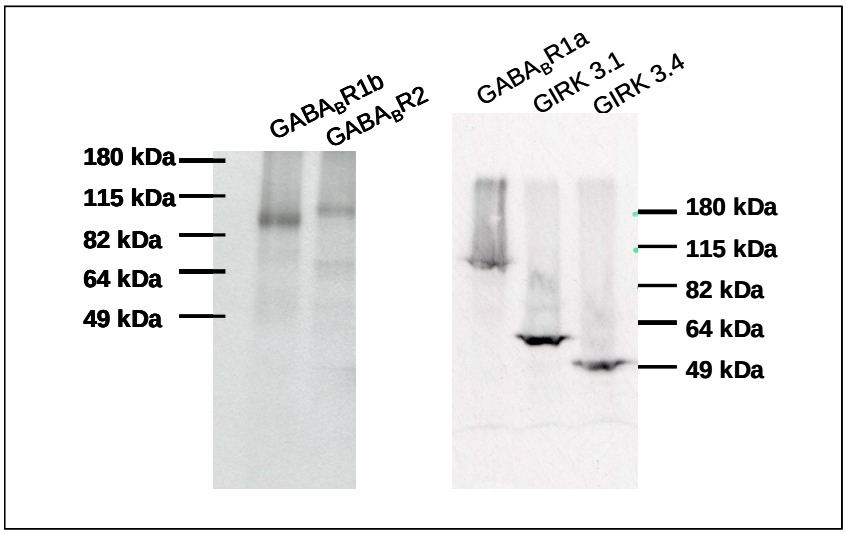

Figure 60 ***Autoradiograph demonstrating the in vitro transcription-translation of all constructs used in the TEVC studies***
The GABA$_B$R1a, GABA$_B$R1b, GABA$_B$R2 GIRK3.1 and 3.4 constructs used in the present study all successfully produced protein of the expected size.

4.4 Results

4.4.1 Characterization of the $GABA_B$ receptor using *Xenopus laevis* oocytes as a model system

4.4.1.1 Successful generation of RNA encoding for $GABA_B$ receptors and potassium channels

The pharmacology of $GABA_B$ receptors were studied by expressing the receptor subtypes $GABA_BR1a$ or R1b together with $GABA_BR2$ and the potassium channels GIRK3.1 and GIRK3.4 in *Xenopus* oocytes. Responses of oocyte-expressed $GABA_B$ receptor isoforms R1a/R2 and R1b/R2 evoked by agonist baclofen and antagonist CGP55845 were recorded by two-electrode voltage clamp (TEVC).

The RNA sequences corresponding to the $GABA_B$ receptor subunits $GABA_BR1b$ and $GABA_BR2$, and the ion channels, GIRK3.1 and GIRK3.4, were generated successfully by synthesising cRNA from the plasmids which incorporated the genes. The initial $GABA_BR1a$ construct failed to transcribe cRNA *in vitro (*as discussed in 4.3.3.1). New $GABA_BR1a$ constructs was therefore generated in the pcDNA3.1D/V5-His-TOPO vector as well as in the pRSSP vector; both constructs were tested and the latter construct was used for further studies as the vector pRSSP possessed similar advantages, with respect to optimisation for expression in *Xenopus* oocytes, as did pSGEM. It was subsequently confirmed, using a transcription-translation approach, that

the new $GABA_BR1a$ construct used in this study was able to express protein of the expected size *in vitro* (Figure 60).

4.4.1.2 Co-expression of both $GABA_B$ receptor subunits is required for function

It was confirmed in the current study that none of the individual $GABA_B$ receptor subunits $GABA_BR1a$, $GABA_BR1b$ or $GABA_BR2$, were able to activate potassium inwardly rectifying currents when expressed alone in oocytes together with GIRKs. On the other hand, when expressed together, $GABA_BR1a/GABA_BR2$ or $GABA_BR1b/GABA_BR2$, are able to activate GIRK currents in response to the application of 10 µM baclofen. The results of this study are thus consistent with the fact that $GABA_B$ receptors expressed in oocytes can recruit endogenous G-proteins and thereby activate inwardly rectifying potassium channels. The results also confirmed that co-expression of both $GABA_B$ subunits (together with GIRK subunits) is required for activity.

4.4.1.3 Optimisation of $GABA_BR1a$ expression and recording conditions

A major aim of this work was to compare pharmacological responses of $GABA_BR1a/R2$ versus $GABA_BR1b/R2$ as a step towards establishing biological roles for the two CCP modules that are unique to the $GABA_BR1a$ subunit. The results of this

study indicated that oocytes expressing $GABA_BR1a/GABA_BR2$ evoked a consistently smaller and less stable baclofen-mediated response compared to the response obtained with $GABA_BR1b/GABA_BR2$ under the same conditions.

To enhance the baclofen-evoked response of $GABA_BR1a/GABA_BR2$ several steps were taken. Firstly, $[K^+]$ in the TEVC external buffer was increased from its physiological value (2.5 mM) to 25 mM. Initially 40 mM potassium was tried, however this created a very high holding potential, resulting in short lifespans for the oocytes. This intermediate (25 mM) concentration of external potassium resulted in holding currents in the range of ~ -3-4 μA. Secondly, the amounts of injected cRNAs encoding the various proteins were optimised. It was suspected that excessive amounts of any particular cRNA would overload the translation machinery of the cell, leading to poor expression and rapid deterioration of the oocyte. By injecting less of GIRK cRNA, fewer potassium channels were expressed, this meant that a lower holding current needed to clamp the oocyte at -100 mV and resulted in a longer recording-life of the oocyte. Thirdly, it was found that in the case of $GABA_BR1b/GABA_BR2$, on average two days of incubation of oocytes, post-injection, was required to attain a useful level of protein expression. Prior to this time, no baclofen-evoked currents could be observed. Longer incubation resulted in very high recording currents (possibly due to high expression of receptors) followed by deterioration of oocytes. The $GABA_BR1a/GABA_BR2$ constructs, on the other hand, required longer incubation, post-injection - typically three to five days - in order to observe detectable baclofen-evoked responses. Thus incubation times were extended for the $GABA_BR1a/GABA_BR2$ constructs.

These measures improved baclofen-evoked response observed for $GABA_BR1a/R2$-expressing oocytes and enhanced oocyte lifespan while recording. However, the overall response of the oocytes expressing the $GABA_BR1a$ isoform (Figure 61) was still lower than for $GABA_BR1b$ expressing oocytes (Figure 62).

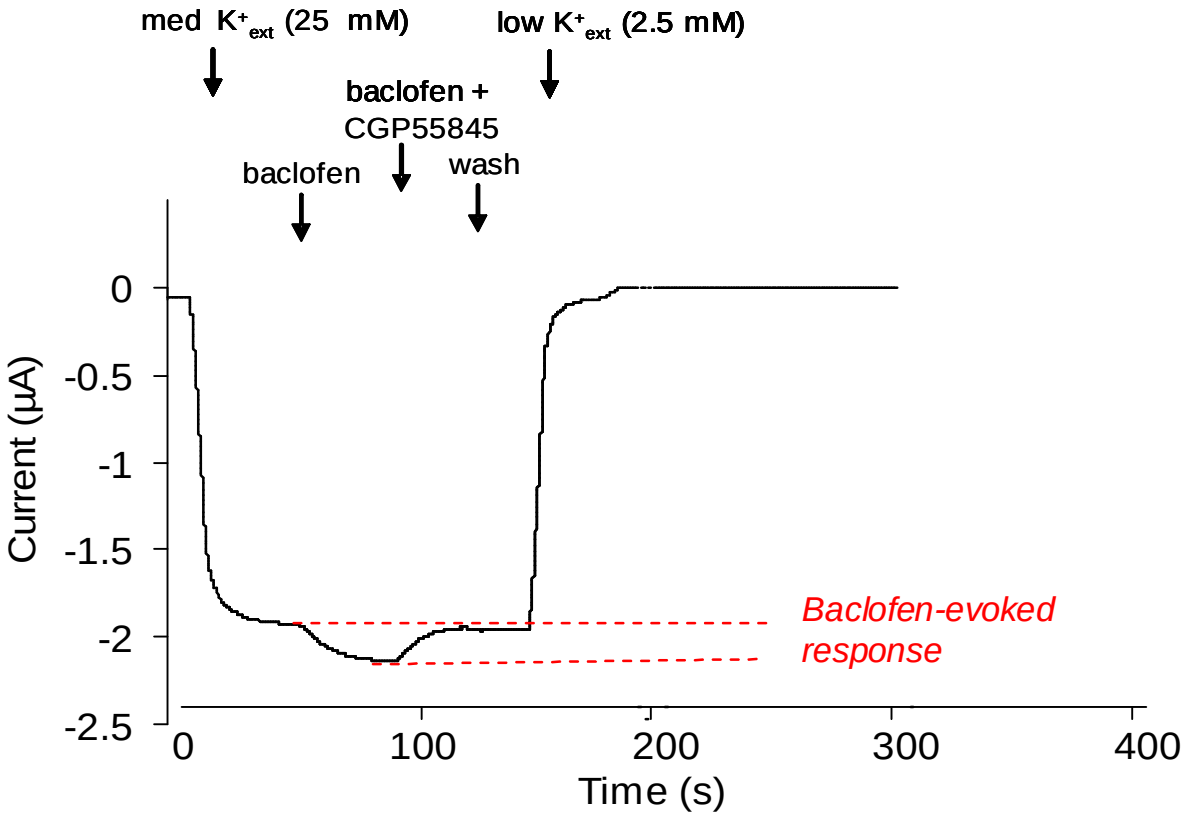

Figure 61 ***A representative trace of baclofen-evoked $GABA_BR1a/R2$ currents***
It was demonstrated that 10 µM baclofen evokes a smaller response compared to that obtained with the R1b/R2 isoform. The R1a/R2 response is blocked by 5 µM of the $GABA_B$ receptor antagonist CGP55845. The drug was washed off with medium-potassium buffer and the current brought back to baseline with low-potassium buffer.

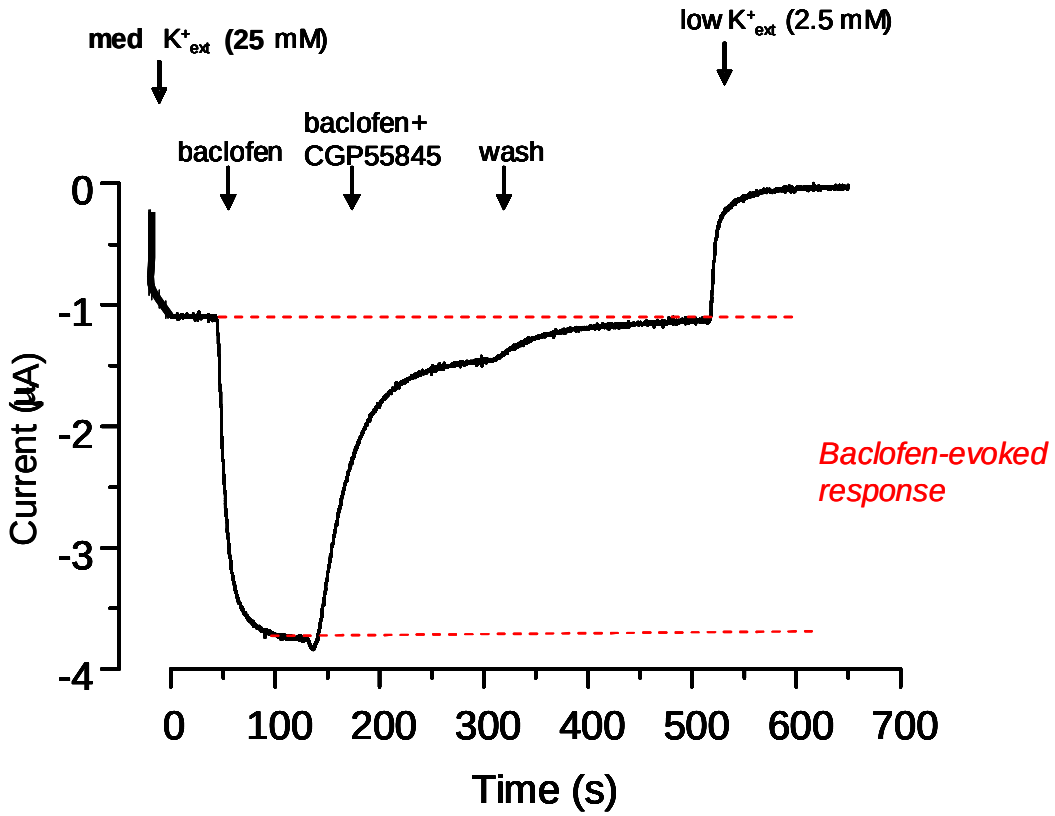

Figure 62 ***A representative trace of baclofen-evoked GABA$_B$R1b/R2 currents***
It was demonstrated that 10 µM baclofen evokes a large response, which can be blocked by 5 µM of the GABA$_B$ receptor antagonist CGP55845. The drug was washed off with medium-potassium buffer and the current was brought back to baseline with low-potassium buffer.

4.4.1.4 Current-voltage curves (IV)

Current-voltage (IV) curves demonstrate the characteristic behaviour of the potassium channels used in the system. It was successfully confirmed from the current-voltage curves (Figure 63 and Figure 64) that both GABA$_B$R1a/R2 and GABA$_B$R1b/R2, when co-expressed with GIRK3.1/3.4, demonstrate inward rectification which is an expected behaviour from potassium channels. The theoretical equilibrium potential for

K^+ ions is -31 mV according to the Nernst equation, when $[K^+]^{ext}$ = 40 mM. Pleasingly, this theoretical value is very similar to the experimental values seen in Figure 63 and Figure 64.

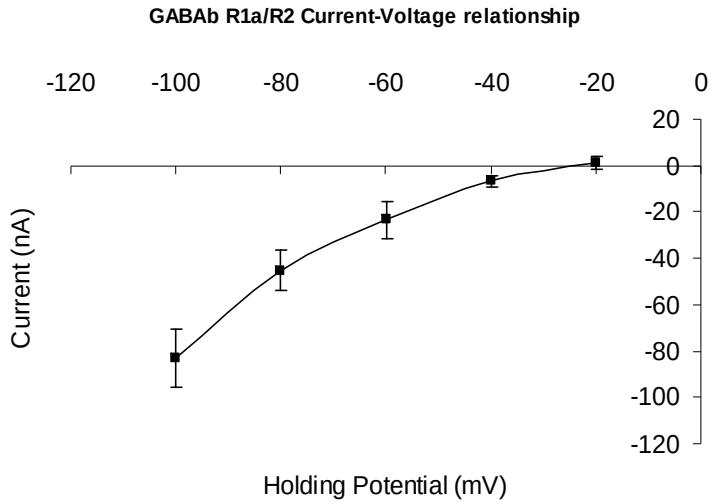

Figure 63 ***GABA$_B$R1a/R2 current-voltage relationship***
Current-voltage plot demonstrating the inward current behaviour of potassium channels coupled to the GABA$_B$R1a/R2 receptor and expressed in oocytes (n=4, error bars illustrate standard error of mean (SEM) values.)

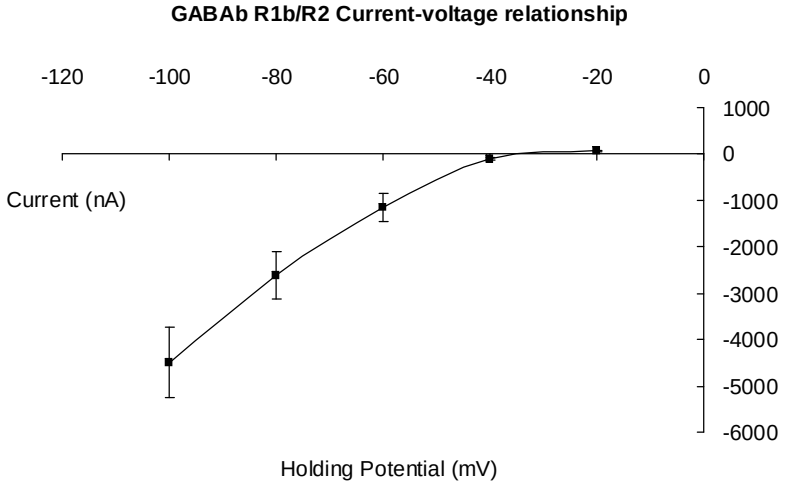

Figure 64 ***GABA$_B$R1b/R2 current-voltage relationship***
Current-voltage plot demonstrating the inward current behaviour of potassium channels coupled to the GABA$_B$R1b/R2 receptor and expressed in oocytes (n=5, error bars illustrate SEM values).

4.4.2 Pharmacological differences between the oocyte-expressed isoforms $GABA_BR1a$ and $GABA_BR1b$

4.4.2.1 Exploration of differences in potency of baclofen at the two $GABA_B$ receptors isoforms

Throughout this study baclofen-evoked currents and CGP55845-mediated block of these currents were investigated at the holding potential of -100 mV. Figure 61 and Figure 62 show typical TEVC traces recorded from oocytes expressing $GABA_BR1b/R2$ and $GABA_BR1a/R2$ receptors where baclofen-evoked inward currents are detected that are blocked by CGP55845. No apparent pharmacological differences have previously been proven for the two isoforms $GABA_BR1a$ and R1b, although some that were originally suggested (Leaney and Tinker, 2000; Ng et al., 2001; Parker et al., 2004) proved to be controversial (Jensen et al., 2002; Lanneau et al., 2001; Shimizu et al., 2004; Sills et al., 2005). Their affinities for baclofen were originally reported to be very similar (Malitschek et al., 1998), however an investigation of the receptor behaviour over a range of high and low concentrations of agonist was needed to test wether they display identical pharmacological behaviour in our system.

4.4.2.1.1 Saturating concentrations of baclofen

In order to determine a concentration of baclofen that is sufficient to saturate the receptor, baclofen-evoked responses were measured at concentrations of 10 µM and 100 µM, both of which have previously been reported to be suitable (Nehring et al., 2000;

Uezono et al., 2006). The experiments were initiated with the lower concentration of baclofen, and then the oocytes were perfused with TEVC external buffer for four minutes to wash off the agonist, followed by application of the higher concentration of baclofen. Very little difference in response was obtained, for either of the two $GABA_B$ receptor isoforms, when the concentration of baclofen was increased from 10 to 100 μM [for $GABA_BR1a$-expressing oocytes: 274 nA (10 μM baclofen) versus 283 nA (100 μM baclofen); for $GABA_BR1b$-expressing oocytes: 3360 nA (10 μM baclofen) versus 3270 nA (100 μM baclofen)] (Figure 65**)**. The experiment was also carried out in the reverse order, *i.e.* with 100 μM baclofen applied first followed by 10 μM - this reversal produced identical results. A value of 10 μM baclofen was therefore regarded as near-saturating and was chosen for future experiments on this basis. It is worth noting for all experiments in the present study that a delay in response was observed in oocytes expressing $GABA_BR1a/R2$ receptors, while $GABA_BR1b/R2$ receptors responded almost instantly to drug application. This could be related to differences in receptor activation via different G protein isoforms (Leaney and Tinker, 2000).

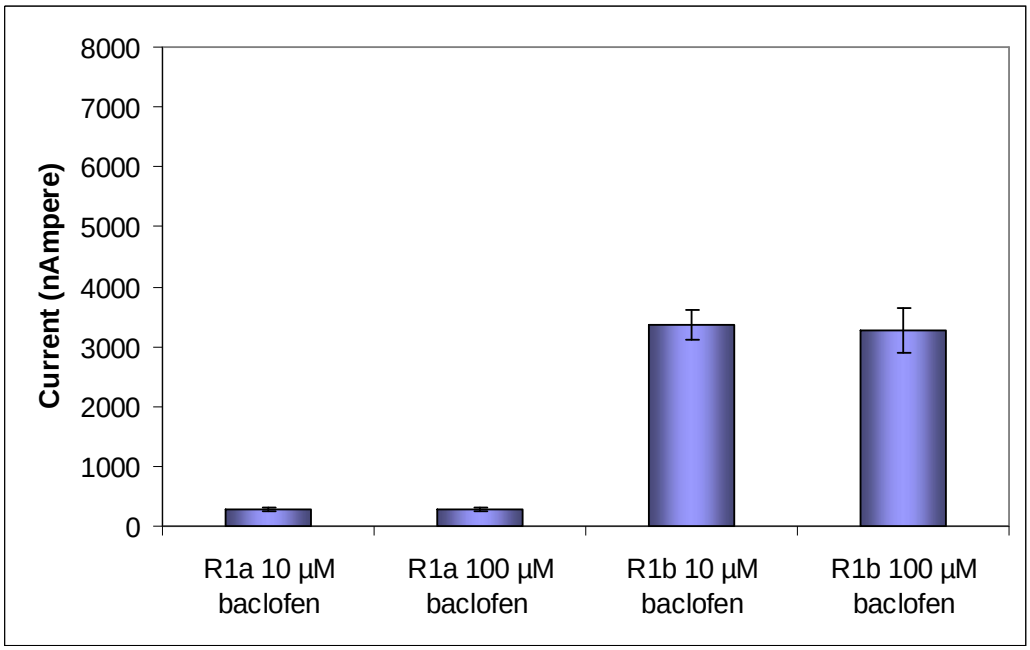

Figure 65 ***Saturation is achieved at 10 µM baclofen***
Currents were measured for the $GABA_BR1a/R2$ and $GABA_BR1b/R2$ receptors when perfused with 10 µM and 100 µM baclofen (n=3, error bars illustrate SEM values). Very little difference in response for the same isoform was observed between the two concentrations studied.

4.4.2.1.2 Lower concentrations of baclofen

The GIRK currents obtained for the two isoforms $GABA_BR1a/GABA_BR2$ and $GABA_BR1b/GABA_BR2$ in response to 1, 3 and 10 µM baclofen were measured, as shown in Figure 66 (Raw data in Appendix C.III). A representative TEVC trace for each of the $GABA_B$receptor isoforms are displayed in Figure 68 and Figure 69.

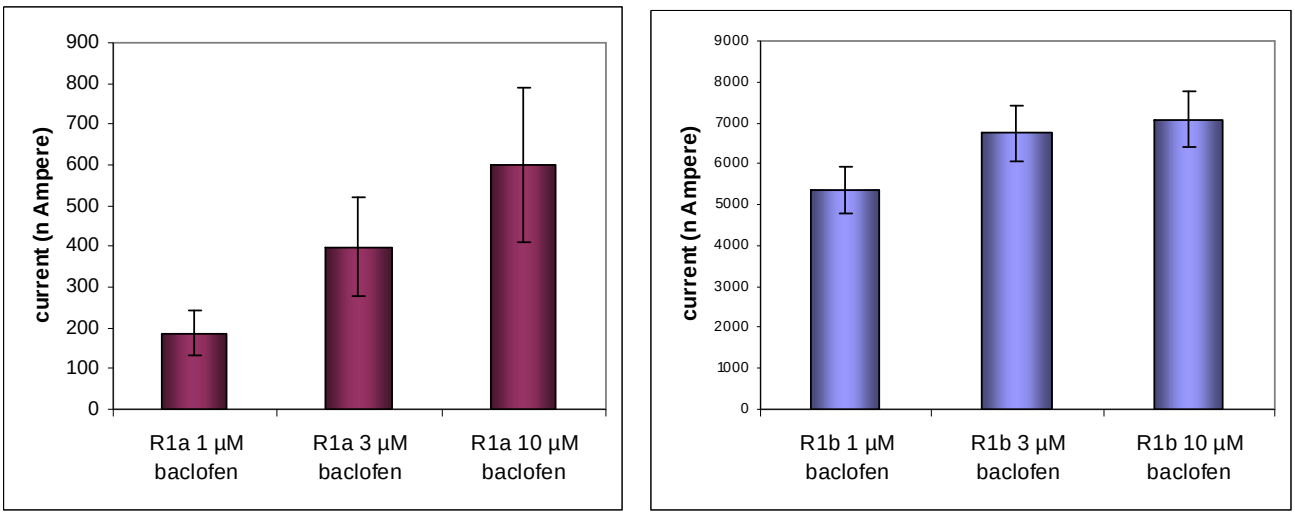

Figure 66 ***Differences in responses to low concentrations of baclofen***
Currents were measured for the $GABA_B$ R1a/R2 and $GABA_B$ R1b/R2 receptor when perfused with 1 µM, 3 µM and 10 µM baclofen (R1a/R2, n= 5; R2/R1b, n= 3; error bars illustrate the SEM values). Note that the responses for $GABA_B$R1b/R2 are 10 fold larger than for $GABA_B$R1a/R2

In the case of $GABA_B$R1a/R2, the GIRK currents measured in response to 1 µM and 3 µM baclofen are ~30% and 65%, respectively, of the response for 10 µM baclofen (n=5). For $GABA_B$R1b/R2, the values were 75% (1 µM) and 95% (3 µM) of the 10 µM response (n=3) as seen in Figure 67. One explanation is that baclofen saturates at lower concentrations, and thereby is more potent at $GABA_B$R1b/ R2 compared to $GABA_B$R1a/R2.

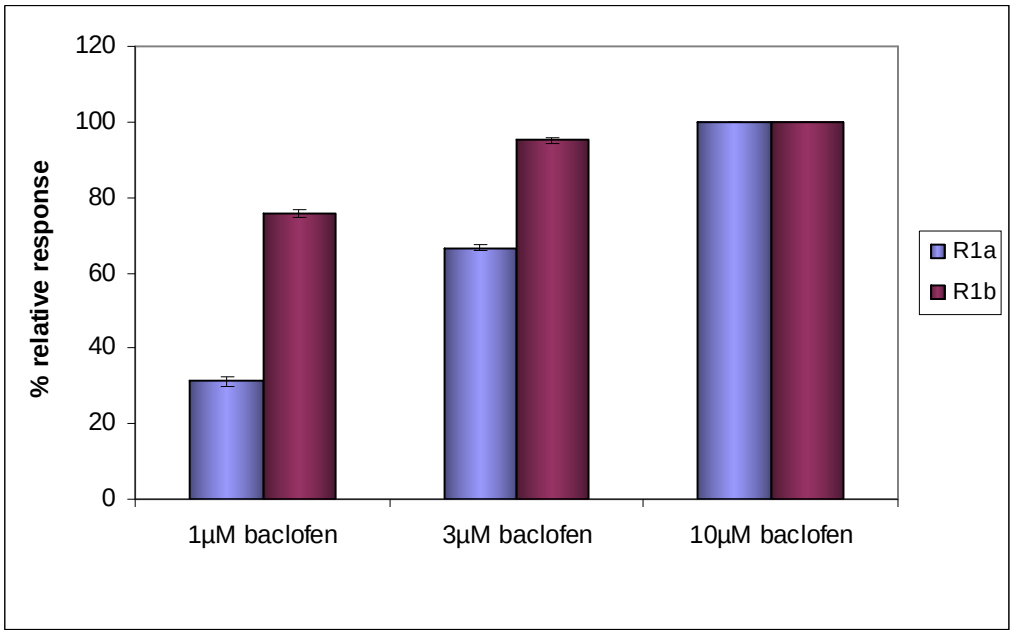

Figure 67 ***Illustration of relative responses to variation of baclofen concentrations***
The response value recorded at 10 µM for each construct is labelled '100%' and the responses at 3 µM and 1 µM is determined as relative percentage in relation to the 10 µM value. The standard error of mean (SEM) is indicated as error bars.

4.4.2.1.3 Step-wise application of baclofen

The difference in response to various baclofen concentrations was further demonstrated by recording TEVC traces (Figure 68 and Figure 69). While IV plots demonstrate the characteristic behaviour of an inwardly rectifying ion channel, TEVC traces show drug-evoked responses of the receptor in 'real-time'. Figure 68 illustrates how, in the case of oocytes expressing $GABA_BR1a/R2$ receptors, incremental additions of baclofen (from 1 µM to 3 µM to 10 µM) produce an approximately steady enhancement of the response for each stepwise increment in baclofen concentration. This implies the binding site for baclofen is not fully saturated at 10 µM. Figure 69, on

the other hand, illustrates how similar incremental increases of baclofen - from 1 µM to 3 µM to 10 µM - to $GABA_BR1b/R2$, result in a different pattern. There is a relatively large initial response to 1 µM baclofen, followed by smaller increases, as baclofen is incremented, indicating that baclofen has nearly saturated its binding site on the receptor at a concerntation of 10 µM. Thus these data also indicate a higher potency of baclofen for $GABA_BR1b/R2$ compared to $GABA_BR1a/R2$. However, the affinity for baclofen has been stated to be similar for both isoforms (Malitschek et al., 1998).

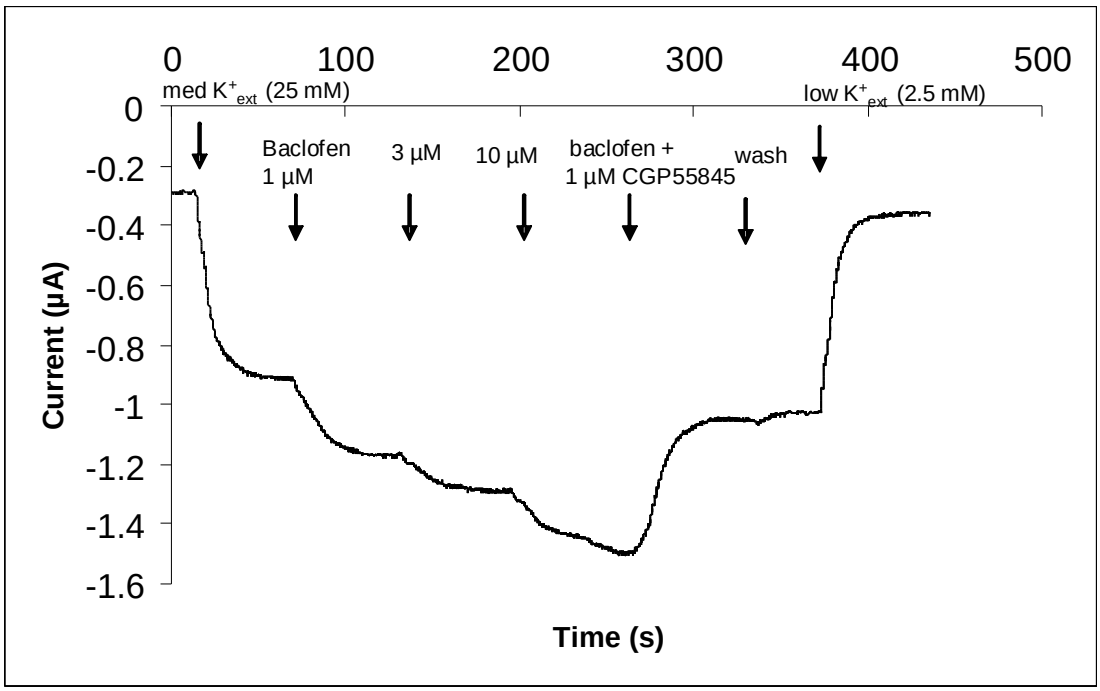

Figure 68 ***Baclofen-evoked response of an oocyte expressing $GABA_BR1a/R2$ receptors.*** Stepwise increases of baclofen concentration from 1 µM to 10 µM evoke a steadily increasing response. TEVC external 'low K^+ buffer' was switched to 25 mM K^+ solution. 1 µM, 3 µM and 10 µM baclofen were applied in a stepwise manner followed by 10 µM baclofen + 1 µM CGP55845. The oocyte was washed with 25 mM K^+ solution, followed by 2.5 mM K^+ solution.

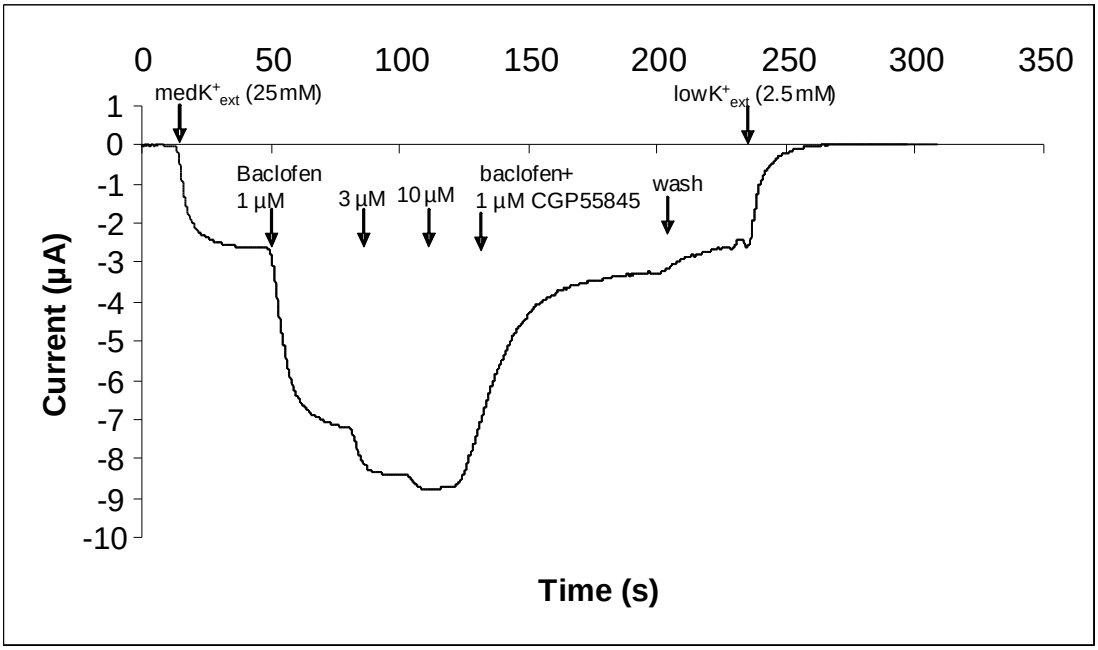

Figure 69 ***Baclofen-evoked response of an oocyte expressing $GABA_BR1b/R2$ receptors.*** Stepwise increase of baclofen from 1 µM to 10 µM produce only small differences in response consistent with an approach to saturation at the highest baclofen concentration used.

4.4.2.2 Assessing differences in response between the two isoforms of the $GABA_B$ receptor elicited by the antagonist CGP55845

4.4.2.2.1 Lower concentrations of CGP55845

The $GABA_B$ receptor selective antagonist CGP55845 was used throughout this study to investigate the inhibition of baclofen-evoked currents on $GABA_BR1a$ and $GABA_BR1b$ when expressed together with $GABA_BR2$ in *Xenopus* oocytes. The inhibition of GIRK currents obtained for $GABA_BR1a/R2$ and $GABA_BR1b/R2$, in response to 0.3, 1 or 3 µM CGP55845 after application of 10 µM baclofen, was

measured. The results appear to demonstrate that the potency of the antagonist CGP55845 is lower for $GABA_BR1a/R2$ than for $GABA_BR1b/R2$ (Figure 72). In the case of $GABA_BR1a/R2$, CGP55845 reduced by some 60% the GIRK currents measured in response to 10 µM baclofen. In the case of $GABA_BR1b/R2$, the GIRK currents measured in response to 10 µM baclofen were about 90% inhibited by the $GABA_B$ receptor antagonist CGP55845. This was explored as described further in the next section.

4.4.2.2.2 Step-wise application of CGP5584

Differences in response to stepwise application of CGP55845 were observed between the two isoforms as seen in Figure 70 and Figure 71. CGP55845 appears to block a 10 µM baclofen-evoked GIRK current in oocytes expressing $GABA_BR1b/R2$ in a more pronounced way, and at lower concentrations, compared to its effect on $GABA_BR1a/R2$. This indicates the antagonist is more potent at (*i.e*. less drug is needed to produce a given effect on) $GABA_BR1b/R2$. A solution of 0.3 µM CGP55845 blocked the measured current by about 50 % in the case of $GABA_BR1a/R2$ compared to 90% for $GABA_BR1b/R2$. Higher concentrations of antagonist, up to 10 µM, result in only a very slight further reduction in the case of $GABA_BR1b/R2$, indicating the lower concentration of antagonist used is able to compete effectively with the near-saturating concentration of baclofen used in this experiment (Figure 71). In the case of $GABA_BR1a/R2$ on the other hand, incremental additions of CGP55845 above the starting concentration of 0.3 µM further reduced the baclofen-evoked response up to a maximum of 64% (10 µM CGP55845) as illustrated in Figure 70. This suggests that CGP55845 has a stronger

potency for $GABA_BR1b/R2$. Thus the antagonist CGP55845 appears to be less potent at blocking baclofen-evoked responses in $GABA_BR1a/R2$, despite the fact that baclofen is also less potent at this receptor isoform. These results imply that this antagonist struggles to compete with baclofen in the case of $GABA_BR1a/R2$ but competes effectively in the case of $GABA_BR1b/R2$. Potency depends on both affinity and efficacy of the drug. However, the system used in this study is not suitable to measure affinity of the ligand; further studies would be needed to look at affinities.

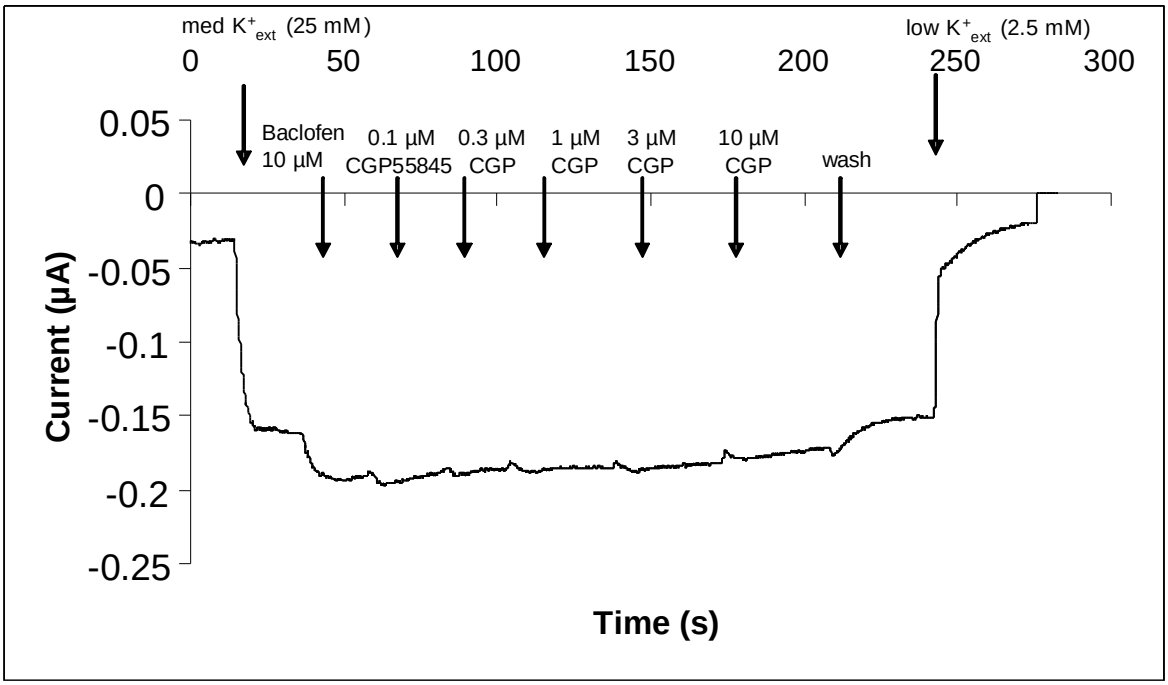

Figure 70 ***Effects of stepwise application of CGP55845 on currents recorded from an oocyte expressing $GABA_B$ R1a/R2 receptors***
A dose of 10 µM of antagonist CGP55845 blocks the baclofen-evoked response by an average of about 65%. External K^+ buffer was switched to 25 mM K^+ solution. 10 µM baclofen was applied followed by a stepwise application of 10 µM baclofen plus 0.1 µM, 0.3 µM , 1 µM, 3 µM and 10 µM CGP55845 The oocyte was washed with 25 mM K^+ solution, followed by 2.5 mM K^+ solution.

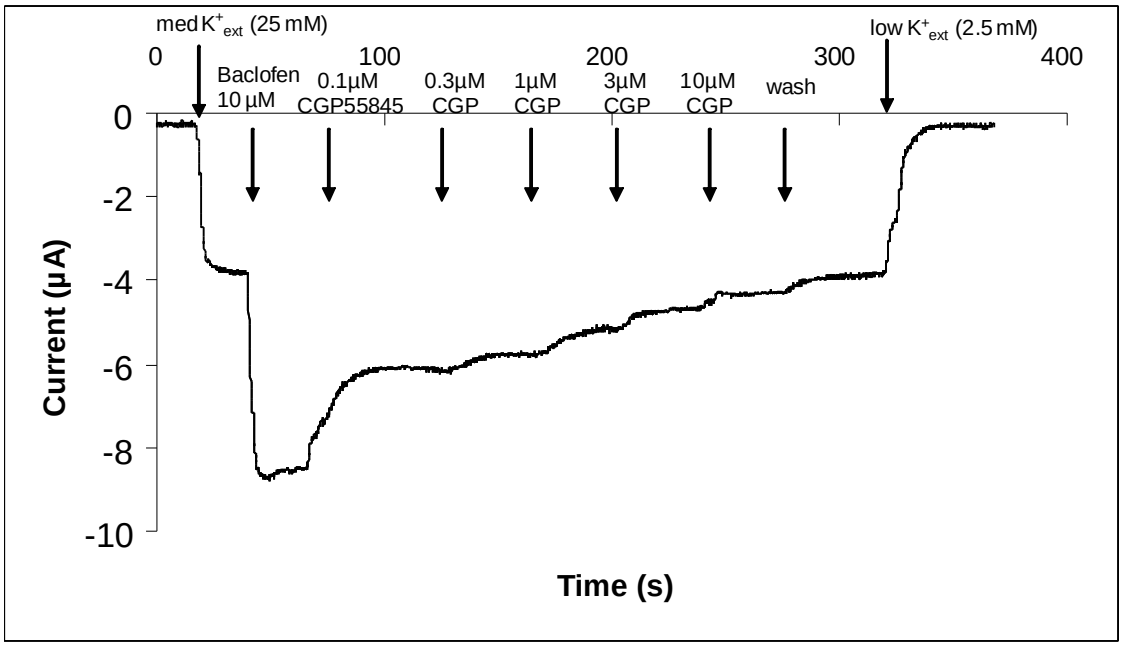

Figure 71 ***Effects of stepwise application of CGP55845 on currents recorded from an oocyte expressing GABA$_B$R1b/R2 receptors***
A dose of 10 µM of antagonist CGP55845 blocks the baclofen evoked response by an average of 90%.

To summarise, although no differences in affinity for baclofen or CGP55845 have previously been reported for the individual isoforms GABA$_B$R1a/R2 and GABA$_B$R1b/R2, differences in potency of CGP55845 were revealed in the current study, which may be linked to differences in affinity. CGP55845 shows a less efficient block of baclofen-evoked responses, at the investigated concentrations, in oocytes expressing GABA$_B$R1a/R2 receptors, compared to GABA$_B$R1b/R2, indicating a higher concentration of the antagonist is required for the same level of blocking of responses (Figure 72).

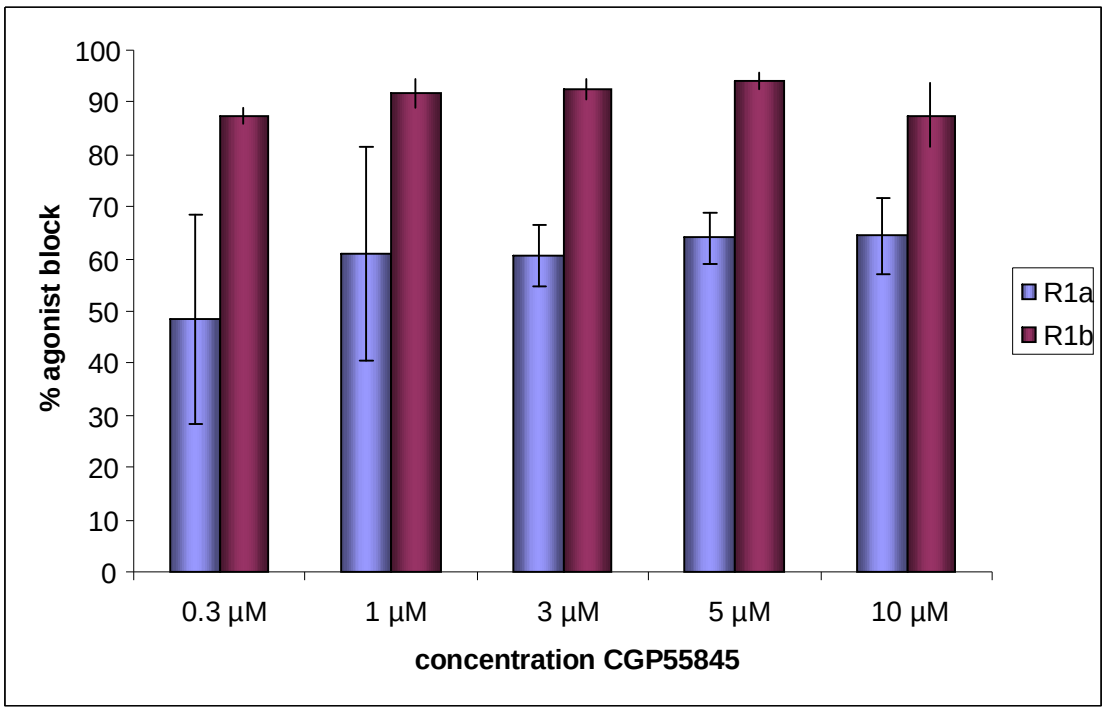

Figure 72 ***Percentage blocking of a baclofen-evoked response in $GABA_BR1a/R2$- (blue) or $GABA_BR1b/R2$- (purple) expressing oocytes.***
Blocking was measured at different concentrations of CGP55845 as seen in the figure**.** The difference in antagonist potency between isoforms is significant for the two concentrations of 3 µM ($p=1.48*10^{-05}$) and 5 µM ($p=2.03*10^{-06}$). The standard error of mean (SEM) is indicated as error bars (n= 20-30 for 3 µM and 5 µM, and n= 5-10 for the remaining concentrations.

4.4.3 Pharmacological responses to baclofen of $GABA_BR1a$ and $GABA_BR1b$ in the presence of laminin

It was determined previously in the current study (Chapter 2 and Chapter 3) that the CCP modules of the $GABA_B$ receptor and the extracellular protein laminin can interact with one another. It is not known, however, whether this interaction occurs *in vivo*, nor is it known if the interaction has any effect on the function of the receptor. To investigate this further in the oocyte model system, an experiment was set up in which

oocytes expressing $GABA_BR1a/R2$ or $GABA_BR1b/R2$ receptors were perfused with baclofen, and the response recorded to obtain a baseline. The individual oocytes were thereafter incubated with laminin or buffer (as a negative control) for two hours; this incubation period was followed by an identical perfusion of baclofen, and the response was recorded.

Surprisingly, in the cases of both laminin-incubated and buffer-incubated $GABA_BR1b/R2$-expressing oocytes, the detected responses appear to be consistently larger after the incubation compared to before the incubation (Table 12). The increase in response to baclofen for $GABA_BR1b/R2$-expressing oocytes incubated in the presence of laminin is greater than that for control oocytes incubated in buffer. On the other hand, and in contrast, $GABA_BR1a/R2$-expressing oocytes incubated in the presence of laminin showed a complete loss of response to baclofen post-incubation (Figure 73). A smaller decrease in response to baclofen was observed in the case of $GABA_BR1a/R2$-expressing oocytes that had been incubated in buffer without laminin.

Table 12. Results show precentage difference in baclofen-evoked response after incubation with laminin or buffer respectively.

R1a	**Oocyte 1**	**Oocyte 2**		**Average**
Laminin incubation	-100%	-100%	-	-100%
Buffer incubation	**-** 33%	- 53%	-	- 43%
R1b	**Oocyte 1**	**Oocyte 2**	**Oocyte 3**	**Average**
Laminin incubation	+96%	+84%	+120%	+100%
Buffer incubation	+17%	+34%	+74%	+42%

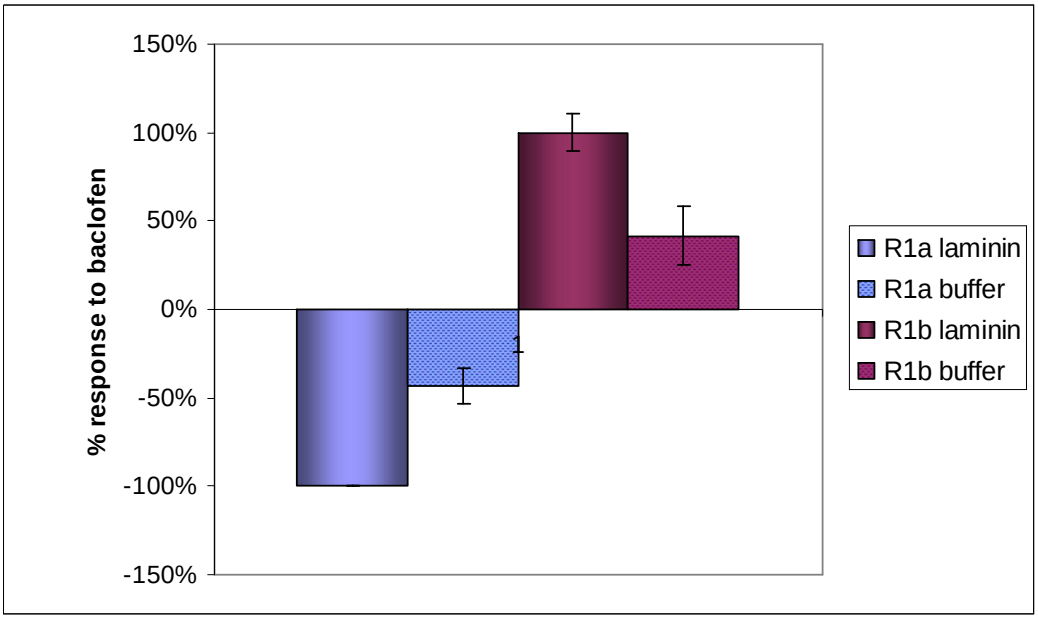

Figure 73 ***Effect of laminin on baclofen-evoked responses in GABA$_B$ receptors*****.**
Oocytes expressing GABA$_B$R1a/R2 or GABA$_B$R1b/R2 were incubated with laminin or buffer (negative control) and the difference in response to baclofen before and after incubation was determined. Laminin completely inhibited the response to baclofen in GABA$_B$R1a/R2 expressing oocytes (n=2) while the response was enlarged in oocytes expressing GABA$_B$R1a/R2 post laminin incubation (n=3)**.**

4.5 Discussion

4.5.1 *Xenopus laevis* oocytes as a model system for characterizing the $GABA_B$ receptor

For the purposes of the present study it was essential to establish a means of measuring the functional activity of $GABA_BR2/R1a$ and $GABA_BR2/R1$. In this respect, the *Xenopus* oocyte system adopted in the current work has many advantages including the following: the oocyte is well characterized and widely used and accepted as a model system; the oocyte contains histones, RNA polymerases, tRNA, ribosomes *etc.*, which enables the study of transcription and translation of injected cDNA or cRNA (Colman et al., 1984); the translation of exogenous RNA occurs in a normal living cell, and is therefore devoid of the artifacts that might be associated with a cell-free (*in vitro*) system; foreign proteins expressed in oocytes are correctly post-translationally modified and proteins containing multiple subunits are correctly oriented (Baker et al., 2007)

A potential disadvantage is that the *Xenopus* oocyte system necessitates the study of mammalian $GABA_B$ receptors expressed in a non-native cell, but this is not regarded as a major limitation given our aim of comparing the characteristics of different isoforms of the same functional receptor. The use of oocytes has, however, some more serious experimental limitations. Oocytes can be very sensitive to seasonal variations, which affect the level of protein expression as well as the survival time of the cell (Witchel et al., 2002). Indeed, oocytes sometimes deteriorate within a few days of removal from the

ovary, which complicates experiments where long incubation times (more than three days) are essential for protein expression. Moreover, expression levels can vary between individual oocytes and batches of oocytes because expression is transient. These issues can rapidly increase the number of experiments (and thereby the time) needed to achieve consistent and statistically significant results. A further consideration is that the physiological functions of oocyte proteins and mammalian proteins are optimal at different temperatures due to body temperature differences (16-20 ºC versus 37 ºC) – this could potentially affect the biochemical properties of the mammalian proteins under study (Witchel et al., 2002).

The present study was conducted to extend knowledge of the $GABA_B$ receptor, and in particular of the isoforms, $GABA_BR1a$ and $GABA_BR1b$. In the current work, the $GABA_B$ receptor was successfully expressed in *Xenopus* oocytes together with inwardly rectifying potassium channels. It was subsequently demonstrated that the expression of both subunits R1 and R2 of the receptor is required for activity. This observation is consistent with previous work (Bettler et al., 2004; Marshall et al., 1999; Mohler and Fritschy, 1999). Furthermore, the $GABA_B$ receptor was shown in this work (and in previous studies) to be coupled to inwardly rectifying potassium channels. The typical behaviour of an inwardly rectifying ion channel was demonstrated in the form of a current-voltage (I-V) plot. The responses obtained for $GABA_BR1a/R2$ recorded in this study were in good agreement with the responses for both $GABA_BR1a/R2$ and for $GABA_BR1b/R2$ previously reported (White et al., 1998). Unexpectedly, however, $GABA_BR1b/R2$ consistently evoked much larger responses to baclofen when expressed

in oocytes, compared to $GABA_BR1a/R2$ in the present study and compared to both isoforms as previously reported (White et al., 1998).

It seems unlikely that this difference between the baclofen-induced responses elicited by the two isoforms has a genuine pharmacological explanation, as no such differences have been reported previously for this well-studied receptor. Instead, the discrepancy could be due to variations in expression levels between the two isoforms. In this respect it is worth noting that the $GABA_BR1a$ and $GABA_BR1b$ trasncripts used here originated from different vectors. On the other hand, these vectors are highly similar in that they both contain 3'- and 5'-untranslated regions from a *Xenopus* β-globin gene. Nonetheless it remains a possibility that different expression levels prevail, despite injection of the same amounts of RNA, due to variation in cRNA stability between constructs; this could result in degradation of RNA in the cytoplasm (Tokmakov et al., 2006). Alternatively, it could be that the $GABA_BR1a/R2$ isoform is in fact being expressed well but is retained within the oocyte due to trafficking problems related to the presence of the two CCP modules at its N-terminus (not present in $GABA_BR1b$). Given that protein trafficking is a temperature-sensitive process, it may be altered in the case of $GABA_BR1a$ due to the fact that oocytes are maintained at lower temperatures (Wagner et al., 2000). A further possibility is that reduced signalling in the case of $GABA_BR1a$ may be due to differences in G-protein coupling between the two receptor isoforms, whereas R1a has been reported to signal preferentially through $G_{o\alpha}$, R1b signals equally through $G_{o\alpha}$ and $G_{i\alpha}$ (Leaney and Tinker, 2000). A final possibility is that *Xenopus* endogenous proteins interact selectively with the R1a isoform, and thereby

interfere with the interaction of R1a and R2, as has been reported for IKs channels (Wagner et al., 2000).

The two receptor isoforms, $GABA_BR1a/R2$ and $GABA_BR1b/R2$, appeared to exhibit differences in response to baclofen at lower concentrations (3 and 5 μM). The expression levels of the two receptors may vary between the two isoforms, as discussed above, which would explain a difference in the absolute response to baclofen. However, this does not explain the differences in potency of baclofen towards the two isoforms, *i.e.* the observation that less agonist is required to saturate the response in $GABA_BR1b/R2$ than in $GABA_BR1a/R2$. In a similar vein, CGP55845 is less potent at $GABA_BR1a/R2$ compared to $GABA_BR1b/R2$.

Differences in sensitivity between $GABA_B$ receptor isoforms towards other drugs – such as saclophen and CGP35348 - have been reported (Deisz et al., 1997). It was originally reported that gabapentin is an agonist for the $GABA_BR2/R1a$ but not for $GABA_BR2/R1b$ (Ng et al., 2001). It was claimed that this isoform-selective agonist was the first proof of pharmacologically distinct isoforms. This remains a controversial finding. Several research groups have been unable to confirm any agonistic (or antagonistic) properties for gabapentin at the $GABA_B$ receptor, let alone an isoform-specific agoinst (Jensen et al., 2002; Lanneau et al., 2001). In the present study, a further unexpected observation was that a delay in response was noted in oocytes expressing $GABA_BR1a/R2$ receptors upon application of drugs. For $GABA_BR1b/R2$ receptors, on the other hand, the response was immediate.

A particularly puzzling aspect of putatively isoform-specific agonists and antagonists is the fact that the ligand-binding site has been reported to be located well

away from the N-terminal domains that distinguish the two isoforms (Deriu et al., 2005). On the other hand, in the absence of structural data it is impossible to know this for sure. Moreover in the current work it was the downstream effects of ligand engagement (as opposed to direct measurements of affinity) that were observed - it is possible that the CCPs have a subtle, indirect, effect on the response of the receptor to occupation of the ligand-binding site. There might be differences, for example, in the conformational changes that are proposed to occur in the ectodomain upon binding of agonist/antagonist (Billinton et al., 2001; Bridges and Lindsley, 2008).

According to the Venus fly-trap model, the two major subdomains within the ectodomain of $GABA_BR1$ are conformationally mobile and can hinge towards one another; this closed conformation is stabilised by ligand. Closure of the "fly-trap" causes changes in the conformation of the transmembrane helical domain that are transmitted to the inside of the cell. The presence of the CCP modules could destabilise the active (closed) conformation such that higher occupancy of the ligand-binding site is required for a comparable amount of transduction to occur although the actual affinity for ligand is not altered (Bridges and Lindsley, 2008). It is also possible that different G-proteins are involved in coupling the receptor isoforms to the ion channels (Leaney and Tinker, 2000), explaining the delayed responses observed for $GABA_BR1a/R2$, but this has not been fully assessed in this study and further work is needed to investigate such a possibility.

It is tempting to speculate on possible a functional role for the isoform specificity observed in the current study. Of note is that the isoforms have distinct different expression patterns, both in regional and developmental distributions. $GABA_BR1a$ is

evenly distributed across the brain while $GABA_BR1b$ is predominantly expressed in cerebral cortex, thalamus and cerebellum (Fritschy et al., 1999). Moreover, $GABA_BR1a$ is the predominant isoform during development, while $GABA_BR1b$ becomes the main isoform in adult brain (Fritschy et al., 1999; Mohler et al., 2001). This is discussed further in Chapter 5.

The levels of expression of mRNA for the receptor subunits R1 and R2 are differentially regulated. This is unexpected given that the receptor requires a functionally obligate heterodimer. One possible explanation is that dimerisation of $GABA_B$ R1 and R2 represents just one out of several functions of these two proteins. Additional functions could include dimerisation with an as-yet unidentified receptor subunit (Billinton et al., 2001; Clark et al., 2000), or with another GPCR; indeed, such an interaction was reported for the $GABA_A\gamma2S$ and $GABA_B1$ receptor subunits (Balasubramanian et al., 2004), allowing the $GABA_BR1$ subunit to be trafficked to the cell surface in the absence of the R2 subunit. Furthermore, functional crosstalk between the two receptor types A and B has been reported (Balasubramanian et al., 2004), increasing internalisation of the $GABA_B$ receptor when bound to the $GABA_A$ subunit, and thereby opening up the possibility of multiple receptor combinations and pharmacological diversity.

4.5.2 Pharmacological responses to baclofen on $GABA_B$ receptor isoforms R1a and R1b in the presence of Laminin

The pharmacological diversity of the metabotropic $GABA_B$ receptor observed *in vivo* remains (Bettler et al., 2004; Marshall et al., 1999) a matter of contention *in vitro*, notwithstanding the results described in the previous sections. The *in vitro* diversity may require auxillary proteins, possibly interacting with the CCP modules of $GABA_B$R1a. As outlines in the introduction, laminin and fibulin could act in this way.

The preliminary results of the present study indicated an inhibition of the response to baclofen of $GABA_B$R1a/R2 following incubation with laminin (compared to the smaller effect in the control that was incubated with buffer). No such inhibition was seen for $GABA_B$R1b/R2. Instead, a slightly increased response to baclofen was seen for oocytes expressing $GABA_B$R1b/R2 after incubation with both laminin and buffer.

It should be noted that it proved difficult to maintain healthy $GABA_B$R1a/R2-expressing oocytes able to sustain the multiple recordings required for this experiment. Surprisingly these oocytes deteriorated more rapidly than oocytes expressing $GABA_B$R1b/R2 or non-injected oocytes. This led to a very small sample size being used for these experiments. The loss of responsiveness in the buffer control for $GABA_B$R1a/R2 underlines the difficulty of maintaining stable $GABA_B$R1a/R2-expressing oocytes throughout the experiments. Nonetheless, it is intriguing that the $GABA_B$R1a/R2-expressing control (buffer-incubated) oocytes responded to baclofen, whereas the laminin-treated $GABA_B$R1a/R2-expressing oocytes did not. It would be of

interest to investigate whether a smaller interacting fragment of laminin, like α5LG4-5, would exert a similar effect. This remains to be explored.

CHAPTER 5

Overall conclusions and future work

5 Chapter 5 Overall conclusions and future work

A central question in metabotropic GABA receptor biology is: how can the wide functional diversity observed *in vivo* be reconciled with the very limited or unknown pharmacological variations that have been detected *in vitro*? The current work set out to investigate the functional consequences of the presence of two CCP modules within the extodomain of the R1a subunit of the $GABA_BR1a/R2$ dimer.

The results of the current study on laminin and fibulin, based primarily on yeast-two-hybrid assay and surface plasmon resonance, strongly suggest that these modules, which are of a type found in dozens of mammalian extracellular proteins, recognise and bind directly to two proteins of the ECM, laminin and fibulin. Moreover, the results have helped to pin down the domains involved – namely the C-terminal LG domain of the laminin alpha5 chain, and the C-terminal fragment of fibulin-2. In the case of laminin, the involvement of LG domains is in agreement with observations of interactions involving these types of domains in other proteins (Fernandez and Griffin, 1994; Hardig and Dahlback, 1996; Hardig et al., 1993; Hillarp and Dahlback, 1990). In addition, laminin-1 was identified as an interacting partner, suggesting multiple laminins acting as binding parners to the $GABA_B$ receptor. In a follow-up study (discussed further below), our collaborators in the Bettler group (University of Basel) have gone on to show that a splice variant ($GABA_BR1j$), consisting solely of the two CCP modules, binds to specific sites on neurones with low-nM affinity, although they were unable to identify the targeted protein.

The physiological purpose of the interaction between the $GABA_B$ receptor R1a and the ECM is intriguing, especially in the light of literature that was published during the course of the present study (further details below). In the current work, this issue was addressed by expression of functional $GABA_BR1a/R2$ and $GABA_BR1b/R2$ receptors in the *Xenopus laevis* model system. This approach yielded surprising results in that $GABA_BR1b/R2$ receptors exhibited a larger response to baclofen than had previously been reported; on the other hand, baclofen-evoked responses were consistently more difficult to measure for $GABA_BR1a/R2$. In the current study, the agonist baclofen as well as the antagonist CGP55845 was also more potent at $GABA_BR1b/R2$ compared to $GABA_BR1a/R2$. Thus the current study has contributed to the controversy over differential responsiveness of isoforms to small-molecule ligands. Moreover the small-ligand results are hard to explain from a structural perspective although it is worth remembering that no experimentally derived structure yet exists for the $GABA_B$ receptor. As was discussed in Chapter 4, the intriguing differences in spatial and temporal distribution of the two isoforms are not irreconcilable with putative differences in ligand affinities. But further work is needed to clarify these issues.

In the light of these unexpected trace data, the results obtained in the presence of laminin have to be regarded with caution. Nonetheless, and despite the limited number of observations, the apparent abolition of the baclofen-evoked response in $GABA_BR1a/R2$–expressing oocytes following incubation with laminin is noteworthy. By contrast the response to baclofen in the $GABA_BR1b/R2$-expressing oocytes remained unperturbed, or was increased, by treatment of the oocytes with laminin. While these experiments need to be repeated a sufficient number of times to establish statistically

rigorous data, such differences between R1a and R1b in the effects of laminin could have major implications for the field.

Thanks to numerous recent reports, it is becoming ever more widely accepted that several neurotransmitter receptors have extracellular binding partners, and these interactions are suspected to modulate both synaptic localisation and signaling of the receptors. For example, both agrin and laminin have been linked to the clustering of acetylcholine receptors at neuromuscular junctions (Sugiyama et al., 1997; Weston et al., 2007). Neural agrin was named after its function in aggregating acetylcholine receptors in development of neuromuscular junctions. The C-terminal laminin-LG domain of agrin is involved in clustering of the receptor (Ferns et al., 1993; Ngo et al., 2007), by signaling through muscle specific kinase (MuSK) and thereby activating the proteins 'downstream-of-tyrosine-kinase-7' (Dok-7), casein kinase 2 (CK-2) and rapsyn (Ngo et al., 2007). Laminin-1 ($\alpha1\beta1\gamma1$) was identified as being involved in the clustering of acetylcholine receptor (Sugiyama et al., 1997). The α1-chain is most likely the interacting chain (as laminin-2 ($\alpha2\beta1\gamma1$) and laminin-11 ($\alpha5\beta2\gamma1$) were reported not involved), by signalling through a different pathway than agrin. Laminin-clustering has been shown not to require MuSk but to require Rac, Rho and rapsyn (Weston et al., 2007). In another example, the N-terminal 92 residues of the extracellular domain of the ionotropic AMPA receptor subunit GluR2 was shown to make a specific and direct interaction with the ectodomain of N-cadherin, a single-pass transmembrane protein that plays a key role in synaptogenesis, neurite outgrowth, axon guidance and dendrite arborisation (Saglietti et al., 2007). Moreover, candidates for clustering of the AMPA receptor are the neuronal pentraxins. Pentraxins are thought to be involved in neuronal

uptake and clearing proteins away during synaptic remodeling (Kirkpatrick et al., 2000). The AMPA subunit GluR4 binds neuronal pentraxin 1 (NP1) and neuronal pentraxin receptor (NPR) via its N-terminal extracellular domain**;** this interaction was reported to be involved in recruitment of the subunit to synapses (Sia et al., 2007). Furthermore, naturally occurring secreted isoforms of other receptors comprising CCP modules have been found to have a physiological effect on receptor function. The CCP domain-containing soluble receptor IL-15 receptor α for example, can inhibit IL-15 activity while a truncated soluble form of the same receptor increases IL-15 activity (Bulanova et al., 2007).

Recently our collaborators performed studies of the truncated isoform $GABA_BR1j$, which consists solely of the two CCP modules. These provide further context for interpretation of the laminin/fibulin interactions. This small two-CCP module protein was found to inhibit the effect of pre-synaptic $GABA_B$ heteroreceptors on glutamate release. Such an observation is striking since the affected heteroreceptors contain the R1a subunit (Vigot et al., 2006), not the R1b subunit. Indeed, no such effect was measurable on autoreceptors or post-synaptic heteroreceptors that contain the R1b subunit. These important results suggest that R1j is competing selectively with the CCP portion of R1a, presumably for an extracellular binding partner protein. An appropriate interaction partner presumably lies on, or in the vicinity of, the pre-synaptic release machinery, although the physiological role of this putative interaction remains a matter of speculation. To test the hypothesis that the binding partner is, in fact, fibulin-2 we supplied samples of recombinant fibulin-2 to the Bettler group (Tiao et al., 2008). These co-workers showed that incubation of hippocampal slices with recombinant fibulin-2 (40

nM) did not perturb baclofen-mediated antagonism of evoked glutamate release. Nor did 40-nM fibulin-2 neutralize the inhibitory action of 40-nM recombinant R1j at heteroreceptors. Thus we concluded that the impairment of heteroreceptors by the R1j protein does not involve scavenging of fibulin-2. On the other hand, we did not test any laminin fragments in these studies and laminin remains a potential partner. In order to complete the characterization of the interaction with laminin *in vivo*, a study involving hippocampal slices expressing $GABA_BR1a/R2$ heteroreceptors could be studied with an addition of laminin, similarly to the study by Tiao (2008), to investigate if the laminin interaction is involved in the localisation of the R1a subunit to glutamatergic release sites.

In addition to a strengthening precedent amongst neuroreceptors for ectodomain-mediated functionally critical protein:protein interactions, there is growing evidence for distinct differences in regional and developmental expression patterns of $GABA_BR1a$ versus R1b. Thus $GABA_BR1a$ expression appears to be evenly distributed throughout the brain, while $GABA_BR1b$ is predominantly expressed in cerebral cortex, thalamus and cerebellum. Moreover, $GABA_BR1a$ is the predominant isoform during development, while $GABA_BR1b$ becomes the main isoform after postnatal-week three (Fritschy et al., 1999; Mohler et al., 2001). Recently, differences in the subcellular localisation of the two receptor isoforms was reported which supports the possibility of distinct functions *in vivo* (Vigot et al., 2006). $GABA_BR1a$ was reported to be primarily expressed at glutamatergic terminals, while $GABA_BR1b$ was found opposite glutamate release sites, supporting distinct pre- and postsynaptic functions. Distinct physiological roles have been suggested, where R1a plays a role in synaptic plasticity but R1b does not (Vigot et

al., 2006). while R1b is responsible for the long lasting inhibition of dentric Ca^{2+} spikes (Perez-Garci et al., 2006). Together, these observations suggest distinct additional roles of $GABA_BR1a$ over $GABA_BR1b$ that are likely attributable to its CCP modules. Thus, precedent and differential expression both support a hypothesis that the interaction of $GABA_BR1a$ with laminin, demonstrated in the current study, may play a role in development of neural pathways or synaptic connections.

To investigate further the role of the CCP modules, it would be of interest to study the receptor isoforms *in vivo*, where the presence of auxilary proteins may modify pharmacology of the receptor through interaction with the R1a CCPs. An *in vivo* system consisting of brain slices from homozygous mice lacking the R1a or R1b isoform respectively ($R1a^{-/-}$ and $R1b^{-/-}$), as described by Vigot *et al* 2006, would aid the study of such an effect. Furthermore one could use brain preparations from different stages of development, or supplement with specific laminin modules of interest, to exhaust the possibility of pharmacological differences between the $GABA_B$ receptor isoforms.

In conclusion, this thesis has emphasised the complexity of the different isoforms of the $GABA_B$ receptor, highlighting the involvement of CCP modules binding to the extracellular partners laminin and fibulin. Interactions involving the CCP modules might introduce as of yet unobserved pharmacological distinctions between the receptor isoforms, or they might be important in establishing differences in spatial or temporal distributions of the receptor sub-types. The biological significance of the interaction remains to be investigated further.

APPENDICES

Appendix A.

I. Primers for YTH construct:

Laminin alpha5 chain LG domains 1-5 (residues 2733-3695) was amplified from a human cDNA library using the following primers

Forward: 5’ GTC AAG GTG CCC ATG AAG TT 3’

Reverse: 5’ C TGT GTC CTA GGC GGC TG 3’

Laminin alpha5 for cloning into pGADT7

Forward (Nde1 site): 5’ GG GAA TTC CAT ATG CCC ATG AAG TTC AAC 3’

Reverse (Xho1 site): 5’ CC TGT CTC GAG CTA GGC GGC TGG 3’

No primers were used for the other constructs used in this study, as they could be transferred from other plasmids using restriction digests.

Appendix B.

I. Pre-concentrations

Laminin 1 (CM5):

Laminin-1 (L2020) was diluted in four different pH buffers, injected over the chip surface and analysed for electrostatic attraction to the chip surface. pH 5 was chosen as a suitable pH for immobilisation.

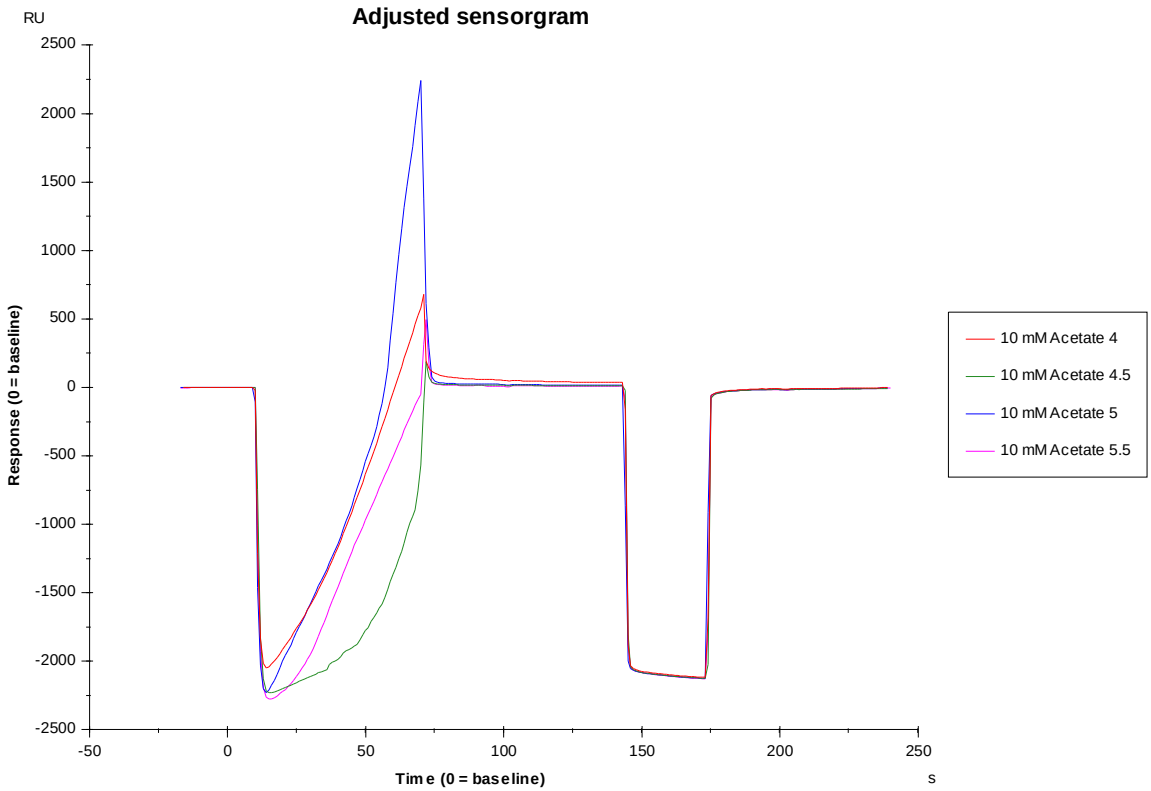

Laminin-10/11 (CM5):

Laminin-10/11 (AG56P) was diluted in four different pH buffers, injected over the chip surface and analysed for electrostatic attraction to the chip surface. pH 4 was chosen as a suitable pH for immobilisation.

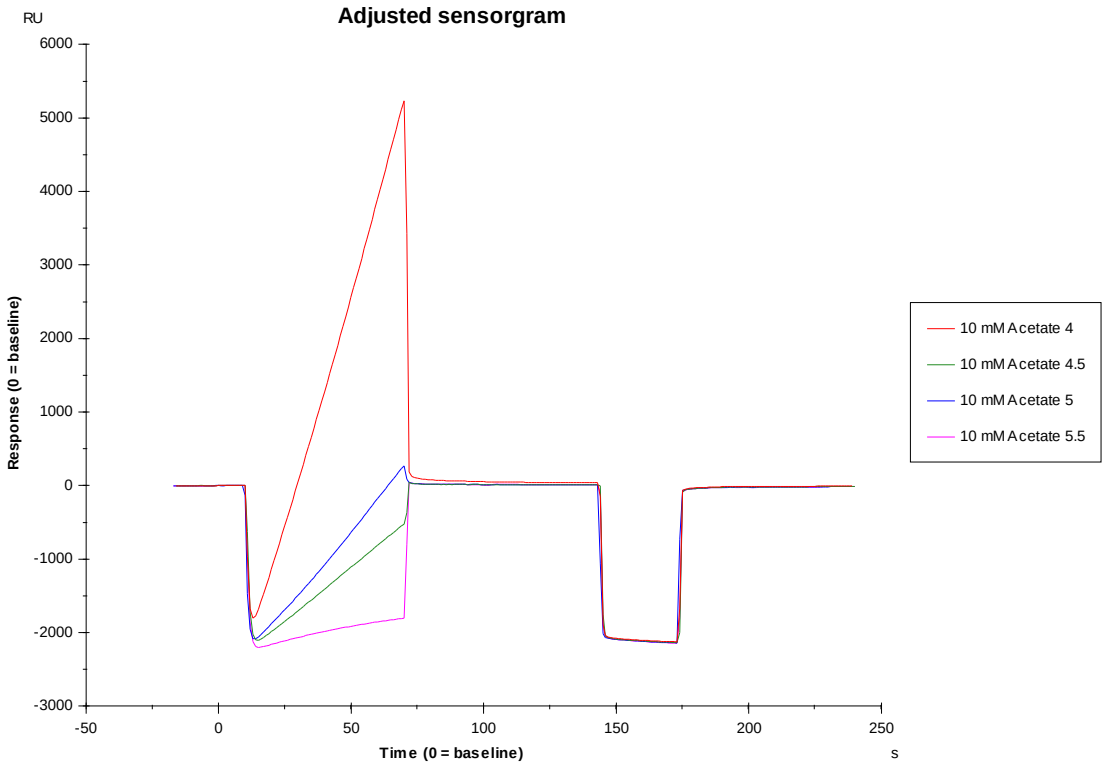

Laminin alpha1 LG1-3 (CM5):

Due to insufficient amount of protein available, Laminin alpha1 LG1-3 was diluted in only two different pH buffers (pH5 and pH5.5), injected over the chip surface and analysed for electrostatic attraction to the chip surface. pH 5 was chosen as a suitable pH for immobilisation.

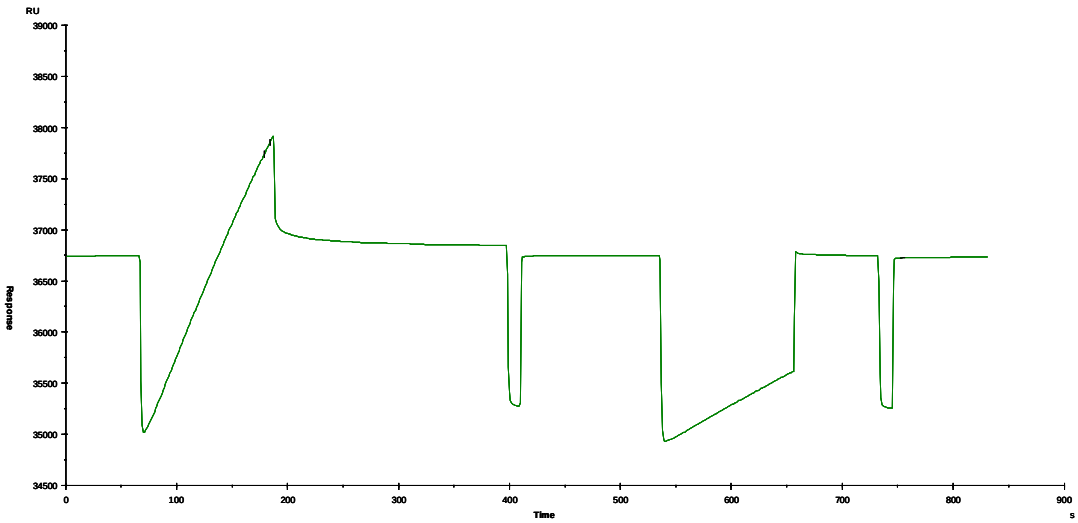

pH5 pH5.5

Laminin alpha1 LG4-5 (CM5):

Laminin alpha1 LG4-5 was diluted in four different pH buffers, injected over the chip surface and analysed for electrostatic attraction to the chip surface. The ligand appears to be highly attracted to the chip surface. Acetate buffer pH 5.5 was therefore chosen for immobilisation.

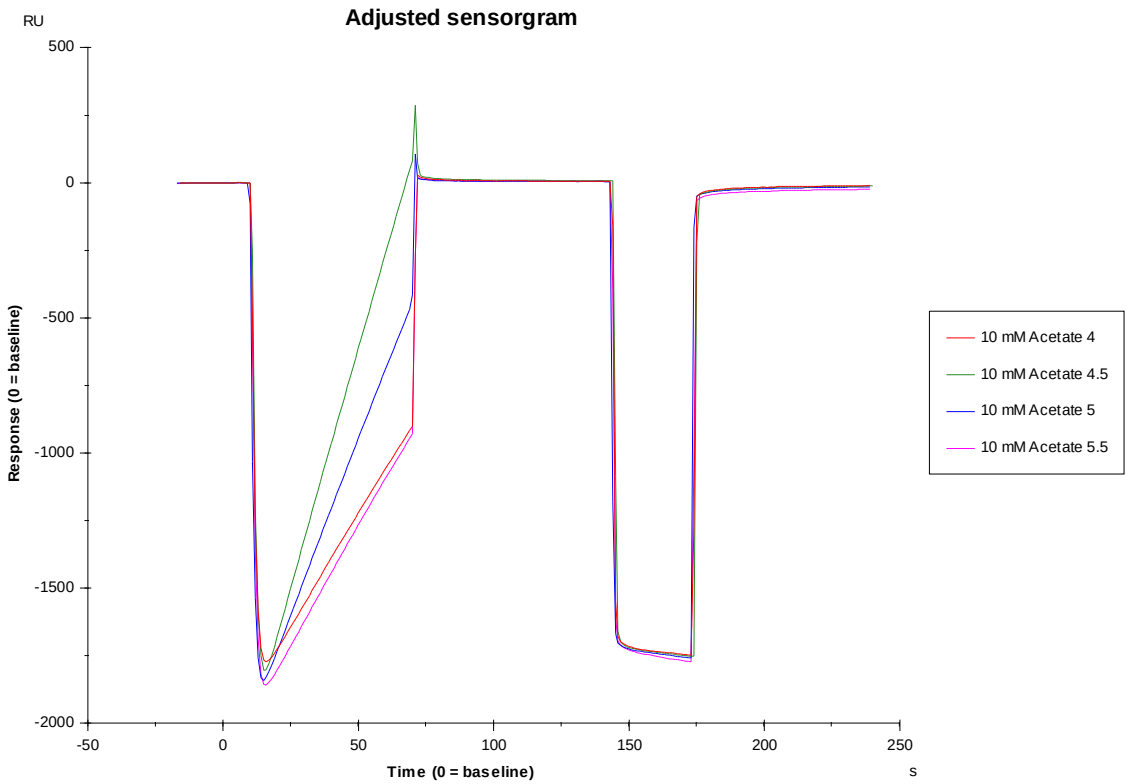

$GABA_B$ CCP1-2 (CM5):

$GABA_B$R1a CCP1-2 was diluted in four different pH buffers, injected over the chip surface and analysed for electrostatic attraction to the chip surface. The reaction appears to be very fast. pH 5.5 was therefore chosen for immobilisation. Furthermore, the ligand was diluted to 10 µg/ml.

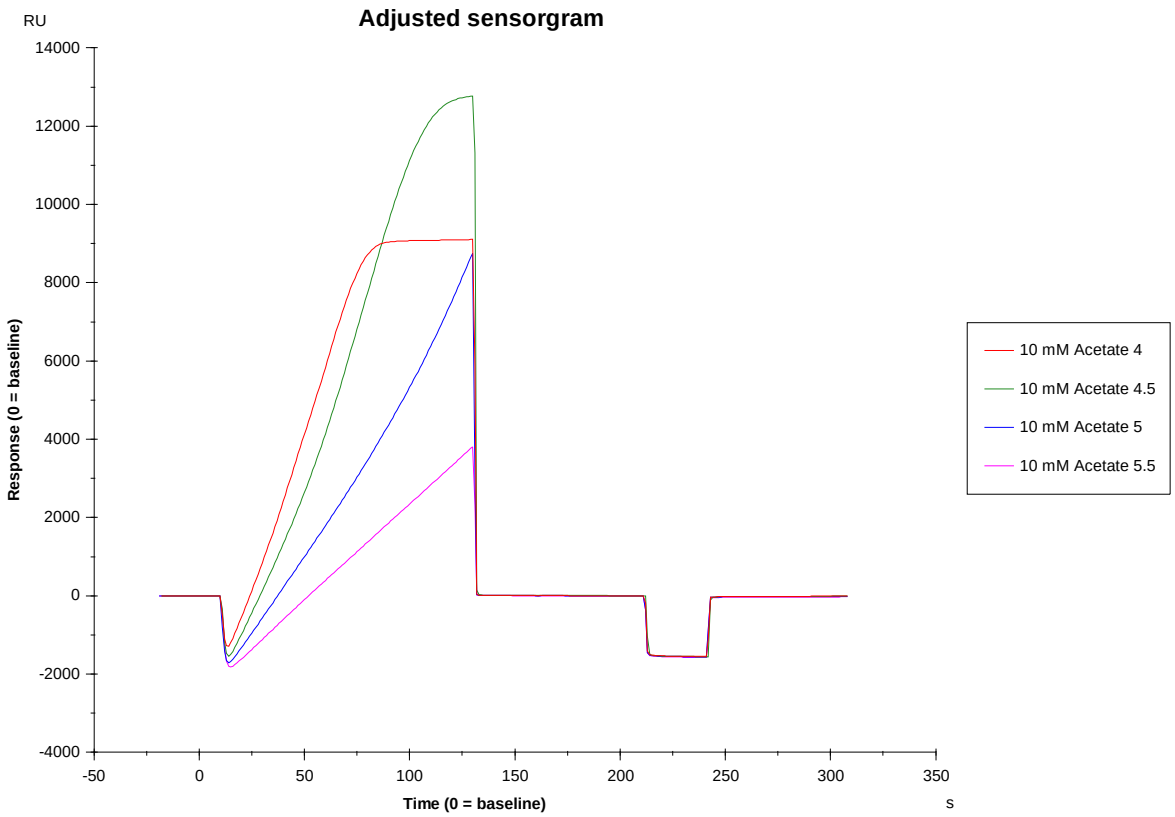

II. Immobilisation of ligands

Laminin-1 (CM5):

The theoretical amount of Laminin L2020 immobilised on the chip (R_L) was calculated to be 4938 Response units (Ru), as illustrated below.

$$R_{\max} = \frac{analyte\ M_W}{ligand\ M_W} * R_L * S_m$$

R_{max} describes the binding capacity of the sensor surface and is normally set to 100-300 Ru.

R_{max} was set to 100 Ru
R_L : immobilisation level
S_m : stocichiometric ratio (=1)

analyte (CCP1-2) : 16 200 Da
ligand (laminin-1) : 800 000 Da
R_L was calculated to be : 4938 Ru

Immobilisation of the ligand, laminin-1 on a CM5 sensor chip. The actual amount of ligand immobilised produced a response of 5070 Ru.

Flow cell	Procedure	Method	Ligand	Response Bound (RU)	Response Final (RU)	Target Reached
1	Blank	Amine			165.5	N/A
2	Target level	Amine	L2020	5014.5	5070.3	Yes

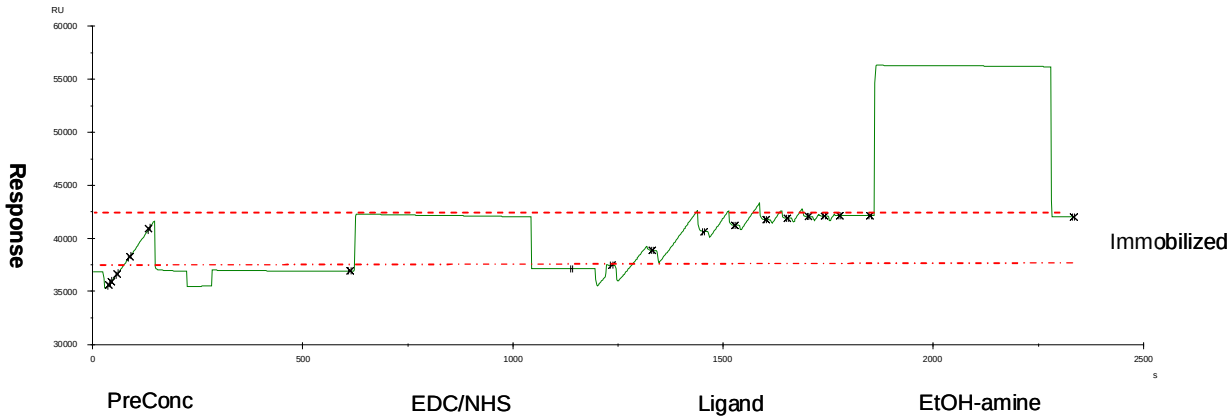

Laminin10/11 (CM5):

The theoretical amount of laminin 10/11 immobilised on the chip (R_L) was calculated to be 455 Response units (Ru), as illustrated below.

$$R_{\max} = \frac{analyte\ M_W}{ligand\ M_W} * R_L * S_m$$

R_{max} describes the binding capacity of the sensor surface and is normally set to 100-300 Ru.

R_{max} was set to 100 Ru

R_L : immobilisation level

S_m : stocichiometric ratio (=1)

analyte (CCP1-2) : 16 200 Da

ligand (laminin10/11:) : 75 000 Da (estimation of smaller fragment, as protein is pepsinised)

R_L was calculated to be 455Ru

Immobilisation of laminin-10/11 on a CM5 sensor chip. The amount of ligand actually immobilised produced a response of 390 Ru,

Flow cell	Procedure	Method	Ligand	Response Bound (RU)	Response Final (RU)	Target Reached
1	Blank	Amine			167,5	N/A
2	Target level	Amine	AG56P	222.7	390.2	Yes

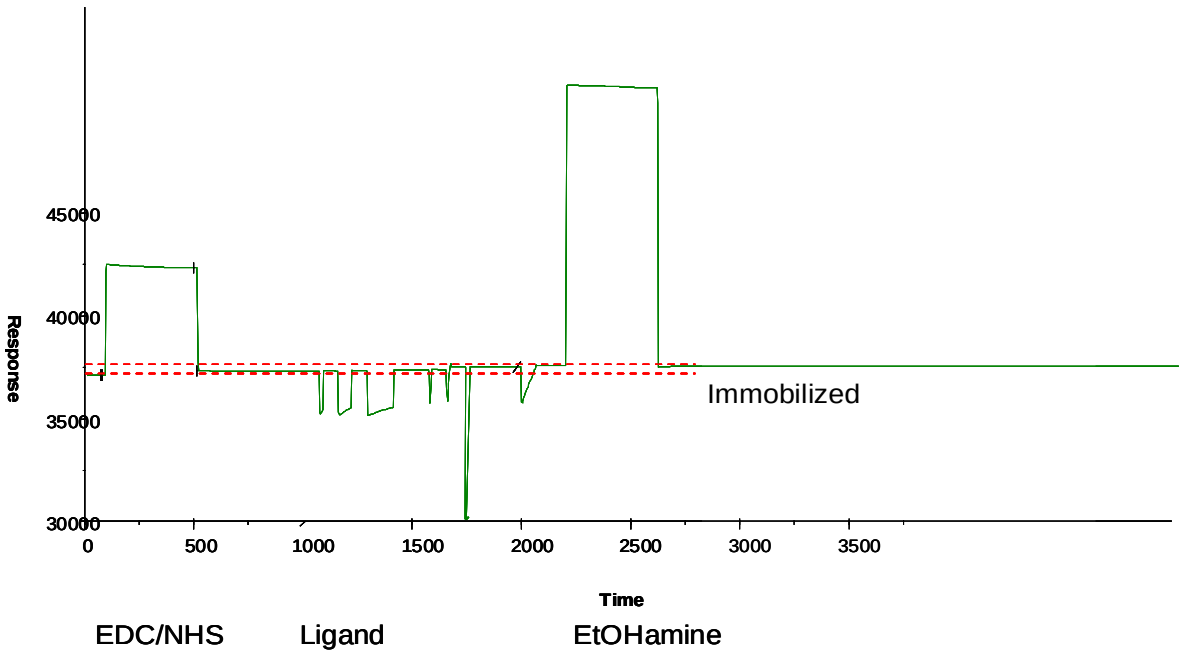

CCP1-2 (CM5):

The theoretical amount of CCP1-2 immobilised on the chip (R_L) was calculated to be 81 Response units (Ru), as illustrated below.

$$R_{\max} = \frac{analyte\ M_W}{ligand\ M_W} * R_L * S_m$$

R_{max} describes the binding capacity of the sensor surface and is normally set to 100-300 Ru.

R_{max} was set to 300 Ru
R_L : immobilisation level
S_m : stocichiometric ratio (=1)

analyte (laminin fragments:) 60 000 Da (estimated average fragment size)
ligand (CCP1-2) : 16 200 Da
R_L was calculated to be 81Ru

Immobilisation of CCP1-2 on a CM5 sensor chip. The amount of ligand actually immobilised produced a response of 235 Ru,

Flow cell	Procedure	Method	Ligand	Bound (RU)	Final (RU)	Target Reached
1	Blank	Amine			167.8	N/A
2	Target level	Amine	CCP1-2 pH 5.5	70.1	235.3	Yes

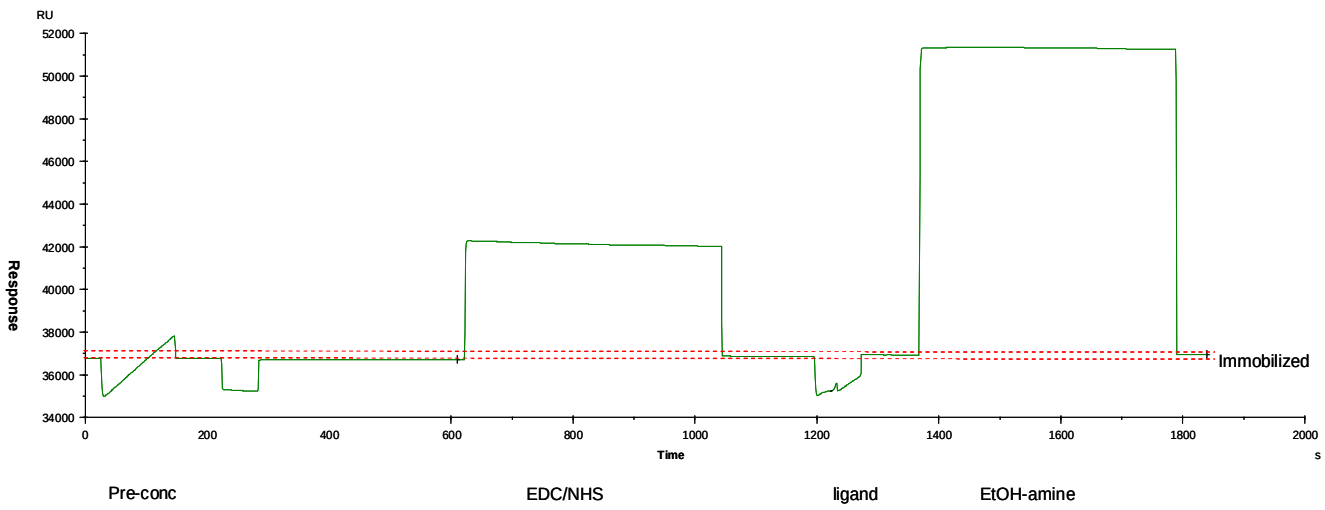

Immobilisation of biotinylated CCP1-2 (SA chip):

Conditioning of SA chip surface with three injections of 1M NaCl + 50 mM NaOH to prepare surface for biotinylated ligand.

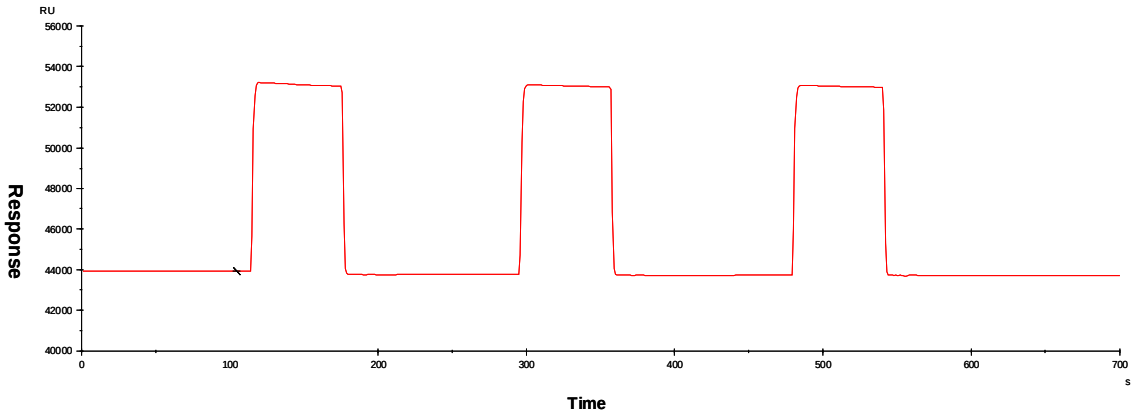

Immobilisation of CCP1-2 on a SA sensor chip. The amount of ligand immobilised produced a response of 225 Ru, which was adjusted to 230 Ru after blocking of unreacted groups with an injection of biotin.

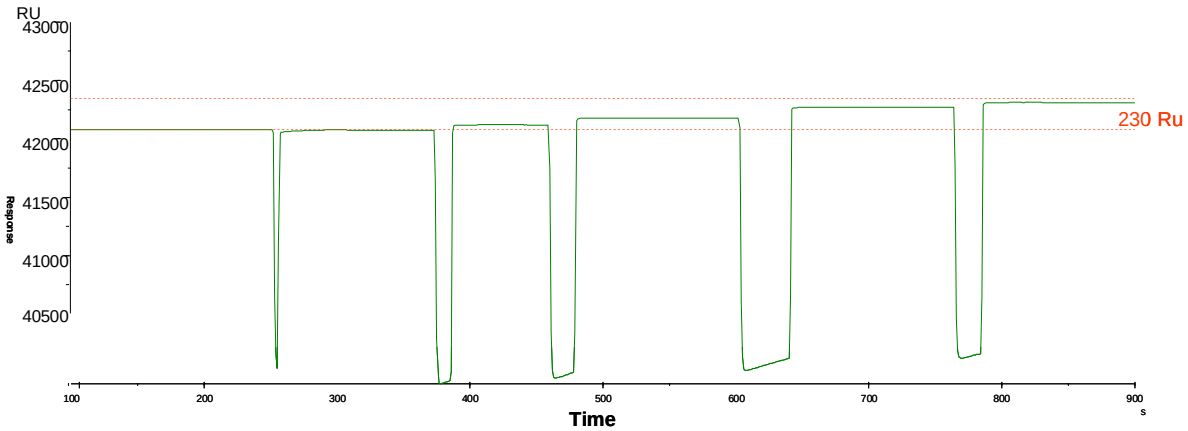

Laminin α1 LG1-3 (CM5):

The theoretical amount of Laminin α1 LG1-3 immobilised on the chip (R_L) was calculated to be 506 Response units (Ru), as illustrated below.

$$R_{\max} = \frac{analyte\ M_W}{ligand\ M_W} * R_L * S_m$$

R_{max} describes the binding capacity of the sensor surface and is normally set to 100-300 Ru.

R_{max} was set to 100 Ru
R_L : immobilisation level
S_m : stocichiometric ratio (=1)

analyte (CCP1-2) : 16 200 Da
ligand (α1 LG1-3:) : 82000 Da
R_L was calculated to be : 506 Ru

Immobilisation of Laminin α1 lg1-3 on a CM5 sensor chip. The amount of ligand actually immobilised produced a response of 455 Ru, due to insufficient amount of protein available.

Flow cell	Procedure	Method	Ligand	Response Bound (RU)	Response Final (RU)	Target Reached
2	Target level	Amine	alpha1 LG1-3	455.4	611.8	No - Out of ligand

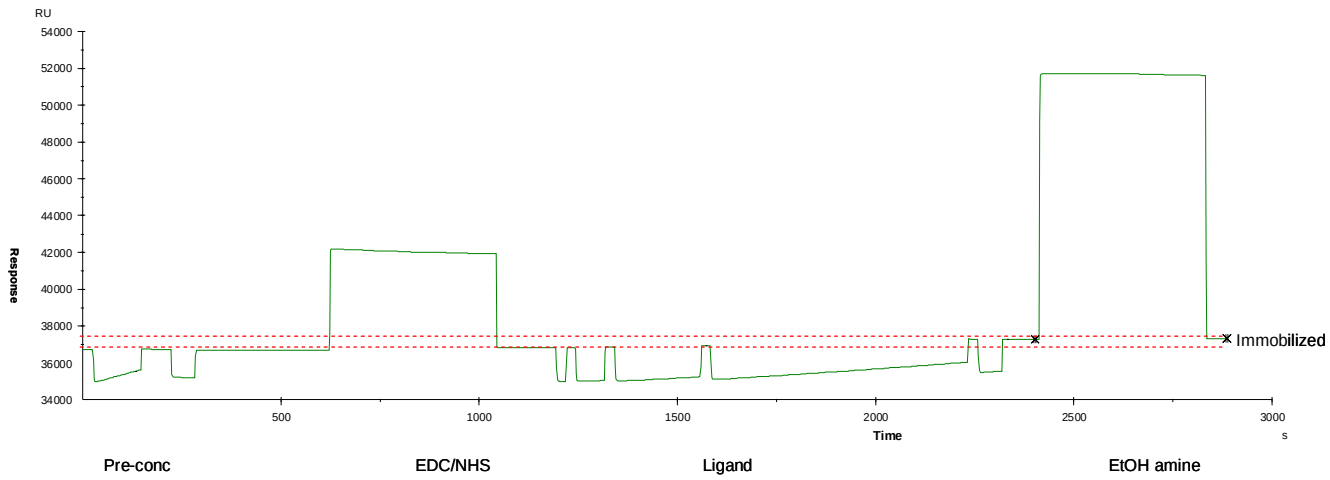

Laminin α1 LG 4-5 (CM5):

The theoretical amount of Laminin α1 LG4-5 immobilised on the chip chip (R_L) was calculated to be 272 Response units (Ru), as illustrated below.

$$R_{\max} = \frac{analyte\ M_W}{ligand\ M_W} * R_L * S_m$$

R_{max} describes the binding capacity of the sensor surface and is normally set to 100-300 Ru.

R_{max} was set to 100 Ru
R_L : immobilisation level
S_m : stocichiometric ratio (=1)

analyte (CCP1-2) : 16 200 Da
ligand (α1 LG 4-5) : 44 000 Da
R_L was calculated to be : 272 Ru

Immobilisation of Laminin α1 LG4-5 on a CM5 sensor chip. The amount of ligand actually immobilised produced a response of 295 Ru, after reference cell adjustment 465 Ru.

Flow cell	Procedure	Method	Ligand	Response Bound (RU)	Response Final (RU)	Target Reached
3	Blank	Amine			189.2	N/A
4	Target level	Amine	alpha1 lg4-5	295.8	465.4	Yes

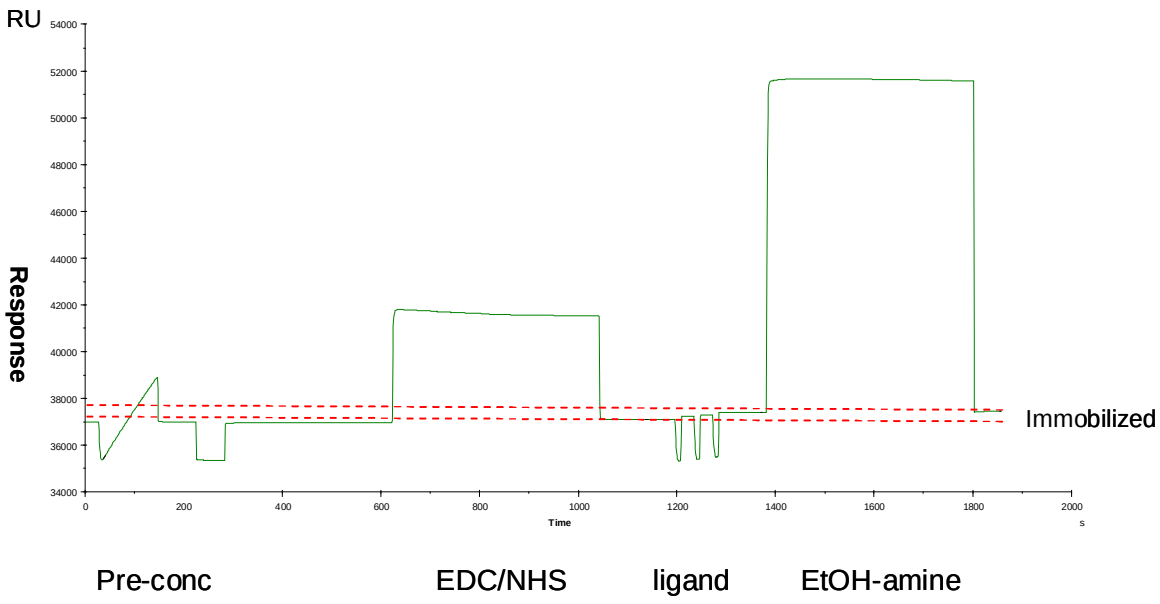

His-tagged α5 LG 4-5 (NTA chip):

The theoretical amount of Laminin α5 LG4-5 immobilised on the chip chip (R_L) was calculated to be 493 Response units (Ru), as illustrated below.

$$R_{\max} = \frac{analyte\ M_W}{ligand\ M_W} * R_L * S_m$$

R_{max} describes the binding capacity of the sensor surface and is normally set to 100-300 Ru.

R_{max} was set to 200 Ru
R_L : immobilisation level
S_m : stocichiometric ratio (=1)

analyte (CCP1-2) : 16 200 Da
ligand (α1 LG 4-5) : 40 000 Da
R_L was calculated to be : 493Ru

Immobilisation of Laminin α1 LG4-5 on a CM5 sensor chip. The amount of ligand actually immobilised produced a response of 429 Ru. The chip surface was regenerated, the surface was reactivated and new ligand was immobilised for each cycle.

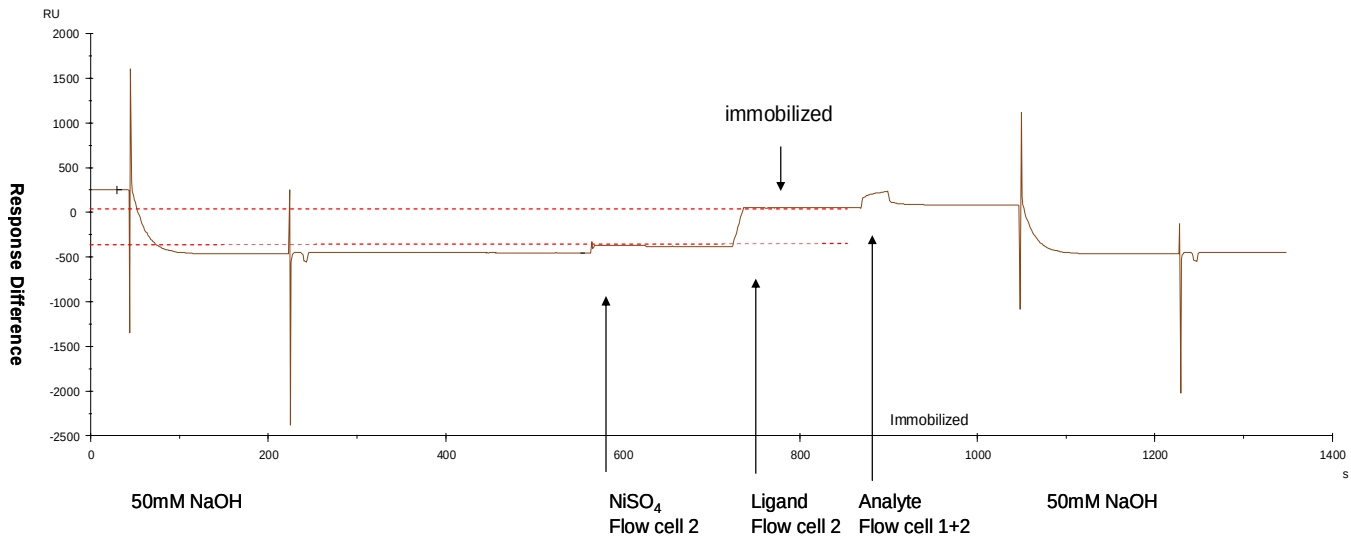

Appendix C.

I. Primers for constructs used in electrophysiology study:

Primers used: for cloning of full length $GABA_BR1a$ in pcDNA3.1/V5-His TOPO

Forward: *5' C ACC ATG TTG CTG CTG CTG*

Reverse: *3'TCA CTT ATA AAG CA*

Primers used: for two-step cloning approach of R1a in pRSSP

Forward: *5' CTT CTA CAT GTT GCT GCT G*

The forward primer was designed to incorporate the restriction digest site for AflIII

Reverse: *3' ATC CAC TGT GCA GTT GAT AG*

The reverse primer was design to amplify the gene up to just past a naturally occurring restriction digest site for BGlII

II. Plasmids

pcDNA3.1 (Invitrogen)

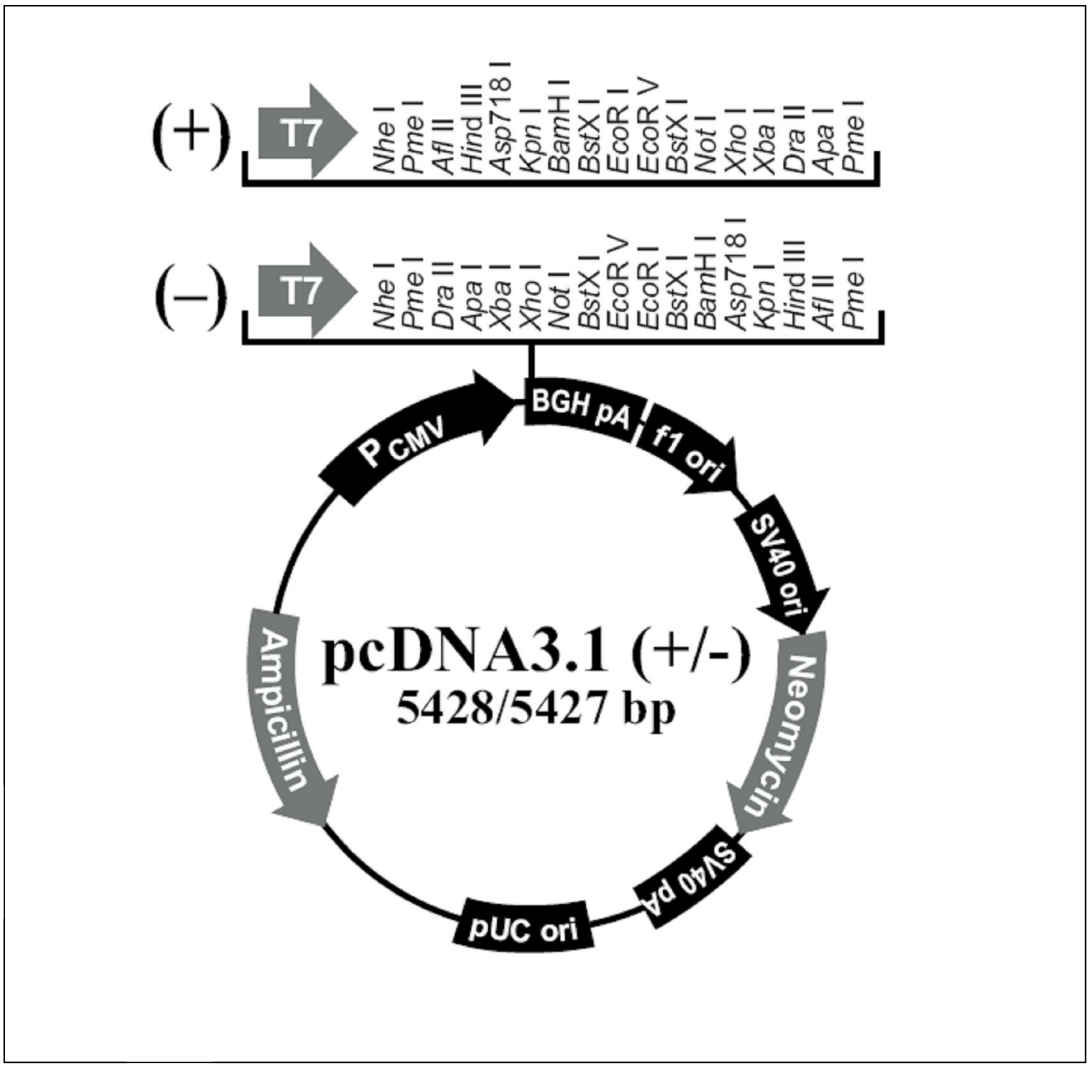

pcDNA3.1D/V5-HIS TOPO (Invitrogen)

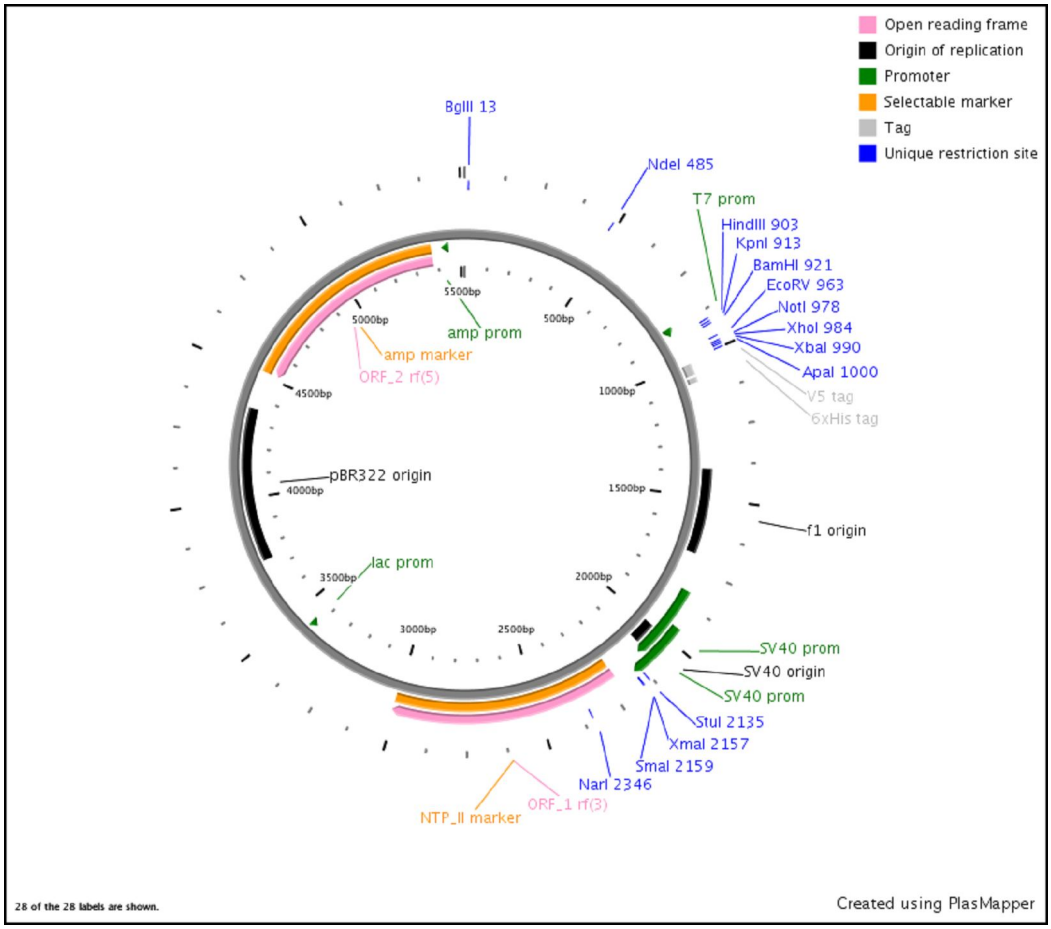

pRSSP

(Veyhl et al., 2006)

The vector contains an SP6 promoter for in vitro RNA transcription, 3’ and 5’ UTR from Xenopus β-globin gene. In addition a polyA sequence has been added to the 3' end of the gene.

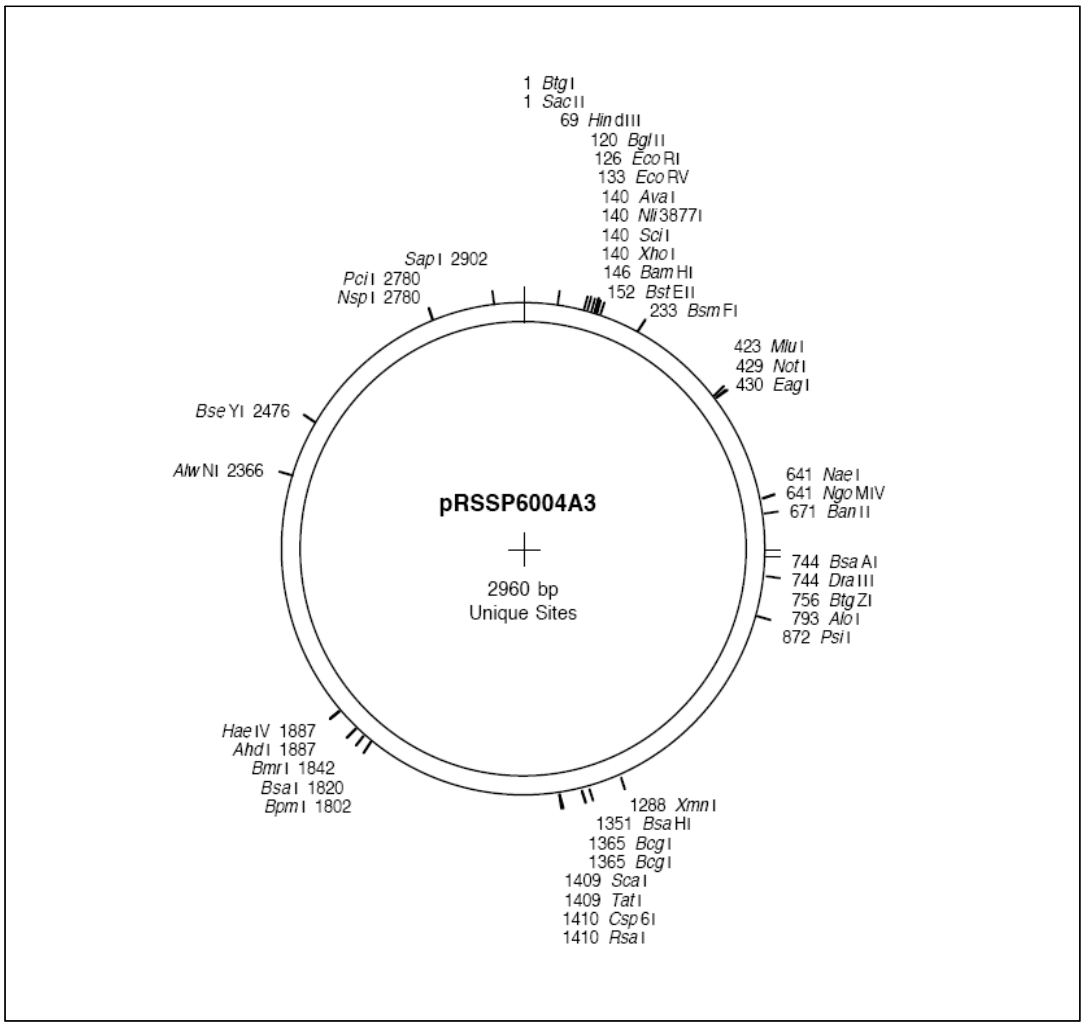

pSGEM (derrived from the pGEMHE vector)

(Villmann et al., 1997)

The vector contains 3’ and 5’ UTR from Xenopus β-globin gene, flanking a polylinker derived from the multi-cloning site of pBluescript vector.

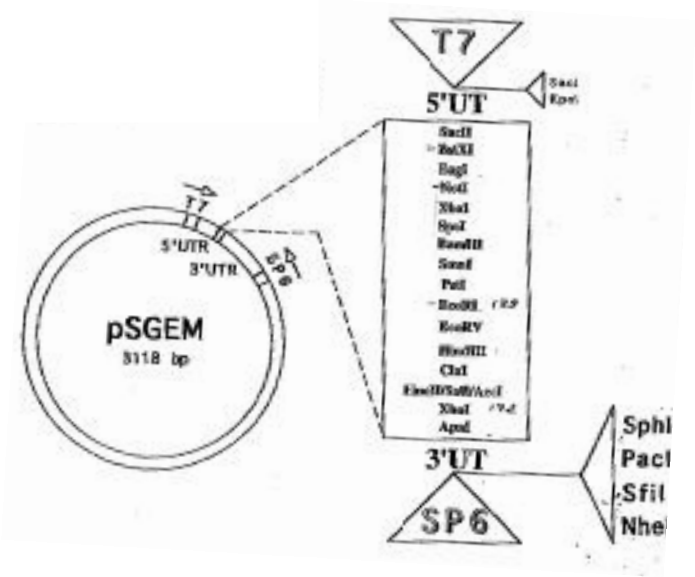

III. Data related to low concentrations of baclofen

$GABA_B$ receptor responses at 1, 3 and 10 µM baclofen, including standard error of mean (SEM) for each concentration.

	R1a			**R1b**		
	1 µM baclofen	**3 µM baclofen**	**10 µM baclofen**	**1 µM baclofen**	**3 µM baclofen**	**10 µM baclofen**
nAmpere	60	139	203	6510	8090	8430
	375	810	1250	4650	5910	6310
	110	205	302	4960	6230	6510
	142	324	467	-	-	-
	248	517	776	-	-	-
mean	187	399	600	5373	6743	7083
SD	126	271	424	997	1177	1171
SEM	56	121	189	575	680	676

$GABA_B$ receptor relative percentage responses at 1, 3 and 10 µM baclofen.

Concentration of baclofen	$GABA_BR1a/GABA_BR2$ percentage response	$GABA_BR1b/GABA_BR2$ percentage response
1 µM	31. %	75.9 %
3 µM	66.5 %	95.9 %
10 µM	100 %	100 %

IV. Data related to antagonist blocking

i. Percentage of baclofen-evoked response blocked by antagonist CGP55845 in oocytes expressing $\underline{GABA_BR1a/GABA_BR2}$.

The percentage block is measured at the following concentrations of CGP55845; 10µM, 5µM, 3µM, 1µM, 0.3µM

R1a 10µM	R1a 5µM	R1a 3µM	R1a 1µM	R1a 0.3µM
76	47	51	95	93
79	47	100	72	60
75	28	60	2	87
80	100	28	75	2
85	45	59	-	0
36	45	88	-	-
51	53	93	-	-
33	100	81	-	-
-	89	35	-	-
-	50	67	-	-
-	34	76	-	-
-	73	79	-	-
-	100	82	-	-
-	75	59	-	-
-	71	62	-	-
-	90	70	-	-
-	65	50	-	-
-	86	100	-	-
-	75	84	-	-
-	75	65	-	-
-	60	42	-	-
-	100	0	-	-
-	79	0	-	-
-	100	0	-	-
-	61	85	-	-
-	15	-	-	-
-	76	-	-	-
-	85	-	-	-
-	64	-	-	-
-	53	-	-	-
-	100	-	-	-
-	35	-	-	-
-	0	-	-	-
-	0	-	-	-
-	0	-	-	-
-	0	-	-	-
-	100	-	-	-
-	70	-	-	-
-	0	-	-	-

ii. Percentage of baclofen-evoked response blocked by the antagonist CGP55845 in oocytes expressing $\underline{GABA_BR1b/\ GABA_BR2.}$

The percentage block is measured at the following concentrations of CGP55845; 10µM, 5µM, 3µM, 1µM, 0.3µM

R1b 10µM	R1b 5µM	R1b 3µM	R1b 1µM	R1b 0.3µM
82	100	100	88	89
100	100	93	90	86
91	96	70	89	-
92	91	93	100	-
60	100	100	-	-
100	100	86	-	-
-	100	92	-	-
-	90	94	-	-
-	99	95	-	-
-	98	89	-	-
-	75	96	-	-
-	99	100	-	-
-	78	81	-	-
-	96	70	-	-
-	83	100	-	-
-	83	100	-	-
-	96	91	-	-
-	96	100	-	-
-	96	96	-	-
-	10	91	-	-
-	98	97	-	-
-	98	100	-	-
-	82	-	-	-
-	100	-	-	-
-	96	-	-	-

The GIRK currents obtained for the two isoforms $GABA_BR1a/GABA_BR2$ and $GABA_BR1b/GABA_BR2$ in response to 1, 3 and 10 µM baclofen as illustrated in Figure 66

	R1a			R1b		
	1 µM bac	**3 µM bac**	**10 µM bac**	**1 µM bac**	**3 µM bac**	**10 µM bac**
	60	139	203	6510	8090	8430
	375	810	1250	4650	5910	6310
	110	205	302	4960	6230	6510
	142	324	467			
	248	517	776			
mean	187	399	599.6	5373.333	6743.333	7083.333
SD	125.6463	270.9732	423.5496	996.5106	1177.172	1170.527
SEM	56.19075	121.1829	189.4172	575.3357	679.6404	675.804

Values in relative percent, where the value for 10 µM baclofen is set to 100% as illustrated in Figure 67.

	R1a			R1b		
	1 µM bac	**3 µM bac**	**10 µM bac**	**1 µM bac**	**3 µM bac**	**10 µM bac**
	29.5	68.5	100	77.22	95.96	100
	30	64.8	100	73.69	93.66	100
	36.4	67.9	100	76.19	95.69	100
	30.4	69.4	100			
	31.95	66.6	100			
mean	31.66	67.4	100	75.7	95.10333	100
SD	2.799	1.776	0	1.815	1.257	0
SEM	1.252	0.794	0	1.0481	0.726	0

A statistical overview of the blocking properties by the antagonist CGP55845 of the baclofen induced responses displayed in the table below, indicating the standard deviation (SD) and the Standard Error of Mean (SEM)

	R1a				
	10µM	**5µM**	**3µM**	**1µM**	**0.3µM**
mean	64.4	58.7	60.6	61	48.4
Median	75.5	64.5	65	73.5	60
SD	21	33	29.5	40.6	45
SEM	7.4	5.2	5.9	20.3	20
95% conf	17.6	10.6	12	64.6	55.9
99% conf	26	14	16.5	118.5	92.7
size	9	41	26	5	6
min	33	0	0	2	0
max	85	100	100	95	93

	R1b				
	10µM	**5µM**	**3µM**	**1µM**	**0.3µM**
mean	87.5	94	92.5	91.8	87.5
median	91.5	96	94.5	89.5	87.5
SD	15	7.6	8.9	5.6	2
SEM	6	1.5	1.9	2.8	1.5
95% conf	15.8	3	3.9	8.8	18
99% conf	24.8	4.3	5.4	16.2	73.5
size	7	26	23	5	3
min	60	75	70	88	86
max	100	100	100	100	89

Bibliography

Airenne, T., H. Haakana, K. Sainio, T. Kallunki, P. Kallunki, H. Sariola, and K. Tryggvason. 1996. Structure of the human laminin gamma 2 chain gene (LAMC2): alternative splicing with different tissue distribution of two transcripts. *Genomics*. 32:54-64.

Argraves, W.S., L.M. Greene, M.A. Cooley, and W.M. Gallagher. 2003. Fibulins: physiological and disease perspectives. *EMBO Rep*. 4:1127-31.

Aumailley, M., L. Bruckner-Tuderman, W.G. Carter, R. Deutzmann, D. Edgar, P. Ekblom, J. Engel, E. Engvall, E. Hohenester, J.C. Jones, H.K. Kleinman, M.P. Marinkovich, G.R. Martin, U. Mayer, G. Meneguzzi, J.H. Miner, K. Miyazaki, M. Patarroyo, M. Paulsson, V. Quaranta, J.R. Sanes, T. Sasaki, K. Sekiguchi, L.M. Sorokin, J.F. Talts, K. Tryggvason, J. Uitto, I. Virtanen, K. von der Mark, U.M. Wewer, Y. Yamada, and P.D. Yurchenco. 2005. A simplified laminin nomenclature. *Matrix Biol*. 24:326-32.

Baker, G., S. Dunn, and A. Holt. 2007. Expression and study of ligand-gated ion channels in Xenopus laevis Oocytes. *In* Handbook of neurochemistry and molecular neurobiology. Springer US.

Balasubramanian, S., J.A. Teissere, D.V. Raju, and R.A. Hall. 2004. Hetero-oligomerization between GABAA and GABAB receptors regulates GABAB receptor trafficking. *J Biol Chem*. 279:18840-50.

Barlow, P.N., M. Baron, D.G. Norman, A.J. Day, A.C. Willis, R.B. Sim, and I.D. Campbell. 1991. Secondary structure of a complement control protein module by two-dimensional 1H NMR. *Biochemistry*. 30:997-1004.

Beck, K., I. Hunter, and J. Engel. 1990. Structure and function of laminin: anatomy of a multidomain glycoprotein. *FASEB J*. 4:148-60.

Bettler, B., K. Kaupmann, and N. Bowery. 1998. GABAB receptors: drugs meet clones. *Curr Opin Neurobiol*. 8:345-50.

Bettler, B., K. Kaupmann, J. Mosbacher, and M. Gassmann. 2004. Molecular structure and physiological functions of GABA(B) receptors. *Physiol Rev*. 84:835-67.

Bettler, B., and J.Y. Tiao. 2006. Molecular diversity, trafficking and subcellular localization of GABAB receptors. *Pharmacol Ther*. 110:533-43.

Billinton, A., A.O. Ige, J.P. Bolam, J.H. White, F.H. Marshall, and P.C. Emson. 2001. Advances in the molecular understanding of GABA(B) receptors. *Trends Neurosci*. 24:277-82.

Billinton, A., N. Upton, and N.G. Bowery. 1999. GABA(B) receptor isoforms GBR1a and GBR1b, appear to be associated with pre- and post-synaptic elements respectively in rat and human cerebellum. *Br J Pharmacol*. 126:1387-92.

Blein, S., R. Ginham, D. Uhrin, B.O. Smith, D.C. Soares, S. Veltel, R.A. McIlhinney, J.H. White, and P.N. Barlow. 2004. Structural analysis of the complement control protein (CCP) modules of GABA(B) receptor 1a: only one of the two CCP modules is compactly folded. *J Biol Chem*. 279:48292-306.

Bockaert, J., L. Fagni, A. Dumuis, and P. Marin. 2004. GPCR interacting proteins (GIP). *Pharmacol Ther*. 103:203-21.

Bockaert, J., and J.P. Pin. 1999. Molecular tinkering of G protein-coupled receptors: an evolutionary success. *EMBO J*. 18:1723-9.
Bolteus, A.B., A. 2006. Non synaptic GABAeric communication and postnatal neurogenesis. *In* the cell cycle in the central nervous system. D. Janigro, editor. Human Press Incorporated. 95-104.
Bourne, H.R. 1997. How receptors talk to trimeric G proteins. *Curr Opin Cell Biol*. 9:134-42.
Bourne, H.R., D.A. Sanders, and F. McCormick. 1991. The GTPase superfamily: conserved structure and molecular mechanism. *Nature*. 349:117-27.
Bouvier, M. 2001. Oligomerization of G-protein-coupled transmitter receptors. *Nat Rev Neurosci*. 2:274-86.
Bowery, N.G. 1993. GABAB receptor pharmacology. *Annu Rev Pharmacol Toxicol*. 33:109-47.
Bowery, N.G. 2006. GABAB receptor: a site of therapeutic benefit. *Curr Opin Pharmacol*. 6:37-43.
Bowery, N.G., A. Doble, D.R. Hill, A.L. Hudson, J.S. Shaw, and M.J. Turnbull. 1979. Baclofen: a selective agonist for a novel type of GABA receptor]proceedings]. *Br J Pharmacol*. 67:444P-445P.
Bowery, N.G., D.R. Hill, A.L. Hudson, A. Doble, D.N. Middlemiss, J. Shaw, and M. Turnbull. 1980. (-)Baclofen decreases neurotransmitter release in the mammalian CNS by an action at a novel GABA receptor. *Nature*. 283:92-4.
Bowery, N.G., and A.L. Hudson. 1979. gamma-Aminobutyric acid reduces the evoked release of [3H]-noradrenaline from sympathetic nerve terminals [proceedings]. *Br J Pharmacol*. 66:108P.
Bridges, T.M., and C.W. Lindsley. 2008. G-protein-coupled receptors: from classical modes of modulation to allosteric mechanisms. *ACS Chem Biol*. 3:530-41.
Bulanova, E., V. Budagian, E. Duitman, Z. Orinska, H. Krause, R. Ruckert, N. Reiling, and S. Bulfone-Paus. 2007. Soluble Interleukin IL-15Ralpha is generated by alternative splicing or proteolytic cleavage and forms functional complexes with IL-15. *J Biol Chem*. 282:13167-79.
Calver, A.R., A.D. Medhurst, M.J. Robbins, K.J. Charles, M.L. Evans, D.C. Harrison, M. Stammers, S.A. Hughes, G. Hervieu, A. Couve, S.J. Moss, D.N. Middlemiss, and M.N. Pangalos. 2000. The expression of GABA(B1) and GABA(B2) receptor subunits in the cNS differs from that in peripheral tissues. *Neuroscience*. 100:155-70.
Campbell, I.D., and A.K. Downing. 1998. NMR of modular proteins. *Nat Struct Biol*. 5 Suppl:496-9.
Carafoli, F., N.J. Clout, and E. Hohenester. 2009. Crystal Structure of the LG1-3 Region of the Laminin {alpha}2 Chain. *J Biol Chem*. 284:22786-92.
Carman, C.V., and J.L. Benovic. 1998. G-protein-coupled receptors: turn-ons and turn-offs. *Curr Opin Neurobiol*. 8:335-44.
Chebib, M., and G.A. Johnston. 1999. The 'ABC' of GABA receptors: a brief review. *Clin Exp Pharmacol Physiol*. 26:937-40.
Ciruela, F., M.M. Soloviev, W.Y. Chan, and R.A. McIlhinney. 2000. Homer-1c/Vesl-1L modulates the cell surface targeting of metabotropic glutamate receptor type 1alpha: evidence for an anchoring function. *Mol Cell Neurosci*. 15:36-50.

Clark, J.A., E. Mezey, A.S. Lam, and T.I. Bonner. 2000. Distribution of the GABA(B) receptor subunit gb2 in rat CNS. *Brain Res*. 860:41-52.
Coates, P.J., and P.A. Hall. 2003. The yeast two-hybrid system for identifying protein-protein interactions. *J Pathol*. 199:4-7.
Colman, A., S. Bhamra, and G. Valle. 1984. Post-translational modification of exogenous proteins in Xenopus laevis oocytes. *Biochem Soc Trans*. 12:932-7.
Colognato, H., C. ffrench-Constant, and M.L. Feltri. 2005. Human diseases reveal novel roles for neural laminins. *Trends Neurosci*. 28:480-6.
Colognato, H., and P.D. Yurchenco. 2000. Form and function: the laminin family of heterotrimers. *Dev Dyn*. 218:213-34.
Couve, A., A.K. Filippov, C.N. Connolly, B. Bettler, D.A. Brown, and S.J. Moss. 1998. Intracellular retention of recombinant GABAB receptors. *J Biol Chem*. 273:26361-7.
Cryan, J.F., P.H. Kelly, F. Chaperon, C. Gentsch, C. Mombereau, K. Lingenhoehl, W. Froestl, B. Bettler, K. Kaupmann, and W.P. Spooren. 2004. Behavioral characterization of the novel GABAB receptor-positive modulator GS39783 (N,N'-dicyclopentyl-2-methylsulfanyl-5-nitro-pyrimidine-4,6-diamine): anxiolytic-like activity without side effects associated with baclofen or benzodiazepines. *J Pharmacol Exp Ther*. 310:952-63.
Davies, C.H., M.F. Pozza, and G.L. Collingridge. 1993. CGP 55845A: a potent antagonist of GABAB receptors in the CA1 region of rat hippocampus. *Neuropharmacology*. 32:1071-3.
de Vega, S., T. Iwamoto, T. Nakamura, K. Hozumi, D.A. McKnight, L.W. Fisher, S. Fukumoto, and Y. Yamada. 2007. TM14 is a new member of the fibulin family (fibulin-7) that interacts with extracellular matrix molecules and is active for cell binding. *J Biol Chem*. 282:30878-88.
de Vega, S., T. Iwamoto, and Y. Yamada. 2009. Fibulins: multiple roles in matrix structures and tissue functions. *Cell Mol Life Sci*. 66:1890-902.
Deisz, R.A., J.M. Billard, and W. Zieglgansberger. 1997. Presynaptic and postsynaptic GABAB receptors of neocortical neurons of the rat in vitro: differences in pharmacology and ionic mechanisms. *Synapse*. 25:62-72.
Deriu, D., M. Gassmann, S. Firbank, D. Ristig, C. Lampert, J. Mosbacher, W. Froestl, K. Kaupmann, B. Bettler, and M.G. Grutter. 2005. Determination of the minimal functional ligand-binding domain of the GABAB1b receptor. *Biochem J*. 386:423-31.
DiScipio, R.G. 1992. Ultrastructures and interactions of complement factors H and I. *J Immunol*. 149:2592-9.
Durfee, T., K. Becherer, P.L. Chen, S.H. Yeh, Y. Yang, A.E. Kilburn, W.H. Lee, and S.J. Elledge. 1993. The retinoblastoma protein associates with the protein phosphatase type 1 catalytic subunit. *Genes Dev*. 7:555-69.
Durkin, M.E., M. Gautam, F. Loechel, J.R. Sanes, J.P. Merlie, R. Albrechtsen, and U.M. Wewer. 1996. Structural organization of the human and mouse laminin beta2 chain genes, and alternative splicing at the 5' end of the human transcript. *J Biol Chem*. 271:13407-16.
Dyson, H.J., and P.E. Wright. 2005. Intrinsically unstructured proteins and their functions. *Nat Rev Mol Cell Biol*. 6:197-208.
Ekblom, P. 1995. Extracellular matrix in animal development. Role of extracellular matrix in animal development--an introduction. *Experientia*. 51:851-2.

Engel, J. 1992. Laminins and other strange proteins. *Biochemistry*. 31:10643-51.
Engvall, E. 1995. Structure and function of basement membranes. *Int J Dev Biol*. 39:781-7.
Engvall, E., D. Earwicker, T. Haaparanta, E. Ruoslahti, and J.R. Sanes. 1990. Distribution and isolation of four laminin variants; tissue restricted distribution of heterotrimers assembled from five different subunits. *Cell Regul*. 1:731-40.
Erickson, A.C., and J.R. Couchman. 2000. Still more complexity in mammalian basement membranes. *J Histochem Cytochem*. 48:1291-306.
Ferguson, S.S., J. Zhang, L.S. Barak, and M.G. Caron. 1998. Molecular mechanisms of G protein-coupled receptor desensitization and resensitization. *Life Sci*. 62:1561-5.
Fernandez, J.A., and J.H. Griffin. 1994. A protein S binding site on C4b-binding protein involves beta chain residues 31-45. *J Biol Chem*. 269:2535-40.
Ferns, M.J., J.T. Campanelli, W. Hoch, R.H. Scheller, and Z. Hall. 1993. The ability of agrin to cluster AChRs depends on alternative splicing and on cell surface proteoglycans. *Neuron*. 11:491-502.
Fields, S., and O. Song. 1989. A novel genetic system to detect protein-protein interactions. *Nature*. 340:245-6.
Fisher, S.A., A. Rivera, L.G. Fritsche, C.N. Keilhauer, P. Lichtner, T. Meitinger, G. Rudolph, and B.H. Weber. 2007. Case-control genetic association study of fibulin-6 (FBLN6 or HMCN1) variants in age-related macular degeneration (AMD). *Hum Mutat*. 28:406-13.
Franco, R., V. Casado, A. Cortes, C. Ferrada, J. Mallol, A. Woods, C. Lluis, E.I. Canela, and S. Ferre. 2007. Basic concepts in G-protein-coupled receptor homo- and heterodimerization. *ScientificWorldJournal*. 7:48-57.
Fritschy, J.M., V. Meskenaite, O. Weinmann, M. Honer, D. Benke, and H. Mohler. 1999. GABAB-receptor splice variants GB1a and GB1b in rat brain: developmental regulation, cellular distribution and extrasynaptic localization. *Eur J Neurosci*. 11:761-8.
Fritschy, J.M., C. Sidler, F. Parpan, M. Gassmann, K. Kaupmann, B. Bettler, and D. Benke. 2004. Independent maturation of the GABA(B) receptor subunits GABA(B1) and GABA(B2) during postnatal development in rodent brain. *J Comp Neurol*. 477:235-52.
Gallagher, W.M., C.A. Currid, and L.C. Whelan. 2005. Fibulins and cancer: friend or foe? *Trends Mol Med*. 11:336-40.
Gallagher, W.M., L.M. Greene, M.P. Ryan, V. Sierra, A. Berger, P. Laurent-Puig, and E. Conseiller. 2001. Human fibulin-4: analysis of its biosynthetic processing and mRNA expression in normal and tumour tissues. *FEBS Lett*. 489:59-66.
Galliano, M.F., D. Aberdam, A. Aguzzi, J.P. Ortonne, and G. Meneguzzi. 1995. Cloning and complete primary structure of the mouse laminin alpha 3 chain. Distinct expression pattern of the laminin alpha 3A and alpha 3B chain isoforms. *J Biol Chem*. 270:21820-6.
Galvez, T., B. Duthey, J. Kniazeff, J. Blahos, G. Rovelli, B. Bettler, L. Prezeau, and J.P. Pin. 2001. Allosteric interactions between GB1 and GB2 subunits are required for optimal GABA(B) receptor function. *EMBO J*. 20:2152-9.

Galvez, T., M.L. Parmentier, C. Joly, B. Malitschek, K. Kaupmann, R. Kuhn, H. Bittiger, W. Froestl, B. Bettler, and J.P. Pin. 1999. Mutagenesis and modeling of the GABAB receptor extracellular domain support a venus flytrap mechanism for ligand binding. *J Biol Chem*. 274:13362-9.

Gesty-Palmer, D., M. Chen, E. Reiter, S. Ahn, C.D. Nelson, S. Wang, A.E. Eckhardt, C.L. Cowan, R.F. Spurney, L.M. Luttrell, and R.J. Lefkowitz. 2006. Distinct beta-arrestin- and G protein-dependent pathways for parathyroid hormone receptor-stimulated ERK1/2 activation. *J Biol Chem*. 281:10856-64.

Gether, U. 2000. Uncovering molecular mechanisms involved in activation of G protein-coupled receptors. *Endocr Rev*. 21:90-113.

Ginham, R.L., S. Blein, P. Barlow, J.H. White, and R.A.J. McIlhinney. 2002. Interaction of 'Sushi' domain of GABAbR1a subunit with the extracellular matrix protein, fibulin. *FENS Abstr* 1:6.

Grace, C.R., M.H. Perrin, M.R. DiGruccio, C.L. Miller, J.E. Rivier, W.W. Vale, and R. Riek. 2004. NMR structure and peptide hormone binding site of the first extracellular domain of a type B1 G protein-coupled receptor. *Proc Natl Acad Sci U S A*. 101:12836-41.

Greene, L.M., W.O. Twal, M.J. Duffy, E.W. McDermott, A.D. Hill, N.J. O'Higgins, A.H. McCann, P.A. Dervan, W.S. Argraves, and W.M. Gallagher. 2003. Elevated expression and altered processing of fibulin-1 protein in human breast cancer. *Br J Cancer*. 88:871-8.

Hagg, T., C. Portera-Cailliau, M. Jucker, and E. Engvall. 1997. Laminins of the adult mammalian CNS; laminin-alpha2 (merosin M-) chain immunoreactivity is associated with neuronal processes. *Brain Res*. 764:17-27.

Hall, R.A., L.S. Ostedgaard, R.T. Premont, J.T. Blitzer, N. Rahman, M.J. Welsh, and R.J. Lefkowitz. 1998. A C-terminal motif found in the beta2-adrenergic receptor, P2Y1 receptor and cystic fibrosis transmembrane conductance regulator determines binding to the Na+/H+ exchanger regulatory factor family of PDZ proteins. *Proc Natl Acad Sci U S A*. 95:8496-501.

Hamm, H.E. 1998. The many faces of G protein signaling. *J Biol Chem*. 273:669-72.

Hardig, Y., and B. Dahlback. 1996. The amino-terminal module of the C4b-binding protein beta-chain contains the protein S-binding site. *J Biol Chem*. 271:20861-7.

Hardig, Y., A. Rezaie, and B. Dahlback. 1993. High affinity binding of human vitamin K-dependent protein S to a truncated recombinant beta-chain of C4b-binding protein expressed in Escherichia coli. *J Biol Chem*. 268:3033-6.

Harrison, D., S.A. Hussain, A.C. Combs, J.M. Ervasti, P.D. Yurchenco, and E. Hohenester. 2007. Crystal structure and cell surface anchorage sites of laminin alpha1LG4-5. *J Biol Chem*. 282:11573-81.

Hawrot, E., Y. Xiao, Q.L. Shi, D. Norman, M. Kirkitadze, and P.N. Barlow. 1998. Demonstration of a tandem pair of complement protein modules in GABA(B) receptor 1a. *FEBS Lett*. 432:103-8.

Hebert, T.E., S. Moffett, J.P. Morello, T.P. Loisel, D.G. Bichet, C. Barret, and M. Bouvier. 1996. A peptide derived from a beta2-adrenergic receptor transmembrane domain inhibits both receptor dimerization and activation. *J Biol Chem*. 271:16384-92.

Heuss, C., and U. Gerber. 2000. G-protein-independent signaling by G-protein-coupled receptors. *Trends Neurosci*. 23:469-75.

Hill, D.R., and N.G. Bowery. 1981. 3H-baclofen and 3H-GABA bind to bicuculline-insensitive GABA B sites in rat brain. *Nature*. 290:149-52.

Hillarp, A., and B. Dahlback. 1990. Cloning of cDNA coding for the beta chain of human complement component C4b-binding protein: sequence homology with the alpha chain. *Proc Natl Acad Sci U S A*. 87:1183-7.

Hohenester, E., D. Tisi, J.F. Talts, and R. Timpl. 1999. The crystal structure of a laminin G-like module reveals the molecular basis of alpha-dystroglycan binding to laminins, perlecan, and agrin. *Mol Cell*. 4:783-92.

Holter, J., J. Davies, N. Leresche, V. Crunelli, and D.A. Carter. 2005. Identification of two further splice variants of GABABR1 characterizes the conserved micro-exon 4 as a hot spot for regulated splicing in the rat brain. *J Mol Neurosci*. 26:99-108.

Hoshino, M., F. Matsuzaki, Y. Nabeshima, and C. Hama. 1993. hikaru genki, a CNS-specific gene identified by abnormal locomotion in Drosophila, encodes a novel type of protein. *Neuron*. 10:395-407.

Ige, O.M., and B.O. Onadeko. 2001. An open study to evaluate the safety and efficacy of zafirlukast ("Accolate") in patients with mild to moderate asthma in Ibadan, Nigeria. *West Afr J Med*. 20:220-6.

Indyk, J.A., Z.L. Chen, S.E. Tsirka, and S. Strickland. 2003. Laminin chain expression suggests that laminin-10 is a major isoform in the mouse hippocampus and is degraded by the tissue plasminogen activator/plasmin protease cascade during excitotoxic injury. *Neuroscience*. 116:359-71.

Janatova, J., K.B. Reid, and A.C. Willis. 1989. Disulfide bonds are localized within the short consensus repeat units of complement regulatory proteins: C4b-binding protein. *Biochemistry*. 28:4754-61.

Jensen, A.A., J. Mosbacher, S. Elg, K. Lingenhoehl, T. Lohmann, T.N. Johansen, B. Abrahamsen, J.P. Mattsson, A. Lehmann, B. Bettler, and H. Brauner-Osborne. 2002. The anticonvulsant gabapentin (neurontin) does not act through gamma-aminobutyric acid-B receptors. *Mol Pharmacol*. 61:1377-84.

Johnson, G., C. Swart, and S.W. Moore. 2008. Interaction of acetylcholinesterase with the G4 domain of the laminin alpha1-chain. *Biochem J*. 411:507-14.

Jones, K.A., B. Borowsky, J.A. Tamm, D.A. Craig, M.M. Durkin, M. Dai, W.J. Yao, M. Johnson, C. Gunwaldsen, L.Y. Huang, C. Tang, Q. Shen, J.A. Salon, K. Morse, T. Laz, K.E. Smith, D. Nagarathnam, S.A. Noble, T.A. Branchek, and C. Gerald. 1998. GABA(B) receptors function as a heteromeric assembly of the subunits GABA(B)R1 and GABA(B)R2. *Nature*. 396:674-9.

Kallunki, P., K. Sainio, R. Eddy, M. Byers, T. Kallunki, H. Sariola, K. Beck, H. Hirvonen, T.B. Shows, and K. Tryggvason. 1992. A truncated laminin chain homologous to the B2 chain: structure, spatial expression, and chromosomal assignment. *J Cell Biol*. 119:679-93.

Kato-Takagaki, K., N. Suzuki, F. Yokoyama, S. Takaki, K. Umezawa, J. Higo, M. Mochizuki, Y. Kikkawa, S. Oishi, A. Utani, and M. Nomizu. 2007. Cyclic peptide analysis of the biologically active loop region in the laminin alpha3 chain LG4 module demonstrates the importance of peptide conformation on biological activity. *Biochemistry*. 46:1952-60.

Kaupmann, K., K. Huggel, J. Heid, P.J. Flor, S. Bischoff, S.J. Mickel, G. McMaster, C. Angst, H. Bittiger, W. Froestl, and B. Bettler. 1997. Expression cloning of

GABA(B) receptors uncovers similarity to metabotropic glutamate receptors. *Nature*. 386:239-46.

Kaupmann, K., B. Malitschek, V. Schuler, J. Heid, W. Froestl, P. Beck, J. Mosbacher, S. Bischoff, A. Kulik, R. Shigemoto, A. Karschin, and B. Bettler. 1998. GABA(B)-receptor subtypes assemble into functional heteromeric complexes. *Nature*. 396:683-7.

Kerr, D.I., J. Ong, G.A. Johnston, J. Abbenante, and R.H. Prager. 1988. 2-Hydroxy-saclofen: an improved antagonist at central and peripheral GABAB receptors. *Neurosci Lett*. 92:92-6.

Kerr, D.I., J. Ong, R.H. Prager, B.D. Gynther, and D.R. Curtis. 1987. Phaclofen: a peripheral and central baclofen antagonist. *Brain Res*. 405:150-4.

Kimura, N., T. Toyoshima, T. Kojima, and M. Shimane. 1998. Entactin-2: a new member of basement membrane protein with high homology to entactin/nidogen. *Exp Cell Res*. 241:36-45.

Kirkitadze, M.D., and P.N. Barlow. 2001. Structure and flexibility of the multiple domain proteins that regulate complement activation. *Immunol Rev*. 180:146-61.

Kirkpatrick, L.L., M.M. Matzuk, D.C. Dodds, and M.S. Perin. 2000. Biochemical interactions of the neuronal pentraxins. Neuronal pentraxin (NP) receptor binds to taipoxin and taipoxin-associated calcium-binding protein 49 via NP1 and NP2. *J Biol Chem*. 275:17786-92.

Kniazeff, J., T. Galvez, G. Labesse, and J.P. Pin. 2002. No ligand binding in the GB2 subunit of the GABA(B) receptor is required for activation and allosteric interaction between the subunits. *J Neurosci*. 22:7352-61.

Kobayashi, N., G. Kostka, J.H. Garbe, D.R. Keene, H.P. Bachinger, F.G. Hanisch, D. Markova, T. Tsuda, R. Timpl, M.L. Chu, and T. Sasaki. 2007. A comparative analysis of the fibulin protein family. Biochemical characterization, binding interactions, and tissue localization. *J Biol Chem*. 282:11805-16.

Kohfeldt, E., T. Sasaki, W. Gohring, and R. Timpl. 1998. Nidogen-2: a new basement membrane protein with diverse binding properties. *J Mol Biol*. 282:99-109.

Kristensen, T., and B.F. Tack. 1986. Murine protein H is comprised of 20 repeating units, 61 amino acids in length. *Proc Natl Acad Sci U S A*. 83:3963-7.

Kristiansen, K. 2004. Molecular mechanisms of ligand binding, signaling, and regulation within the superfamily of G-protein-coupled receptors: molecular modeling and mutagenesis approaches to receptor structure and function. *Pharmacol Ther*. 103:21-80.

Kuner, R., G. Kohr, S. Grunewald, G. Eisenhardt, A. Bach, and H.C. Kornau. 1999. Role of heteromer formation in GABAB receptor function. *Science*. 283:74-7.

Kuner, T., and R. Schoepfer. 1996. Multiple structural elements determine subunit specificity of Mg2+ block in NMDA receptor channels. *J Neurosci*. 16:3549-58.

Labasque, M., E. Reiter, C. Becamel, J. Bockaert, and P. Marin. 2008. Physical interaction of calmodulin with the 5-hydroxytryptamine2C receptor C-terminus is essential for G protein-independent, arrestin-dependent receptor signaling. *Mol Biol Cell*. 19:4640-50.

Lalonde, S., D.W. Ehrhardt, D. Loque, J. Chen, S.Y. Rhee, and W.B. Frommer. 2008. Molecular and cellular approaches for the detection of protein-protein interactions: latest techniques and current limitations. *Plant J*. 53:610-35.

Lanneau, C., A. Green, W.D. Hirst, A. Wise, J.T. Brown, E. Donnier, K.J. Charles, M. Wood, C.H. Davies, and M.N. Pangalos. 2001. Gabapentin is not a GABAB receptor agonist. *Neuropharmacology*. 41:965-75.

Leaney, J.L., and A. Tinker. 2000. The role of members of the pertussis toxin-sensitive family of G proteins in coupling receptors to the activation of the G protein-gated inwardly rectifying potassium channel. *Proc Natl Acad Sci U S A*. 97:5651-6.

Lee, N.V., J.C. Rodriguez-Manzaneque, S.N. Thai, W.O. Twal, A. Luque, K.M. Lyons, W.S. Argraves, and M.L. Iruela-Arispe. 2005. Fibulin-1 acts as a cofactor for the matrix metalloprotease ADAMTS-1. *J Biol Chem*. 280:34796-804.

Lefkowitz, R.J. 1998. G protein-coupled receptors. III. New roles for receptor kinases and beta-arrestins in receptor signaling and desensitization. *J Biol Chem*. 273:18677-80.

Legrain, P., and L. Selig. 2000. Genome-wide protein interaction maps using two-hybrid systems. *FEBS Lett*. 480:32-6.

Lehtinen, M.J., S. Meri, and T.S. Jokiranta. 2004. Interdomain contact regions and angles between adjacent short consensus repeat domains. *J Mol Biol*. 344:1385-96.

Liman, E.R., J. Tytgat, and P. Hess. 1992. Subunit stoichiometry of a mammalian K+ channel determined by construction of multimeric cDNAs. *Neuron*. 9:861-71.

Liu, F., Q. Wan, Z.B. Pristupa, X.M. Yu, Y.T. Wang, and H.B. Niznik. 2000. Direct protein-protein coupling enables cross-talk between dopamine D5 and gamma-aminobutyric acid A receptors. *Nature*. 403:274-80.

Lodish, H., Baltimore, D., Berk, A. 1995. Molecular cell biology. Scientific American Books, New York, NY.

Loridon-Rosa, B., P. Vielh, H. Matsuura, H. Clausen, C. Cuadrado, and P. Burtin. 1990. Distribution of oncofetal fibronectin in human mammary tumors: immunofluorescence study on histological sections. *Cancer Res*. 50:1608-12.

Luttrell, L.M., S.S. Ferguson, Y. Daaka, W.E. Miller, S. Maudsley, G.J. Della Rocca, F. Lin, H. Kawakatsu, K. Owada, D.K. Luttrell, M.G. Caron, and R.J. Lefkowitz. 1999. Beta-arrestin-dependent formation of beta2 adrenergic receptor-Src protein kinase complexes. *Science*. 283:655-61.

Luttrell, L.M., B.E. Hawes, T. van Biesen, D.K. Luttrell, T.J. Lansing, and R.J. Lefkowitz. 1996. Role of c-Src tyrosine kinase in G protein-coupled receptor- and Gbetagamma subunit-mediated activation of mitogen-activated protein kinases. *J Biol Chem*. 271:19443-50.

Luttrell, L.M., and R.J. Lefkowitz. 2002. The role of beta-arrestins in the termination and transduction of G-protein-coupled receptor signals. *J Cell Sci*. 115:455-65.

Maatta, M., I. Virtanen, R. Burgeson, and H. Autio-Harmainen. 2001. Comparative analysis of the distribution of laminin chains in the basement membranes in some malignant epithelial tumors: the alpha1 chain of laminin shows a selected expression pattern in human carcinomas. *J Histochem Cytochem*. 49:711-26.

Mackie, E.J., R. Chiquet-Ehrismann, C.A. Pearson, Y. Inaguma, K. Taya, Y. Kawarada, and T. Sakakura. 1987. Tenascin is a stromal marker for epithelial malignancy in the mammary gland. *Proc Natl Acad Sci U S A*. 84:4621-5.

Malitschek, B., D. Ruegg, J. Heid, K. Kaupmann, H. Bittiger, W. Frostl, B. Bettler, and R. Kuhn. 1998. Developmental changes of agonist affinity at GABABR1 receptor variants in rat brain. *Mol Cell Neurosci*. 12:56-64.

Margeta-Mitrovic, M., Y.N. Jan, and L.Y. Jan. 2000. A trafficking checkpoint controls GABA(B) receptor heterodimerization. *Neuron*. 27:97-106.

Marshall, F.H. 2001. Heterodimerization of G-protein-coupled receptors in the CNS. *Curr Opin Pharmacol*. 1:40-4.

Marshall, F.H., K.A. Jones, K. Kaupmann, and B. Bettler. 1999. GABAB receptors - the first 7TM heterodimers. *Trends Pharmacol Sci*. 20:396-9.

Martin, S.C., S.J. Russek, and D.H. Farb. 1999. Molecular identification of the human GABABR2: cell surface expression and coupling to adenylyl cyclase in the absence of GABABR1. *Mol Cell Neurosci*. 13:180-91.

Martin, S.C., S.J. Russek, and D.H. Farb. 2001. Human GABA(B)R genomic structure: evidence for splice variants in GABA(B)R1 but not GABA(B)R2. *Gene*. 278:63-79.

Maurer, K.C., J.H. Urbanus, and R.J. Planta. 1995. Sequence analysis of a 30 kb DNA segment from yeast chromosome XIV carrying a ribosomal protein gene cluster, the genes encoding a plasma membrane protein and a subunit of replication factor C, and a novel putative serine/threonine protein kinase gene. *Yeast*. 11:1303-10.

Mercuri, N.B., A. Bonci, A. Siniscalchi, A. Stefani, P. Calabresi, and G. Bernardi. 1996. Electrophysiological effects of monoamine oxidase inhibition on rat midbrain dopaminergic neurones: an in vitro study. *Br J Pharmacol*. 117:528-532.

Miernyk, J.A., and J.J. Thelen. 2008. Biochemical approaches for discovering protein-protein interactions. *Plant J*. 53:597-609.

Milligan, G., and J.H. White. 2001. Protein-protein interactions at G-protein-coupled receptors. *Trends Pharmacol Sci*. 22:513-8.

Miner, J.H. 2008. Laminins and their roles in mammals. *Microsc Res Tech*. 71:349-56.

Miner, J.H., J. Cunningham, and J.R. Sanes. 1998. Roles for laminin in embryogenesis: exencephaly, syndactyly, and placentopathy in mice lacking the laminin alpha5 chain. *J Cell Biol*. 143:1713-23.

Mohler, H., D. Benke, and J.M. Fritschy. 2001. GABA(B)-receptor isoforms molecular architecture and distribution. *Life Sci*. 68:2297-300.

Mohler, H., and J.M. Fritschy. 1999. GABAB receptors make it to the top--as dimers. *Trends Pharmacol Sci*. 20:87-9.

Montell, D.J., and C.S. Goodman. 1989. Drosophila laminin: sequence of B2 subunit and expression of all three subunits during embryogenesis. *J Cell Biol*. 109:2441-53.

Mukherjee, S., Bal, S., Saha, P. 2001. Protein interaction maps using yeast two-hybrid assay. *Current Science*. 81:458-464.

Nehring, R.B., H.P. Horikawa, O. El Far, M. Kneussel, J.H. Brandstatter, S. Stamm, E. Wischmeyer, H. Betz, and A. Karschin. 2000. The metabotropic GABAB

receptor directly interacts with the activating transcription factor 4. *J Biol Chem*. 275:35185-91.

Ng, G.Y., S. Bertrand, R. Sullivan, N. Ethier, J. Wang, J. Yergey, M. Belley, L. Trimble, K. Bateman, L. Alder, A. Smith, R. McKernan, K. Metters, G.P. O'Neill, J.C. Lacaille, and T.E. Hebert. 2001. Gamma-aminobutyric acid type B receptors with specific heterodimer composition and postsynaptic actions in hippocampal neurons are targets of anticonvulsant gabapentin action. *Mol Pharmacol*. 59:144-52.

Ng, G.Y., J. Clark, N. Coulombe, N. Ethier, T.E. Hebert, R. Sullivan, S. Kargman, A. Chateauneuf, N. Tsukamoto, T. McDonald, P. Whiting, E. Mezey, M.P. Johnson, Q. Liu, L.F. Kolakowski, Jr., J.F. Evans, T.I. Bonner, and G.P. O'Neill. 1999. Identification of a GABAB receptor subunit, gb2, required for functional GABAB receptor activity. *J Biol Chem*. 274:7607-10.

Ngo, S.T., P.G. Noakes, and W.D. Phillips. 2007. Neural agrin: a synaptic stabiliser. *Int J Biochem Cell Biol*. 39:863-7.

Nitkin, R.M., M.A. Smith, C. Magill, J.R. Fallon, Y.M. Yao, B.G. Wallace, and U.J. McMahan. 1987. Identification of agrin, a synaptic organizing protein from Torpedo electric organ. *J Cell Biol*. 105:2471-8.

O'Brien, R.J., D. Xu, R.S. Petralia, O. Steward, R.L. Huganir, and P. Worley. 1999. Synaptic clustering of AMPA receptors by the extracellular immediate-early gene product Narp. *Neuron*. 23:309-23.

O'Hara, P.J., P.O. Sheppard, H. Thogersen, D. Venezia, B.A. Haldeman, V. McGrane, K.M. Houamed, C. Thomsen, T.L. Gilbert, and E.R. Mulvihill. 1993. The ligand-binding domain in metabotropic glutamate receptors is related to bacterial periplasmic binding proteins. *Neuron*. 11:41-52.

Oleszewski, M., P. Gutwein, W. von der Lieth, U. Rauch, and P. Altevogt. 2000. Characterization of the L1-neurocan-binding site. Implications for L1-L1 homophilic binding. *J Biol Chem*. 275:34478-85.

Ong, J., and D.I. Kerr. 1990. GABA-receptors in peripheral tissues. *Life Sci*. 46:1489-501.

Overall, C.M., G.A. McQuibban, and I. Clark-Lewis. 2002. Discovery of chemokine substrates for matrix metalloproteinases by exosite scanning: a new tool for degradomics. *Biol Chem*. 383:1059-66.

Oxford, J.T., J. DeScala, N. Morris, K. Gregory, R. Medeck, K. Irwin, R. Oxford, R. Brown, L. Mercer, and S. Cusack. 2004. Interaction between amino propeptides of type XI procollagen alpha1 chains. *J Biol Chem*. 279:10939-45.

Panayotou, G., P. End, M. Aumailley, R. Timpl, and J. Engel. 1989. Domains of laminin with growth-factor activity. *Cell*. 56:93-101.

Paraoanu, L.E., and P.G. Layer. 2004. Mouse acetylcholinesterase interacts in yeast with the extracellular matrix component laminin-1beta. *FEBS Lett*. 576:161-4.

Parent, C.A., and P.N. Devreotes. 1996. Molecular genetics of signal transduction in Dictyostelium. *Annu Rev Biochem*. 65:411-40.

Parker, D.A., J. Ong, V. Marino, and D.I. Kerr. 2004. Gabapentin activates presynaptic GABAB heteroreceptors in rat cortical slices. *Eur J Pharmacol*. 495:137-43.

Perez-Garci, E., M. Gassmann, B. Bettler, and M.E. Larkum. 2006. The GABAB1b isoform mediates long-lasting inhibition of dendritic Ca2+ spikes in layer 5 somatosensory pyramidal neurons. *Neuron*. 50:603-16.

Pfaff, T., B. Malitschek, K. Kaupmann, L. Prezeau, J.P. Pin, B. Bettler, and A. Karschin. 1999. Alternative splicing generates a novel isoform of the rat metabotropic GABA(B)R1 receptor. *Eur J Neurosci*. 11:2874-82.

Pierce, K.L., and R.J. Lefkowitz. 2001. Classical and new roles of beta-arrestins in the regulation of G-protein-coupled receptors. *Nat Rev Neurosci*. 2:727-33.

Pin, J.P., C. De Colle, A.S. Bessis, and F. Acher. 1999. New perspectives for the development of selective metabotropic glutamate receptor ligands. *Eur J Pharmacol*. 375:277-94.

Pin, J.P., T. Galvez, and L. Prezeau. 2003. Evolution, structure, and activation mechanism of family 3/C G-protein-coupled receptors. *Pharmacol Ther*. 98:325-54.

Powell, S.K., and H.K. Kleinman. 1997. Neuronal laminins and their cellular receptors. *Int J Biochem Cell Biol*. 29:401-14.

Quiocho, F.A. 1990. Atomic structures of periplasmic binding proteins and the high-affinity active transport systems in bacteria. *Philos Trans R Soc Lond B Biol Sci*. 326:341-51; discussion 351-2.

Reiter, E., and R.J. Lefkowitz. 2006. GRKs and beta-arrestins: roles in receptor silencing, trafficking and signaling. *Trends Endocrinol Metab*. 17:159-65.

Rich, R.L., and D.G. Myszka. 2008. Survey of the year 2007 commercial optical biosensor literature. *J Mol Recognit*. 21:355-400.

Robbins, M.J., A.R. Calver, A.K. Filippov, W.D. Hirst, R.B. Russell, M.D. Wood, S. Nasir, A. Couve, D.A. Brown, S.J. Moss, and M.N. Pangalos. 2001. GABA(B2) is essential for g-protein coupling of the GABA(B) receptor heterodimer. *J Neurosci*. 21:8043-52.

Ross, R.A. 2007. Allosterism and cannabinoid CB(1) receptors: the shape of things to come. *Trends Pharmacol Sci*. 28:567-72.

Rual, J.F., K. Venkatesan, T. Hao, T. Hirozane-Kishikawa, A. Dricot, N. Li, G.F. Berriz, F.D. Gibbons, M. Dreze, N. Ayivi-Guedehoussou, N. Klitgord, C. Simon, M. Boxem, S. Milstein, J. Rosenberg, D.S. Goldberg, L.V. Zhang, S.L. Wong, G. Franklin, S. Li, J.S. Albala, J. Lim, C. Fraughton, E. Llamosas, S. Cevik, C. Bex, P. Lamesch, R.S. Sikorski, J. Vandenhaute, H.Y. Zoghbi, A. Smolyar, S. Bosak, R. Sequerra, L. Doucette-Stamm, M.E. Cusick, D.E. Hill, F.P. Roth, and M. Vidal. 2005. Towards a proteome-scale map of the human protein-protein interaction network. *Nature*. 437:1173-8.

Rubinstein, M., S. Peleg, S. Berlin, D. Brass, T. Keren-Raifman, C.W. Dessauer, T. Ivanina, and N. Dascal. 2009. Divergent regulation of GIRK1 and GIRK2 subunits of the neuronal G protein gated K+ channel by GalphaiGDP and Gbetagamma. *J Physiol*. 587:3473-91.

Ryan, M.C., R. Tizard, D.R. VanDevanter, and W.G. Carter. 1994. Cloning of the LamA3 gene encoding the alpha 3 chain of the adhesive ligand epiligrin. Expression in wound repair. *J Biol Chem*. 269:22779-87.

Saghatelyan, A.K., S. Gorissen, M. Albert, B. Hertlein, M. Schachner, and A. Dityatev. 2000. The extracellular matrix molecule tenascin-R and its HNK-1 carbohydrate modulate perisomatic inhibition and long-term potentiation in the CA1 region of the hippocampus. *Eur J Neurosci*. 12:3331-42.

Saghatelyan, A.K., M. Snapyan, S. Gorissen, I. Meigel, J. Mosbacher, K. Kaupmann, B. Bettler, A.V. Kornilov, N.E. Nifantiev, V. Sakanyan, M. Schachner, and A. Dityatev. 2003. Recognition molecule associated carbohydrate inhibits postsynaptic GABA(B) receptors: a mechanism for homeostatic regulation of GABA release in perisomatic synapses. *Mol Cell Neurosci*. 24:271-82.

Saglietti, L., C. Dequidt, K. Kamieniarz, M.C. Rousset, P. Valnegri, O. Thoumine, F. Beretta, L. Fagni, D. Choquet, C. Sala, M. Sheng, and M. Passafaro. 2007. Extracellular interactions between GluR2 and N-cadherin in spine regulation. *Neuron*. 54:461-77.

Sasaki, M., H.K. Kleinman, H. Huber, R. Deutzmann, and Y. Yamada. 1988. Laminin, a multidomain protein. The A chain has a unique globular domain and homology with the basement membrane proteoglycan and the laminin B chains. *J Biol Chem*. 263:16536-44.

Sauter, K., T. Grampp, J.M. Fritschy, K. Kaupmann, B. Bettler, H. Mohler, and D. Benke. 2005. Subtype-selective interaction with the transcription factor CCAAT/enhancer-binding protein (C/EBP) homologous protein (CHOP) regulates cell surface expression of GABA(B) receptors. *J Biol Chem*. 280:33566-72.

Scheele, S., A. Nystrom, M. Durbeej, J.F. Talts, M. Ekblom, and P. Ekblom. 2007. Laminin isoforms in development and disease. *J Mol Med*. 85:825-36.

Schultz, D.W., M.L. Klein, A.J. Humpert, C.W. Luzier, V. Persun, M. Schain, A. Mahan, C. Runckel, M. Cassera, V. Vittal, T.M. Doyle, T.M. Martin, R.G. Weleber, P.J. Francis, and T.S. Acott. 2003. Analysis of the ARMD1 locus: evidence that a mutation in HEMICENTIN-1 is associated with age-related macular degeneration in a large family. *Hum Mol Genet*. 12:3315-23.

Schwarz, D.A., G. Barry, S.D. Eliasof, R.E. Petroski, P.J. Conlon, and R.A. Maki. 2000. Characterization of gamma-aminobutyric acid receptor GABAB(1e), a GABAB(1) splice variant encoding a truncated receptor. *J Biol Chem*. 275:32174-81.

Shimizu-Nishikawa, K., K. Kajiwara, and E. Sugaya. 1995. Cloning and characterization of seizure-related gene, SEZ-6. *Biochem Biophys Res Commun*. 216:382-9.

Shimizu, S., M. Honda, M. Tanabe, and H. Ono. 2004. GABAB receptors do not mediate the inhibitory actions of gabapentin on the spinal reflex in rats. *J Pharmacol Sci*. 96:444-9.

Sia, G.M., J.C. Beique, G. Rumbaugh, R. Cho, P.F. Worley, and R.L. Huganir. 2007. Interaction of the N-terminal domain of the AMPA receptor GluR4 subunit with the neuronal pentraxin NP1 mediates GluR4 synaptic recruitment. *Neuron*. 55:87-102.

Stacey, M., H.H. Lin, S. Gordon, and A.J. McKnight. 2000. LNB-TM7, a group of seven-transmembrane proteins related to family-B G-protein-coupled receptors. *Trends Biochem Sci*. 25:284-9.

Steiger, J.L., S. Bandyopadhyay, D.H. Farb, and S.J. Russek. 2004. cAMP response element-binding protein, activating transcription factor-4, and upstream stimulatory factor differentially control hippocampal GABABR1a and GABABR1b subunit gene expression through alternative promoters. *J Neurosci*. 24:6115-26.

Stelzl, U., U. Worm, M. Lalowski, C. Haenig, F.H. Brembeck, H. Goehler, M. Stroedicke, M. Zenkner, A. Schoenherr, S. Koeppen, J. Timm, S. Mintzlaff, C. Abraham, N. Bock, S. Kietzmann, A. Goedde, E. Toksoz, A. Droege, S. Krobitsch, B. Korn, W. Birchmeier, H. Lehrach, and E.E. Wanker. 2005. A human protein-protein interaction network: a resource for annotating the proteome. *Cell*. 122:957-68.

Stetefeld, J., U. Mayer, R. Timpl, and R. Huber. 1996. Crystal structure of three consecutive laminin-type epidermal growth factor-like (LE) modules of laminin gamma1 chain harboring the nidogen binding site. *J Mol Biol*. 257:644-57.

Stokes, P.H., L.S. Thompson, N.J. Marianayagam, and J.M. Matthews. 2007. Dimerization of CtIP may stabilize in vivo interactions with the Retinoblastoma-pocket domain. *Biochem Biophys Res Commun*. 354:197-202.

Stone, E.M., A.J. Lotery, F.L. Munier, E. Heon, B. Piguet, R.H. Guymer, K. Vandenburgh, P. Cousin, D. Nishimura, R.E. Swiderski, G. Silvestri, D.A. Mackey, G.S. Hageman, A.C. Bird, V.C. Sheffield, and D.F. Schorderet. 1999. A single EFEMP1 mutation associated with both Malattia Leventinese and Doyne honeycomb retinal dystrophy. *Nat Genet*. 22:199-202.

Sugiyama, J.E., D.J. Glass, G.D. Yancopoulos, and Z.W. Hall. 1997. Laminin-induced acetylcholine receptor clustering: an alternative pathway. *J Cell Biol*. 139:181-91.

Sunada, Y., S.M. Bernier, A. Utani, Y. Yamada, and K.P. Campbell. 1995. Identification of a novel mutant transcript of laminin alpha 2 chain gene responsible for muscular dystrophy and dysmyelination in dy2J mice. *Hum Mol Genet*. 4:1055-61.

Tiao, J.Y., A. Bradaia, B. Biermann, K. Kaupmann, M. Metz, C. Haller, A.G. Rolink, E. Pless, P.N. Barlow, M. Gassmann, and B. Bettler. 2008. The sushi domains of secreted GABA(B1) isoforms selectively impair GABA(B) heteroreceptor function. *J Biol Chem*. 283:31005-11.

Tilakaratne, N., and P.M. Sexton. 2005. G-Protein-coupled receptor-protein interactions: basis for new concepts on receptor structure and function. *Clin Exp Pharmacol Physiol*. 32:979-87.

Timpl, R., and J.C. Brown. 1996. Supramolecular assembly of basement membranes. *Bioessays*. 18:123-32.

Timpl, R., H. Rohde, P.G. Robey, S.I. Rennard, J.M. Foidart, and G.R. Martin. 1979. Laminin--a glycoprotein from basement membranes. *J Biol Chem*. 254:9933-7.

Timpl, R., T. Sasaki, G. Kostka, and M.L. Chu. 2003. Fibulins: a versatile family of extracellular matrix proteins. *Nat Rev Mol Cell Biol*. 4:479-89.

Tisi, D., J.F. Talts, R. Timpl, and E. Hohenester. 2000. Structure of the C-terminal laminin G-like domain pair of the laminin alpha2 chain harbouring binding sites for alpha-dystroglycan and heparin. *EMBO J*. 19:1432-40.

Tokmakov, A.A., E. Matsumoto, M. Shirouzu, and S. Yokoyama. 2006. Coupled cytoplasmic transcription-and-translation--a method of choice for heterologous gene expression in Xenopus oocytes. *J Biotechnol*. 122:5-15.

Trakselis, M.A., S.C. Alley, and F.T. Ishmael. 2005. Identification and mapping of protein-protein interactions by a combination of cross-linking, cleavage, and proteomics. *Bioconjug Chem*. 16:741-50.

Tu, J.C., B. Xiao, J.P. Yuan, A.A. Lanahan, K. Leoffert, M. Li, D.J. Linden, and P.F. Worley. 1998. Homer binds a novel proline-rich motif and links group 1 metabotropic glutamate receptors with IP3 receptors. *Neuron*. 21:717-26.

Tzu, J., and M.P. Marinkovich. 2008. Bridging structure with function: structural, regulatory, and developmental role of laminins. *Int J Biochem Cell Biol*. 40:199-214.

Uezono, Y., M. Kanaide, M. Kaibara, R. Barzilai, N. Dascal, K. Sumikawa, and K. Taniyama. 2006. Coupling of GABAB receptor GABAB2 subunit to G proteins: evidence from Xenopus oocyte and baby hamster kidney cell expression system. *Am J Physiol Cell Physiol*. 290:C200-7.

Uhrinova, S., F. Lin, G. Ball, K. Bromek, D. Uhrin, M.E. Medof, and P.N. Barlow. 2003. Solution structure of a functionally active fragment of decay-accelerating factor. *Proc Natl Acad Sci U S A*. 100:4718-23.

Vernon, E., G. Meyer, L. Pickard, K. Dev, E. Molnar, G.L. Collingridge, and J.M. Henley. 2001. GABA(B) receptors couple directly to the transcription factor ATF4. *Mol Cell Neurosci*. 17:637-45.

Veroni, C., M. Grasso, G. Macchia, C. Ramoni, M. Ceccarini, T.C. Petrucci, and P. Macioce. 2007. beta-dystrobrevin, a kinesin-binding receptor, interacts with the extracellular matrix components pancortins. *J Neurosci Res*. 85:2631-9.

Veyhl, M., T. Keller, V. Gorboulev, A. Vernaleken, and H. Koepsell. 2006. RS1 (RSC1A1) regulates the exocytotic pathway of Na+-D-glucose cotransporter SGLT1. *Am J Physiol Renal Physiol*. 291:F1213-23.

Vigot, R., S. Barbieri, H. Brauner-Osborne, R. Turecek, R. Shigemoto, Y.P. Zhang, R. Lujan, L.H. Jacobson, B. Biermann, J.M. Fritschy, C.M. Vacher, M. Muller, G. Sansig, N. Guetg, J.F. Cryan, K. Kaupmann, M. Gassmann, T.G. Oertner, and B. Bettler. 2006. Differential compartmentalization and distinct functions of GABAB receptor variants. *Neuron*. 50:589-601.

Villmann, C., L. Bull, and M. Hollmann. 1997. Kainate binding proteins possess functional ion channel domains. *J Neurosci*. 17:7634-43.

Violin, J.D., and R.J. Lefkowitz. 2007. Beta-arrestin-biased ligands at seven-transmembrane receptors. *Trends Pharmacol Sci*. 28:416-22.

Vogel, B.E., and E.M. Hedgecock. 2001. Hemicentin, a conserved extracellular member of the immunoglobulin superfamily, organizes epithelial and other cell attachments into oriented line-shaped junctions. *Development*. 128:883-94.

Wagner, C.A., B. Friedrich, I. Setiawan, F. Lang, and S. Broer. 2000. The use of Xenopus laevis oocytes for the functional characterization of heterologously expressed membrane proteins. *Cell Physiol Biochem*. 10:1-12.

Wei, H., S. Ahn, S.K. Shenoy, S.S. Karnik, L. Hunyady, L.M. Luttrell, and R.J. Lefkowitz. 2003. Independent beta-arrestin 2 and G protein-mediated pathways for angiotensin II activation of extracellular signal-regulated kinases 1 and 2. *Proc Natl Acad Sci U S A*. 100:10782-7.

Wei, K., J.H. Eubanks, J. Francis, Z. Jia, and O.C. Snead, 3rd. 2001. Cloning and tissue distribution of a novel isoform of the rat GABA(B)R1 receptor subunit. *Neuroreport*. 12:833-7.

Wess, J. 1997. G-protein-coupled receptors: molecular mechanisms involved in receptor activation and selectivity of G-protein recognition. *FASEB J*. 11:346-54.

Weston, C.A., G. Teressa, B.S. Weeks, and J. Prives. 2007. Agrin and laminin induce acetylcholine receptor clustering by convergent, Rho GTPase-dependent signaling pathways. *J Cell Sci*. 120:868-75.

White, J.H., R.A. McIllhinney, A. Wise, F. Ciruela, W.Y. Chan, P.C. Emson, A. Billinton, and F.H. Marshall. 2000. The GABAB receptor interacts directly with the related transcription factors CREB2 and ATFx. *Proc Natl Acad Sci U S A*. 97:13967-72.

White, J.H., A. Wise, M.J. Main, A. Green, N.J. Fraser, G.H. Disney, A.A. Barnes, P. Emson, S.M. Foord, and F.H. Marshall. 1998. Heterodimerization is required for the formation of a functional GABA(B) receptor. *Nature*. 396:679-82.

White, J.H., A. Wise, and F.H. Marshall. 2002. Heterodimerization of gamma-aminobutyric acid B receptor subunits as revealed by the yeast two-hybrid system. *Methods*. 27:301-10.

Witchel, H.J., J.T. Milnes, J.S. Mitcheson, and J.C. Hancox. 2002. Troubleshooting problems with in vitro screening of drugs for QT interval prolongation using HERG K+ channels expressed in mammalian cell lines and Xenopus oocytes. *J Pharmacol Toxicol Methods*. 48:65-80.

Yang, M.Y., J.D. Armstrong, I. Vilinsky, N.J. Strausfeld, and K. Kaiser. 1995. Subdivision of the Drosophila mushroom bodies by enhancer-trap expression patterns. *Neuron*. 15:45-54.